

Methods in breast cancer

Edited by

Luis Costa, Gianluca Franceschini, Dayanidhi Raman
and Antonino Bonaventura D'assoro

Published in

Frontiers in Oncology



FRONTIERS EBOOK COPYRIGHT STATEMENT

The copyright in the text of individual articles in this ebook is the property of their respective authors or their respective institutions or funders. The copyright in graphics and images within each article may be subject to copyright of other parties. In both cases this is subject to a license granted to Frontiers.

The compilation of articles constituting this ebook is the property of Frontiers.

Each article within this ebook, and the ebook itself, are published under the most recent version of the Creative Commons CC-BY licence. The version current at the date of publication of this ebook is CC-BY 4.0. If the CC-BY licence is updated, the licence granted by Frontiers is automatically updated to the new version.

When exercising any right under the CC-BY licence, Frontiers must be attributed as the original publisher of the article or ebook, as applicable.

Authors have the responsibility of ensuring that any graphics or other materials which are the property of others may be included in the CC-BY licence, but this should be checked before relying on the CC-BY licence to reproduce those materials. Any copyright notices relating to those materials must be complied with.

Copyright and source acknowledgement notices may not be removed and must be displayed in any copy, derivative work or partial copy which includes the elements in question.

All copyright, and all rights therein, are protected by national and international copyright laws. The above represents a summary only. For further information please read Frontiers' Conditions for Website Use and Copyright Statement, and the applicable CC-BY licence.

ISSN 1664-8714
ISBN 978-2-8325-3998-9
DOI 10.3389/978-2-8325-3998-9

About Frontiers

Frontiers is more than just an open access publisher of scholarly articles: it is a pioneering approach to the world of academia, radically improving the way scholarly research is managed. The grand vision of Frontiers is a world where all people have an equal opportunity to seek, share and generate knowledge. Frontiers provides immediate and permanent online open access to all its publications, but this alone is not enough to realize our grand goals.

Frontiers journal series

The Frontiers journal series is a multi-tier and interdisciplinary set of open-access, online journals, promising a paradigm shift from the current review, selection and dissemination processes in academic publishing. All Frontiers journals are driven by researchers for researchers; therefore, they constitute a service to the scholarly community. At the same time, the *Frontiers journal series* operates on a revolutionary invention, the tiered publishing system, initially addressing specific communities of scholars, and gradually climbing up to broader public understanding, thus serving the interests of the lay society, too.

Dedication to quality

Each Frontiers article is a landmark of the highest quality, thanks to genuinely collaborative interactions between authors and review editors, who include some of the world's best academicians. Research must be certified by peers before entering a stream of knowledge that may eventually reach the public - and shape society; therefore, Frontiers only applies the most rigorous and unbiased reviews. Frontiers revolutionizes research publishing by freely delivering the most outstanding research, evaluated with no bias from both the academic and social point of view. By applying the most advanced information technologies, Frontiers is catapulting scholarly publishing into a new generation.

What are Frontiers Research Topics?

Frontiers Research Topics are very popular trademarks of the *Frontiers journals series*: they are collections of at least ten articles, all centered on a particular subject. With their unique mix of varied contributions from Original Research to Review Articles, Frontiers Research Topics unify the most influential researchers, the latest key findings and historical advances in a hot research area.

Find out more on how to host your own Frontiers Research Topic or contribute to one as an author by contacting the Frontiers editorial office: frontiersin.org/about/contact

Methods in breast cancer

Topic editors

Luis Costa — Santa Maria Hospital, Portugal

Gianluca Franceschini — Agostino Gemelli University Polyclinic (IRCCS), Italy

Dayanidhi Raman — University of Toledo, United States

Antonino Bonaventura D'assoro — Mayo Clinic, United States

Citation

Costa, L., Franceschini, G., Raman, D., D'assoro, A. B., eds. (2023). *Methods in breast cancer*. Lausanne: Frontiers Media SA. doi: 10.3389/978-2-8325-3998-9

Table of contents

| | |
|-----|--|
| 05 | Editorial: Methods in breast cancer Gianluca Franceschini |
| 08 | Clinical outcomes following robotic versus conventional DIEP flap in breast reconstruction: A retrospective matched study Min Jeong Lee, Jongmin Won, Seung Yong Song, Hyung Seok Park, Jee Ye Kim, Hye Jung Shin, Young In Kwon, Dong Won Lee and Na Young Kim |
| 19 | The effect of respiratory capacity for dose sparing in left-sided breast cancer irradiation with active breathing coordinator technique Hongtao Chen, Ying Piao, Dong Yang, Peipei Kuang, Zihuang Li, Guixiang Liao and Heli Zhong |
| 29 | Symptomatic bone marrow metastases in breast cancer: A retrospective cohort study Ruohan Yang, Lin Jia, Guanyu Lu, Zheng Lv and Jiuwei Cui |
| 38 | Metabolic characteristics of the various incision margins for breast cancer conservation surgery Fang Wang, Zongze Gu, Xunan Zhao, Zhuo Chen, Zhe Zhang, Shihao Sun and Mingli Han |
| 49 | Impact of telehealth interventions on physiological and psychological outcomes in breast cancer survivors: A meta-analysis of randomised controlled trials Puneeta Ajmera, Mohammad Miraj, Sheetal Kalra, Ramesh K. Goyal, Varsha Chorsiya, Riyaz Ahamed Shaik, Msaad Alzhrani, Ahmad Alanazi, Mazen Alqahtani, Shaima Ali Miraj, Sonia Pawaria and Vini Mehta |
| 68 | Impact of clinicopathological factors on extended endocrine therapy decision making in estrogen receptor–positive breast cancer Weilin Chen, Jiayi Wu, Yifei Zhu, Jiahui Huang, Xiaosong Chen, Ou Huang, Jianrong He, Yafen Li, Weiguo Chen, Kunwei Shen and Li Zhu |
| 81 | HER2-positive metastatic breast cancer with brain metastases responds favorably to pyrotinib and trastuzumab-based treatment: A case report and literature review Min-long Chen, Wenjie Yu, Binbin Cui, Yijian Yu and Zhaosheng Ma |
| 88 | Breast cancer patient-derived explant cultures recapitulate <i>in vivo</i> drug responses Solveig Pettersen, Geir Frode Øy, Eivind Valen Egeland, Siri Juell, Olav Engebråten, Gunhild Mari Mælandsmo and Lina Prasmickaite |
| 100 | An ultrasound-based radiomics model to distinguish between sclerosing adenosis and invasive ductal carcinoma Qun Huang, Wanxian Nong, Xiaozhen Tang and Yong Gao |

- 111 **Development and validation of nomograms for predicting axillary non-SLN metastases in breast cancer patients: A retrospective analysis**
Huizi Lei, Pei Yuan, Changyuan Guo and Jianming Ying
- 119 **BOMB trial: First results of stereotactic radiotherapy to primary breast tumor in metastatic breast cancer patients**
Edy Ippolito, Sonia Silipigni, Francesco Pantano, Paolo Matteucci, Sofia Carrafiello, Maristella Marrocco, Rita Alaimo, Vincenzo Palumbo, Michele Fiore, Paolo Orsaria, Rolando Maria D'Angelillo, Vittorio Altomare, Giuseppe Tonini and Sara Ramella
- 125 **Prediction of clinical response to neoadjuvant therapy in advanced breast cancer by baseline B-mode ultrasound, shear-wave elastography, and pathological information**
Siyu Wang, Wen Wen, Haina Zhao, Jingyan Liu, Xue Wan, Zihan Lan and Yulan Peng
- 134 **Analytical validation of the 7-gene biosignature for prediction of recurrence risk and radiation therapy benefit for breast ductal carcinoma *in situ***
David Dabbs, Karuna Mittal, Scott Heineman, Pat Whitworth, Chirag Shah, Jess Savala, Steven C. Shivers and Troy Bremer
- 146 **Efficacy of apatinib 250 mg combined with chemotherapy in patients with pretreated advanced breast cancer in a real-world setting**
Ruyan Zhang, Yifei Chen, Xiaoran Liu, Xinyu Gui, Anjie Zhu, Hanfang Jiang, Bin Shao, Xu Liang, Ying Yan, Jiayang Zhang, Guohong Song and Huiping Li
- 155 **A single-arm study design with non-inferiority and superiority time-to-event endpoints: a tool for proof-of-concept and de-intensification strategies in breast cancer**
Miguel Sampayo-Cordero, Bernat Miguel-Huguet, Andrea Malfettone, Elena López-Miranda, María Gion, Elena Abad, Daniel Alcalá-López, Jhudit Pérez-Escuredo, José Manuel Pérez-García, Antonio Llombart-Cussac and Javier Cortés
- 161 **Discrepancies in ICD-9/ICD-10-based codes used to identify three common diseases in cancer patients in real-world settings and their implications for disease classification in breast cancer patients and patients without cancer: a literature review and descriptive study**
Nora Tu, Mackenzie Henderson, Meera Sundararajan and Maribel Salas



OPEN ACCESS

EDITED AND REVIEWED BY

Kara Britt,
Peter MacCallum Cancer Centre, Australia

*CORRESPONDENCE

Gianluca Franceschini
✉ gianlucafranceschini70@gmail.com

RECEIVED 30 September 2023

ACCEPTED 06 November 2023

PUBLISHED 10 November 2023

CITATION

Franceschini G (2023) Editorial: Methods
in breast cancer.

Front. Oncol. 13:1304941.

doi: 10.3389/fonc.2023.1304941

COPYRIGHT

© 2023 Franceschini. This is an open-access article distributed under the terms of the [Creative Commons Attribution License \(CC BY\)](https://creativecommons.org/licenses/by/4.0/). The use, distribution or reproduction in other forums is permitted, provided the original author(s) and the copyright owner(s) are credited and that the original publication in this journal is cited, in accordance with accepted academic practice. No use, distribution or reproduction is permitted which does not comply with these terms.

Editorial: Methods in breast cancer

Gianluca Franceschini *

Fondazione Policlinico Universitario Agostino Gemelli IRCCS, Breast Unit, Department of Woman and Child Health and Public Health, Università Cattolica del Sacro Cuore, Rome, Italy

KEYWORDS

breast cancer, new methods & methodologies, surgery, oncoplastic breast conserving surgery, mastectomy, breast reconstruction, breast treatment, radiotherapy

Editorial on the Research Topic

Methods in breast cancer

Breast cancer remains one of the most prevalent challenges in oncology and is recognized as an international priority in healthcare; it is currently the most common tumor in women worldwide with demographic trends indicating a continued increase in incidence (1). While clinicians and researchers work to find an optimal strategy in treatment of breast cancer, the introduction of innovative methods is also mandatory.

Nowadays, therapeutic strategies against breast cancer are increasingly personalized for each patient. The appropriate treatment is modulated on clinical characteristics, staging, biological factors such as the status of hormone receptors, Ki67, HER2 overexpression. In particular, endocrine therapy plays a vital role in the management of estrogen receptor-positive breast cancer. Chen et al. examine how clinicopathological factors influence decisions regarding extended endocrine therapy. They report that that age, lymph nodal status and receipt of chemotherapy are independent predictors for the recommendation of extended endocrine therapy.

However, a multidisciplinary management is essential to improve oncological and aesthetic results while increasing patient's quality of life. An accurate discussion should always be carried out with each patient on the benefits and problems related to the chosen treatment.

Accurate coding is crucial for an appropriate disease classification and research; Tu et al. review discrepancies in ICD-9/ICD-10-based codes for breast cancer and other common diseases, highlighting the need for precision in health data. They indicate that researchers should use standardized, validated coding algorithms to reduce risk of misclassification which can significantly alter the findings of a study.

Thanks to the wider diffusion of screening programs, breast cancer is more often detected at an early stage. An innovative ultrasound-based radiomics model can distinguish between sclerosing adenosis and invasive ductal carcinoma while potentially aiding in early diagnosis (Huang et al.). This innovative model can contribute to an effective diagnosis by avoiding misdiagnosis and unnecessary biopsies.

Early-stage breast cancer is usually treated with primary surgery. Breast-conserving treatment or mastectomy are the surgical options. However local control of disease and the patient's aesthetic satisfaction should always be guaranteed in both cases (1). An adequate evaluation of the disease by clinical and radiological assessment is mandatory to choose the

best local treatment (1). The selection of optimal surgical treatment should be based on breast volume, cancer size, multicentricity, ability to obtain clear surgical margins and the patient's wishes.

Breast-conserving surgery (BCS) with adjuvant radiotherapy is considered the gold standard approach for early-stage breast cancer. Some prospective randomized studies have not shown significant differences in disease-free and overall survival rates comparing conservative treatment with mastectomy. However, BCS must always guarantee complete surgical removal of the tumor with negative surgical margins and optimal aesthetic results also using some biomaterials as filler (2, 3). Nowadays, the main method used to evaluate margins in BCS is a pathological evaluation. The designation of surgical margins is controversial and metabolomics may represent a new approach to assess surgical margins. Based on metabolomic analysis, Wang et al. show the negative margin of 1 mm is sufficient for surgery. The six metabolites identified as abnormal (pyruvic acid, N-acetyl-L-aspartic acid, glutamic acid, gamma-aminobutyric acid, fumaric acid and citric acid) may serve as biomarkers to select an appropriate surgical margin.

Adjuvant radiotherapy is a cornerstone after BCS. However, subsequent cardiac toxicity is deemed to be dose-dependent for left breast cancer irradiation. Chen et al. investigate the impact of respiratory capacity on dose sparing during left-sided breast cancer irradiation, highlighting a novel technique for optimizing radiotherapy. They demonstrate the effect of respiratory capacity for dose sparing when the deep inspiration breath hold with Active Breathing Coordinator technique (ABC-DIBH) is used in left-sided breast cancer irradiation. Furthermore, Dabbs et al. present the results on clinical utility for the DCISionRT test for the prediction of recurrence risk and radiotherapy benefit in ductal carcinoma *in situ*.

Mastectomy should be performed when conservative treatment is unable to guarantee adequate local control and appropriate aesthetic results. Common indications for mastectomy include: large tumors that cannot be treated by BCS with a satisfactory cosmetic outcome; multicentric disease; persistent positive margins after multiple re-excisions; inability to perform adjuvant radiotherapy; presence of BRCA pathogenic variants; patient preference (1). Breast reconstruction after mastectomy is a critical aspect of a patient's recovery. Immediate breast reconstruction with autologous tissue or prosthesis should always be performed after mastectomy as it can improve the patient's quality of life (4). The demand for further aesthetic improvement in breast reconstruction is leading to innovative solutions. Lee et al. delves into the clinical outcomes of robot-assisted DIEP (Deep Inferior Epigastric artery Perforator) flap surgery. They suggest that robotic DIEP flap offers enhanced postoperative recovery with a reduction in postoperative pain and hospital stay.

Regarding axillary surgery, sentinel lymph node biopsy is considered the gold standard in early breast cancer with clinically negative nodes. Axillary dissection is indicated in breast cancers with clinically positive nodes although new therapeutic strategies are emerging (1). Lei et al. report a nomogram for predicting positive non-sentinel lymph nodes (non-SLNs) in positive SLN patients.

Primary chemotherapy is used with increasing frequency in the multidisciplinary treatment of breast cancer patients (5). Various

trials have demonstrated that neoadjuvant chemotherapy allows to obtain important advantages such as downstaging of disease favoring surgical de-escalation (6, 7). Wang et al. propose a multimodal approach to predict clinical responses to neoadjuvant therapy in advanced breast cancer, incorporating B-mode ultrasonography, shear wave elastography and pathological information.

The primary aim of management in metastatic breast cancer is to mitigate symptoms, prolong survival and improve quality of life. Patients with metastatic disease can be treated with endocrine therapy, chemotherapy, biologic therapies and immunotherapy (1). HER2-positive patients with brain metastases respond favorably to pyrotinib and trastuzumab-based treatment (Chen et al.). Zhang et al. report the efficacy and safety of apatinib (an oral small-molecule tyrosine kinase inhibitor targeting VEGFR-2) 250 mg combined with chemotherapy in patients with pretreated metastatic breast cancer. Yang et al. explore the clinicopathological characteristics of bone marrow metastases in breast cancer and prognosis using different therapies. Ippolito et al. show the results of the BOMB trial, which explores the use of stereotactic radiotherapy on primary tumor in metastatic patients (20). The study evaluates the maximum tolerated dose of stereotactic body radiotherapy (SABRT) to primary breast cancer in stage IV disease.

Furthermore, some authors take us into personalized medicine by demonstrating how patient-derived explant cultures can recapitulate *in vivo* drug responses, opening the way to innovative treatments (Pettersen et al.). Finally, innovative trials and new technologies are changing breast cancer management; single-arm designs with non-inferiority and superiority analyses are optimal for proof-of-concept and de-escalation studies in oncology (Sampayo-Cordero et al.). The telehealth care is also an adequate approach to reduce the treatment burden and the clinical problems of breast cancer survivors (Ajmera et al.).

In conclusion, this Research Topic presents interesting research in the field of breast cancer treatment. Thanks to results of ongoing studies and collaboration between healthcare professionals and researchers, prognosis and well-being of breast cancer survivors can be constantly improved.

Author contributions

GF: Conceptualization, Writing – original draft, Writing – review & editing.

Conflict of interest

The author declares that the research was conducted in the absence of any commercial or financial relationships that could be construed as a potential conflict of interest.

The author(s) declared that they were an editorial board member of Frontiers, at the time of submission. This had no impact on the peer review process and the final decision.

Publisher's note

All claims expressed in this article are solely those of the authors and do not necessarily represent those of their affiliated

organizations, or those of the publisher, the editors and the reviewers. Any product that may be evaluated in this article, or claim that may be made by its manufacturer, is not guaranteed or endorsed by the publisher.

References

1. Franceschini G, Scardina L, Visconti G, Hayashi A, Masetti R. Editorial: update of current evidences in breast cancer surgery. *Front Oncol* (2022) 12:928467. doi: 10.3389/fonc.2022.928467
2. Franceschini G, Visconti G, Sanchez AM, Di Leone A, Salgarello M, Masetti R. Oxidized regenerated cellulose in breast surgery: experimental model. *J Surg Res* (2015) 198(1):237–44. doi: 10.1016/j.jss.2015.05.012
3. Franceschini G, Masetti R, D'Ugo D, Palumbo F, D'Alba P, Mulè A, et al. Synchronous bilateral Paget's disease of the nipple associated with bilateral breast carcinoma. *Breast J* (2005) 11(5):355–6. doi: 10.1111/j.1075-122X.2005.21722.x
4. Franceschini G, Scardina L, Di Leone A, Terribile DA, Sanchez AM, Magno S, et al. Immediate Prosthetic Breast Reconstruction after Nipple-Sparing Mastectomy: Traditional Subpectoral Technique versus Direct-to-Implant Prepectoral Reconstruction without Acellular Dermal Matrix. *J Pers Med* (2021) 2211(2):153. doi: 10.3390/jpm11020153
5. Franceschini G, Terribile D, Magno S, Fabbri C, D'Alba PF, Chiesa F, et al. Update in the treatment of locally advanced breast cancer: a multidisciplinary approach. *Eur Rev Med Pharmacol Sci* (2007) 11(5):283–9.
6. Nardone L, Valentini V, Marino L, De Santis MC, Terribile D, Franceschini G, et al. A feasibility study of neo-adjuvant low-dose fractionated radiotherapy with two different concurrent anthracycline-docetaxel schedules in stage IIA/B-III breast cancer. *Tumori*. (2012) 98(1):79–85. doi: 10.1177/030089161209800110
7. Franceschini G, Terribile D, Fabbri C, Magno S, D'Alba P, Chiesa F, et al. Management of locally advanced breast cancer. *Mini-review. Minerva Chir.* (2007) 62(4):249–55.



OPEN ACCESS

EDITED BY

Gianluca Franceschini,
Agostino Gemelli University Polyclinic
(IRCCS), Italy

REVIEWED BY

Onur Dülgeroğlu,
Acibadem University, Turkey
Pawel Kabata,
Medical University of Gdansk, Poland

*CORRESPONDENCE

Dong Won Lee
xyphoss@yuhs.ac
Na Young Kim
knnyyy@yuhs.ac

[†]These authors have contributed
equally to this work and share
first authorship

SPECIALTY SECTION

This article was submitted to
Breast Cancer,
a section of the journal
Frontiers in Oncology

RECEIVED 08 July 2022

ACCEPTED 24 August 2022

PUBLISHED 14 September 2022

CITATION

Lee MJ, Won J, Song SY, Park HS, Kim
JY, Shin HJ, Kwon YI, Lee DW and Kim
NY (2022) Clinical outcomes following
robotic versus conventional DIEP flap
in breast reconstruction: A
retrospective matched study.
Front. Oncol. 12:989231.
doi: 10.3389/fonc.2022.989231

COPYRIGHT

© 2022 Lee, Won, Song, Park, Kim, Shin,
Kwon, Lee and Kim. This is an open-
access article distributed under the
terms of the [Creative Commons
Attribution License \(CC BY\)](https://creativecommons.org/licenses/by/4.0/). The use,
distribution or reproduction in other
forums is permitted, provided the
original author(s) and the copyright
owner(s) are credited and that the
original publication in this journal is
cited, in accordance with accepted
academic practice. No use,
distribution or reproduction is
permitted which does not comply with
these terms.

Clinical outcomes following robotic versus conventional DIEP flap in breast reconstruction: A retrospective matched study

Min Jeong Lee^{1†}, Jongmin Won^{2†}, Seung Yong Song², Hyung
Seok Park³, Jee Ye Kim³, Hye Jung Shin⁴, Young In Kwon¹,
Dong Won Lee^{2*} and Na Young Kim^{1*}

¹Department of Anesthesiology and Pain Medicine, Anesthesia and Pain Research Institute, Yonsei University College of Medicine, Seoul, South Korea, ²Department of Plastic and Reconstructive Surgery, Institute for Human Tissue Restoration, Yonsei University College of Medicine, Seoul, South Korea, ³Department of Surgery, Yonsei University College of Medicine, Seoul, South Korea, ⁴Biostatistics Collaboration Unit, Department of Biomedical Systems Informatics, Yonsei University College of Medicine, Seoul, South Korea

Background: A robotic deep inferior epigastric perforator (DIEP) flap created through a totally extraperitoneal approach minimizes violation of the donor site, which may lead to postoperative pain reduction and rapid recovery. The authors compared the clinical outcomes of robotic and conventional DIEP flap breast reconstructions.

Methods: Data from consecutive patients who underwent mastectomy with DIEP flaps for breast reconstruction between July 2017 and January 2021 were retrospectively reviewed. Patients were divided into robotic and conventional DIEP groups, and the two groups were matched using the inverse probability of treatment weighting method. They were compared based on the reconstruction time, drainage amount, postoperative pain, rescue analgesics, hospital stay, complications, and BREAST-Q scores.

Results: After matching, a dataset of 207 patients was formed, including 21 patients in the robotic DIEP group and 186 patients in the conventional DIEP group. The mean reconstruction time was longer in the robotic DIEP group than in the conventional DIEP group ($P < 0.001$). In the robotic group, pain intensity during the postoperative 6–24 hours was significantly reduced ($P = 0.001$) with less use of fentanyl ($P = 0.003$) compared to the conventional DIEP group. The mean length of hospital stay for the robotic DIEP group was shorter than that for conventional DIEP ($P = 0.002$). BREAST-Q scores indicated

a higher level of the abdominal physical well-being domain in the robotic group ($P=0.020$). Complication rates were comparable between the two groups.

Conclusions: This study suggests that a robotic DIEP flap offers enhanced postoperative recovery, accompanied by a reduction in postoperative pain and hospital stay.

KEYWORDS

breast reconstruction, deep inferior epigastric perforator flap, robot surgery, conventional DIEP, robotic DIEP, clinical outcome

Introduction

As surgical techniques have improved and patient expectations have increased, the goal of breast reconstruction is to make breasts natural-looking and esthetically pleasing while minimizing patient morbidity. Autologous breast reconstruction using abdominal tissue has been developed to decrease donor-site morbidities. The deep inferior epigastric perforator (DIEP) flap has gained popularity since its introduction in 1989 and is currently the most commonly performed procedure to reduce the morbidity of the donor site (1–5). There is also the superficial inferior epigastric artery flap, which does not damage the rectus muscle and fascia at all, but its use is limited owing to the inconsistency of a reliable superficial inferior epigastric artery.

However, even during DIEP flap elevation, an incision in the anterior rectus fascia is inevitable. Especially when a reliable perforator is located near the umbilicus, an extensive incision over the fascia is needed. Dissection, splitting, and traction of the upper structures above the pedicle are required to reach the pedicle. These procedures may increase donor-site morbidities. These limitations can be overcome using minimally invasive approaches, such as robotic or laparoscopic approaches (6–10). They are used in the dissection of the pedicle coursing underneath the rectus muscle during harvesting of the DIEP flap. Therefore, violation of the anterior rectus fascia, rectus muscle, and motor nerves can be minimized compared with conventional DIEP flaps. Despite several reports of DIEP flap harvesting using robots, there is still a lack of data comparing the outcomes of robotic and conventional DIEP flaps for reconstruction.

Robotic DIEP flap harvest is expected to provide significant benefits in decreasing donor-site morbidity. This may lead to postoperative pain reduction, rapid recovery, and donor site well-being. This study aimed to perform a robotic DIEP flap harvesting through a totally extraperitoneal approach and compare the postoperative outcomes between robotic and conventional DIEP flap breast reconstruction.

Materials and methods

Study population

This retrospective study was conducted at a single institution. Data from 254 consecutive Korean patients with breast cancer who underwent total mastectomy with immediate conventional DIEP flap or robotic DIEP flap breast reconstruction between July 2017 and January 2021 were identified from specified electronic medical records. To ensure uniformity in patient selection by reducing potential surgical confounding factors, 19 patients who underwent other simultaneous surgeries, 16 patients who underwent combined contralateral breast surgeries, 8 patients who underwent bilateral DIEP flap surgeries, and 7 patients with incomplete data were excluded. Finally, the remaining 204 patients who underwent unilateral DIEP flap breast reconstruction were eligible for the study and were classified into one of two groups: those who underwent conventional DIEP flap surgery (conventional DIEP, $n = 185$) and those who underwent robotic DIEP flap surgery (robotic DIEP, $n = 19$) (Figure 1). The robotic DIEP flap breast reconstruction was performed on patients who had single or closely grouped perforators with a short intramuscular course and consented to robotic surgery before surgery.

Surgical techniques

The conventional DIEP technique was performed in a standard manner by splitting the anterior rectus fascia and rectus abdominis muscles. The robotic DIEP technique was performed as previously reported by the authors (8). Briefly, in the robotic technique, the preselected perforator was dissected with the conventional method until the intramuscular course ended, followed by preperitoneal blunt dissection with a surgeon's finger or balloon device (OMS-PDB1000; Covidien, Dublin, Ireland) through a 1.5-cm fascial incision on the linea

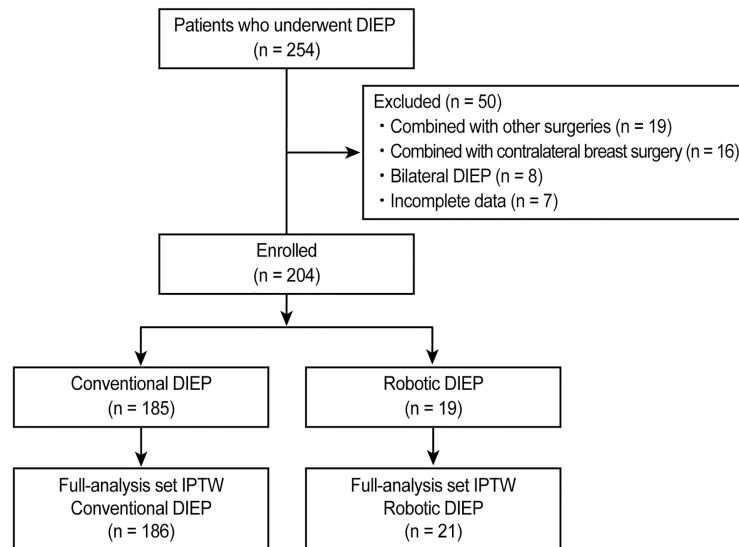


FIGURE 1
CONSORT flow diagram of patient selection. DIEP, deep inferior epigastric perforator; IPTW, inverse probability of treatment weighting.

semilunaris to secure the working space. The port was then inserted directly through the fascia into the preperitoneal space. When using a single-port robotic system (da Vinci SP; Intuitive Surgical, Sunnyvale, CA), the single port penetrates the new umbilicus site and fascia (Figure 2). The operation table was placed in the Trendelenburg position to avoid collision with the

patient's head or chest. Gas insufflation was maintained at 8 mmHg, and the robot was docked. Using the robot, the pedicle was dissected with ligation of all collateral vascular branches and divided near the origin (see Video, Supplemental Material 1, which shows the robotic dissection of the pedicle). After undocking the robot, the remaining attachments from the

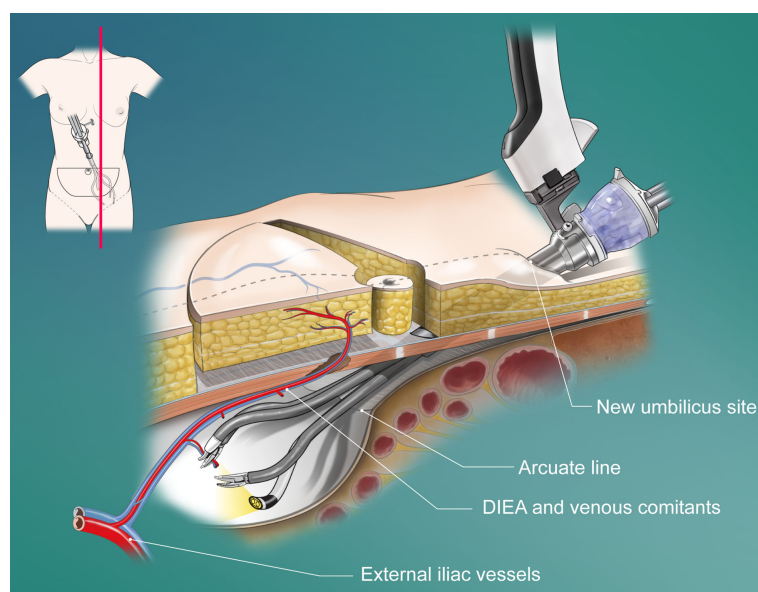


FIGURE 2
Schematic diagram of the penetrating placement of the single port in a robotic DIEP flap harvesting through a totally extraperitoneal approach. DIEA, deep inferior epigastric artery.

intramuscular portion were divided. Finally, the pedicle was delivered through a small fascial incision.

Postoperative pain management

Before the end of the surgery, all patients received 1 µg/kg fentanyl (Hana Pharm, Seoul, Korea) and 0.3 mg of ramosetron (Nasea; Astellas Pharma Korea, Seoul, Korea) to control postoperative pain and postoperative nausea and vomiting (PONV). All patients received an intravenous (IV) patient-controlled analgesia (PCA) device (Anapa plus; E-HWA Biomedics, Seoul, Korea), programmed to 2 mL/h for background infusion, a demand volume of 0.5 mL, and a lock-out interval of 15 min, with a total volume of 100 mL. The PCA regimen comprised fentanyl and 0.3 mg of ramosetron, which were mixed with normal saline to achieve a total volume of 100 mL (11).

Data regarding postoperative pain were obtained from an electronic medical database that was recorded by a PCA management team comprising two qualified nurses. All eligible patients were informed on how to rate their pain intensity using the numerical rating scale (NRS; 0, no pain; 10, worst pain possible) in the pre-anesthetic room (12), after which they were moved to the post-anesthetic care unit (PACU) and had emerged from anesthesia. The recovery nurses assessed their NRS scores. The patients were instructed about the use of the PCA device and encouraged to push the button whenever they experienced pain. In patients who experienced sustained pain with a resting NRS score of ≥ 4 , 50 µg IV fentanyl was administered as an additional rescue analgesic. After the patients were transferred to the admission room, postoperative NRS assessments were performed at 0–6, 6–24, and 24–48 h (11). In patients who suffered from prolonged pain with an NRS score of ≥ 4 in the admission room, 1 g IV paracetamol (Dai Han Pharm, Seoul, Korea), 30 mg ketorolac (Hana Pharm), 50 mg tridol (Yuhan. Co., Seoul, Korea), or 25 µg pethidine HCl (Jeil Pharm. Co. Ltd., Daegu, Korea) as an additional analgesic.

Data collection and outcomes

Demographic, clinical, and laboratory data were collected from the electronic medical records. Demographic data included age, body mass index (BMI), American Society of Anesthesiologists (ASA) physical status classification, comorbidities (hypertension and diabetes mellitus), smoking history, menopausal status, and neoadjuvant chemotherapy. Oncologic characteristics, such as tumor pathology and pathological stage, were also evaluated. Data on intraoperative characteristics, operation times, blood loss, red blood cell transfusion, type of mastectomy, lymph node procedure, and specimen weight were collected. Postoperative variables, including drainage amount, laboratory values, length of hospital

stay, postoperative adjuvant therapy, postoperative complications, postoperative pain, rescue analgesics, and PONV, were evaluated. Postoperative complications included hematoma, flap loss, infection, donor site wound problem, seroma, fat necrosis, and abdominal hernia (11). Furthermore, patient-reported outcomes were assessed using the BREAST-Q questionnaire. Patients included in this cohort were asked to complete the BREAST-Q questionnaire using a paper survey when visiting an outpatient clinic at least 6 months after the completion of reconstruction. The authors assessed the following domains: satisfaction with breasts, psychosocial well-being, physical well-being of the chest and abdomen, and satisfaction with the abdomen. Scores on the BREAST-Q domains ranged from 0 to 100, with higher scores indicating higher levels of satisfaction or improved well-being.

Statistical analysis

Continuous variables were expressed as mean \pm standard deviation and compared using Student's *t*-test. Categorical variables are expressed as numbers (percentages) and compared using the chi-squared or Fisher's exact test, depending on the size of the cell frequencies. Since data were retrospectively collected, the inverse probability of treatment weighting (IPTW) method was applied to adjust for confounding factors, including age, BMI, ASA physical status classification, hypertension, diabetes mellitus, smoking history, menopause, and neoadjuvant therapy (13). Logistic regression was used to regress the group variable on these confounding variables to calculate propensity scores (PSs). The goodness-of-fit of this logistic regression model was evaluated using the Hosmer–Lemeshow test ($P=0.896$). Moreover, 1/PS and 1/(1-PS) were weighed in the treatment and control groups, respectively. We stabilized and trimmed the weights to minimize the influence of extreme weights (14). To analyze the inverse probability of treatment-weighted data, we performed a *t*-test with the R command `svyttest` for continuous variables and the Rao-Scott Chi-square test for categorical variables with R command `svychisq` in the R package `survey` (the R Foundation). Statistical analysis was conducted using R version 4.0.4 (R Environment). Statistical significance was set at $P < 0.05$.

Ethics

This study was performed in a single-center university hospital following approval from the Institutional Review Board (IRB) and the Hospital Research Ethics Committee of Severance Hospital, Yonsei University Health System, Seoul, Korea (IRB number: 4-2020-1397) and following the ethical standards of the current version of the Declaration of Helsinki. The need for prior consent was waived because of the retrospective nature of the anonymous data.

Results

The patients' demographic characteristics are demonstrated in Table 1. After applying the IPTW method, a dataset with 207 patients was formed, including 21 patients in the robotic DIEP group and 186 patients in the conventional DIEP group. No significant differences were noted in demographic characteristics before and after IPTW adjustment.

A comparison of crude and IPTW-adjusted operative variables is presented in Table 2. The mean reconstruction time was significantly longer in the robotic DIEP group than in the conventional DIEP group (both $P < 0.001$). The number of patients who underwent nipple-sparing mastectomy was significantly higher in the robotic DIEP group than in the conventional DIEP group. The specimen weights were not

significantly different between the two groups. In addition, there were no differences in blood loss, patients transfused during surgery, lymph node procedure, or specimen weight between the two groups.

In the 19 robotic surgeries, the mean intramuscular course of the pedicle was 4.1 cm, and the mean fascial incision length around the pedicle was 4.3 cm. The mean robot console time was 68.8 min. There was one case of open conversion in which the pedicle was ligated because the main pedicle was misrecognized as a side branch during the robotic surgery, and the pedicle on the opposite side was used. No peritoneal perforation or uncontrolled bleeding was observed.

The postoperative clinical and laboratory variables of the two groups are presented in Table 3. There was a significant difference in the amount of drainage from the donor site on postoperative day 0

TABLE 1 Demographic characteristics by using Inverse Probability of Treatment Weighting.

| Variables | Before IPTW | | | After IPTW * | | |
|--------------------------|--------------------------------|--------------------------|---------|--------------------------------|--------------------------|---------|
| | Conventional DIEP (N = 185) | Robotic DIEP (N = 19) | P-value | Conventional DIEP (N = 186) | Robotic DIEP (N = 21) | P-value |
| Age, year | 48.6 ± 7.9 | 47.8 ± 5.7 | 0.663 | 48.5 ± 7.8 | 48.5 ± 6.6 | 0.998 |
| BMI, kg/m ² | 24.0 ± 3.1 | 23.6 ± 3.5 | 0.631 | 23.9 ± 3.0 | 23.9 ± 3.6 | 0.942 |
| ASA physical status | | | >.999 | | | 0.710 |
| I | 113 (61) | 12 (63) | | 114 (61) | 13 (63) | |
| II | 65 (35) | 7 (37) | | 66 (35) | 8 (37) | |
| III | 7 (4) | 0 (0) | | 6 (3) | 0 (0) | |
| Co-morbidities | | | | | | |
| Hypertension | 22 (12) | 1 (5) | 0.702 | 21 (11) | 2 (7) | 0.639 |
| Diabetes | 10 (5) | 0 (0) | 0.603 | 9 (5) | 0 (0) | 0.295 |
| Smoking history | | | >.999 | | | 0.672 |
| Non-smoker | 178 (96) | 19 (100) | | 179 (97) | 21 (100) | |
| Ex-smoker | 4 (2) | 0 (0) | | 4 (2) | 0 (0) | |
| Current smoker | 3 (2) | 0 (0) | | 3 (2) | 0 (0) | |
| Postmenopausal status | 46 (25) | 2 (11) | 0.255 | 44 (24) | 4 (20) | 0.768 |
| Neoadjuvant chemotherapy | 30 (16) | 4 (21) | 0.530 | 31 (17) | 3 (15) | 0.807 |
| Tumor pathology | | | 0.939 | | | 0.962 |
| DCIS | 53 (29) | 6 (32) | | 52 (28) | 5 (25) | |
| IDC | 110 (60) | 11 (58) | | 111 (60) | 13 (62) | |
| Infiltrative other | 22 (12) | 2 (11) | | 22 (12) | 3 (12) | |
| Stage | | | 0.715 | | | 0.560 |
| 0 | 51 (28) | 7 (37) | | 51 (27) | 6 (28) | |
| 1 | 71 (38) | 8 (42) | | 71 (39) | 11 (51) | |
| 2 | 56 (30) | 4 (21) | | 57 (30) | 4 (20) | |
| 3 | 7 (4) | 0 (0) | | 7 (4) | 0 (0) | |

Values are mean ± standard deviation or number (%) of patients.

DIEP, deep inferior epigastric artery perforator; ASA, American Society of Anesthesiologists; BMI, body mass index; CEA, carcinoembryonic antigen; CA 15-3, cancer antigen 15-3; DCIS, ductal carcinoma in situ; IDC, invasive ductal carcinoma; IPTW, Inverse Probability of Treatment Weighting.

*Counts in the weighted data may not sum to expected totals owing to rounding. Percentage may not total 100 because of rounding, and disagreements between numbers and percentages in the weighted data are the result of rounding of non-integer number value.

TABLE 2 Operative variables .

| Variables | Before IPTW | | | After IPTW | | |
|-------------------------------|--------------------------------|----------------------|---------|--------------------------------|--------------------------|---------|
| | Conventional DIEP (N = 185) | Robotic DIEP(N = 19) | P-value | Conventional DIEP (N = 186) | Robotic DIEP (N = 21) | P-value |
| Reconstruction time, min | 438 ± 83 | 507 ± 72 | <.001* | 438 ± 84 | 509 ± 71 | <.001* |
| Blood loss, mL/hr | 0.2 ± 0.2 | 0.3 ± 0.2 | 0.290 | 0.2 ± 0.2 | 0.3 ± 0.2 | 0.779 |
| Intraoperative transfusion, n | 13 (7) | 2 (11) | 0.636 | 13 (7) | 2 (7) | 0.986 |
| Type of mastectomy | | | 0.002* | | | 0.006* |
| Nipple sparing | 91 (49) | 17 (90) | | 92 (49) | 18 (87) | |
| Skin sparing | 94 (51) | 2 (10) | | 94 (51) | 3 (13) | |
| Lymph node procedure | | | | | | |
| SLNB then ALND | 56 (30) | 4 (21) | 0.565 | 57 (31) | 4 (20) | 0.364 |
| Specimen weight, g | 548 ± 214 | 494 ± 181 | 0.291 | 546 ± 214 | 507 ± 177 | 0.361 |

Values are mean ± standard deviation or number (%) of patients. *P < 0.05.

DIEP, deep inferior epigastric artery perforator; RBC, red blood cell; SLNB, sentinel lymph node biopsy; ALND, axillary lymph node dissection; IPTW, Inverse Probability of Treatment Weighting.

(conventional group, 68 ± 29 mL vs. robot group, 55 ± 26 mL; P=0.031 after IPTW). Patients in the robotic DIEP group showed significantly lower white blood cell (WBC) count and neutrophil count on postoperative day 0 than those in the conventional DIEP group; however, no group difference in WBCs was observed after IPTW adjustment. Patients in the robotic DIEP group showed a significantly shorter postoperative hospital stay than those in the conventional DIEP group (7.92 ± 1.20 days vs. 8.77 ± 1.74 days, respectively; P=0.002 after IPTW). Other variables, including the complication rate, were comparable between the two groups.

Figure 3 illustrates the postoperative pain intensity in the two groups. The pain intensity at 0–6 h was the highest during the 48-h postoperative period. The pain intensity 6–24 h after surgery in the robotic DIEP group was significantly lower than that in the conventional DIEP group (2.3 ± 0.9 vs 3.1 ± 1.1, respectively; P=0.001), although a significantly lower dose of fentanyl in the PCA device was used in the robotic DIEP group. Furthermore, there were no differences between groups in the number of patients receiving other rescue analgesics, including paracetamol, ketorolac, and pethidine HCl, except for the number of patients receiving tridol during the 6–24 h postoperative period; no patients in the robotic DIEP group received tridol during the 6–24 h postoperative period, while about 20% of patients in the conventional DIEP group did (Table 4). There were no differences in the incidence or number of patients receiving antiemetics between groups.

In this cohort, 75 women (16 in the robotic DIEP group, 59 in the conventional DIEP group) completed the BREAST-Q. Patients in the robotic DIEP group had significantly higher scores for postoperative psychosocial well-being (77.7 ± 19.5 vs. 64.4 ± 16.1; P=0.007), physical well-being of the chest (73.9 ± 12.8 vs. 65.8 ± 12.9; P=0.028), and physical well-being of the

abdomen (79.8 ± 13.6 vs. 71.4 ± 12.2; P=0.020) compared to those in the conventional DIEP group. There were no significant differences in the scores for satisfaction with the breasts and abdomen (Supplementary Material 2).

Discussion

Among the various breast reconstruction techniques, the DIEP flap is known as one of the most advanced procedures because the abdominal rectus muscle areas are not harvested and thus has the advantage of minimizing morbidities in the donor site areas, which leads to an increased level of satisfaction (1–3, 15, 16). However, during DIEP flap elevation, anterior rectus fascia, rectus muscle, and motor nerve violations can potentially occur (7, 17). To overcome this problem, Hivelin et al. harvested a DIEP flap with a totally extraperitoneal approach using a laparoscope (9); Gunclapalli et al. (6) and Selber (7) reported the use of a transabdominal preperitoneal approach with a multiport robotic system. Subsequently, the study's senior author (DWL) introduced a robotic DIEP flap harvest through a totally extraperitoneal approach with a single-port robotic system (8). Although a totally extraperitoneal approach is less invasive compared to the transabdominal preperitoneal approach that penetrates the peritoneum, it has a steep learning curve owing to the narrow preperitoneal space. He indicated that a single-port robot optimized for narrow surgical spaces permits DIEP flap harvesting using a totally extraperitoneal approach. In recent years, reports of minimally invasive procedures for the methodological part of robotic DIEP flaps for breast reconstruction have increased, while reports of postoperative prognosis are still lacking.

TABLE 3 Postoperative variables and laboratory values.

| Variables | Before IPTW | | | After IPTW | | |
|---|--------------------------------|--------------------------|---------|--------------------------------|--------------------------|---------|
| | Conventional DIEP (N = 185) | Robotic DIEP (N = 19) | P-value | Conventional DIEP (N = 186) | Robotic DIEP (N = 21) | P-value |
| Drainage amounts from the donor site, mL | | | | | | |
| POD 0 | 68 ± 29 | 58 ± 29 | 0.147 | 68 ± 29 | 55 ± 26 | 0.031* |
| POD 1 | 93 ± 29 | 95 ± 34 | 0.801 | 93 ± 29 | 93 ± 36 | 0.961 |
| POD 2 | 81 ± 39 | 87 ± 31 | 0.472 | 81 ± 38 | 82 ± 30 | 0.832 |
| Patients who received RBC transfusion, n | | | | | | |
| POD 0 | 9 (5) | 3 (16) | 0.088 | 9 (5) | 2 (11) | 0.215 |
| POD 1 | 7 (4) | 1 (5) | 0.549 | 7 (4) | 1 (4) | 0.940 |
| POD 2 | 2 (1) | 0 (0) | >.999 | 2 (1) | 0 (0) | 0.635 |
| White blood cell count, 10 ³ /μL | | | | | | |
| Preoperative | 5.8 ± 1.8 | 6.0 ± 1.9 | 0.657 | 5.8 ± 1.8 | 6.1 ± 1.8 | 0.519 |
| POD 0 | 12.0 ± 2.8 | 10.4 ± 2.9 | 0.033* | 12.0 ± 2.8 | 10.7 ± 2.6 | 0.061 |
| POD 1 | 10.2 ± 3.0 | 9.3 ± 2.0 | 0.274 | 10.2 ± 3.0 | 9.5 ± 1.7 | 0.145 |
| Neutrophil count, 10 ³ /μL | | | | | | |
| Preoperative | 3.5 ± 1.5 | 3.7 ± 1.8 | 0.610 | 3.5 ± 1.5 | 3.7 ± 1.6 | 0.582 |
| POD 0 | 10.0 ± 2.6 | 8.4 ± 2.6 | 0.022* | 10.0 ± 2.6 | 8.5 ± 2.5 | 0.027* |
| POD 1 | 8.4 ± 2.6 | 7.6 ± 1.8 | 0.303 | 8.4 ± 2.6 | 7.8 ± 1.5 | 0.135 |
| Lymphocyte count, 10 ³ /μL | | | | | | |
| Preoperative | 1.8 ± 0.6 | 1.8 ± 0.6 | 0.891 | 1.8 ± 0.6 | 1.8 ± 0.6 | 0.706 |
| POD 0 | 1.2 ± 0.5 | 1.2 ± 0.5 | 0.725 | 1.2 ± 0.5 | 1.3 ± 0.5 | 0.548 |
| POD 1 | 1.0 ± 0.5 | 0.9 ± 0.3 | 0.437 | 1.0 ± 0.5 | 1.0 ± 0.4 | 0.676 |
| Neutrophil-lymphocyte ratio | | | | | | |
| Preoperative | 2.2 ± 1.2 | 2.2 ± 1.6 | 0.912 | 2.2 ± 1.2 | 2.1 ± 1.5 | 0.922 |
| POD 0 | 9.5 ± 4.8 | 8.6 ± 4.9 | 0.435 | 9.5 ± 4.7 | 7.9 ± 4.6 | 0.143 |
| POD 1 | 9.5 ± 5.2 | 8.8 ± 3.4 | 0.619 | 9.5 ± 5.2 | 8.7 ± 3.3 | 0.388 |
| Postop-hospital stay, day | 8.78 ± 1.74 | 7.95 ± 1.22 | 0.044* | 8.77 ± 1.74 | 7.92 ± 1.20 | 0.002* |
| Postoperative adjuvant treatment | | | | | | |
| Radiation therapy, n | 48 (26) | 4 (21) | 0.786 | 49 (27) | 4 (18) | 0.392 |
| Chemotherapy, n | 69 (37) | 5 (26) | 0.486 | 70 (38) | 6 (27) | 0.422 |
| Hormonal therapy, n | 121 (65) | 13 (68) | 0.992 | 122 (66) | 15 (72) | 0.605 |
| Postoperative complications | | | | | | |
| Flap loss | 4 (2.2) | 1 (5.3) | 0.399 | 4 (2.3) | 1 (3.8) | 0.640 |
| Fat necrosis | 3 (1.6) | 1 (5.3) | 0.326 | 3 (1.7) | 2 (9.4) | 0.085 |
| Donor-site hematoma | 2 (1.1) | 0 (0) | >.999 | 2 (1.1) | 0 (0) | 0.634 |
| Donor-site seroma | 2 (1.1) | 0 (0) | >.999 | 2 (1.1) | 0 (0) | 0.634 |
| Donor-site wound problem | 12 (6.5) | 0 (0) | 0.608 | 12 (6.3) | 0 (0) | 0.244 |
| Abdominal hernia | 0 (0) | 0 (0) | - | 0 (0) | 0 (0) | - |

Values are mean ± standard deviation or number (%) of patients. *P < 0.05.

DIEP, deep inferior epigastric artery perforator; Postop, postoperative; POD, postoperative day; RBC, red blood cell; IPTW, Inverse Probability of Treatment Weighting.

There has been an increased focus in studies examining the enhanced recovery after surgery for patients with breast cancer after breast reconstruction (18–20). Since the development and implementation of early postoperative recovery in gastrointestinal surgery has been shown to improve perioperative outcomes and decrease the length of hospitalization, such protocols have been

extended to patients with a wide variety of surgical diseases in an effort to enhance early postoperative recovery (21). Postoperative length of stay is commonly employed as an outcome measure for early postoperative recovery and serves as an indicator of functional recovery and return to normal activity, which is the ultimate aim of early postoperative recovery (18). Meanwhile, the

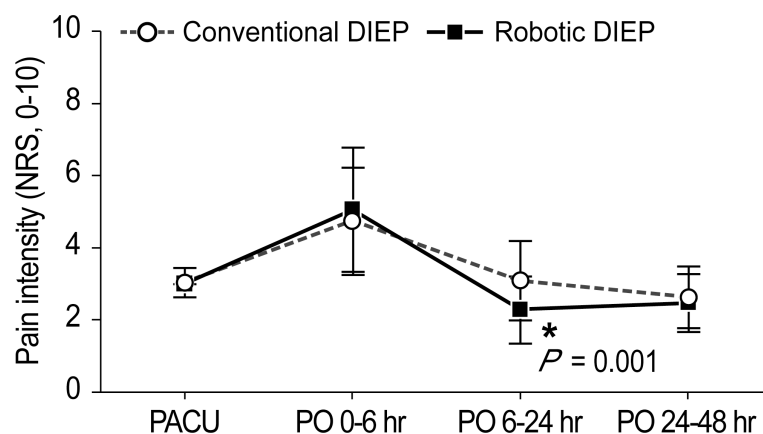


FIGURE 3

Pain intensity during the 48-h postoperative period. DIEP, deep inferior epigastric perforator; PACU, post-anesthesia care unit; PO, postoperative; NRS, numeric rating scale.

absolute number of hospital days in the current study seems to be longer than that for microvascular breast reconstruction in the United States. According to Holoyda et al. (22), the mean length of hospital stay in the U.S. was 3.90 days in 2018. However, a direct comparison of hospital stays between two countries with different healthcare systems is not appropriate. In this study, postoperative hospital stay was significantly shorter in the robotic DIEP group than in the conventional DIEP group, which was consistent with the reports regarding robotic procedures in other types of surgery (23, 24). Flap-based reconstruction is one of the surgeries with the highest morbidities and longest hospital stays within the field of plastic and reconstructive surgery; in these fields, it is clinically significant that robotic DIEP can shorten the postoperative hospital stay by one day.

This study compared the effects of robotic DIEP flap breast reconstruction with those of conventional DIEP on postoperative pain intensity. There were no significant differences in postoperative NRS scores at 0–6 h; however, patients in the robotic DIEP group showed significantly lower NRS scores during the 6–24 h postoperative period (2.3 ± 0.9 vs. 3.1 ± 1.1 , respectively; $P=0.001$). The amount of fentanyl mixed in the PCA device was significantly lower in the robotic DIEP group (851 ± 195 μ g) than in the conventional DIEP group (1051 ± 490 μ g) ($P=0.003$). However, the morphine equivalent dose of fentanyl mixed with PCA in the conventional DIEP group was higher than that in previous studies (25, 26), which may be the reason why there was not much of a difference in NRS scores, despite the statistically significant differences in the dose of fentanyl. Furthermore, the fentanyl amounts in the PACU and other rescue analgesics in the admission room were comparable between the two groups, while a significant difference in the number of patients receiving tridol during the 6–24 h postoperative period was noted. Postoperative pain has been

reported to interfere with early postoperative recovery and cause chronic pain after surgery, which reduces physical activity and quality of life (27, 28). Such significant attenuation in NRS during the 6–24 h postoperative period may have contributed to shortening the postoperative hospital stay in robotic DIEP (29, 30).

Significant group differences were observed in operation time. The results showed that the duration of the robotic DIEP operation was significantly longer than that of the conventional DIEP procedure, which is consistent with the findings of other types of robotic surgery (11, 31, 32). This longer operative time is thought to be due to the additional time for preparation of the robot and a relatively longer robotic dissection time compared to conventional surgery (33). In the current study, the mean robot console time was 68.8 min and showed a decreasing pattern over time (data not shown). In addition to the longer operation time, another common drawback in the use of robotics is the cost (34). However, to claim that robotic surgery is expensive, a cost-effectiveness analysis is required. As robotic surgery becomes more popular, there have been discussions about the high cost of robotic surgery and its effectiveness. Although there is a report that states that robot-assisted radical prostatectomy has a higher cost compared to the open and laparoscopic approach, with relatively fewer health benefits (35), many studies predict that the high cost would be balanced by favorable clinical outcomes, such as a reduction in blood transfusion requirement, hospital stay, and perioperative complications (36–39). In addition, robotic thymectomy was associated with a lower total hospital cost than that with open surgery since it reduced the duration of intensive care unit and hospital stay (40). The increase in the number of robotic surgeries may lead to a significant reduction in the future operation time and better postoperative outcomes (41). The presence of more experienced professionals and

TABLE 4 Postoperative nausea and vomiting, and analgesics profile.

| Variables | Before IPTW | | | After IPTW | | |
|--|--------------------------------|--------------------------|---------|--------------------------------|--------------------------|---------|
| | Conventional DIEP (N = 185) | Robotic DIEP (N = 19) | P-value | Conventional DIEP (N = 186) | Robotic DIEP (N = 21) | P-value |
| Fentanyl amounts in PCA, μg | 1051 \pm 483 | 853 \pm 184 | 0.001* | 1051 \pm 490 | 851 \pm 195 | 0.003* |
| Additional fentanyl in PACU, μg | 13 \pm 23 | 20 \pm 28 | 0.211 | 13 \pm 23 | 16 \pm 26 | 0.614 |
| Patients receiving paracetamol | | | | | | |
| PO 0-6 hr | 7 (4) | 1 (5) | 0.549 | 7 (4) | 1 (5) | 0.829 |
| PO 6-24 hr | 46 (25) | 8 (42) | 0.177 | 46 (25) | 8 (38) | 0.246 |
| PO 24-48 hr | 52 (28) | 6 (32) | 0.958 | 52 (28) | 6 (30) | 0.880 |
| Patients receiving ketorolac | | | | | | |
| PO 0-6 hr | 179 (97) | 19 (100) | >.999 | 180 (97) | 21 (100) | 0.411 |
| PO 6-24 hr | 181 (98) | 19 (100) | >.999 | 182 (98) | 21 (100) | 0.500 |
| PO 24-48 hr | 166 (90) | 19 (100) | 0.227 | 167 (90) | 21 (100) | 0.135 |
| Patients receiving tridol | | | | | | |
| PO 0-6 hr | 1 (1) | 1 (5) | 0.178 | 1 (1) | 1 (3) | 0.170 |
| PO 6-24 hr | 40 (22) | 0 (0) | 0.028* | 40 (22) | 0 (0) | 0.023* |
| PO 24-48 hr | 30 (16) | 4 (21) | 0.530 | 30 (16) | 5 (24) | 0.447 |
| Patients receiving pethidine HCL | | | | | | |
| PO 0-6 hr | 1 (1) | 0 (0) | >.999 | 1 (1) | 0 (0) | 0.737 |
| PO 6-24 hr | 13 (7) | 0 (0) | 0.616 | 13 (7) | 0 (0) | 0.221 |
| PO 24-48 hr | 8 (4) | 0 (0) | >.999 | 8 (4) | 0 (0) | 0.341 |
| Patients who PONV were experienced | | | | | | |
| PACU | 31 (17) | 2 (11) | 0.745 | 31 (17) | 2 (9) | 0.338 |
| PO 0-6 hr | 107 (58) | 12 (63) | 0.839 | 108 (58) | 13 (61) | 0.824 |
| PO 6-24 hr | 87 (47) | 9 (47) | >.999 | 87 (47) | 10 (46) | 0.920 |
| PO 24-48 hr | 49 (27) | 6 (32) | 0.838 | 49 (27) | 7 (32) | 0.641 |
| Patients receiving antiemetics | | | | | | |
| PACU | 31 (17) | 2 (11) | 0.745 | 31 (17) | 2 (9) | 0.335 |
| PO 0-6 hr | 17 (9) | 2 (11) | 0.692 | 17 (9) | 3 (14) | 0.516 |
| PO 6-24 hr | 6 (3) | 0 (0) | >.999 | 6 (3) | 0 (0) | 0.409 |
| PO 24-48 hr | 5 (3) | 1 (5) | 0.448 | 5 (3) | 1 (4) | 0.786 |

Values are mean \pm SD or number (%) of patients. *P < 0.05.

DIEP, deep inferior epigastric artery perforator; PONV, postoperative nausea and vomiting; PACU, post-anesthesia care unit; PO, postoperative; PCA, patient controlled analgesia; IPTW, Inverse Probability of Treatment Weighting.

optimal teamwork have caused a reduction in the operation time and led to cost-effectiveness, with more experienced centers having lower costs (41–43).

This study had a few limitations. First, the data were retrospectively collected from a single center, primarily from Korean patients. It is difficult to generalize these results to patients from different ethnic backgrounds or those treated under different institutional conditions. Second, the sample size was small, especially in patients who underwent robotic DIEP surgery, which may have contributed to the higher incidence of postoperative complications in the conventional DIEP group without a statistically significant difference. Therefore, to add clinical significance to the existing literature,

further large-scale prospective controlled trials are required, especially with a greater number of samples of robotic DIEP surgery. However, this study provides evidence for future prospective trials in terms of reconstruction outcomes, such as donor site morbidity, enhanced recovery after surgery, and functional restoration at the donor site.

In conclusion, this is the first study to compare the effects of robotic DIEP flap breast reconstruction with those of conventional DIEP reconstruction on the postoperative clinical outcomes. We demonstrated that robotic DIEP flap breast reconstruction offers enhanced postoperative recovery, which was accompanied by attenuated pain intensity and reduced postoperative hospital stay. Furthermore, a significantly

superior abdominal physical well-being score on patient-reported outcomes was noted in patients who underwent robotic DIEP flap breast reconstruction.

Data availability statement

The original contributions presented in the study are included in the article/Supplementary Material. Further inquiries can be directed to the corresponding authors.

Ethics statement

The studies involving human participants were reviewed and approved by Institutional Review Board and the Hospital Research Ethics Committee of Severance Hospital, Yonsei University Health System, Seoul, Korea. Written informed consent for participation was not required for this study in accordance with the national legislation and the institutional requirements.

Author contributions

ML and JW, designed this project, data collection, processing, and manuscript writing. SS, HP, and JK, data collection, and review. HS and YK, data analysis, and

processing. DL and NK, designed this project, interpretation, manuscript writing, review and editing. All authors contributed to the article and approved the submitted version.

Conflict of interest

The authors declare that the research was conducted in the absence of any commercial or financial relationships that could be construed as a potential conflict of interest.

Publisher's note

All claims expressed in this article are solely those of the authors and do not necessarily represent those of their affiliated organizations, or those of the publisher, the editors and the reviewers. Any product that may be evaluated in this article, or claim that may be made by its manufacturer, is not guaranteed or endorsed by the publisher.

Supplementary material

The Supplementary Material for this article can be found online at: <https://www.frontiersin.org/articles/10.3389/fonc.2022.989231/full#supplementary-material>

References

- Gill PS, Hunt JP, Guerra AB, Dellacroce FJ, Sullivan SK, Boraski J, et al. A 10-year retrospective review of 758 DIEP flaps for breast reconstruction. *Plast Reconstr Surg* (2004) 113(4):1153–60. doi: 10.1097/01.prs.0000110328.47206.50
- Ireton JE, Lakhiani C, Saint-Cyr M. Vascular anatomy of the deep inferior epigastric artery perforator flap: a systematic review. *Plast Reconstr Surg* (2014) 134(5):810e–21e. doi: 10.1097/prs.0000000000000625
- Selber JC, Nelson J, Fosnot J, Goldstein J, Bergey M, Sonnad SS, et al. A prospective study comparing the functional impact of SIEA, DIEP, and muscle-sparing free TRAM flaps on the abdominal wall: part i. unilateral reconstruction. *Plast Reconstr Surg* (2010) 126(4):1142–53. doi: 10.1097/PRS.0b013e3181f02520
- Koshima I, Soeda S. Inferior epigastric artery skin flaps without rectus abdominis muscle. *Br J Plast Surg* (1989) 42(6):645–8. doi: 10.1016/0007-1226(89)90075-1
- Allen RJ, Treece P. Deep inferior epigastric perforator flap for breast reconstruction. *Ann Plast Surg* (1994) 32(1):32–8. doi: 10.1097/0000637-199401000-00007
- Gundlapalli VS, Ogunleye AA, Scott K, Wenzinger E, Ulm JP, Tavana L, et al. Robotic-assisted deep inferior epigastric artery perforator flap abdominal harvest for breast reconstruction: A case report. *Microsurgery* (2018) 38(6):702–5. doi: 10.1002/micr.30297
- Selber JC. The robotic DIEP flap. *Plast Reconstr Surg* (2020) 145(2):340–3. doi: 10.1097/prs.00000000000006529
- Choi JH, Song SY, Park HS, Kim CH, Kim JY, Lew DH, et al. Robotic DIEP flap harvest through a totally extraperitoneal approach using a single-port surgical robotic system. *Plast Reconstr Surg* (2021) 148(2):304–7. doi: 10.1097/prs.00000000000008181
- Hivelin M, Soprani A, Schaffer N, Hans S, Lantieri L. Minimally invasive laparoscopically dissected deep inferior epigastric artery perforator flap: An anatomical feasibility study and a first clinical case. *Plast Reconstr Surg* (2018) 141(1):33–9. doi: 10.1097/prs.00000000000003989
- Shakir S, Spencer AB, Kozak GM, Nathan SL, Soriano IS, Kanchwala SK. Laparoscopically assisted DIEP flap harvest minimizes fascial incision in autologous breast reconstruction. *Plast Reconstr Surg* (2020) 146(3):265e–75e. doi: 10.1097/prs.00000000000007048
- Moon J, Lee J, Lee DW, Lee HS, Nam DJ, Kim MJ, et al. Postoperative pain assessment of robotic nipple-sparing mastectomy with immediate prepectoral prosthesis breast reconstruction: a comparison with conventional nipple-sparing mastectomy. *Int J Med Sci* (2021) 18(11):2409–16. doi: 10.7150/ijms.56997
- Williamson A, Hoggart B. Pain: a review of three commonly used pain rating scales. *J Clin Nurs* (2005) 14(7):798–804. doi: 10.1111/j.1365-2702.2005.01121.x
- Austin PC. An introduction to propensity score methods for reducing the effects of confounding in observational studies. *Multivariate Behav Res* (2011) 46(3):399–424. doi: 10.1080/00273171.2011.568786
- Harder VS, Stuart EA, Anthony JC. Propensity score techniques and the assessment of measured covariate balance to test causal associations in psychological research. *Psychol Methods* (2010) 15(3):234–49. doi: 10.1037/a0019623
- Chang EI, Chang EI, Soto-Miranda MA, Zhang H, Nosrati N, Robb GL, et al. Comprehensive analysis of donor-site morbidity in abdominally based free flap breast reconstruction. *Plast Reconstr Surg* (2013) 132(6):1383–91. doi: 10.1097/PRS.0b013e3182a805a3
- Damen TH, Timman R, Kunst EH, Gopie JP, Bresser PJ, Seynaeve C, et al. High satisfaction rates in women after DIEP flap breast reconstruction. *J Plast Reconstr Aesthet Surg* (2010) 63(1):93–100. doi: 10.1016/j.bjps.2008.08.019
- DellaCrocce FJ, DellaCrocce HC, Blum CA, Sullivan SK, Trahan CG, Wise MW, et al. Myth-busting the DIEP flap and an introduction to the abdominal

- perforator exchange (APEX) breast reconstruction technique: A single-surgeon retrospective review. *Plast Reconstr Surg* (2019) 143(4):992–1008. doi: 10.1097/prs.0000000000005484
18. Tan YY, Liaw F, Warner R, Myers S, Ghanem A. Enhanced recovery pathways for flap-based reconstruction: Systematic review and meta-analysis. *Aesthetic Plast Surg* (2021) 45(5):2096–115. doi: 10.1007/s00266-021-02233-3
19. Fan KL, Luvisa K, Black CK, Wirth P, Nigam M, Camden R, et al. Gabapentin decreases narcotic usage: Enhanced recovery after surgery pathway in free autologous breast reconstruction. *Plast Reconstr Surg Glob Open* (2019) 7(8):e2350. doi: 10.1097/gox.0000000000002350
20. Batdorf NJ, Lemaine V, Lovely JK, Ballman KV, Goede WJ, Martinez-Jorge J, et al. Enhanced recovery after surgery in microvascular breast reconstruction. *J Plast Reconstr Aesthet Surg* (2015) 68(3):395–402. doi: 10.1016/j.bjps.2014.11.014
21. Nicholson A, Lowe MC, Parker J, Lewis SR, Alderson P, Smith AF. Systematic review and meta-analysis of enhanced recovery programmes in surgical patients. *Br J Surg* (2014) 101(3):172–88. doi: 10.1002/bjs.9394
22. Holoyda KA, Magno-Padron DA, Carter GC, Agarwal JP, Kwok AC. National trends in length of stay for microvascular breast reconstruction: An evaluation of 10,465 cases using the American college of surgeons national surgical quality improvement program database. *Plast Reconstr Surg* (2022) 149(2):306–13. doi: 10.1097/prs.00000000000008706
23. Ma J, Li X, Zhao S, Wang J, Zhang W, Sun G. Robot-assisted thoracic surgery versus video-assisted thoracic surgery for lung lobectomy or segmentectomy in patients with non-small cell lung cancer: a meta-analysis. *BMC Cancer* (2021) 21(1):498. doi: 10.1186/s12885-021-08241-5
24. Crocero F, Carbonara U, Cantello F, Marchioni M, Dittono P, Mir MC, et al. Robot-assisted radical nephrectomy: A systematic review and meta-analysis of comparative studies. *Eur Urol* (2021) 80(4):428–39. doi: 10.1016/j.eururo.2020.10.034
25. Bar-Meir ED, Yueh JH, Hess PE, Hartmann CE, Maia M, Tobias AM, et al. Postoperative pain management in DIEP flap breast reconstruction: Identification of patients with poor pain control. *Eplasty* (2010) 10:e59.
26. Azizi AA, Mohan AT, Tomouk T, Brickley EB, Malata CM. Does surgical procedure type impact postoperative pain and recovery in deep inferior epigastric artery perforator flap breast reconstruction? *Arch Plast Surg* (2020) 47(4):324–32. doi: 10.5999/aps.2019.01417
27. Andersen KG, Kehlet H. Persistent pain after breast cancer treatment: a critical review of risk factors and strategies for prevention. *J Pain* (2011) 12(7):725–46. doi: 10.1016/j.jpain.2010.12.005
28. Andersen KG, Duriaud HM, Jensen HE, Kroman N, Kehlet H. Predictive factors for the development of persistent pain after breast cancer surgery. *Pain* (2015) 156(12):2413–22. doi: 10.1097/j.pain.0000000000000298
29. Walker CT, Gullotti DM, Prendergast V, Radosevich J, Grimm D, Cole TS, et al. Implementation of a standardized multimodal postoperative analgesia protocol improves pain control, reduces opioid consumption, and shortens length of hospital stay after posterior lumbar spinal fusion. *Neurosurgery* (2020) 87(1):130–6. doi: 10.1093/neuros/nyz312
30. Shaffer EE, Pham A, Woldman RL, Spiegelman A, Strassels SA, Wan GJ, et al. Estimating the effect of intravenous acetaminophen for postoperative pain management on length of stay and inpatient hospital costs. *Adv Ther* (2017) 33(12):2211–28. doi: 10.1007/s12325-016-0438-y
31. Park HS, Lee J, Lee DW, Song SY, Lew DH, Kim SI, et al. Robot-assisted nipple-sparing mastectomy with immediate breast reconstruction: An initial experience. *Sci Rep* (2019) 9(1):15669. doi: 10.1038/s41598-019-51744-2
32. Lai HW, Chen ST, Mok CW, Lin YJ, Wu HK, Lin SL, et al. Robotic versus conventional nipple sparing mastectomy and immediate gel implant breast reconstruction in the management of breast cancer- a case control comparison study with analysis of clinical outcome, medical cost, and patient-reported cosmetic results. *J Plast Reconstr Aesthet Surg* (2020) 73(8):1514–25. doi: 10.1016/j.bjps.2020.02.021
33. Winocour S, Tarassoli S, Chu CK, Liu J, Clemens MW, Selber JC. Comparing outcomes of robotically assisted latissimus dorsi harvest to the traditional open approach in breast reconstruction. *Plast Reconstr Surg* (2020) 146(6):1221–5. doi: 10.1097/prs.00000000000007368
34. Manrique OJ, Bustos SS, Mohan AT, Nguyen MD, Martinez-Jorge J, Forte AJ, et al. Robotic-assisted DIEP flap harvest for autologous breast reconstruction: A comparative feasibility study on a cadaveric model. *J Reconstr Microsurg* (2020) 36(5):362–8. doi: 10.1055/s-0040-1701666
35. Health Quality Ontario. Robotic Surgical System for Radical Prostatectomy: A Health Technology Assessment. *Ont Health Technol Assess Ser* (2017) 17(11):1–172.
36. Hemli JM, Patel NC. Robotic cardiac surgery. *Surg Clin North Am* (2020) 100(2):219–36. doi: 10.1016/j.suc.2019.12.005
37. Caba Molina D, Lamberton F, Arrangoiz Majul R. Trends in robotic pancreaticoduodenectomy and distal pancreatectomy. *J Laparoendosc Adv Surg Tech A* (2019) 29(2):147–51. doi: 10.1089/lap.2018.0421
38. Tewari A, Sooriakumaran P, Bloch DA, Seshadri-Kreaden U, Hebert AE, Wiklund P. Positive surgical margin and perioperative complication rates of primary surgical treatments for prostate cancer: a systematic review and meta-analysis comparing retropubic, laparoscopic, and robotic prostatectomy. *Eur Urol* (2012) 62(1):1–15. doi: 10.1016/j.eururo.2012.02.029
39. Rodrigues Martins YM, Romanelli de Castro P, Drummond Lage AP, Alves Wainstein AJ, de Vasconcellos Santos FA. Robotic surgery costs: Revealing the real villains. *Int J Med Robot* (2021) 17(6):e2311. doi: 10.1002/rcs.2311
40. Imielski B, Kurihara C, Manerikar A, Chaudhary S, Koterski S, Odell D, et al. Comparative effectiveness and cost-efficiency of surgical approaches for thymectomy. *Surgery* (2020) 168(4):737–42. doi: 10.1016/j.surg.2020.04.037
41. Leow JJ, Chang SL, Meyer CP, Wang Y, Hanske J, Sammon JD, et al. Robot-assisted versus open radical prostatectomy: A contemporary analysis of an all-payer discharge database. *Eur Urol* (2016) 70(5):837–45. doi: 10.1016/j.eururo.2016.01.044
42. Forsmark A, Gehrman J, Angenete E, Bjartell A, Björholt I, Carlsson S, et al. Health economic analysis of open and robot-assisted laparoscopic surgery for prostate cancer within the prospective multicentre LAPPRO trial. *Eur Urol* (2018) 74(6):816–24. doi: 10.1016/j.eururo.2018.07.038
43. Budäus L, Abdollah F, Sun M, Johal R, Morgan M, Thuret R, et al. The impact of surgical experience on total hospital charges for minimally invasive prostatectomy: a population-based study. *BJU Int* (2011) 108(6):888–93. doi: 10.1111/j.1464-410X.2010.09906.x



OPEN ACCESS

EDITED BY

Gianluca Franceschini,
Agostino Gemelli University Polyclinic
(IRCCS), Italy

REVIEWED BY

Vladimir Jurisic,
University of Kragujevac, Serbia
Kengo Ito,
Tohoku Medical and Pharmaceutical
University, Japan

*CORRESPONDENCE

Heli Zhong
zhongheli@tom.com
Ying Piao
gloriapiao@163.com

SPECIALTY SECTION

This article was submitted to
Breast Cancer,
a section of the journal
Frontiers in Oncology

RECEIVED 08 July 2022

ACCEPTED 14 September 2022

PUBLISHED 03 October 2022

CITATION

Chen H, Piao Y, Yang D, Kuang P, Li Z,
Liao G and Zhong H (2022) The effect
of respiratory capacity for dose
sparing in left-sided breast cancer
irradiation with active breathing
coordinator technique.
Front. Oncol. 12:989220.
doi: 10.3389/fonc.2022.989220

COPYRIGHT

© 2022 Chen, Piao, Yang, Kuang, Li,
Liao and Zhong. This is an open-access
article distributed under the terms of
the [Creative Commons Attribution
License \(CC BY\)](https://creativecommons.org/licenses/by/4.0/). The use, distribution
or reproduction in other forums is
permitted, provided the original
author(s) and the copyright owner(s)
are credited and that the original
publication in this journal is cited, in
accordance with accepted academic
practice. No use, distribution or
reproduction is permitted which does
not comply with these terms.

The effect of respiratory capacity for dose sparing in left-sided breast cancer irradiation with active breathing coordinator technique

Hongtao Chen, Ying Piao*, Dong Yang, Peipei Kuang,
Zihuang Li, Guixiang Liao and Heli Zhong*

Department of Radiation Oncology, Shenzhen People's Hospital, the Second Clinical Medical College, Jinan University, Shenzhen, China

Background and aim: A subsequent cardiac toxicity is deemed to be dose-dependent for left-sided breast cancer irradiation. This study aims to demonstrate the effect of respiratory capacity for dose sparing when the deep inspiration breath hold with Active Breathing Coordinator technique (ABC-DIBH) is used in left-sided breast cancer irradiation.

Methods: 74 left-sided breast cancer patients, who received whole breast or post-mastectomy chest wall radiotherapy with ABC-DIBH between 2020 and 2021 in our center, were retrospectively reviewed in this study. CT scans of free breath (FB) and ABC-DIBH were done for each patient, and two treatment plans with a prescription dose of 5000 cGy/25 Fr were designed separately. The dose to heart, left anterior descending artery (LAD) and lungs was compared between FB and ABC-DIBH. The correlation between individual parameters (dose to organs at risk (OARs) and minimum heart distance (MHD)) was analyzed, and the effect of respiratory capacity for dose sparing was assessed.

Results: The plans with ABC-DIBH achieved lower Dmean for heart (34.80%, $P < 0.01$) and LAD (29.33%, $P < 0.01$) than those with FB. Regression analysis revealed that both Dmean and D2 of heart were negatively correlated with MHD in the plans with FB and ABC-DIBH, which decreased with the increase in MHD by 37.8 cGy and 309.9 cGy per 1mm, respectively. Besides, a lower Dmean of heart was related to a larger volume of ipsilateral lung in plans with FB. With the increase in volume of ipsilateral lung, the linear correlation was getting weaker and weaker until the volume of ipsilateral lung reached 1700 cc. Meanwhile, a negative linear correlation between Dmean of LAD and MHD in plans with FB and ABC-DIBH was observed, whose slope was 162.5 and 135.9 cGy/mm, respectively. Furthermore, when the respiratory capacity of ABC-DIBH reached 1L, and the relative ratio (ABC-DIBH/FB) reached 3.6, patients could obtain the benefit of dose sparing. The larger difference in respiratory

capacity had no significant effect in the larger difference of MHD, Dmean of heart and Dmean of LAD between FB and ABC-DIBH.

Conclusion: This study demonstrates the sufficiently good effect of ABC-DIBH when utilizing for cardiac sparing. It also reveals the correlations among individual parameters and the effect of respiratory capacity for dose sparing. This helps take optimal advantage of the ABC-DIBH technique and predict clinical benefits.

KEYWORDS

ABC, DIBH, radiotherapy, breast cancer, cardiac sparing

Introduction

Adjuvant radiotherapy is an important part of curative-intent treatment for patients after breast conservation surgery or mastectomy (1). Adjuvant radiotherapy contributes to a favorable prognosis and reduces the risk of local-regional recurrence compared to surgery alone (2–4). However, toxicities associated with radiotherapy compromise the quality of life post-treatment (5). Particularly, due to the tangential fields, large amounts of radiation dose may locate in the anterior part of the heart, including the left anterior descending (LAD) artery, which is one of the structures closest to PTV. Incidental radiation dose to the left ventricle and LAD results in an increased risk of ischemic heart disease for left-sided breast cancer patients (6–9). Although there is no clear dose threshold for radiation-induced cardiac complications, the excess risk of ischemic heart disease increases linearly with the mean heart dose, which is evident within four years after radiotherapy and even continues for decades (7, 10). The study based on 2168 women who underwent radiotherapy for breast cancer by Darby et al. found that the rate of coronary events increased linearly with the Dmean of heart by 7.4% per Gy (7).

Improvements in techniques of radiotherapy minimize the dose to heart and cardiac structures over the years, such as patient positioning methods (11), gating (12) and proton therapy (13). Respiratory management is regarded as another promising strategy applied in breast cancer radiotherapy (14–20). Accuracy of PTV dose delivery and protection of organs at risk (OARs) is adversely affected by respiratory motion. Deep inspiration breath hold with the Active Breathing Coordinator device (ABC-DIBH) can minimize breathing motion and consequently augments cardiac sparing in radiotherapy of breast cancer by increasing the distance between heart and PTV. In contrast to self-sustained breath hold (4.1% variability of lung volume), the ABC device was proved with better intra-session and inter-session reproducibility of respiratory capacity

(1.8% and 3% variability of lung volume) on account of the function that induced breath hold automatically at a preset inhaled or exhaled air volume during a predetermined time (14, 15). Note that the ABC device utilizes the sensor to count the rotations of turbine impeller for a known respiratory capacity. Once the inhaled or exhaled air volume reaches the preset threshold, the balloon valve shuts off and stops airflow (Figure 1A).

In the ABC-DIBH feasibility study, Kunheri et al. demonstrated that the mean dose to the heart and LAD was reduced by 48.5% and 53.81% (ABC-DIBH VS. Free breath (FB)) (1). The study by Quirk et al. presented that the median heart dose and the median LAD dose in deep inspiration breath hold (DIBH) cohort are 10% lower than those of FB cohort (5). However, the samples of the two cohorts are different and without one-to-one correspondence. Eldredge-Hindy et al. showed that the median values of the relative and absolute reduction of mean heart dose were 62% and 1.7 Gy as use of the ABC-DIBH (21). The above studies have indicated that left-sided breast cancer patients benefited greatly from the ABC-DIBH technique, but there lacked consideration for individual parameters. More correlations among dose of OARs minimum heart distance (MHD), lung volume and inspiratory capacity are expected to reveal (22).

In this study, we have examined the individual parameters of dose and volume in left-sided breast cancer patients treated with adjuvant radiotherapy with FB or ABC-DIBH to demonstrate the advantages of respiratory management. Moreover, the novel objective was to characterize implicit correlations of individual parameters and assess the relationship between the dose of OARs and MHD. Despite the clear evidence of ABC-DIBH for reducing the dose to heart and LAD, the effect of respiratory capacity for dose sparing has remained unknown. This study quantified these correlations and effects that would help to take optimal advantage of the ABC-DIBH technique and predict clinical benefits.

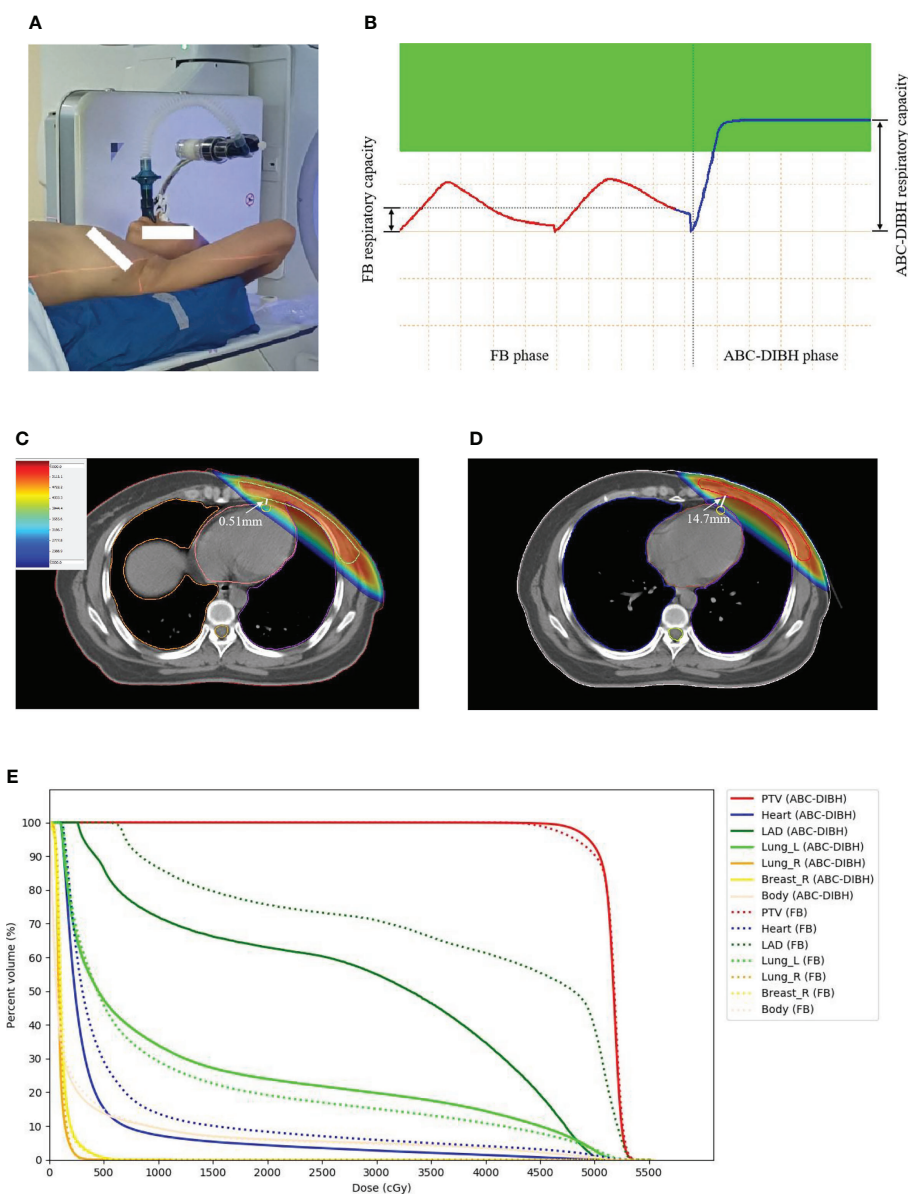


FIGURE 1

(A) ABC device applied in left-sided breast cancer radiotherapy. (B) FB and ABC-DIBH breathing curves. (C) Dose distribution on CT image in FB plan. (D) Dose distribution on CT image in ABC-DIBH plan. (E) DVH of structures in FB plan and ABC-DIBH plan.

Materials and methods

74 left-sided breast cancer patients were retrospectively reviewed in this study who received whole breast (41 patients) or post-mastectomy chest wall (33 patients) radiotherapy with ABC-DIBH technique between 2020 and 2021 in our center. The median age was 43 (27–64). Patient characteristics are shown in Table 1. These retrospective data were deidentified and approved by the ethics committee of our institute. For this retrospective study, formal consent was not required. Eligible patients were

required with no history of cardiac and lung diseases, no previous radiotherapy of the breast, and breath hold for 40 seconds at 80% of maximum deep inspiration. All of these patients underwent multiple simulations of thoracic breathing with the ABC device from Elekta before CT scan. The difference of position of mark point on the patient's body among multiple deep inspiration breath holds was less than 2mm (5, 23, 24). All patients were scanned and treated in a supine position with arms above the head. CT scans of FB and ABC-DIBH with a slice thickness of 2.5 mm were acquired for per patient successively.

TABLE 1 Patient characteristics.

| Characteristic | Patients |
|---------------------------|------------|
| Total patients | 74 |
| Age, median (range) | 43 (27–64) |
| Stages | |
| IA | 26 |
| IB | 1 |
| IIA | 17 |
| IIB | 16 |
| IIIA | 7 |
| IIIB | 1 |
| IIIC | 4 |
| IVA | 2 |
| Surgery | 73 |
| Breast conserving surgery | 40 |
| Implant | 5 |
| Chemotherapy | 52 |
| ER (+) | 53 |
| PR (+) | 51 |
| HER-2 amplification | 20 |

On each CT scan, OARs and PTV were contoured by the same qualified physician as per the Radiation Therapy Oncology Group breast contouring guidelines. Both treatment plans were done by the same and qualified physicist in the Monaco planning system. Monte Carlo algorithm was adopted in all plans. The clinical treatment plans were prescribed according to the condition of individuals and the discretion of physicians, which was 5000 cGy/25 Fr, 4320 cGy/16 Fr or 4050 cGy/15 Fr. To ensure consistency, all plans adopted an experimental prescription dose of 5000 cGy/25 Fr in the final analysis. 95% of the prescribed dose covered at least 95% of the PTV volume while the dose to OARs was minimized as much as possible. These patients with whole breast radiotherapy also received sequential tumor bed boost delivered by electron ray or X ray, which depended on the physician's consideration. Boost dose therefore was not included in the analysis.

For each patient, delineated structures volumes (i.e., PTV, lungs, heart) were documented for both CT scans, and dose

volume histograms (DVHs) were generated for these structures in both treatment plans. For PTV, conformal index (CI) and homogeneity index (HI) were calculated to assess the dose coverage. For heart, D2, Dmean, V30, V20, V10 and V5 were recorded. For LAD, Dmax, Dmean, V40, V30 and V20 were recorded. For ipsilateral lung, Dmean, V20 and V5 were recorded. The minimum heart distance (MHD), defined as the minimum vertical distance from the posterior edge of PTV to the heart border, was measured to detect the variation of location between heart and PTV in both plans. Moreover, the respiratory capacity with ABC-DIBH for consistent breath-holds during CT scan was recorded for each patient (Figure 1B). The waveform of respiratory capacity with FB was similar to a sine wave. CT reconstruction of FB was performed on all respiratory phases. The end expiration of FB was set as the origin. The amplitude of free breathing curve was considered as respiratory capacity with FB (Figure 1B).

SPSS 20.0 software was used for statistical analysis. The calculated data was expressed as mean and standard deviation. The paired t-test was adopted to analyze these statistic variables. $P < 0.05$ was considered as a statistically significant difference. Additionally, regression analysis was performed to search for correlations between these parameters. The Pearson test (r) and Spearman test (ρ) were adopted to assess the correlation between MHD and dose to heart, MHD and dose to LAD, volume of ipsilateral lung and dose to heart, respectively.

Results

All the 74 patients' data of 148 CT scans and 148 treatment plans were analyzed. Patients' variability was noted in volume and dose parameters of PTV and OARs. As shown in Table 2, the PTV volume was comparable and without significant difference between the FB and ABC-DIBH plans. CT scans with ABC-DIBH showed significantly larger ipsilateral lung and contralateral lung than those with FB, where the mean increase was 53.83% and 46.41% under $P < 0.01$, respectively. Although the ABC-DIBH increased the intrathoracic pressure and thus enlarged the distance between the heart and PTV (an increase of 82.61% for MHD, distribution shown in

TABLE 2 Volumes and MHD between FB and ABC-DIBH plans.

| | FB | ABC-DIBH | P value |
|--------------------------|----------------------|----------------------|---------|
| PTV (cc) | 631.16 \pm 221.32 | 636.97 \pm 227.55 | 0.18 |
| Ipsilateral lung (cc) | 1175.95 \pm 245.96 | 1808.96 \pm 286.77 | 0.00 |
| Contralateral lung (cc) | 1435.70 \pm 240.91 | 2102.03 \pm 299.68 | 0.00 |
| Heart (cc) | 537.38 \pm 99.75 | 529.94 \pm 86.38 | 0.23 |
| MHD (cm) | 0.46 \pm 0.29 | 0.84 \pm 0.32 | 0.00 |
| Respiratory capacity (L) | 0.24 \pm 0.05 | 1.43 \pm 0.24 | 0.00 |

FB, free breath; ABC-DIBH, deep inspiration breath hold with Active Breathing Coordinator technique; MHD, minimum heart distance.

Figure 2G), no significant variation in heart volume was observed. Moreover, in comparison with FB, the average respiratory capacity of ABC-DIBH increased by 495.83% ($P < 0.01$, Figure 2H).

While ensuring prescribed dose coverage of the PTV (FB, CI=0.70, HI=1.09; ABC-DIBH, CI=0.71, HI=1.09), exposure to OARs was decreased as much as possible. As shown in Table 3, the plans with ABC-DIBH achieved distinctly lower D2, Dmean,

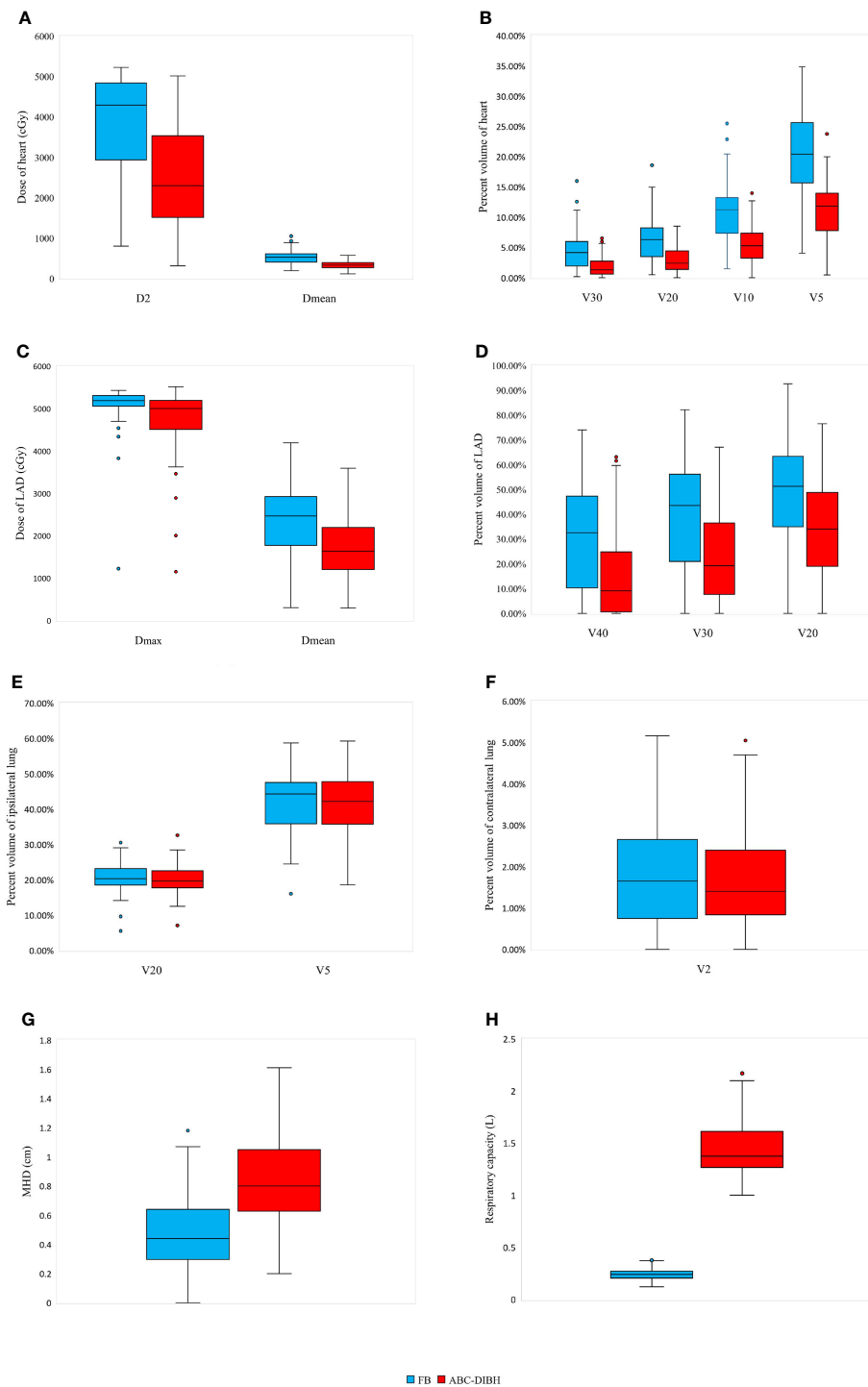


FIGURE 2

Distribution of parameters of heart (A: D2 and Dmean; B: V30, V20, V10 and V5), LAD (C: Dmax and Dmean; D: V40, V30 and V20), ipsilateral lung (E: V20 and V5), contralateral lung (F: V2), MHD (G) and respiratory capacity (H) with FB and ABC-DIBH.

V30, V20, V10 and V5 of heart than the plans with FB, where the relative reductions were 32.72%, 34.80%, 58.78%, 52.74%, 48.30% and 44.31% under $P < 0.01$, respectively. The distribution of these parameter values was presented in Figures 2A, B. Meanwhile, it relatively reduced the Dmax, Dmean, V40, V30 and V20 of LAD by 8.47%, 29.33%, 53.00%, 42.69% and 32.31%, $P < 0.01$, whose distribution was observed in Figures 2C, D. In addition, the plans with ABC-DIBH outperform FB on V20 reduction of ipsilateral lung (3.12%, $P < 0.05$, Figure 2E) and Dmean reduction of contralateral lung (4.82%, $P < 0.01$). Whereas, there is no significant reduction for the Dmean and V5 of ipsilateral lung (7.86%, 0.47%) and V2 of contralateral lung (7.18%, Figure 2F) in both plans.

Regression analysis demonstrated that both Dmean and D2 of heart were negatively correlated with MHD in plans with FB and ABC-DIBH respectively, as shown in Figures 3A, B. In general, Dmean and D2 of heart decreased with the increase of MHD by 37.8 cGy and 309.9 cGy per 1mm, respectively. Meanwhile, a lower Dmean of heart was related to a larger volume of ipsilateral lung in plans with FB ($r = -0.631$, $\rho = -0.673$, Figure 3C). With the increase in volume of ipsilateral lung, this correlation was getting weaker and weaker until the volume of ipsilateral lung reached 1700 cc. Therefore, this correlation was nonsignificant in plans with DIBH ($r = -0.269$, $\rho = -0.311$). Furthermore, the analysis revealed a negative linear correlation between Dmean of LAD and MHD in plans with FB ($r = -0.549$, $\rho = -0.510$, Figure 3D) and

ABC-DIBH ($r = -0.557$, $\rho = -0.505$, Figure 3D), whose slope was 162.5 and 135.9 cGy/mm, respectively.

In terms of respiratory capacity with FB and ABC-DIBH, a positive correlation between the difference of respiratory capacity and difference of ipsilateral lung volume was found ($r = 0.665$, $\rho = 0.556$, Figure 3E). However, as revealed by Figures 4A, B, with the absolute difference and relative ratio of respiratory capacity between ABC-DIBH and FB increased, there lacked correlation for the difference of Dmean of heart. The same was true for the differences of Dmean of LAD. There was an apparent separation for MHD, Dmean of heart and Dmean of LAD plotted against respiratory capacity between the two groups (Figures 4C-E). The ABC-DIBH group had a larger MHD and lower overall Dmean of heart and LAD than the FB group without a distribution pattern. Hence, the larger difference of respiratory capacity between ABC-DIBH and FB had no significant effect on the larger difference of MHD, Dmean of heart and Dmean of LAD. In this study, when the respiratory capacity of ABC-DIBH reached 1L and the relative ratio (ABC-DIBH/FB) reached 3.6, patients could obtain the benefit of dose sparing from the ABC-DIBH.

Conclusion and discussion

Radiation-induced toxicities are a severe concern for left-sided breast cancer patients, which not only discount the quality

TABLE 3 Dosimetric parameters of PTV and OARs between FB and ABC-DIBH plans.

| Parameters | | FB | ABC-DIBH | P value |
|----------------------|----------------------|-------------------|-------------------|---------|
| PTV | CI | 0.70 ± 0.06 | 0.71 ± 0.05 | 0.00 |
| | HI | 1.09 ± 0.02 | 1.09 ± 0.03 | 0.33 |
| Heart | D ₂ (cGy) | 3774.77 ± 1297.68 | 2539.69 ± 1295.97 | 0.00 |
| | Dmean (cGy) | 520.83 ± 181.42 | 339.56 ± 100.57 | 0.00 |
| | V30 (%) | 4.44 ± 3.24 | 1.83 ± 1.65 | 0.00 |
| | V20 (%) | 6.20 ± 3.79 | 2.93 ± 2.12 | 0.00 |
| | V10 (%) | 10.60 ± 4.89 | 5.48 ± 3.04 | 0.00 |
| | V5 (%) | 19.93 ± 7.97 | 11.10 ± 4.36 | 0.00 |
| | Dmax (cGy) | 5145.65 ± 259.94 | 4709.84 ± 767.23 | 0.00 |
| LAD | Dmean (cGy) | 2498.46 ± 828.79 | 1765.67 ± 740.22 | 0.00 |
| | V40 (%) | 33.17 ± 21.44 | 15.59 ± 16.76 | 0.00 |
| | V30 (%) | 42.68 ± 20.26 | 24.46 ± 19.04 | 0.00 |
| | V20 (%) | 51.28 ± 18.16 | 34.71 ± 19.17 | 0.00 |
| | Dmean (cGy) | 1219.70 ± 500.35 | 1123.81 ± 204.36 | 0.08 |
| Ipsilateral lung | V20 (%) | 20.54 ± 3.92 | 19.90 ± 4.07 | 0.04 |
| | V5 (%) | 42.11 ± 8.12 | 41.91 ± 8.41 | 0.79 |
| | Dmean (cGy) | 83.62 ± 9.14 | 79.59 ± 9.78 | 0.00 |
| Contralateral lung | V2 (%) | 1.81 ± 1.28 | 1.68 ± 1.19 | 0.29 |
| | Dmean (cGy) | 111.18 ± 16.21 | 112.78 ± 17.34 | 0.13 |
| Contralateral breast | V5 (%) | 0.24 ± 0.52 | 0.33 ± 0.60 | 0.08 |

CI, conformal index, $CI = (V_{P, ref}/V_P) * (V_{P, ref}/V_{ref})$, ($V_{P, ref}$, the volume of PTV covered by the prescription dose, V_P , the volume of PTV, V_{ref} , the volume covered by the prescription dose); HI, homogeneity index, $HI = D5/D95$, (D5, the dose at 5% volume of PTV, D95, the dose at 95% volume of PTV); LAD, left anterior descending artery; Dmax, maximum dose; D2, the dose at 2% volume; Dmean, mean dose; Vx, the percent of volume covered by dose of x Gy.

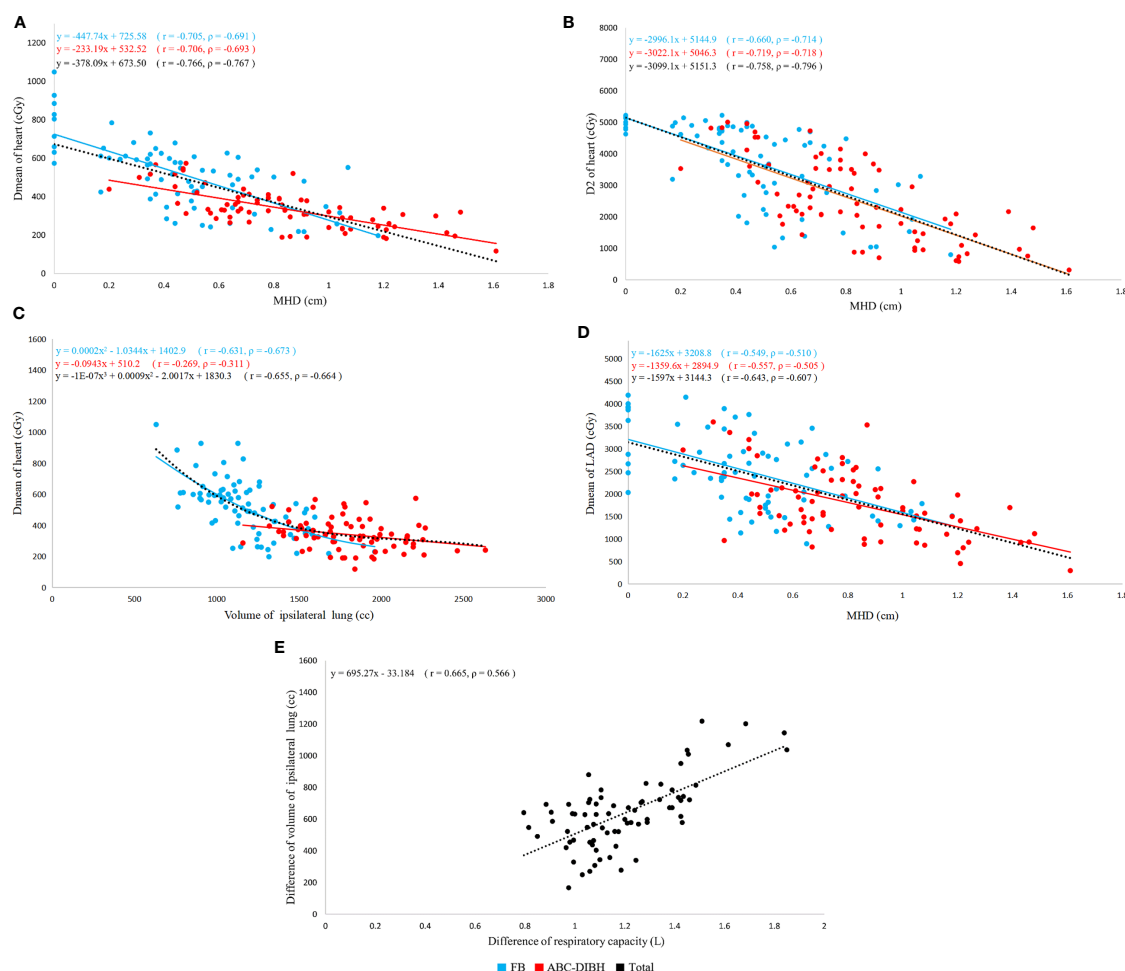


FIGURE 3

Correlation of individual parameters (r , Pearson's rank correlation coefficient; p , Spearman's rank correlation coefficient). (A) Correlation between Dmean of heart and MHD with FB and ABC-DIBH. (B) Correlation between D2 of heart and MHD with two modes. (C) Correlation between Dmean of heart and volume of ipsilateral lung with two modes. (D) Correlation between Dmean of LAD and MHD with two modes. (E) Correlation between difference of volume of ipsilateral lung and difference of respiratory capacity with two modes.

of life but also increase the likelihood of mortality due to the cardiac impairment and failure. Although the subsequent risk is uncertain, the excess events of ischemic heart disease increase linearly with the mean dose of heart. Respiratory motion management of ABC-DIBH is therefore an appropriate method applied in treatment delivery, which can decrease the heart and LAD exposure to radiation dramatically.

The results from our study not only demonstrate the encouraging effect that ABC-DIBH is utilized for the reduction of cardiac dose but also reveal the correlation among individual parameters in left-sided breast cancer patients treated with adjuvant radiotherapy. Similar to the results of our study, Azam Eskandari et al. in their study of 17 left-sided breast cancer patients had performed dosimetric comparison for FB and DIBH plans. They demonstrated that the DIBH plans achieved lower the Dmean of heart with respect to those with FB (3.83 Gy

VS. 5.79 Gy) (25). C. S. Chang et al. in their review of 21 left-sided breast cancer patients acknowledged that the mean heart dose and mean LAD dose of DIBH plans was reduced by 41% and 42% separately. It also revealed that Dmean of heart and LAD were negatively correlated with the volume of ipsilateral lung. They suggested the difference of lung volume between the two groups could be adopted to screen patients for DIBH (22). Diana Lee et al. in their analysis of 47 patients treated with FB and 41 patients treated with ABC-DIBH had shown an inverse relationship between Dmean of heart and volume of left lung. Likewise, Dmean of LAD decreased with increasing volume of left lung for all patients (26). We can conclude that DIBH is a practical way for cardiac sparing in radiotherapy of left-sided breast cancer. ABC is employed for this purpose.

While for the reduction of dose to lungs by DIBH, there seems to be controversy. C. S. Chang et al. held that the DIBH

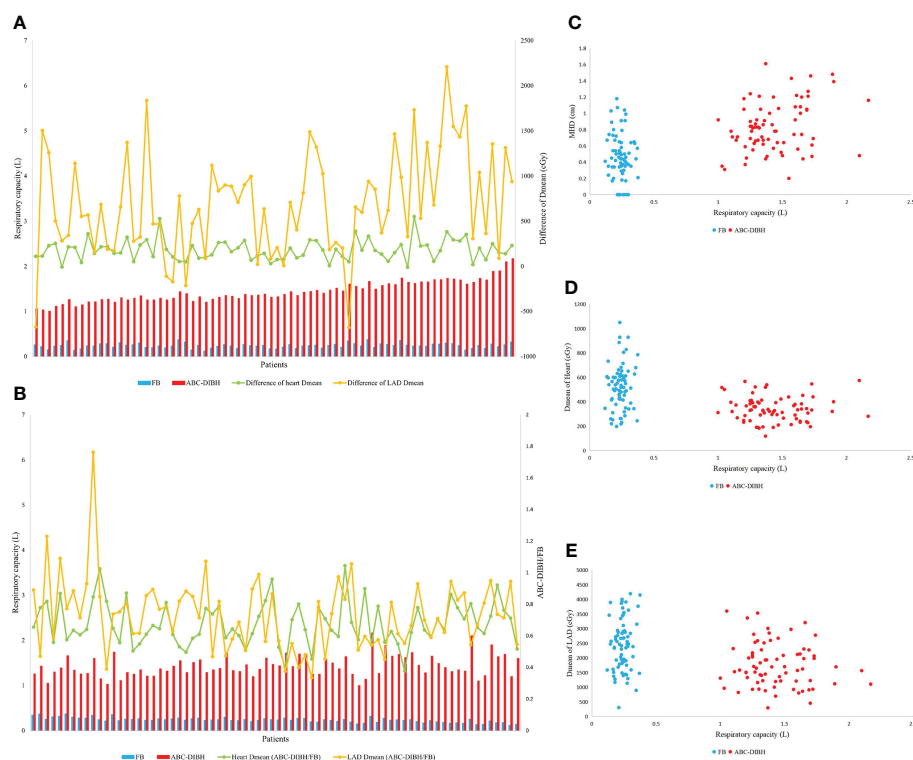


FIGURE 4

(A) Respiratory capacity, difference of Dmean of heart and LAD of per patient between FB and ABC-DIBH (in order of absolute difference of respiratory capacity). (B) Respiratory capacity, ratio of Dmean of heart and LAD of per patient between FB and ABC-DIBH (ABC-DIBH/FB, in order of ratio of respiratory capacity). (C) Distribution of MHD against respiratory capacity between FB and ABC-DIBH. (D) Distribution of Dmean of heart against respiratory capacity between FB and ABC-DIBH. (E) Distribution of Dmean of LAD against respiratory capacity between FB and ABC-DIBH.

had no significant reduction of V5, V20 and Dmean of ipsilateral lung and whole lung (22). Azam Eskandari et al. and Diana Lee et al. considered that DIBH would increase Dmean and V20 of ipsilateral lung despite the fact that it lacking of statistical significance (25, 26). However, Harriet et al. presented statistically significant reductions in the dose of ipsilateral lung and whole lung with ABC-DIBH (21). In our work, the plans with ABC-DIBH outperform FB on V20 reduction of ipsilateral lung and Dmean reduction of contralateral lung with statistical significance. Whereas, there is nonsignificant reduction for the Dmean and V5 of ipsilateral lung and V2 of contralateral lung in both plans. This is mainly because that while the volume of whole lungs becomes larger after inhalation, the part within or near the radiation fields also becomes larger without correspondence (Figures 1C, D) as the lower lobes of lung exhibit a higher degree of airflow exchange than other lobes (27, 28). The volume of exposure to radiation gets complicated (Figure 1E). In terms of dose to lung, not all patients can receive the significant benefit from the DIBH on account of some outliers. A larger number of samples are needed for this purpose in further investigations. Differently,

Song et al. held that it is wrong as the larger absolute lung volume of exposure to radiation with DIBH results in an increased risk of radiation-induced lung toxicity (27). The density of functional units such as alveoli and bronchioles should be considered, which is negatively correlated with the volume of lung. Radiation damage to these functional units is more likely to lead to functional impairment (28). The effects may even be evaluated on a molecular level with the help of micronucleus testing (29).

We have found that MHD is a crucial factor which determines the cardiac dose. Dose to heart and LAD is negatively correlated with MHD in plans with FB and ABC-DIBH, respectively. The expansion of ipsilateral lung with DIBH pushes the heart away from the radiation field and broadens the MHD, which decreases cardiac dose by leaps and bounds. Nevertheless, it is patient-specific for the difference of lung volume between FB and ABC-DIBH, which doesn't determine the difference of MHD and therefore doesn't determine the difference of cardiac dose between the two modes. Similarly, although the difference of respiratory capacity is associated with the difference of lung volume between FB and ABC-DIBH, it is

not associated with the difference of MHD, and thus was not associated with the difference of cardiac dose. In brief, deep inspiratory can increase lung volume and MHD, thereby reducing the cardiac dose. Whereas, it does not mean that more respiratory capacity decreases more cardiac dose. Our data demonstrate that patients can obtain the desired benefit when the respiratory capacity of ABC-DIBH reaches 1L and the relative ratio (ABC-DIBH/FB) reaches 3.6. It needs to be cautious that the threshold of inspiration volume is set too close to the maximum breath-hold. Comfort is the other factor that has to be considered. Angela et al. found through paper questionnaires that more than half of patients felt moderately to highly nervous and starved for air when using the ABC-DIBH technique (30). Discomfort may lead to rapid breaths and chaotic breath-holds (15). Therefore, an appropriate threshold is significant to keep the stable breath-hold with comfort when the respiratory capacity of ABC-DIBH reaches 1L, and the relative ratio (ABC-DIBH/FB) reaches 3.6.

In addition, the variation of airflow rate in a sense affects respiratory capacity measured by the ABC device. The work by Soyoung Lee et al. with 12 patients received ABC breath-hold treatment indicated a positive correlation that the recorded respiratory capacity increased as the airflow rate increased on inhalation mode. They measured air volume with a specific syringe at several airflow rates and confirmed the accuracy within 5% tolerance. In terms of respiratory capacity of patients, the maximum difference with respect to the reference volume of conventional radiotherapy and SBRT was 1.0 L and 0.16 L, with airflow rates of 0.77 L/s and 0.29 L/s range, respectively (15). The wide range of airflow rates of patients affects the actual measured inspiratory results, and thus the impact of this on our statistics cannot be ignored. It affects the repeatability in breath-hold volume during patients' treatment fractions. Additionally, although ABC can monitor the breathing curve in real time, it cannot display the intra-fractional and inter-fractional position variation. If a patient has false breath-holding, such as leaking air from the corner of mouth or breathing through the nose, it is difficult to judge from the breath curve.

In conclusion, this study has demonstrated the significant impact on cardiac sparing from radiation on account of variation in lung volume or expansion, as well as suggests the effect of respiratory capacity in left-sided breast cancer irradiation with ABC-DIBH compared with FB. MHD plays a significant role which determines the cardiac dose. The larger difference of respiratory capacity has no significant effect on the larger difference of MHD, Dmean of heart and Dmean of LAD between ABC-DIBH and FB. When the respiratory capacity of ABC-DIBH reached 1L and the relative ratio (ABC-DIBH/FB) reached 3.6, patients could obtain the benefit of dose sparing. Further investigation of the effect of respiratory capacity

considering the intra-fractional and inter-fractional variation will be implemented.

Data availability statement

The original contributions presented in the study are included in the article/[Supplementary Material](#). Further inquiries can be directed to the corresponding authors.

Ethics statement

The studies involving human participants were reviewed and approved by The ethics committee of Shenzhen People's hospital. Written informed consent for participation was not required for this study in accordance with the national legislation and the institutional requirements.

Author contributions

HTC recorded and analyzed the data, and wrote the manuscript. YP, DY, PPK, ZHL and GXL helped with the statistical analysis. YP and HLZ revised the manuscript. All authors contributed to the study and approved the submitted manuscript.

Conflict of interest

The authors declare that the research was conducted in the absence of any commercial or financial relationships that could be construed as a potential conflict of interest.

Publisher's note

All claims expressed in this article are solely those of the authors and do not necessarily represent those of their affiliated organizations, or those of the publisher, the editors and the reviewers. Any product that may be evaluated in this article, or claim that may be made by its manufacturer, is not guaranteed or endorsed by the publisher.

Supplementary material

The Supplementary Material for this article can be found online at: <https://www.frontiersin.org/articles/10.3389/fonc.2022.989220/full#supplementary-material>

References

- Kunheri B, Kotne S, Nair SS, Makuny D. A dosimetric analysis of cardiac dose with or without active breath coordinator moderate deep inspiratory breath hold in left sided breast cancer radiotherapy. *J Cancer Res Ther* (2017) 13(1):56–61. doi: 10.4103/jcrt.JCRT_1414_16
- Darby S, McGale P, Correa C, Taylor C, Arriagada R, Clarke M, et al. Effect of radiotherapy after breast-conserving surgery on 10-year recurrence and 15-year breast cancer death: meta-analysis of individual patient data for 10,801 women in 17 randomised trials. *Lancet* (2011) 378(9804):1707–16. doi: 10.1016/S0140-6736(11)61629-2
- Whelan TJ, Julian J, Wright J, Jadad AR, Levine ML. Does locoregional radiation therapy improve survival in breast cancer? a meta-analysis. *J Clin Oncol* (2000) 18:1220–9. doi: 10.1200/JCO.2000.18.6.1220
- McGale P, Taylor C, Correa C, Cutter D, Duane F, Ewertz M, et al. Effect of radiotherapy after mastectomy and axillary surgery on 10-year recurrence and 20-year breast cancer mortality: meta-analysis of individual patient data for 8135 women in 22 randomised trials. *Lancet* (2014) 383(9935):2127–35. doi: 10.1016/S0140-6736(14)60488-8
- Quirk S, Grendarova P, Phan T, Conroy L, Burke B, Long K, et al. A retrospective analysis to demonstrate achievable dosimetry for the left anterior descending artery in left-sided breast cancer patients treated with radiotherapy. *Radiother Oncol* (2020) 148:167–73. doi: 10.1016/j.radonc.2020.04.022
- Darby SC, McGale P, Taylor CW, Peto R. Long-term mortality from heart disease and lung cancer after radiotherapy for early breast cancer: prospective cohort study of about 300,000 women in US SEER cancer registries. *Lancet Oncol* (2005) 6:557–65. doi: 10.1016/S1470-2045(05)70251-5
- Darby SC, Ewertz M, McGale P, Bennet AM, Blom-Goldman U, Brønnum D, et al. Risk of ischemic heart disease in women after radiotherapy for breast cancer. *N Engl J Med* (2013) 368:987–98. doi: 10.1056/NEJMoa1209825
- Bouillon K, Haddy N, Delaloge S, Garbay JR, Garsi JP, Brindel P, et al. Long-term cardiovascular mortality after radiotherapy for breast cancer. *J Am Coll Cardiol* (2011) 57:445–52. doi: 10.1016/j.jacc.2010.08.638
- Zhu Q, Kirova YM, Cao L, Arsene-Henry A, Chen J. Cardiotoxicity associated with radiotherapy in breast cancer: a question-based review with current literatures. *Cancer Treat Rev* (2018) 68:9–15. doi: 10.1016/j.ctrv.2018.03.008
- Jacob S, Camilleri J, Derreumaux S, Walker V, Lairez O, Lapeyre M, et al. Is mean heart dose a relevant surrogate parameter of left ventricle and coronary arteries exposure during breast cancer radiotherapy: a dosimetric evaluation based on individually-determined radiation dose (BACCARAT study). *Radiat Oncol* (2019) 14:29. doi: 10.1186/s13014-019-1234-z
- Kahán Z, Ráosi F, Gaál S, Cserhádi A, Boda K, Darázs B, et al. A simple clinical method for predicting the benefit of prone vs. supine positioning in reducing heart exposure during left breast radiotherapy. *Radiother Oncol* (2018) 126:487–92. doi: 10.1016/j.radonc.2017.12.021
- D'Agostino GR, Diletto B, Mantini G, Nardone L, Mattiucci GC, Catucci F, et al. Reducing heart dose during left breast cancer radiotherapy: comparison among 3 radiation techniques. *Tumori* (2016) 102(2):184–9. doi: 10.5301/tj.5000414
- Stick LB, Yu J, Maraldo MV, Aznar MC, Pedersen AN, Bentzen SM, et al. Joint estimation of cardiac toxicity and recurrence risks after comprehensive nodal photon versus proton therapy for breast cancer. *Int J Radiat Oncol* (2017) 97:754–61. doi: 10.1016/j.ijrobp.2016.12.008
- Kaza E, Dunlop A, Panek R, Collins DJ, Orton M, Symonds-Taylor R, et al. Lung volume reproducibility under ABC control and self-sustained breath-holding. *J Appl Clin Med Phys* (2017) 18(2):154–62. doi: 10.1002/acm2.12034
- Lee S, Zheng Y, Podder T, Biswas T, Verma V, Goss M, et al. Tumor localization accuracy for high-precision radiotherapy during active breath-hold. *Radiother Oncol* (2019) 137:145–52. doi: 10.1016/j.radonc.2019.04.036
- Yang D, Piao Y, Yuan F, Chen H, Zhang D, Li X. Gastric side effects and the stomach dosimetric analysis in left-sided breast cancer radiotherapy in free-breathing and deep inspiration breath-hold technique. *Radiat Oncol* (2022) 17(1):2. doi: 10.1186/s13014-021-01963-7
- Farrugia B, Khor R, Foroudi F, Chao M, Knight K, Wright C. Protocol of a study investigating breath-hold techniques for upper-abdominal radiation therapy (BURDIE): addressing the challenge of a moving target. *Radiat Oncol* (2020) 15(1):250. doi: 10.1186/s13014-020-01688-z
- Zhang W, Li R, You D, Su Y, Dong W, Ma Z. Dosimetry and feasibility studies of volumetric modulated arc therapy with deep inspiration breath-hold using optical surface management system for left-sided breast cancer patients. *Front Oncol* (2020) 10:1711. doi: 10.3389/fonc.2020.01711
- Mkanna A, Mohamad O, Ramia P, Thebian R, Makki M, Tamim H, et al. Predictors of cardiac sparing in deep inspiration breath-hold for patients with left sided breast cancer. *Front Oncol* (2018) 8:564. doi: 10.3389/fonc.2018.00564
- Lu YK, Yang D, Zhang XW, Teng Y, Yuan W, Zhang Y, et al. Comparison of deep inspiration breath hold versus free breathing in radiotherapy for left sided breast cancer. *Front Oncol* (2022) 12:845037. doi: 10.3389/fonc.2022.845037
- Eldredge-Hindy H, Lockamy V, Crawford A, Nettleton V, Werner-Wasik M, Siglin J, et al. Active breathing coordinator reduces radiation dose to the heart and preserves local control in patients with left breast cancer: report of a prospective trial. *Pract Radiat Oncol* (2015) 5(1):4–10. doi: 10.1016/j.prr.2014.06.004
- Chang CS, Chen CH, Liu KC, Ho CS, Chen MF. Selection of patients with left breast cancer for IMRT with deep inspiration breath-hold technique. *J Radiat Res* (2020) 61(3):431–9. doi: 10.1093/jrr/rraa003
- Mittauer KE, Deraniyagala R, Li JG, Lu B, Liu C, Samant SS, et al. Monitoring ABC-assisted deep inspiration breath hold for left-sided breast radiotherapy with an optical tracking system. *Med Phys* (2015) 42(1):134–43. doi: 10.1118/1.4903511
- Conroy L, Yeung R, Watt E, Quirk S, Long K, Hudson A, et al. Evaluation of target and cardiac position during visually monitored deep inspiration breath-hold for breast radiotherapy. *J Appl Clin Med Phys* (2016) 17:25–36. doi: 10.1120/jacmp.v17i4.6188
- Eskandari A, Nasser S, Gholamhosseini H, Hosseini S, Farzaneh MJ, Keramati A, et al. Evaluation of the heart and lung dosimetric parameters in deep inspiration breath hold using 3D slicer. *Radiat Oncol J* (2020) 38(1):68–76. doi: 10.3857/roj.2019.00654
- Lee D, Dinniwel R, Lee G. A retrospective analysis of lung volume and cardiac dose in left-sided whole breast radiotherapy. *J Med Imaging Radiat Sci* (2016) 47(3S):S10–4. doi: 10.1016/j.jmir.2016.04.008
- Song J, Tang T, Caudrelier JM, Bélec J, Chan J, Lacasse P, et al. Dose-sparing effect of deep inspiration breath hold technique on coronary artery and left ventricle segments in treatment of breast cancer. *Radiother Oncol* (2021) 154:101–9. doi: 10.1016/j.radonc.2020.09.019
- Hope AJ, Lindsay PE, El Naqa I, Alaly JR, Vicic M, Bradley JD, et al. Modeling radiation pneumonitis risk with clinical, dosimetric, and spatial parameters. *Int J Radiat Oncol Biol Phys* (2006) 65(1):112–24. doi: 10.1016/j.ijrobp.2005.11.046
- Mrdjanović J, Šolajić S, Srđenić-Čonić B, Bogdanović V, Dea KJ, Kladar N, et al. The oxidative stress parameters as useful tools in evaluating the DNA damage and changes in the complete blood count in hospital workers exposed to low doses of antineoplastic drugs and ionizing radiation. *Int J Environ Res Public Health* (2021) 18(16):8445. doi: 10.3390/ijerph18168445
- Cashell A, Qadeer J, Rosewall T. Exploring the experiences of left-sided breast cancer patients receiving radiation therapy using the active breathing coordinator. *J Med Imaging Radiat Sci* (2016) 47(4):323–8. doi: 10.1016/j.jmir.2016.08.004



OPEN ACCESS

EDITED BY

Sophia Ran,
Southern Illinois University
Carbondale, United States

REVIEWED BY

Govind Babu Kanakasetty,
HCG Cancer Hospital, India
Robert Wesolowski,
Comprehensive Cancer Center, The
Ohio State University, United States

*CORRESPONDENCE

Zheng Lv
lvz@jlu.edu.cn
Jiuwei Cui
cuijw@jlu.edu.cn

SPECIALTY SECTION

This article was submitted to
Breast Cancer,
a section of the journal
Frontiers in Oncology

RECEIVED 13 September 2022

ACCEPTED 18 November 2022

PUBLISHED 19 December 2022

CITATION

Yang R, Jia L, Lu G, Lv Z and Cui J
(2022) Symptomatic bone marrow
metastases in breast cancer: A
retrospective cohort study.
Front. Oncol. 12:1042773.
doi: 10.3389/fonc.2022.1042773

COPYRIGHT

© 2022 Yang, Jia, Lu, Lv and Cui. This is
an open-access article distributed under
the terms of the [Creative Commons
Attribution License \(CC BY\)](#). The use,
distribution or reproduction in other
forums is permitted, provided the
original author(s) and the copyright
owner(s) are credited and that the
original publication in this journal is
cited, in accordance with accepted
academic practice. No use,
distribution or reproduction is
permitted which does not comply with
these terms.

Symptomatic bone marrow metastases in breast cancer: A retrospective cohort study

Ruohan Yang, Lin Jia, Guanyu Lu, Zheng Lv* and Jiuwei Cui*

Cancer Center, The First Hospital of Jilin University, Changchun, China

Objective: Breast cancer symptomatic bone marrow metastasis (BMM) is rare and has a poor prognosis. Chemotherapy is usually the primary treatment, but it has limited efficacy, resulting in dose reduction and a decrease in quality of life due to the adverse effects of the agent. Other than chemotherapy, there are no other treatment studies for BMM. This study aimed to explore the clinicopathological characteristics of BMM patients with breast cancer, the prognosis using different treatment modalities, and the risk factors that affect the prognosis.

Methods: This retrospective study included patients diagnosed with breast cancer BMM from January 2018 to January 2022 in the Cancer Center of the First Hospital of Jilin University. The analysis focused on the characteristics of the patients, the treatment regimen, and the prognosis.

Results: Of 733 patients with advanced breast cancer, 33 patients were identified with BMM. All patients showed a hemoglobin decrease, and 25 (75.75%) presented with a fever of unknown origin. As for the metastasis breast cancer subtype, 25 (75.75%) were hormone receptor (HR) positive/human epidermal growth factor receptor 2 (HER2) negative, three (9.09%) had HER2 overexpression, and five (15.15%) were triple negative. The BMM patients had a median progression-free survival (PFS) of 7 months (1–21 months) and a median overall survival (OS) of 18 months (2–108 months). Among 25 HR⁺/HER2⁻ BMM patients treated with different modalities, the median OS of the endocrine therapy (ET) group was 23 months, compared with 5 months in the chemotherapy group. Cox proportional hazards models suggested that higher Eastern Cooperative Oncology Group (ECOG) scores and old age were associated with shorter survival.

Conclusion: When breast cancer patients present with anemia and fever of unknown origin, BMM should be considered. For HR⁺/HER2⁻ patients with good physical status and can receive active treatment, CDK4/6 inhibitors combined with ET can be used to control disease progression, improve quality of life, and prolong survival.

KEYWORDS

breast cancer, bone marrow metastasis, prognosis, retrospective, cohort study

Introduction

Symptomatic bone marrow metastases (BMM) are the hematogenous spread of circulating tumor cells and the invasion of highly vascularized bone marrow. They manifested as hematopoietic function suppression, such as anemia, thrombocytopenia, and abnormal coagulation (1). Diffuse bone marrow involvement leading to profound cytopenias is rare in solid malignant tumors of nonhematologic diseases (2). Xiao et al. retrospectively analyzed 10,122 solid tumor bone marrow biopsy samples and found that lung, gastric, and breast cancer patients were prone to bone marrow infiltration (3). Although the specific mechanism of breast cancer BMM is not fully understood. It has been confirmed that bone marrow adipocytes (BMAs) and adipokines secreted by breast cancer cells are essential mediators in promoting breast cancer metastasis (4). BMAs secrete cytokines such as leptin, adiponectin, IL-1 β , IL-6, TNF- α , and VEGF to promote breast cancer cell metastasis (5). BMAs can also release cytokines to activate dormant mesenchymal stem cells (MSCs) and cancer stem cells (CSCs) to increase their proliferation and promote breast cancer BMM (6).

Current literature suggests that chemotherapy prolongs survival in breast cancer patients with BMM (7, 8). Chemotherapy, however, can promote the growth of BMAs in the bone marrow, especially in the sacrum (9). Increased BMAs will further promote tumor cell escape and bone destruction around the tumor to promote tumor progression. At the same time, the adverse reactions of chemotherapy agents affected the patient's quality of life (4). Kopp et al. found that the initial chemotherapy of BMM alleviated the patient's cytopenias but did not significantly improve the patient's prognosis (2). Only one case report highlights the positive role of anti-HER2 therapy in breast cancer BMM (10). Furthermore, there is a lack of large-scale studies on the prognosis of treatment regimens other than chemotherapy.

Therefore, we conducted a retrospective analysis based on our center's cases to investigate the clinical characteristics of breast cancer BMM, the prognosis of patients with different treatment methods, and the risk factors affecting the prognosis.

Methods

Study population

Through the medical record system of our hospital, from January 2018 to January 2022, breast cancer BMM patients were retrospectively analyzed. The inclusion criteria were as follows:

1. Clinical manifestations are hypocytosis with or without fever of unknown origin; bone marrow aspiration biopsy confirmed cancer infiltration.
2. Patients who had complete medical records

The exclusion criteria included patients with primary tumors concurrently at other sites and those with metastases from which the tumor origin could not be determined.

Data collection

Clinicopathological information was systematically extracted by reviewing medical records and included the following variables: hormone receptor (estrogen and progesterone) status, HER2 status, age at diagnosis of bone marrow metastases, disease stage at initial diagnosis, number of previous lines of treatment received, ECOG scores at diagnosis of BMM, regimens received, adverse events, time to disease progression, and time to death.

Endocrine therapy (ET) following the diagnosis of BMM includes aromatase inhibitors (AI) and cyclin-dependent kinase (CDK) 4/6 inhibitors.

Statistical analysis

Survival was assessed using Kaplan–Meier analysis, and the log-rank test was used to determine overall survival (OS) rates between groups treated with different regimens. The Cox proportional hazards model was used to search for risk factors that affect OS in patients with bone marrow metastases. Progression-free survival (PFS) is defined as the time from the occurrence of BMM on any regimen to disease progression or death from any cause. OS was defined as the time from the occurrence of BMM receiving any treatment regimen to death.

Statistical significance was defined as a two-sided *p*-value of < 0.05. All statistical tests were performed using SPSS 23.0 (IBM Corporation Released 2013. IBM SPSS Statistics for Windows, Version 23.0, Armonk, NY, USA).

Result

Clinical features of patients with bone marrow metastases

A total of 33 patients were included in this study. All denied a family history of breast cancer. The median age was 49.5 years (29–68 years); 25 (75.75%) were HR positive/HER2 negative, three (9.09%) had HER2 overexpression, and five (15.15%) were triple negative. As for metastasis breast cancer pathological type, 28 (84.85%) were invasive ductal carcinoma. In total, 28 patients

(84.85%) had a high Ki-67 index expression, 14 (42.42%) were primarily diagnosed as *de novo*, and 15 (45.46%) had an ECOG score of 3. Clinically, all patients complained of fatigue, and 25 (75.75%) had fever with a negative etiological test. Blood routine revealed that all patients had a decrease in hemoglobin. Three of the cases (9.09%) showed thrombocytopenia, and two (6.25%) showed pancytopenia with no apparent cause. We also analyzed factors such as menstrual status, histological grade, and the number of previous lines of therapy (Table 1). All of the patients had bone metastases when they developed BMM. We analyzed the specific sites of bone metastases and found that the spine was the most common (78.78%), followed by the ribs (63.63%) and the femur (30.20%) (Figure 1).

TABLE 1 Clinical characteristics of patients with BMM.

| Variable | N (%) |
|------------------------------------|--------------|
| Age (years) | |
| Median age | 49.5 (29–68) |
| ≤60 | 25 (75.75%) |
| >60 | 7 (24.25%) |
| Menstrual status | |
| Postmenopause | 11 (33.33%) |
| Premenopausal | 22 (66.67%) |
| Molecular typing | |
| HR ⁺ /HER2 [−] | 25 (75.75%) |
| HER2 overexpression | 3 (9.09%) |
| Triple negative | 5 (15.15%) |
| Pathological type | |
| Invasive ductal carcinoma | 28 (84.85%) |
| Invasive lobular carcinoma | 2 (6.06%) |
| Others | 3 (9.09%) |
| Ki-67 expression | |
| ≥15% | 28 (84.85%) |
| <15% | 5 (15.15%) |
| Histological grading | |
| I | 1 (3.03%) |
| II | 18 (54.55%) |
| III | 14 (42.42%) |
| <i>De novo</i> metastasis | |
| Yes | 14 (42.42%) |
| No | 19 (57.58%) |
| ECOG scores | |
| 1 | 10 (30.30%) |
| 2 | 8 (24.24%) |
| 3 | 15 (45.46%) |
| Treatment after BMM | |
| Chemotherapy | 18 (54.25%) |
| Targeted therapy | 2 (6.06%) |
| Endocrine therapy | 13 (39.39%) |
| CDK4/6+AI | 9 (27.28%) |

(Continued)

TABLE 1 Continued

| Variable | N (%) |
|---|-------------|
| AI | 4 (12.12%) |
| Number of lines of therapy received before bone marrow metastases | |
| 0 | 12 (36.36%) |
| 1 | 7 (21.22%) |
| ≥2 | 14 (42.42%) |
| Combined with bone metastases | |
| Yes | 33 (100%) |
| No | 0 (0%) |
| Clinical manifestations | |
| Fatigue | 33 (100%) |
| Fever | 25 (75.75%) |
| Blood routine | |
| Pancytopenia | 2 (6.25%) |
| Decreased hemoglobin (g/L) | 32 (100%) |
| 100–80 | 18 (54.55%) |
| <80 | 15 (45.45%) |
| Thrombocytopenia (10 ⁹ /L) | 4 (12.12%) |
| 75–99 | 3 (9.09%) |
| <75 | 1 (3.03%) |

Prognosis

The patients had a median PFS of 7 months (1–22 months) and a median OS of 18 months (2–108 months). We used different treatment regimens to compare the OS and PFS of 25 patients with HR positive/HER2 negative. The median OS for chemotherapy was 5 months (2–30 months), while the median OS for ET was 23 months (7–108 months). The median PFS for chemotherapy was 2 months (1–18 months), and the median PFS for ET was 11 months (4–22 months). Due to the small number of HER2 overexpressing and triple-negative patients, no survival analysis was performed (Figures 2–5).

In order to investigate the factors affecting the prognosis of patients with BMM, we incorporated elements such as age, menstrual status, initial diagnosis stage, histological grade, ECOG score, and Ki-67 index into the Cox proportional hazards model. We found that a higher ECOG score (95% CI: 2.15–29.28, $p = 0.002$) and older age (95% CI: 2.57–210.84, $p = 0.005$) were associated with shorter survival (Table 2).

Adverse events

Adverse events (AEs) are summarized in Table 3. The most common hematologic adverse event in the chemotherapy group was hemoglobin reduction (61.11%), and 15 (83.33%) patients had AEs of grade ≥3. Alopecia was the most common nonhematologic AE (100%) in the chemotherapy group. The common hematologic AEs in the ET group were neutropenia

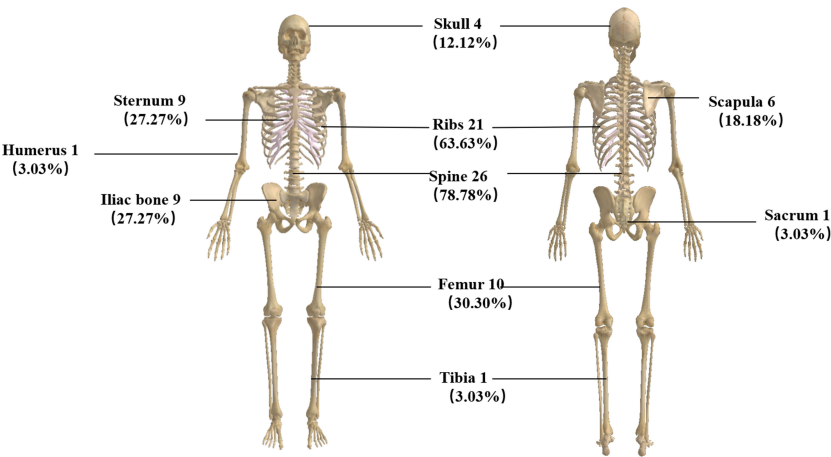


FIGURE 1
Pattern of bone metastases in patients with breast cancer BMM.

(38.46%) and decrease in hemoglobin (38.46%), and only two (15.38%) patients had grade ≥ 3 AEs. No patient had a grade 1 hematologic adverse event.

Fatigue was the most common nonhematologic AE (46.15%) in the ET group. Six (33.33%) patients in the chemotherapy group and two (15.38%) in the ET group had dose reductions due to AEs. No patients experienced treatment-related serious adverse events (SAEs). SAEs are life-threatening or fatal events that require hospitalization or prolonged hospitalization, result in permanent or significant disability/loss of function, and congenital anomaly or congenital disability.

AEs are graded according to the Common Terminology Criteria for Adverse Events (CTCAE) Version 5.0.

Discussion

Clinically relevant bone marrow carcinomatosis (that causes severe cytopenia) is a rare event in patients with breast cancer, with a reported incidence of only 0.17% (2). We retrospectively reviewed 733 patients with advanced breast cancer and found that 33 (4.5%) developed bone marrow metastases, which is higher than previously reported studies and may be related to aggressive bone marrow biopsy and vigilance for patients presenting with anemia and unexplained febricity. Our study found that the median age of patients with bone marrow metastases was 49.5 years old (29–68 years), the pathological type was invasive ductal carcinoma, the

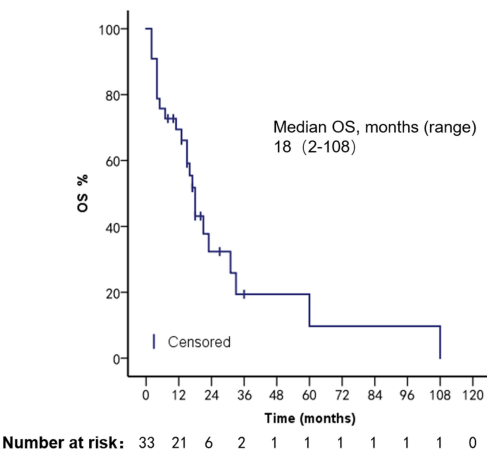


FIGURE 2
PFS in patients with bone marrow metastases.

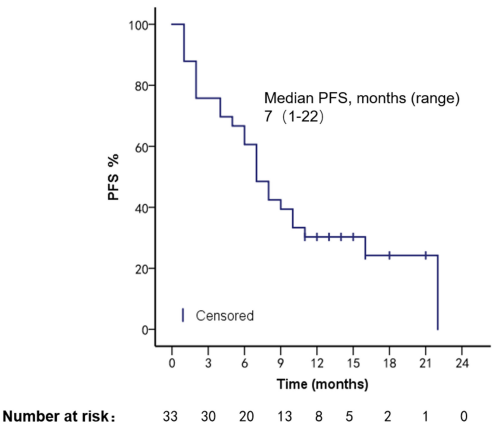


FIGURE 3
OS in patients with bone marrow metastases.

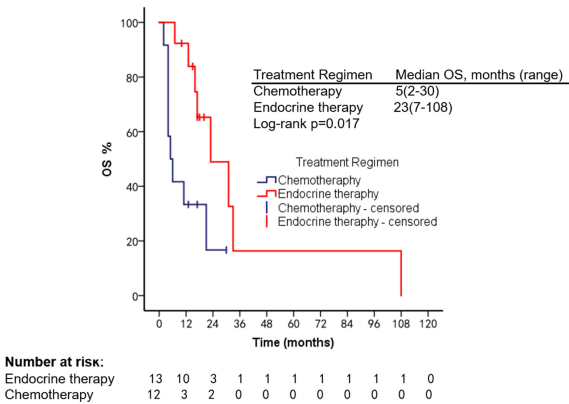


FIGURE 4
Comparison of PFS in HR⁺/HER2⁻ patients used different treatment regimens.

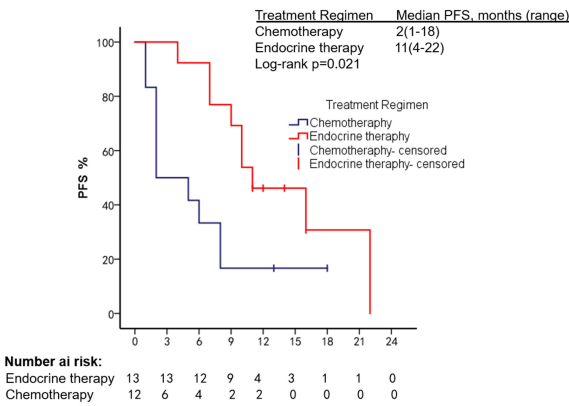


FIGURE 5
Comparison of OS in HR⁺/HER2⁻ patients using different treatment regimens.

TABLE 2 Multivariate Cox-regression of overall survival from time of bone marrow metastasis.

| Factor | Number (%) | Median OS (months, 95%CI) | Hazard ratio value (95%CI) | p-value |
|------------------------------------|------------|---------------------------|----------------------------|---------|
| Age (years) | | | | |
| ≥60 | 25, 78.79% | 15 (9.0–27.0) | 23.27 (2.57–210.84) | 0.005 |
| <60 | 7, 21.21% | 3 (5.6–21.1) | | |
| Menstrual status | | | | |
| Postmenopause | 11, 33.33% | 15 (3.4–37.8) | 0.22 (0.047–1.039) | 0.056 |
| Premenopausal | 22, 66.67% | 17 (10.4–22.8) | | |
| Molecular typing | | | | |
| HR ⁺ /HER2 [−] | 25, 75.75% | 15.5 (7.9–28.7) | 0.979 (0.532–1.802) | 0.945 |
| HER2 overexpression | 3, 9.09% | 15 (−7.2–40.5) | | |
| Triple negative | 5, 15.15% | 15 (0.68–21.3) | | |
| Ki-67 expression | | | | |
| ≥15% | 28, 84.85% | 15 (9.0–19.4) | 1.721 (0.29–10.09) | 0.547 |
| <15% | 5, 15.15% | 13 (23.0–84.0) | | |
| Histological grading | | | | |
| 1 | 1, 3.03% | NA | 0.398 (0.11–1.44) | 0.162 |
| 2 | 18, 54.55% | 15 (8.9–17.2) | | |
| 3 | 14, 42.42% | 15.5 (4.2–38.7) | | |
| ECOG scores | | | | |
| 1 | 10, 30.30% | 17 (6.7–44.8) | 7.940 (2.15–29.28) | 0.002 |
| 2 | 8, 24.24% | 4 (0.6–13.6) | | |
| 3 | 15, 45.46% | 4 (5.5–24.7) | | |
| De novo metastasis | | | | |
| Yes | 14, 42.42% | 15 (5.0–25.3) | 1.998 (0.41–9.52) | 0.385 |
| No | 19, 57.58% | 16 (6.9–28.6) | | |
| Pathological type | | | | |
| Invasive ductal carcinoma | 28, 84.85% | 15 (8.6–18.4) | 1.359 (0.27–6.83) | 0.71 |
| Invasive lobular carcinoma | 2, 6.06% | NA | | |
| Papillary carcinoma | 3, 9.09% | 1.5 (12.5–25.5) | | |
| Number of previous treatment lines | | | | |
| 0 | 12, 36.36% | 16 (1.7–38.5) | 1.10 (0.47–2.57) | 0.82 |
| 1 | 7, 21.22% | 15 (4.8–19.1) | | |
| ≥2 | 14, 42.42% | 15 (6.3–26.2) | | |
| Hemoglobin level (g/L) | | | | |
| 75–99 | 18, 54.55% | 12 (6.9–21.2) | 1.49 (0.38–5.70) | 0.56 |
| <75 | 15, 45.45% | 13 (4.8–35.7) | | |

OS, Overall Survival; CI, Confidence Interval; NA, Not Available.

molecular type was HR positive/HER2 negative, the Ki-67 index was highly expressed, and histological grades 2–3 were more common, which is similar to the clinical features of breast cancer patients with BMM in a retrospective study by Abdullah Sakin et al. (2, 7). All our patients' clinical manifestations presented with fatigue, consistent with reported studies (11, 12). There were 25 patients with fever; we performed relevant tests for etiology, and all were negative. Empirical antibiotic therapy did not significantly improve the patient's symptoms, and immediately we performed a bone marrow aspiration biopsy which revealed BMM. Xiao et al. also reported the phenomenon of unexplained febricity in BMM patients with solid tumors (3). We found that all

patients had BMM accompanied by bone metastases. The reported articles did not analyze the specific sites of bone metastases. We found that the weight-bearing bone (spine, 26 cases) was the most common site of metastasis, which may be because the level of CXC3L1/CXC3R1 in the spine bone is higher than that in other bones, which can promote the adhesion and migration of breast cancer cells (13).

We summarized the literature on breast cancer BMM retrieved from PubMed (Table 4). The published kinds of literature are mainly case reports. After BMM, chemotherapy is the first choice (11, 14–16). Although some patients' diseases were controlled, some reports mentioned that chemotherapy-related adverse events led to dose reduction

TABLE 3 Statistics of adverse events after treatment (CTCAE 5.0).

| | Chemotherapy (<i>n</i> = 18) | | | Endocrine therapy (<i>n</i> = 13) | | |
|-------------------------------------|-------------------------------|-------------|------------|------------------------------------|------------|-----------|
| | Grade 1 | Grade 2 | Grade ≥3 | Grade 1 | Grade 2 | Grade ≥3 |
| Hematologic AEs | | | | | | |
| Neutropenia | 0 (0%) | 4 (22.22%) | 1 (5.56%) | 0 (0%) | 5 (38.46%) | 0 (0%) |
| Leukopenia | 0 (0%) | 4 (22.22%) | 1 (5.56%) | 0 (0%) | 0 (0%) | 1 (7.69%) |
| Decreased hemoglobin | 0 (0%) | 4 (22.22%) | 7 (38.89%) | 0 (0%) | 4 (30.77%) | 1 (7.69%) |
| Thrombocytopenia | 0 (0%) | 3 (16.67%) | 6 (33.33%) | 0 (0%) | 2 (15.38%) | 0 (0%) |
| Nonhematologic AEs | | | | | | |
| Hair loss | 8 (44.44%) | 10 (55.56%) | 0 (0%) | 0 (0%) | 0 (0%) | 0 (0%) |
| Fatigue | 7 (38.89%) | 3 (16.66%) | 1 (5.55%) | 0 (0%) | 6 (46.15%) | 0 (0%) |
| Nausea and vomiting | 5 (27.78%) | 4 (22.22%) | 0 (0%) | 0 (0%) | 0 (0%) | 0 (0%) |
| AEs result in dose reduction | | 6 (33.33%) | | | 2 (15.38%) | |

TABLE 4 Summary of clinical characteristics and prognosis of reported breast cancer BMM.

| Type of study | Sample | Age/ median age | Pathological type | Molecular typing | Histological grading | Treatment | OS | Results |
|---------------------|--------|-----------------------|--|--|--------------------------------|---|--------------|---|
| Retrospective study | 30 | 44.5 | Invasive ductal carcinoma: 27 Invasive lobular carcinoma: 3 | Triple negative: 4 HR positive, HER2 negative: 21 HER2 overexpression: 4 | II: 17 III: 13 | Chemotherapy | 6 months | Chemotherapy significantly prolongs survival in breast cancer patients with bone marrow metastases. Among them, paclitaxel treatment achieved the best survival rate (7). |
| Retrospective study | 22 | 47 | Invasive ductal carcinoma: 14 Invasive lobular carcinoma: 7 Missing: 1 | HR positive, HER2 negative: 18 HER2 overexpression: 1 Triple negative: 3 | III: 10 II: 8 Missing: 4 | Chemotherapy | 11 months | Breast cancer patients with bone marrow metastases should receive rescue therapy with a high response rate (2). |
| Case report | 1 | 62 | Invasive ductal carcinoma | HR positive, HER2 negative | III | Chemotherapy | 57 months | Aggressive standard-dose chemotherapy may be feasible and beneficial in selected patients with bone marrow cancer-related severe thrombocytopenia without major bleeding events (14). |
| Pilot study | 5 | 47 | – | HR positive, HER2 negative: 3 Missing: 2 | – | Palliative hormone therapy combined with low-dose chemotherapy. | 12–38 months | Low-dose chemotherapy and oral or intravenous bisphosphonates prolong survival in patients with bone marrow metastases (15). |
| Case report | 1 | 58 | Occult breast cancer | – | – | Symptomatic treatment | – | Bone marrow aspirate has essential implications for diagnosing rare OBC patients (12). |
| Case report | 5 | 66 | Invasive ductal carcinoma: 4 Invasive lobular carcinoma: 1 | HR positive, HER2 negative: 5 | – | Chemotherapy | 19 months | For capecitabine as a treatment option for patients with breast cancer and bone marrow metastases, a study involving many patients is warranted (16). |
| Case report | 1 | 62 | Invasive lobular carcinoma | HR positive, HER2 negative | – | Chemotherapy | 44 months | In patients with bone marrow metastases with a good PS score, medical therapy is a consideration (8). |

(Continued)

TABLE 4 Continued

| Type of study | Sample | Age/ median age | Pathological type | Molecular typing | Histological grading | Treatment | OS | Results |
|---------------|--------|-----------------------|----------------------------|----------------------------|-------------------------|---|-----------|--|
| Case report | 1 | 62 | Invasive lobular carcinoma | HR positive, HER2 negative | – | Chemotherapy | 38 months | Breast cancer metastases to the bone marrow can be life-threatening, and chemotherapy improves survival (11). |
| Case report | 1 | 41 | Invasive ductal carcinoma | HER2 overexpression | – | Trastuzumab | 11 months | Trastuzumab may be a beneficial treatment option for patients with HER2-positive bone marrow metastases (10). |
| Case report | 1 | 46 | Invasive lobular carcinoma | HR positive, HER2 negative | – | Palbociclib +letrozole +ovarian suppression | 26 months | A combination of endocrine therapy and CDK4/6 inhibitor may have more extended clinical benefits than chemotherapy, and combination therapy of ET and CDK4/6 inhibitor is less toxic and leads to a better quality of life than chemotherapy (17). |
| Case report | 1 | 58 | – | HR positive, HER2 negative | – | Aromatase inhibitor | 7 months | After hormonal treatment with an aromatase inhibitor. The patient's condition improved (18). |

or even discontinuation (11). Turner et al. found that CDK4/6 inhibitor combined with ET can significantly improve the survival of hormone receptor-positive breast cancer patients with visceral metastases (not visceral crisis) (19). Giovanna Garufi et al. reported a patient with hormone receptor-positive breast cancer with BMM who received letrozole in combination with palbociclib and leuprolide and achieved a 26-month sustained complete remission (17). Sakin et al. retrospectively studied 30 patients with breast cancer BMM who had received chemotherapy and had a median OS of only 6 months (7), which is shorter than the median OS of 18 months in our study. Among the 25 patients with HR⁺/HER2[−] in our research, we were pleasantly surprised to find that the median PFS of 13 patients treated with endocrine therapy was 11 months, which was significantly better than the chemotherapy group of 2 months (Log-rank $p = 0.021$). The maximum PFS was 22 months, and the patient had progressive disease at our follow-up cutoff. The median OS was 23 months longer than the chemotherapy group (5 months). We found that the prognosis of patients in the ET group was significantly improved. The multivariate Cox regression results found that higher ECOG scores and higher age were risk factors affecting the OS of patients, which was consistent with the reported results (2). We counted the AEs after the patients received the two treatment regimens and found that the incidence of AEs of grades ≥ 3 in patients receiving ET was significantly lower than in the chemotherapy group. The proportion of patients with dose reductions due to AEs was also lower in the ET group. Furthermore, no treatment-related SAEs occurred in either group. Indicates that ET may become the most effective and safest treatment option for HR⁺/HER2 patients with BMM, and the sample size should be expanded for further research in the future.

To the best of our knowledge, a larger number of patients with symptomatic BMM were included in this study. The clinical characteristics, prognosis, and adverse events were described in detail. We believe that our current study represents the first thorough evaluation of the efficacy and safety of CDK4/6 inhibitor combined with ET applied to patients with symptomatic BMM and provides valuable information for optimizing therapy.

However, there are limitations to this study. Given the limitations inherent to a retrospective, single-center, small sample size study associated with the challenges in identifying patients considered to be in BMM, our results need to be validated in appropriately designed prospective multicenter prognostic studies and clinical trials comparing different treatment modalities for patients with this condition.

Conclusion

When breast cancer patients present with anemia and fever despite a negative etiological test, BMM should take this into account. For HR⁺/HER2[−] patients with good physical status and can receive active treatment, CDK4/6 inhibitors combined with endocrine therapy can be used to control disease progression, improve quality of life, and prolong survival.

Data availability statement

The raw data supporting the conclusions of this article will be made available by the authors, without undue reservation.

Ethics statement

Ethical review and approval was not required for the study on human participants in accordance with the local legislation and institutional requirements. Written informed consent for participation was not required for this study in accordance with the national legislation and the institutional requirements.

Author contributions

RY: writing—original draft; review and editing. GL: writing—review and editing. ZL: writing—review and editing. LJ: methodology, funding acquisition, writing—review and editing. JC: conceptualization, methodology, supervision, writing—original draft; review and editing. All authors contributed to the article and approved the submitted version.

Funding

This research was funded by the National Natural Science Youth Foundation of China (Grant No. 82001670)

Acknowledgments

We thank all the patients and the authors involved in this study.

Conflict of interest

The authors declare that the research was conducted in the absence of any commercial or financial relationships that could be construed as a potential conflict of interest.

Publisher's note

All claims expressed in this article are solely those of the authors and do not necessarily represent those of their affiliated organizations, or those of the publisher, the editors and the reviewers. Any product that may be evaluated in this article, or claim that may be made by its manufacturer, is not guaranteed or endorsed by the publisher.

References

- Khan S, Awan SA, Jahangir S, Kamran S, Ahmad IN. Bone marrow metastasis in clear cell renal cell carcinoma: A case study. *Cureus* (2019) 11(3):e4181. doi: 10.7759/cureus.4181
- Kopp HG, Krauss K, Fehm T, Staebler A, Zahm J, Vogel W, et al. Symptomatic bone marrow involvement in breast cancer—clinical presentation, treatment, and prognosis: A single institution review of 22 cases. *Anticancer Res* (2011) 31(11):4025–30.
- Xiao L, Luxi S, Ying T, Yizhi L, Lingyun W, Quan P. Diagnosis of unknown nonhematological tumors by bone marrow biopsy: a retrospective analysis of 10,112 samples. *J Cancer Res Clin Oncol* (2009) 135(5):687–93. doi: 10.1007/s00432-008-0503-2
- Luo G, He Y, Yu X. Bone marrow adipocyte: An intimate partner with tumor cells in bone metastasis. *Front Endocrinol (Lausanne)* (2018) 9:339. doi: 10.3389/fendo.2018.00339
- Shin E, Koo JS. The role of adipokines and bone marrow adipocytes in breast cancer bone metastasis. *Int J Mol Sci* (2020) 21(14):4967. doi: 10.3390/ijms21144967
- Walker ND, Patel J, Munoz JL, Hu M, Guio K, Sinha G, et al. The bone marrow niche in support of breast cancer dormancy. *Cancer Lett* (2016) 380(1):263–71. doi: 10.1016/j.canlet.2015.10.033
- Sakin A, Sakalar T, Sahin S, Yasar N, Demir C, Geredeli C, et al. Factors affecting survival and treatment efficacy in breast cancer patients with bone marrow metastasis. *Breast J* (2020) 26(4):815–8. doi: 10.1111/tbj.13647
- Pahouja G, Wesolowski R, Reinbolt R, Tozbikian G, Berger M, Mangini N, et al. Stabilization of bone marrow infiltration by metastatic breast cancer with continuous doxorubicin. *Cancer Treat Commun* (2015) 3:28–32. doi: 10.1016/j.ctcr.2014.11.002
- Cawthorn WP, Scheller EL, Learman BS, Parlee SD, Simon BR, Mori H, et al. Bone marrow adipose tissue is an endocrine organ that contributes to increased circulating adiponectin during caloric restriction. *Cell Metab* (2014) 20(2):368–75. doi: 10.1016/j.cmet.2014.06.003
- Xu L, Guo F, Song S, Zhang G, Liu Y, Xie X. Trastuzumab monotherapy for bone marrow metastasis of breast cancer: A case report. *Oncol Lett* (2014) 7(6):1951–3. doi: 10.3892/ol.2014.1999
- Akagi H, Shimada A, Chin K, Domoto H. Successful stabilization of symptomatic bone marrow metastasis two times in a breast cancer patient. *Anticancer Res* (2021) 41(6):3139–44. doi: 10.21873/anticancer.15099
- Liu L, Zhang J, Chen M, Ren S, Liu H, Zhang H. Anemia, and thrombocytopenia as initial symptoms of occult breast cancer with bone marrow metastasis: A case report. *Med (Baltimore)* (2017) 96(45):e8529. doi: 10.1097/MD.00000000000008529
- Meng Q, Zhou L, Liang H, Hu A, Zhou H, Zhou J, et al. Spinespecific downregulation of LAPTM5 expression promotes the progression and spinal metastasis of estrogen receptorpositive breast cancer by activating glutamindependent mTOR signaling. *Int J Oncol* (2022) 60(4):47. doi: 10.3892/ijo.2022.5337
- Bjelic-Radicic V, Stöger H, Winter R, Beham-Schmid C, Petru E. Long-term control of bone marrow carcinosis and severe thrombocytopenia with standard-dose chemotherapy in a breast cancer patient: a case report. *Anticancer Res* (2006) 26(2b):1627–30.
- Freyer G, Ligneau B, Trillet-Lenoir VV. Palliative hormone therapy, low-dose chemotherapy, and bisphosphonate in breast cancer patients with bone marrow involvement and pancytopenia: Report of a pilot experience. *Eur J Internal Med* (2000) 11(6):329–33. doi: 10.1016/s0953-6205(00)00121-7
- Ardavanis A, Kountourakis P, Orphanos G, Rigatos G. Low-dose capecitabine in breast cancer patients with symptomatic bone marrow infiltration: a case study. *Anticancer Res* (2008) 28(1b):539–41.
- Garufi G, Carbognin L, Orlandi A, Palazzo A, Tortora G, Bria E. The therapeutic challenge of disseminated bone marrow metastasis from HR-positive HER2-negative breast cancer: Case report and review of the literature. *Front Oncol* (2021) 11:651723. doi: 10.3389/fonc.2021.651723
- Rahmat C, Ikhwan R. Hormonal treatment for symptomatic bone marrow metastasis in breast cancer patients. *Maedica (Bucur)* (2018) 13(3):238–40. doi: 10.26574/maedica.2018.13.3.238
- Turner NC, Finn RS, Martin M, Im SA, DeMichele A, Ettl J, et al. Clinical considerations of the role of palbociclib in the management of advanced breast cancer patients with and without visceral metastases. *Ann Oncol* (2018) 29(3):669–80. doi: 10.1093/annonc/mdx797



OPEN ACCESS

EDITED BY
Dayanidhi Raman,
University of Toledo, United States

REVIEWED BY
Assie Olfatbakhsh,
Motamed Cancer Institute, Iran
Teodora Alexa-Stratulat,
Grigore T. Popa, University of
Medicine and Pharmacy, Romania

*CORRESPONDENCE
Mingli Han
✉ Minglihan@126.com

†These authors have contributed
equally to this work and share
first authorship

SPECIALTY SECTION
This article was submitted to
Breast Cancer,
a section of the journal
Frontiers in Oncology

RECEIVED 01 June 2022
ACCEPTED 14 December 2022
PUBLISHED 04 January 2023

CITATION
Wang F, Gu Z, Zhao X, Chen Z,
Zhang Z, Sun S and Han M (2023)
Metabolic characteristics of the
various incision margins for breast
cancer conservation surgery.
Front. Oncol. 12:959454.
doi: 10.3389/fonc.2022.959454

COPYRIGHT
© 2023 Wang, Gu, Zhao, Chen, Zhang,
Sun and Han. This is an open-access
article distributed under the terms of
the [Creative Commons Attribution
License \(CC BY\)](https://creativecommons.org/licenses/by/4.0/). The use, distribution
or reproduction in other forums is
permitted, provided the original author
(s) and the copyright owner(s) are
credited and that the original
publication in this journal is cited, in
accordance with accepted academic
practice. No use, distribution or
reproduction is permitted which does
not comply with these terms.

Metabolic characteristics of the various incision margins for breast cancer conservation surgery

Fang Wang[†], Zongze Gu[†], Xunan Zhao, Zhuo Chen,
Zhe Zhang, Shihao Sun and Mingli Han*

Department of Breast Surgery, The First Affiliated Hospital of Zhengzhou University,
Zhengzhou, China

Background: Breast cancer (BC) has recently become the most prevalent malignancy in women. There are many alternative treatments for BC, and for aesthetic and postoperative quality of life concerns, breast-conserving surgery and corresponding adjuvant therapy have become the predominant treatment for early invasive BC. Currently, the main method used to assess the margins for breast-conserving surgery is intraoperative pathological diagnosis. However, the designation of surgical margins is controversial, and metabolomics may be a novel approach to evaluate surgical margins.

Methods: We collected specimens from 10 breast cancer patients and samples from its surrounding tissues and divided them into cancerous tissue and 1 mm, 2 mm, 3 mm, 5 mm and 10 mm cutting edge tissues, with a total of 60 samples. The samples were analyzed by mass spectrometry on an ultra-performance liquid chromatography-quadrupole/Orbitrap high resolution platform. The data were then statistically analyzed to detect metabolic changes in the different cutting edges and to identify possible surgical cutting edges with statistically significant findings. Abnormal metabolic pathways were identified by Kyoto Encyclopedia of Genes and Genomes (KEGG), which elucidated potential markers.

Results: Statistical analysis indicated that there were substantial differences between the 1 mm margin tissue and the cancer tissue, while there were no statistically significant differences between the 1 mm tissue and tissues from the other margins. The levels of 6 metabolites in the 1 mm tissue were significantly different from those in the cancer tissue and were not significantly different from those in the 2 mm tissue. The six metabolites were pyruvate, N-acetyl-L-aspartate, glutamic acid, γ -aminobutyric acid, fumaric acid, and citric acid. Metabolic pathways such as amino acid metabolism and amino t-RNA synthesis in the margin tissue were significantly distinct from those in cancer tissues based on KEGG analysis.

Conclusion: There was a significant difference between the 1 mm margin tissue and the cancerous tissue. Based on metabolomic analysis, the 1 mm negative margin is sufficient for surgery, and the six metabolites that we identified as abnormal, including pyruvic acid, N-acetyl-L-aspartic acid, glutamic acid, gamma-aminobutyric acid, fumaric acid and citric acid, may serve as biomarkers for a negative margin and help surgeons select an appropriate surgical margin.

KEYWORDS

breast cancer, breast-conserving surgery, surgical margin, metabolomics, potential biomarker

Introduction

Among the malignancies to occur in women in recent years, breast cancer is the most common malignancy in terms of incidence (1), which has exhibited a slow increase of approximately 0.5% per year since 2000; this increase is related to the current decline in fertility and the increasing prevalence of overweightness in society (2), and breast cancer is the leading cause of death from malignancies in women aged 20 to 59 years (1). There are many treatment options available for breast cancer, with surgery, radiotherapy, chemotherapy, endocrine therapy and immunosuppressive agents all offering a good chance of survival. Breast-conserving surgery and the corresponding adjuvant treatment are now the accepted treatment for early invasive breast cancer, providing patients with better quality of life and cosmetic results and more psychological benefits than traditional radical surgery. It has been demonstrated through various trials that breast-conserving surgery does have acceptable morbidity and mortality rates (3, 4). There are many factors that influence the recurrence and prognosis of breast cancer, such as pathological classification, tumor size, presence of distant metastases and depth of infiltration; additionally, regarding breast-conserving surgery, the impact of the surgical margins should not be underestimated (5, 6).

The designation of surgical margins for breast-conserving surgery has long been controversial, with a wider margin affecting the patient's postoperative aesthetics and a narrower margin increasing the risk of reoperation and local recurrence. Some studies have shown that most surgeons currently prefer a 2 mm margin (7). However, guidelines suggest that with good preoperative diagnostic and ancillary techniques, excessive excision of healthy tissue is of no better benefit, leading to the "no tumor ink" guideline (8). Currently, the main method used to diagnose negative margins is intraoperative freezing as judged by the pathologist, but this technique has limitations and can

also increase the duration of the procedure, with a considerable physical and financial impact on the patient. In recent years, new techniques have also emerged, such as microcomputed tomography for intraoperative assessment (9). However, this technique has not been widely used in clinical practice. We applied metabolomics to analyze and assess the surgical margins and identify possible surgical margins and potential markers. However, metabolomics has certain limitations that are not associated with traditional intraoperative rapid frozen pathology and other detection methods. The preprocessing of tissue specimens and the processing of data after mass spectrometry analysis take a longer time and do not provide timely feedback to clinicians; additionally, the technology is more costly, which increases the financial pressure on patients.

A distinctive feature of cancer is metabolic reprogramming, whereby cancer tissues exhibit altered metabolic pathways to adapt to their environment and meet their own growth requirements; for example, cancer tissues can preferentially undergo anaerobic glycolysis under aerobic conditions (10), which is a phenomenon known as the "Warburg effect". Metabolomics has been extensively used to study breast cancer, offering novel approaches to its diagnosis, treatment and prognosis. Triple-negative breast cancer, which is a substantial challenge, is characterized by a high recurrence rate, few treatment options and a poor prognosis (11, 12). Jiang et al. (13, 14) have provided new possibilities for triple-negative breast cancer through metabolomics studies. Research has shown that triple-negative breast cancer can be classified into three types, namely, the lipogenic subtype, glycolytic subtype and mixed subtype, based on the main abnormal metabolic pathways (13), with various subtypes exhibiting different sensitivities to different treatments. This typing can provide new therapeutic tools; studies investigating these approaches are unlike the numerous studies aiming to identify a more precise method for pathological subtyping (15, 16). Metabolomics has been understudied in the context of breast-conserving surgery; thus, we used metabolomics techniques to

analyze different incision margins to provide the possibility for a negative incision margin for breast-conserving surgery.

In this study, we used ultrahigh-performance liquid chromatography-quadrupole/Orbitrap high-resolution mass spectrometry (UHPLC-Q-Orbitrap HRMS) to metabolically analyze 60 specimens that were collected and then statistically analyzed the data to identify tissue at cut edges with significant differences from the tumor tissue and to identify potential markers that might be present.

Materials and methods

Sample collection

After obtaining informed consent from patients, we collected cancer tissue specimens from 10 breast cancer patients at the First Affiliated Hospital of Zhengzhou University and samples from the surrounding tissue in 2021 and maintained them in a -80°C refrigerator until they were machine-processed and examined. We separated each specimen into six groups of cancer tissues, tissues with a 1 mm cut edge, tissues with a 2 mm cut edge, tissues with a 3 mm cut edge, tissues with a 5 mm cut edge and tissues with a 1 cm cut edge, for a total of 60 samples for UHPLC-MS/MS processing.

Sample preparation

First, we weighed each specimen, added 100 µl of pure methanol solution to 10 mg of tissue, added small steel beads and placed the samples into a grinder (SCIENTZ-48 high throughput tissue grinder) for 30 minutes. After removal, each sample was placed in a centrifuge (Centrifuge CF16RN HITACHI, Tokyo, Japan) and centrifuged at 3000 rpm for 30 minutes at 4°C. After extraction of the supernatant, the specimens were concentrated in a concentrator, removed and added to 300 µl of pure methanol solution and placed in a redissolution machine (Mutil-Tube Vortexer) at 2500 rpm for 3 minutes. Then, we placed the samples in a centrifuge at 3000 rpm for 30 minutes at 4°C. One hundred microliters of supernatant was extracted from each sample and transferred to an autosampler vial for in-machine UHPLC-MS/MS processing. The reproducibility and reliability of the UHPLC-MS/MS system was assessed by means of quality control (QC) samples.

UHPLC-Q-Orbitrap HRMS analysis

We used an ultra-performance liquid chromatography system (Thermo Fisher Scientific Dionex, Waltham,

Massachusetts, USA) and an Acquity UHPLC BEH C18 column (2.1 mm × 100 mm, 1.7 µm, Waters, USA) to achieve chromatographic separation and gradient elution. We used acetonitrile as mobile phase A and water containing 0.1% formic acid as mobile phase B at a flow rate of 0.2 mL/min. The elution gradient was employed as follows: 0–0.5 min, 5% A, 0.5–2 min, 5–40% A; 3–8 min, 40–60% A; 9–11 min, 80–90% A, 12–13 min, 90–100% A, 14–15 min, 100% A.

- We performed MS separations in full scan mode using a Q-Orbitrap mass spectrometer equipped with thermoelectric spray ionization (HESI) (Thermo Scientific, San Jose, USA). We used a mass spectrometer in full scan mode to obtain positive and negative mode mass spectra. Substances in the mass range of 80 to 1200 m/z could be scanned by the instrument. The speed of the auxiliary gas was set to 10 arb, and the temperature was set to 300°C. The capillary temperature was set to 320°C. The spray voltages in positive and negative mode were set to 3.5 kV and 2.8 kV, respectively.

Data processing

We used Compound Discoverer 3.1 software (version 3.0, Thermo Scientific) to extract metabolites from the raw data file to generate a comprehensive peak table containing retention times (RT), molecular weights and peak areas. The data were then visualized using Xcalibur™ (Version 3.0, Thermo Fisher Scientific) software and compared to the Human Metabolomics Database (HMDB, <http://hmdb.ca/>) to identify metabolites from different sources. The metabolites screened by the HMDB were then subjected to enrichment analysis using the KEGG database to identify pathways with $p < 0.05$ and a false discovery rate (FDR) < 0.05 .

Statistical analysis

Each sample corresponding to a metabolite contains m/z values, ion peak areas and RT. We used SIMCA software (Version 14.0 Umetrics, Umea, Sweden) to perform principal component analysis (PCA) and orthogonal partial least squares (OPLS-DA) and to obtain projected variable importance (VIP) values. Fold change and t test (p value < 0.05 , FDR < 0.05) results were obtained by MetaboAnalyst (<https://www.MetaboAnalyst.ca/>). Receiver operating characteristic (ROC) curves and area under the curve (AUC) were used to assess the sensitivity and accuracy of analyses performed using the metrics.

Results

Clinical characteristics of the breast cancer patients

We collected tissue samples from 10 clinical breast cancer patients and the adjacent tissue and divided the 60 samples into 6 groups, including tumor tissue and tissues located 1 mm, 2 mm, 3 mm, 5 mm and 10 mm from the tumor margin, for analysis by UHPLC-MS/MS. The clinical characteristics of the 10 patients are shown in [Supplementary Table 1](#).

Metabolomic analysis

To identify a possible negative cut edge, we performed UHPLC-MS/MS analysis on the tumor tissue and tissues from different cut edges, analyzed and processed the data, and imported the analyzed data into SIMCA version 14.0 for statistical analysis. First, we performed PCA on the data obtained from the 1 mm cut edge and data obtained from cancer tissue in negative ion mode ([Figure 1A](#)). Immediately afterward, we performed OPLS-DA ([Figure 1B](#)) with an R^2Y of 0.96 and a Q^2 of 0.801. Significant detachment was found between the cancerous tissue and the 1 mm incision margin tissue, with the same result observed in the positive ion mode; these data are shown in [Supplementary Table 2](#) and [Supplementary Figure S1](#). There was also apparent separation between other margin tissues and cancerous tissues ([Figure 2](#)). The variation among the different cut edge tissues was analyzed by PCA ([Figure 3](#)). The data showed no statistically significant difference between the tissue at the 1 mm margin and the tissue at the other margins, so we designated the margin closest to the

cancerous tissue with a statistically significant difference as the possible negative margin, which was the 1 mm margin. We identified over 50 endogenous differentially expressed metabolites from a set of metabolites, with $P < 0.05$, $VIP > 1.0$ and fold change > 1.5 as the cutoff. We screened the metabolites with statistically significant differences in levels between the 1 mm cut margin tissue and cancer tissue by KEGG, and the results of the statistically significant aberrant metabolic pathways found to be enriched are shown in [Table 1](#); the results indicated that 18 differential metabolites were enriched in statistically significant aberrant metabolic pathways. The statistically significant abnormal metabolic pathways included those for amino acids such as glutamate, alanine, aspartate, histidine, arginine, proline, glutamine, tyrosine and phenylalanine, abnormal synthesis of aminyl-tRNA, and abnormal pantothenic acid biosynthesis. We generated a heatmap of the levels of metabolites capable of being enriched in statistically significant aberrant metabolic pathways by MetaboAnalyst to demonstrate the differences in metabolite levels between 1 mm cut edge tissue and cancerous tissue ([Figure 4](#)). The topological analysis of the aberrant metabolic pathways indicated that amino acid metabolism was the main deviant metabolic pathway in cancerous tissues ([Figure 5](#)).

Identification of potential markers

We selected six metabolites from a large number of metabolites with statistically significant differences in levels (p value < 0.05 , $VIP > 1.0$ and included in all statistically significant differences between margin tissue and cancer tissue). The OPLS-DA of N-acetyl-aspartate, alanine, glutamic acid, aminobutyric acid, citric acid and fumaric acid values were found to be

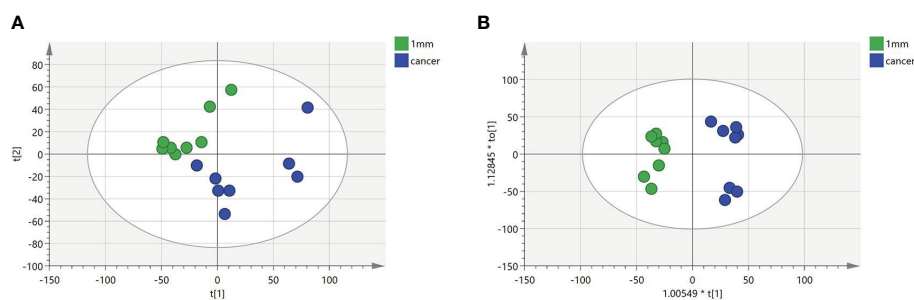


FIGURE 1

Multivariate statistical analysis of two groups. Principal component analysis (PCA) plot comparing between 1 mm cut edge tissue and cancer tissue in (A) negative ion mode; orthogonal partial least squares discriminant analysis (OPLS-DA) score plots comparing between 1 mm cut edge tissue and cancer tissue in (B) negative ion mode.

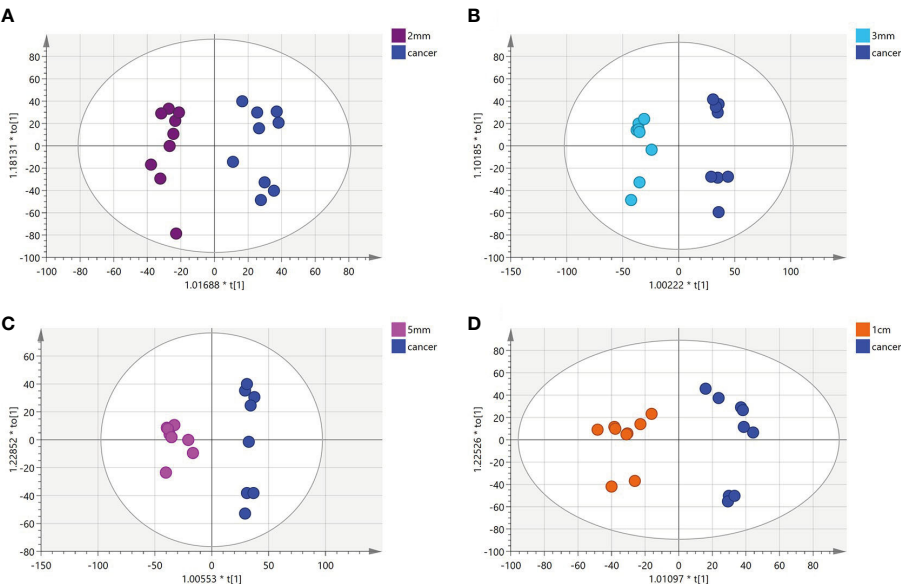


FIGURE 2
(A-D) Orthogonal partial least squares discriminant analysis (OPLS-DA) score plots comparing between tissue located at other surgical margins and cancer tissue.

separated between the 1-mm cut edge tissue and the cancer tissue (Figure 6A). We also performed OPLS-DA of these six metabolites using the 1-mm cut edge tissue and the 2-mm cut edge tissue and found no significant difference between them

(Figure 6B). The information for these six metabolites is shown in Table 2. We then analyzed the differences in the levels of each of these six metabolites between the cancerous tissue and the 1-mm cut edge tissue (Figure 7). As expected, each metabolite had

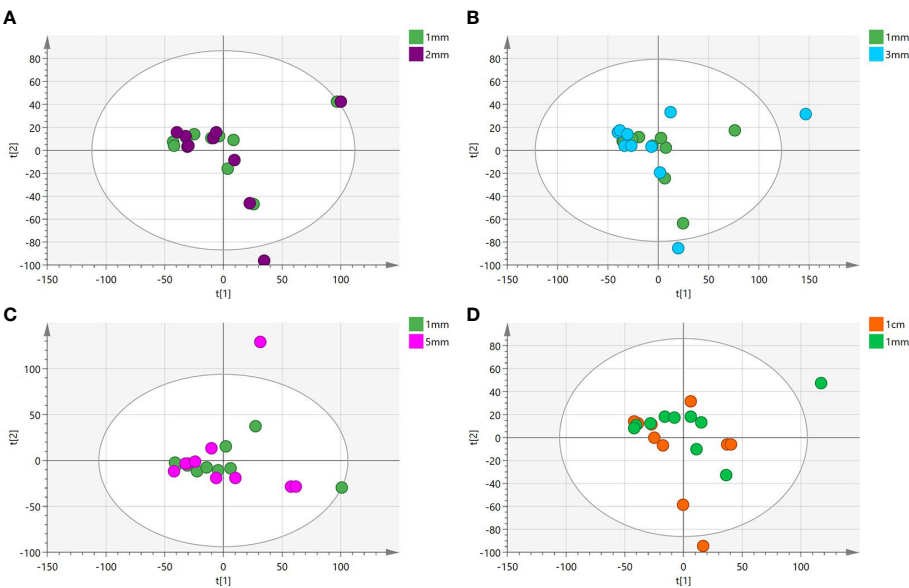


FIGURE 3
(A-D) Principal component analysis(PCA) plot comparing between tissue located at the 1mm surgical margin and other surgical margins.

TABLE 1 Statistically significant metabolic pathways that differed between 1 mm cut margin tissue and cancer tissue identified by KEGG analysis.

| Metabolite Set | Total | Hits | Expect | P Value | FDR |
|---|-------|------|--------|---------|--------|
| Alanine, aspartate and glutamate metabolism | 28 | 7 | 1.34 | 2.31E-4 | 0.0127 |
| Aminoacyl-tRNA biosynthesis | 48 | 9 | 2.3 | 2.31E-4 | 0.0127 |
| Pantothenate and CoA biosynthesis | 19 | 4 | 0.911 | 0.0109 | 0.269 |
| Phenylalanine, tyrosine and tryptophan biosynthesis | 4 | 2 | 0.192 | 0.0128 | 0.269 |
| D-Glutamine and D-glutamate metabolism | 6 | 2 | 0.288 | 0.03 | 0.451 |
| Arginine and proline metabolism | 38 | 5 | 1.82 | 0.0322 | 0.451 |
| Histidine metabolism | 16 | 3 | 9.767 | 0.0378 | 0.451 |

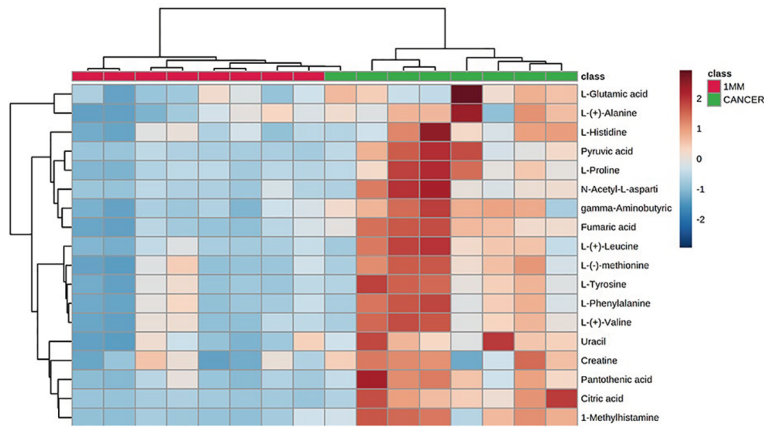


FIGURE 4 Heatmap indicating the relative levels of statistically significant differential metabolites in 1-mm cut edge tissue and cancerous tissue.

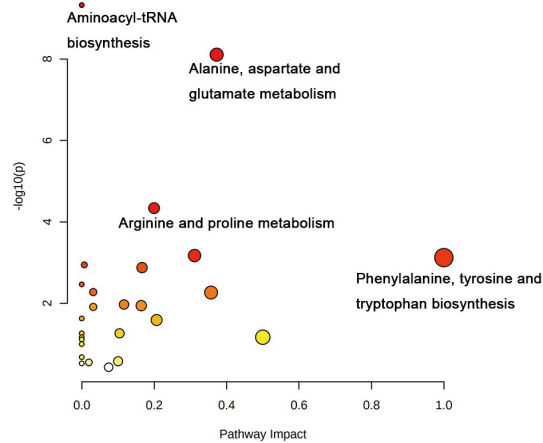


FIGURE 5 Correlation network analysis of metabolites identified in untargeted metabolomics. Correlation analysis of 18 differential metabolites with statistical differences between 1 mm surgical margin and cancerous tissue.

significantly different levels between the cancerous tissue and the 1-mm cut edge tissue. This finding was consistent with our expectations, suggesting that these differential metabolites may be potential markers of negative cut margins. We tested the ability of these six metabolites to distinguish between cancer and negative margins by plotting ROC curves using the levels of five metabolites, which resulted in an AUC > 0.9 and one metabolite with an AUC > 0.8 (Figure 8), demonstrating the good sensitivity and specificity of these indicators.

Discussion

Breast cancer is already the most prevalent cancer in women in today's society (1); although there are many treatments available, breast-conserving surgery is one of the accepted treatments for early invasive breast cancer, with most surgeons preferring a 2-mm margin (7). The Society of Surgical Oncology (SSO) and the American Society of Radiation Oncology

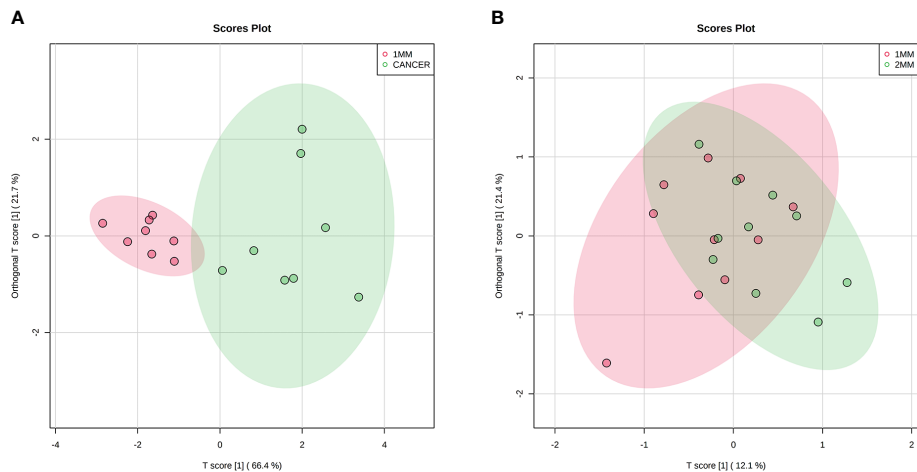


FIGURE 6 Orthogonal partial least squares discriminant analysis (OPLS-DA) score plots of 6 potential biomarkers in tissue located at 1 mm surgical margin and cancerous tissue (A), showing a clear separation. Orthogonal partial least squares discriminant analysis (OPLS-DA) score plots of 6 potential biomarkers in tissue located at the 1 mm surgical margin and 2 mm surgical margin (B), with no significant difference.

(ASTRO)-American Society of Clinical Oncology (ASCO) consensus guidelines state that the principle of “no tumor ink” is recommended for breast-conserving surgical margins in stage I and II invasive breast cancer, which can also achieve a reduction in local recurrence rates (8). The main method used to diagnose cut margins is currently intraoperative rapid cytopathology; however, this method has limitations and is less sensitive than conventional pathology using paraffin blocks (17). Other techniques are also used in the diagnosis of cut edges, such as mammography, intraoperative breast ultrasound, the adjunctive use of magnetic resonance imaging (MRI) techniques and, in recent years, optical techniques and isotope methods. Macroscopic margin assessment is also a diagnostic method used to evaluate cutting edges (18–20); however, these methods have limitations and have developed slowly.

Metabolomics is a field that has experienced rapid growth in recent years and has a promising future as a complement to genomics, proteomics and other “downstream” omics approaches. Metabolomics has great potential for use in relatively noninvasive liquid tests that can be used in the diagnosis and prognosis of cancer (21). In this study, we investigated the metabolism of different cut edge tissues and cancer tissues using 10 breast cancer samples by UHPLC-MS/MS and found statistically significant differences between 1 mm cut edge tissues and cancer tissues and no statistically significant differences between 1 mm cut edge tissues and other tissues from the remaining cut edges. We also identified six metabolites involved in abnormal metabolism ($P < 0.05$, $VIP > 1.0$, $AUC > 0.8$) that could be potential markers for identifying negative incision margins. However, metabolomics has certain limitations that are not associated with traditional intraoperative rapid frozen

TABLE 2 Statistical analysis of potential metabolic biomarkers.

| No. | Metabolities | Lon mode | RT(min) | Molecular | VIP | P Value |
|-----|--------------------------|----------|---------|-----------|------|-----------|
| 1 | Pyruvic acid | N | 1.407 | 88.01493 | 1.80 | 0.001385 |
| 2 | N-Acetyl-L-aspartic acid | N | 1.432 | 175.0479 | 1.57 | 0.005883 |
| 3 | L-Glutamic acid | N | 0.938 | 147.052 | 1.80 | 0.000828 |
| 4 | gamma-Aminobutyric acid | N | 0.963 | 103.0637 | 1.85 | 0.000196 |
| 5 | Fumaric acid | N | 1.630 | 116.0098 | 1.94 | 0.0000652 |
| 6 | Citric acid | N | 1.433 | 192.0262 | 1.97 | 0.000104 |

RT, retention time; VIP, variable importance in projection.

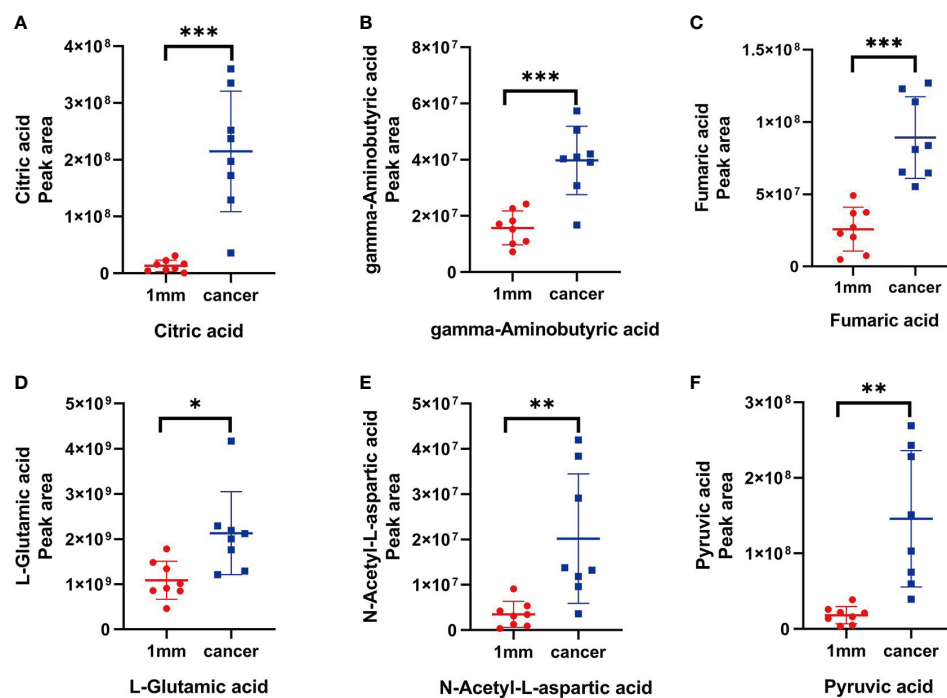


FIGURE 7

(A–F) The peak areas of citric acid, gamma-aminobutyric acid, fumaric acid, L-glutamic acid, N-acetyl-L-aspartic acid and pyruvic acid in tissue located at the 1 mm surgical margin and tumor tissue, with significant differences ($P < 0.05$). "*" stands for the $p < 0.05$, "***" stands for the $p < 0.01$, "****" stands for the $p < 0.001$.

pathology and other detection methods. The preprocessing of tissue specimens and the processing of data after mass spectrometry analysis take a longer time and do not provide timely feedback to clinicians; additionally, the technology is more costly, which increases the financial pressure on patients.

In the present study, amino acid metabolism was significantly abnormal in the tumor tissue, and many diseases are known to be associated with abnormal amino acid metabolism (22, 23). We found significantly higher concentrations of glutamate, which plays an important physiological role in the body as a nonessential amino acid and excitatory neurotransmitter, in the cancer tissues in this study. It has been shown that glutamate levels are significantly elevated in cancer tissues (24). Glutamate is produced from glutamine by the action of glutaminase, an enzyme found in the internal mitochondrial membrane, and it has been shown that glutaminase activity is increased by its overexpression in cancer tissues (25, 26), leading to increased levels of glutamate in cancer tissues, which is consistent with our findings.

Aspartate metabolism was found to be significantly active in the cancer tissues in this study, and concentrations were significantly increased in the cancer tissues. It has been suggested that aspartate, asparagine and asparagine synthase

may be potential markers for surgical cutting edges in oral squamous cell carcinoma (27), and studies have found significantly higher concentrations of aspartate and significantly increased activity of asparagine synthase in cancer tissue; the exact mechanism underlying this phenomenon is unclear, as indicated by our experimental results.

In addition to abnormal amino acid metabolism, abnormal aminyl-tRNA biosynthesis in cancer tissues was a distinctive feature of the results in this study. Aminyl-tRNA biosynthesis has been found to be significantly elevated in metabolomic studies of gastric cancer (28), in which metabolomic and bioinformatics analysis of gastric and paracancerous tissues revealed that aminyl-tRNA biosynthesis exhibited abnormally increased activation in gastric cancer tissues, the expression level of phenylalanine-tRNA synthetase was associated with poor survival, and the expression level of threonine-tRNA synthetase was associated with tumor grade. In addition, amyl-tRNA synthetase and its interacting proteins play an important role in tumorigenesis (29, 30), suggesting that the amyl-tRNA biosynthetic pathway offers a new possibility for limiting tumor growth in the future.

In conclusion, by using UHPLC-MS/MS to investigate the metabolism of different marginal tissues and cancerous tissues from 10 breast cancer specimens, we identified the 1-mm margin

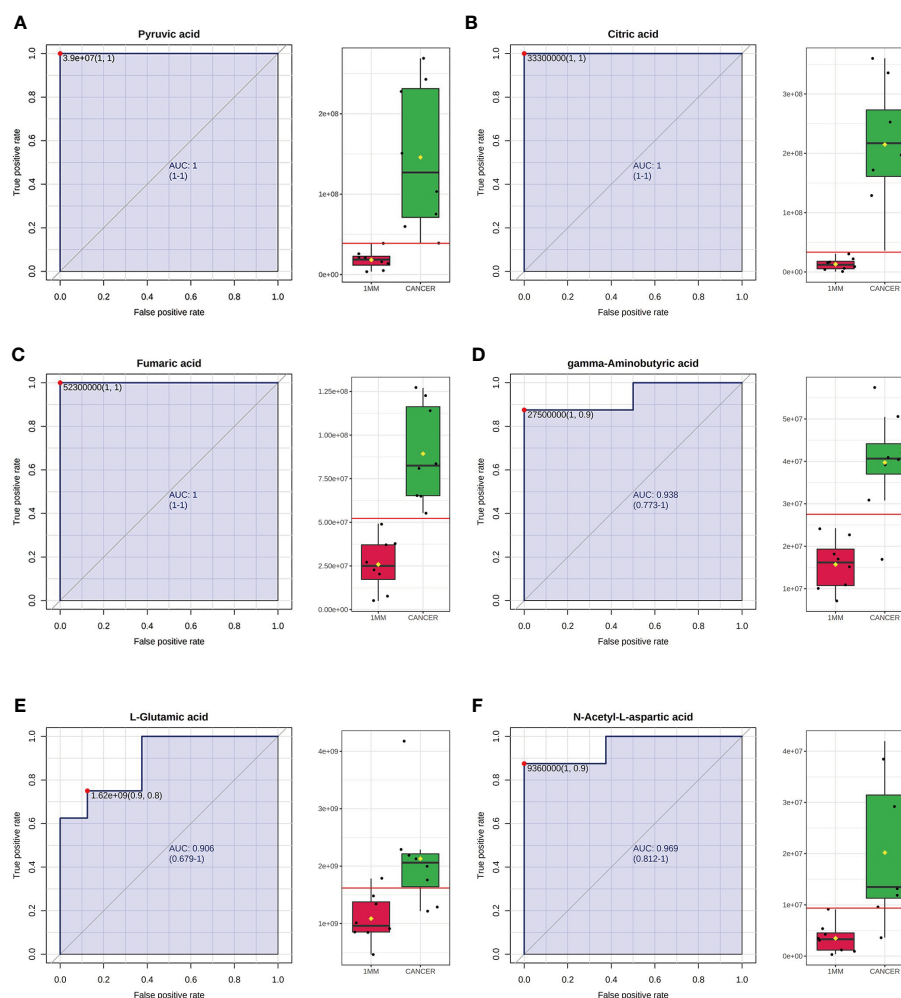


FIGURE 8

Receiver operating characteristic (ROC) curves using the levels of pyruvic acid (A), citric acid (B), fumaric acid (C), gamma-aminobutyric acid (D), L-glutamic acid (E) and N-acetyl-L-aspartic acid (F). The AUCs obtained using the levels of pyruvic acid, citric acid, fumaric acid, gamma-aminobutyric acid, L-glutamic acid and N-acetyl-L-aspartic acid were 1 (95% CI=1-1), 1 (95% CI=1-1), 1 (95% CI=1-1), 0.938 (95% CI=0.773-1), 0.906 (95% CI=0.679-1) and 0.969 (95% CI=0.812-1), respectively. The box plots show the median, quartiles, and whole range of peak areas of the levels of these metabolites.

as a possible margin for breast-conserving surgery. The results of this study are limited in that we collected specimens from only 10 breast cancer patients, which is a small sample size. This study is a preliminary study that performed an initial examination of the surgical margins of breast-conserving surgery from a metabolomics perspective to provide possibilities for clinicians. We have also identified six potential markers, but the value of these markers has yet to be further validated, and we will recruit more clinical patients in the future for further research and to validate the results. Therefore, the method is still experimental and has certain limitations. The pretreatment of tissues and data processing after mass spectrometry analysis require a longer time, and the expensive cost is also a nonnegligible problem, so the method may take a long time to enter clinical practice.

Data availability statement

The raw data supporting the conclusions of this article will be made available by the authors, without undue reservation.

Ethics statement

The studies involving human participants were reviewed and approved by Ethics Committee of Scientific Research Project of The First Affiliated Hospital of Zhengzhou Unive. The patients/participants provided their written informed consent to participate in this study.

Author contributions

MH and FW designed the study. ZG and SS carried out the experiments. ZG and XZ undertook the data analysis and wrote the manuscript. ZC and ZZ assisted in Data curation and editing the manuscript. All authors contributed to the article and approved the submitted version.

Funding

The study was supported by the Henan Provincial Medical Science and Technology Tackling Program Project (201702016).

Acknowledgments

We thank professor Zhi Sun (Pharmacy Department of the First Affiliated Hospital of Zhengzhou University) and the Pharmacy Department of the First Affiliated Hospital of Zhengzhou University for helpful bioinformatic analysis of data and UHPLC-MS analysis. The authors thank all the participants who contributed to this study and the clinical patients who agreed to participate in contributing to our study.

References

1. Sigel RL, Miller KD, Fuchs HE, Jemal A. Cancer statistics. *CA Cancer J Clin* (2021) 71(1):7–33. doi: 10.3322/caac.21654
2. Sigel RL, Miller KD, Fuchs HE, Jemal A. Cancer statistics. *CA Cancer J Clin* (2022) 71(1). doi: 10.3322/caac.21708
3. Fisher B, Anderson S, Bryant J, Margolese RG, Deutsch M, Fisher ER, et al. Twenty-year follow-up of a randomized trial comparing total mastectomy, lumpectomy, and lumpectomy plus irradiation for the treatment of invasive breast cancer. *N Engl J Med* (2002) 347(16):1233–41. doi: 10.1056/NEJMoa022152
4. Margenthaler JA, Gao F, Klimberg VS. Margin index: a new method for prediction of residual disease after breast-conserving surgery. *Ann Surg Oncol* (2010) 17(10):2696–701. doi: 10.1245/s10434-010-1079-z
5. Fleming FJ, Hill ADK, Mc Dermott EW, O'Doherty A, O'Higgins NJ, Quinn CM. Intraoperative margin assessment and re excision rate in breast conserving surgery. *Eur J Surg Oncol* (2004) 30(3):233–7. doi: 10.1016/j.ejso.2003.11.008
6. Silverstein MJ, Lagios MD, Groshen S, Waisman JR, Lewinsky BS, Martino S, et al. The influence of margin width on local control of ductal carcinoma in situ of the breast cancer. *CancerRes* (1999) 340(19):1455–61. doi: 10.1056/NEJM199905133401902
7. Blair SL, Thompson K, Rococco J, Malcarne V, Beitsch PD, Ollia DW. Attaining negative margins in breast-conservation operations: Is there a consensus among breast surgeons? *J Am Coll Surg* (2009) 209(5):608–13. doi: 10.1016/j.jamcollsurg.2009.07.026
8. Moran MS, Schnitt SJ, Giuliano AE, Harris JR, Khan SA, Horton J, et al. Society of surgical oncology-American society for radiation oncology consensus guideline on margins for breast-conserving surgery with whole-breast irradiation in stages I and II invasive breast cancer. *J Clin Oncol* (2014) 32(14):1507–15. doi: 10.1200/JCO.2013.53.3935
9. Qiu SQ, Dorrius MD, de Jongh SJ, Jansen L, de Vries J, Schröder CP, et al. Micro-computed toography (micro-CT) for intraoperative surgical margin assessment of breast cancer: a feasibility study in breast conserving surgery. *Eur J Surg Oncol* (2018) 11:44(11):1708–13. doi: 10.1016/j.ejso.2018.06.022
10. Warburg O. On the origin of cancer cells. *Science* (1956) 123:309–14. doi: 10.1126/science.123.3191.309

Conflict of interest

The authors declare that the research was conducted in the absence of any commercial or financial relationships that could be construed as a potential conflict of interest.

Publisher's note

All claims expressed in this article are solely those of the authors and do not necessarily represent those of their affiliated organizations, or those of the publisher, the editors and the reviewers. Any product that may be evaluated in this article, or claim that may be made by its manufacturer, is not guaranteed or endorsed by the publisher.

Supplementary material

The Supplementary Material for this article can be found online at: <https://www.frontiersin.org/articles/10.3389/fonc.2022.959454/full#supplementary-material>

11. Denkert C, Liedtke C, Tutt A, von Minckwitz G. Molecular alterations in triple-negative breast cancer-the road to new treatment strategied. *Lancet* (2017) 389(10087):2430–22. doi: 10.1016/S0140-6736(16)32454-0
12. Dignam JJ, Dukic V, Anderson SJ, Mamounas EP, Wickerham DL, Wolmark N. Hazard of recurrence and adjuvant treatment effects over time in lymph node-negative breast cancer. *Breast Cancer Res Treat* (2009) 116(3):595–602. doi: 10.1007/s10549-008-0200-5
13. Gong Y, Ji P, Yang YS, Xie S, Jiang YZ, Xiao Y, et al. Metabolic-Pathway-Based subtyping of triple-negative breast cancer reveals potential therapeutic targets. *Cell Metab* (2021) 33(1):51–64. doi: 10.1016/j.cmet.2020.10.012
14. Xiao Y, Ma D, Yang YS, Yang F, Jiang YZ, Shao ZM, et al. Comprehensive metabolomics expands precision medicine for triple-negative breast cancer. *Cell Res* (2022) 32(5):477–90. doi: 10.1038/s41422-022-00614-0
15. Bareche Y, Venet D, Ignatiadis M, Aftimos P, Piccart M, Rothe F, et al. Unravelling triple-negative breast cancer molecular heterogeneity using an integrative multiomic analysis. *Ann Oncol* (2018) 29(4):895–902. doi: 10.1093/annonc/mdy024
16. Garrido-Castro AC, Lin NU, Polyak K. Insights into molecular classification of triple-negative breast cancer: Improving patient selection for treatment. *Cancer Discovery* (2019) 9(2):176–98. doi: 10.1158/2159-8290.CD-18-1177
17. Nowikiewicz T, Srutek E, Glowacka-Mrotek I, Tarkowska M, Zyromska A, Zegarski W. Clinical outcomes of an intraoperative surgical margin assessment using the fresh frozen section method in patients with invasive breast cancer undergoing breast-conserving surgery – a single center analysis. *Sci Rep* (2019) 9(1):13441. doi: 10.1038/s41598-019-49951-y
18. Butler-Henderson K, Lee AH, Price RI, Waring K. Intraoperative assessment of margins in breast conserving therapy: A systematic review. *Breast* (2014) 23(2):112–9. doi: 10.1016/j.breast.2014.01.002
19. Nowikiewicz T, Nowak A, Zegarski W, Wiśniewska M, Wiśniewski M. Diagnostic value of preoperative axillary lymph node ultrasound assessment in patients with breast cancer qualified for sentinel lymph node biopsy. *Wideochir Inne Tech Maloinwazyjne* (2015) 10(2):170–7. doi: 10.5114/wiitm.2015.52264

20. Rubio IT, Ahmed M, Kovacs T, Marco V. Margins in breast conserving surgery: A practice-changing process. *Eur J Surg Oncol* (2016) 42(5):631–40. doi: 10.1016/j.ejso.2016.01.019
21. Hart CD, Tenori L, Luchinat C, Leo AD. Metabolomics in breast cancer: current status and perspectives. *Adv Exp Med Biol* (2016) 882:217–34. doi: 10.1007/978-3-319-22909-6_9
22. Nagao K, Kimura T. Use of plasma-free amino acids as biomarkers for detecting and predicting disease risk. *Nutr Rev* (2020) 78(12 Suppl 2):79–85. doi: 10.1093/nutrit/nuaa086
23. Kok G, Tseng L, Schene IF, Dijkstra ME, Salomons G, Mendes MI, et al. Treatment of ARS deficiencies with specific amino acids. *Genet Med* (2021) 23(11):2202–7. doi: 10.1038/s41436-021-01249-z
24. Koochekpour S, Majumdar S, Azabdaftari G, Attwood K, Scioneaux R, Subramani D, et al. Serum glutamate levels correlate with Gleason score and glutamate blockade decreases proliferation, migration, and invasion and induces apoptosis in prostate cancer cells. *Clin Cancer Res* (2012) 18(21):5888–901. doi: 10.1158/1078-0432.CCR-12-1308
25. Cluntun AA, Lukey MJ, Cerione RA, Locasale JW. Glutamine metabolism in cancer: Understanding the heterogeneity. *Trends Cancer* (2017) 3(3):169–80. doi: 10.1016/j.trecan.2017.01.005
26. Katt WP, Cerione RA, Ramachandran S, Erickson JW. Dibenzophenanthridines as inhibitors of glutaminase c and cancer cell proliferation. *Mol Cancer Ther* (2012) 11(6):1269–78. doi: 10.1158/1535-7163.MCT-11-0942
27. Yang XH, Zhang XX, Jing Y, Ding L, Fu Y, Wang S, et al. Amino acids signatures of distance-related surgical margins of oral squamous cell carcinoma. *EBioMedicine* (2019) 48:81–91. doi: 10.1016/j.ebiom.2019.10.005
28. Gao X, Guo R, Li Y, Kang G, Wu Y, Li Z, et al. Contribution of upregulated aminoacyl-tRNA biosynthesis to metabolic dysregulation in gastric cancer. *J Gastroenterol Hepatol* (2021) 36(11):3113–26. doi: 10.1111/jgh.15592
29. Kwon NH, Lee JY, Ryu YL, Kim C, Kong J, Oh S, et al. Stabilization of cyclin-dependent kinase 4 by methionyl-tRNA synthetase in p16^{INK4a} – negative cancer. *ACS Pharmacol Transl Sci* (2018) 1(1):21–31. doi: 10.1021/acspsci.8b00001
30. Ko YG, Kim EY, Kim T, Park H, Park HS, Choi EJ, et al. Glutamine-dependent antiapoptotic interaction of human glutamyl-tRNA synthetase with apoptosis signal-regulating kinase 1. *J Biol Chem* (2001) 276(8):6030–6. doi: 10.1074/jbc.M006189200



OPEN ACCESS

EDITED BY

Gianluca Franceschini,
Agostino Gemelli University Polyclinic
(IRCCS), Italy

REVIEWED BY

Marco Invernizzi,
University of Eastern Piedmont, Italy
Xingchen Peng,
Sichuan University, China
Donovan Anthony McGrowder,
University of the West Indies, Jamaica

*CORRESPONDENCE

Mohammad Miraj
m.molla@mu.edu.sa

SPECIALTY SECTION

This article was submitted to
Breast Cancer,
a section of the journal
Frontiers in Oncology

RECEIVED 11 August 2022

ACCEPTED 15 November 2022

PUBLISHED 05 January 2023

CITATION

Ajmera P, Miraj M, Kalra S, Goyal RK,
Chorsiya V, Shaik RA, Alzhrani M,
Alanazi A, Alqahtani M, Miraj SA,
Pawaria S and Mehta V (2023) Impact
of telehealth interventions on
physiological and psychological
outcomes in breast cancer survivors:
A meta-analysis of randomised
controlled trials.
Front. Oncol. 12:1017343.
doi: 10.3389/fonc.2022.1017343

COPYRIGHT

© 2023 Ajmera, Miraj, Kalra, Goyal,
Chorsiya, Shaik, Alzhrani, Alanazi,
Alqahtani, Miraj, Pawaria and Mehta. This
is an open-access article distributed
under the terms of the [Creative
Commons Attribution License \(CC BY\)](#).
The use, distribution or reproduction
in other forums is permitted, provided
the original author(s) and the
copyright owner(s) are credited and
that the original publication in this
journal is cited, in accordance with
accepted academic practice. No use,
distribution or reproduction is
permitted which does not comply
with these terms.

Impact of telehealth interventions on physiological and psychological outcomes in breast cancer survivors: A meta-analysis of randomised controlled trials

Puneeta Ajmera¹, Mohammad Miraj^{2*}, Sheetal Kalra³,
Ramesh K. Goyal⁴, Varsha Chorsiya³, Riyaz Ahamed Shaik⁵,
Msaad Alzhrani², Ahmad Alanazi², Mazen Alqahtani⁶,
Shaima Ali Miraj⁷, Sonia Pawaria⁸ and Vini Mehta⁹

¹Department of Public Health, School of Allied Health Sciences, Delhi Pharmaceutical Sciences and Research University, New Delhi, India, ²Department of Physical Therapy and Health Rehabilitation, College of Applied Medical Sciences, Majmaah University, AlMajmaah, Saudi Arabia, ³School of Physiotherapy, Delhi Pharmaceutical Sciences and Research University, New Delhi, India, ⁴Department of Pharmacology, Delhi Pharmaceutical Sciences and Research University, New Delhi, India, ⁵Department of Family and Community Medicine, College of Medicine, Majmaah University, Al Majmaah, Saudi Arabia, ⁶College of Applied Medical Sciences, AlMaarefa University, Daryah, Riyadh, Saudi Arabia, ⁷Department of Public Health, College of Health Science, Saudi Electronic University, Riyadh, Saudi Arabia, ⁸Faculty of Physiotherapy, SGT University, Gurugram, India, ⁹Department of Public Health Dentistry, Dr. D.Y. Patil Dental College and Hospital, Dr. D.Y. Patil Vidyapeeth, Pune, India

Introduction: The use of telehealth interventions has been evaluated in different perspectives in women and also supported with various clinical trials, but its overall efficacy is still ascertained. The objective of the present review is to identify, appraise and analyze randomized controlled trials on breast cancer survivors who have participated in technology-based intervention programs incorporating a wide range of physical and psychological outcome measures.

Material and methods: We conducted electronic search of the literature during last twenty years i.e., from 2001 till August 10, 2021 through four databases. Standardized mean difference with 95% confidence interval was used.

Results: A total of 56 records were included in the qualitative and 28 in quantitative analysis. Pooled results show that telehealth interventions were associated with improved quality of life (SMD 0.48, 95% CI 0.03 to 0.92, $p=0.04$), reduced depression (SMD -1.27, 95% CI -2.43 to -0.10 $p=0.03$), low distress and less perceived stress (SMD -0.40, 95% CI -0.68 to -0.12, $p=0.005$). However, no significant differences were observed on weight change (SMD -0.27, 95% CI -2.39 to 1.86, $p=0.81$) and anxiety scores (SMD -0.09, 95% CI -0.20 to 0.02,

$p=0.10$) between the two groups. Improvement in health care competence and fitness among participants was also reported.

Conclusion: Study concludes that telehealth care is a quick, convenient and assuring approach to breast cancer care in women that can reduce treatment burden and subsequent disturbance to the lives of breast cancer survivors.

KEYWORDS

Breast Cancer, Neoplasm, Tele-health, Meta-analysis, Physiological outcomes, Psychological outcomes

Introduction

Breast cancer is the most common diagnosed cancer in women (1) and accounted for 2.1 million diagnosed cases and an estimated 626,679 deaths worldwide in 2018 (2). Due to advancements in diagnostic techniques and therapeutic treatment during the last few decades, 5-year survival rate of breast cancer patients has exceeded 85 percent (3). “Breast Cancer survivors” is a term commonly used for women living with cancer since the inception (diagnosis) of the disease and for the balance of life (4). Once a woman acquires breast cancer and even if she is treated, a continuous interdisciplinary supportive care is desired (5–7). Majority of the women experience various psychological problems like anxiety, depression and perceived stress which are generally substantial and prolonged (8–10) and require considerable healthcare support that may help them overcome psychological barriers and perceive their situation more positively (11). Every woman plays multifaceted roles in any normal scenario. For women, whether it is job or household responsibilities it is difficult for her to manage a separate time slot for visiting the consultant and get guidance in person (12). Such circumstances consequently brought in demand for alternative provision for health care service delivery, which prioritize the technology guided tele-intervention to come into role (13, 14). The technology acts as a boon in such cases where they can use telehealth consultation or regime and be a part of any fitness protocol during the micro breaks of their already scheduled activities (15, 16). Digital technology guided tele-intervention though are “complex” but have the potential for outreach, cost effectiveness and accessibility in managing the health related issues for consultation and treatment purposes using various application and online web services (13, 17–19). This trend is facilitated more with the inculcation of digital technology of mobile, application and dependency on artificial intelligence (20).

Researchers have investigated the effectiveness of variety of telehealth intervention for breast cancer survivors in a range of

domains like quality of life, mental health, nutritional aspects etc (13, 14, 21–23). Tele-interventions targeting various spectrum of ages of women in multiple aspects across diverse racial and cultural perspectives have been shown to be satisfactory to the end-user and realistic to implement (24, 25). Although the use of telehealth interventions have been evaluated in different perspectives in women and also supported with various clinical trials, but its overall efficacy is still ascertain due to difficulty in designing or implementing non-biased randomized controlled trials (RCT) exploring its true effect. A generalized search in data bases indicates that most of the reviews performed on breast cancer survivors has targeted only Quality of life and psychological outcome measures (13). There is a dearth of published systematic reviews on the impact of telehealth guided interventions on outcomes other than Quality of life and psychological measures in breast cancer survivors and that has formed the basis of this review. To the best of author’s knowledge, this meta-analysis is first of its kind to access the effectiveness of spectrum of telehealth interventions on a variety of clinical and psychological outcomes in breast cancer survivors.

The objective of the present review is to identify, appraise and analyze qualitative and quantitative research evidence for breast cancer survivors who have participated in technology based tele-intervention programs incorporating a wide range of physical, physiological and psychological outcome measures. The intent of the present systematic review will help in providing important consideration for potential outcome of telehealth guided tele intervention with a future insight on its successful uptake.

Materials and methods

Preferred reporting items for systematic review and meta-analysis protocols (PRISMA) statement was used for to develop and report this systematic review (26) (Figure 1).

Search strategy

We conducted electronic search of the literature during last twenty years i.e. from 2001 till August 10, 2021 through four databases viz. Google Scholar, PubMed, Web of Science and Cochrane library. To search more precisely, MeSH terms and Boolean operators were used in library databases. Search strategy used was: [Tele OR Tele health OR Tele technology OR Tele intervention OR Tele technologies OR Telemedicine OR Teleconsultation OR Telecommunication OR E health OR e Health OR Mobile Health OR mHealth OR Cell Phones OR Telephones OR Text Messaging OR SMS OR Videoconference OR Video-conference OR Videoconferencing OR Skype] AND [Breast cancer OR Breast neoplasm OR Breast cancer survivor OR Breast cancer survivor OR Breast neoplasm survivor OR Breast neoplasm survivors] AND [Woman OR Women OR Woman health OR Women health OR Health of Woman OR Health of Women].” To maximize literature coverage and cross check the results we followed multivaried methodology covering multiple databases. We used PICOS framework to select articles from the databases. *P* (Population) breast cancer patients. Telehealth intervention is compared to usual medical care alone in *I* (intervention) and *C* (comparison) respectively. Usual care referred to standard medical procedures such routine hospital visits for in-person treatment, conventional breast cancer education, and so on. *O* (Outcomes: Weight

change, Quality of life and psychological outcomes, such as distress and perceived stress, anxiety, and depression. *S* (study design) only RCTs were included. Case reports, reviews, non-randomized controlled trials, duplicate reports, and studies with uninteresting data were excluded from consideration. PICOS framework is presented in Table 1.

Study selection

The process of eligibility was divided into subsequent phases with definite inclusion or exclusion criteria. Only full text academic articles published in peer-reviewed journals were included in the review whereas magazine and newspaper articles were excluded. Using the search strings, 324 papers from the four databases were identified in the phase, I. In phase II, duplicate papers in each search string and papers for which only abstracts were available were excluded. In the IIIrd phase, a new search category with papers impending under all established search strings was introduced and duplicates were removed across all search strings.

In phase IV, all full-length texts were thoroughly assessed and papers that had no relevance to objectives and research questions of our study were excluded. Twenty Eight papers were finally selected and a descriptive analysis was executed to summarize the results.

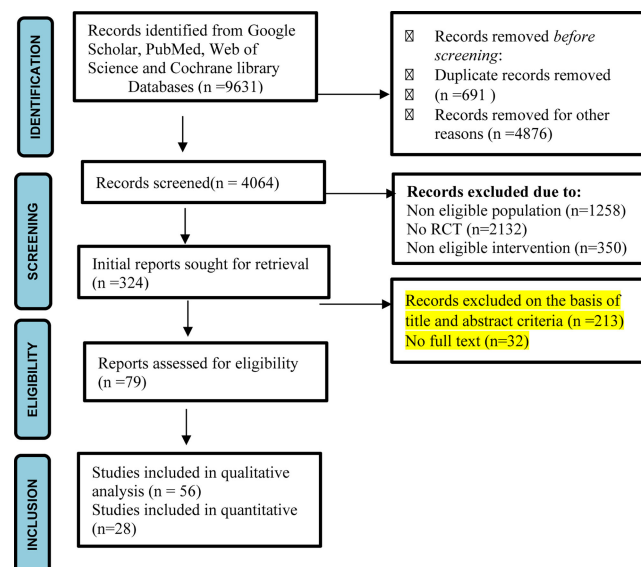


FIGURE 1
PRISMA flow diagram of study (27).

TABLE 1 Search strategy - PICOS framework.

| Framework | Search items |
|------------------|--|
| Population (P) | Breast cancer survivor OR Breast neoplasm survivor OR Breast neoplasm survivors OR Women diagnosed with breast cancer |
| Intervention (I) | (Tele OR Tele health OR Tele technology OR Tele intervention OR Tele technologies OR Telemedicine OR Teleconsultation OR Telecommunication OR E health OR e Health OR Mobile Health OR mHealth OR Cell Phones OR Telephones OR Text Messaging OR SMS OR Videoconference OR Video-conference OR Videoconferencing OR Skype) |
| Comparison (C) | (Usual care) |
| Outcome (O) | (Weight change, QOL and psychological outcome measures including depression, anxiety, distress and perceived stress.) |
| Study design | Randomized Controlled Trials |

Inclusion and exclusion criteria

* Randomized Controlled Trials that examined the role of telehealth technologies in breast cancer survivors were included. Non randomized controlled trials, cross sectional studies, cohort and case control studies were excluded from the study.

* Full text articles written only in English language and published in peer-reviewed journals were included while articles in any other language, book chapters were excluded.

Data extraction and management

Data was independently extracted by two reviewers, (SK) and (PA) on characteristics of study location, year of study, participants, study duration, sample size, inclusion and exclusion criteria, details of intervention, study duration, outcome measures and results of study. Wherever possible, post intervention mean scores and standard deviation were retrieved and recorded. Data was rechecked by third reviewer, (SP) and any discrepancy or doubt pertaining to the selection of particular study was resolved after exhaustive discussion among all the authors.

Risk of bias

Risk of bias in individual studies and methodological quality assessment was performed by 2 independent reviewers SK and PA with more than 15 years of experience in empirical research. Cochrane collaboration tool was used to assess bias risk in randomized control trials in selected articles (28). The tool assesses bias risk on basis of 7 domains. The judgment regarding bias was categorized under 3 categories- a. Low risk b. High risk and c. unclear risk. PRISMA guidelines were used for reporting results of systematic reviews and Meta-analysis. Any disagreements between the 2 reviewers regarding appraisal recommendation were resolved by another reviewer (MM). Review Manager (RevMan) software version 5.4 is used for meta-analysis.

Results

Study selection search results

Initially, during literature search, 9631 records were identified from selected databases. During first screening 691 articles were removed due to duplication while 1258 records were removed as population was found to be non-eligible. Further 2132 records were non-RCTs and in 350 records intervention was not as per our eligibility, hence they were also removed. After initial screening, 324 titles emerged out to be relevant studies. After removal of duplicates and studies not fulfilling eligibility criteria, seventy nine full text records were identified and screened again. Fifty-six records were found to be relevant and directly within the scope of this review and therefore included in the qualitative analysis. Twenty three studies were included in quantitative analysis. Data was summarized narratively and descriptive analysis was carried out. Tables and graphs were prepared to convey significant features of the literature.

Study characteristics

Fifty-six RCT's met our inclusion criteria involving a total of 20,746 women. The earliest study meeting eligibility criteria was published in year 2001 (29). Thirty two trials were conducted in USA (22, 29–58), 7 in Australia (59–64), 4 in Netherland (65–68), 3 each in Denmark (14, 69, 70) and Spain (71–73), 2 in Germany (74, 75) and 1 each in Turkey (76), Finland (77), Taiwan (42), Canada (78), UK (39) and Korea (79). Sample size ranged from 53 in the study of Owen et al, 2005 (76) to 3088 in the study of Pierce et al. in 2007 (30). The trials were conducted in different set ups ranging from cancer societies, multi center institutes, hospitals, medical centers, oncology clinics and Medical University. Age of Participants recruited in different studies ranged from minimum of 18 years to maximum of 80 years. Longest follow up of 4 years for events and mortality related to cancer was done by Pierce et al, 2007 (30). Characteristics of studies are shown in Tables 2, 3. The types of technology used for telehealth interventions varied

throughout the studies that were included. Twenty nine studies used telephone based interventions (22, 29–32, 34–36, 38–40, 42, 44–47, 49, 51, 52, 58–62, 66, 69, 75, 78, 80). Twelve studies used web based interventions (33, 47, 50, 53, 57, 63, 65, 68, 72, 74, 76, 77). Telemedicine was used in two studies (70, 73), eight studies utilized combination of Internet, web, telephone and videoconferencing (14, 37, 41, 43, 48, 56, 67, 71) where as in three studies wearable technology was used for weight management or physical activity tracking (33, 54, 64). Two studies used mobile health based app for self-management of symptoms and mobile gaming in cancer patients (42, 56).

Varied outcome measures were evaluated in the trials. Studies targeting weight management in cancer survivors evaluated weight status, calorie intake and Body Composition. Studies that assessed psycho behavioral aspects used different outcomes like depression, anxiety, sleep and sexual dysfunctions, spiritual and emotional wellbeing, psychological morbidity, self-reported functional status, adjustment to life and adherence to treatment. Studies that examined effects of exercise interventions evaluated Physical activity status, quality of life, self-related health outcomes and functional status. Recurrence of cancer and death was also evaluated in 1 study by Pierce et al, 2007 (30). Interventions and outcome measures are presented in Table 3.

Risk of bias

Four trials were judged with high risk of bias in the domain of random sequence generation (33, 38, 47, 74), as methods of randomization were not given in detail. Twenty trials were judged with low risk of bias in the domain of allocation concealment (29–32, 38, 39, 42, 44, 51, 54, 60, 63–65, 67, 69, 71–73, 80). Eleven studies reported blinding of participants and personnel (14, 29, 32, 38, 42, 51, 63, 64, 72, 75, 80) while twelve trials mentioned about blinding of outcome assessors (38, 39, 42, 51, 60, 64, 67, 69–72, 80) and hence were regarded at low risk of bias. Six studies were reported at high risk in the domain of incomplete outcome data (35, 39, 56, 61, 62, 73). Therefore, in future researches, the allocation concealment, blinding of participants, personnel and outcome assessors should be emphasized to bring out better and reliable conclusions. Risk of bias is presented in Table 4.

Treatment Outcomes

Meta-analysis of depression

Four trials with 547 participants reported the outcomes of depression in meta-analysis. Random-effects model was used due to significant heterogeneity across these trials ($I^2 = 96\%$, $\text{Tau}^2 = 1.08$). Pooled results indicated that telehealth intervention were associated with reduced depression levels in

breast cancer patients (SMD -1.27, 95% CI = -2.43 to -0.10 $p=0.03$) (Figure 2A).

Meta-analysis of anxiety

Seven studies incorporating 1246 patients were included in meta-analysis to examine the impact of telehealth interventions on anxiety levels. Fixed effects model was used as no significant heterogeneity was observed between studies ($I^2 = 0\%$). Pooled results show no significant impact of telehealth interventions on anxiety levels (SMD -0.09, 95% CI = -0.20 to 0.02, $p=0.10$) (Figure 2B).

Sub group analysis of distress and perceived stress

Six studies involving 628 patients were included in meta-analysis to determine the impact of telehealth interventions on distress. Random effects model was used as high heterogeneity was observed among studies ($I^2 = 81\%$). Pooled results depict that a significant impact of telehealth interventions was observed on distress (SMD -0.27, 95% CI = -0.44 to -0.09, $p=0.003$) (Figure 2C).

Subgroup analysis including 825 patients was carried out to determine the impact of telehealth interventions on perceived stress and distress levels. Random effects model was used as high heterogeneity was observed among studies ($I^2 = 74\%$). Six studies involving 628 patients were included to determine the impact of telehealth interventions on distress while two studies including 197 patients were included to determine the impact of telehealth interventions on perceived stress. Pooled results depict that a significant impact of telehealth interventions was observed on distress and perceived stress levels (SMD -0.40, 95% CI = -0.68 to -0.12, $p=0.005$) (Figure 2C).

Dietary status and weight change Meta-analysis of weight change

Five studies incorporating 1624 subjects were incorporated in the meta-analysis of weight change. Random effects model was used due to more heterogeneity among studies ($I^2 = 99\%$). Pooled results depict that no significant impact of telehealth interventions was observed on weight change levels also (SMD -0.48, 95% CI = -1.90 to 0.94, $p=0.50$) (Figure 2D).

Quality of Life

Meta-analysis of Quality of life

Seventeen RCTs including 3055 breast cancer patients were included in the meta-analysis of QOL. Different QOL measurement scales reported in these trials are: FACT G, EORTC QLQ-C30, SF36, FACT-B, FACT-B+4, BCPT and Impact of Cancer Scale. Standardized mean difference (SMD) was used because of variety of measurement scales used in trials. Pooled results depict that telehealth interventions significantly improved the QOL score in

TABLE 2 Characteristics of included trials.

| S No. | Author/year/source | Country | Setting/Data Collection | Participants demographics/Age in years (Mean+SD) |
|-------|-----------------------------|------------|--|---|
| 1 | Rock et al, 2001 (29) | USA | Multi-centre/started in 1995 | N=1010 Age: Intervention group: 54.3± 0.4 Control group: 54.0 ± 0.4 |
| 2 | Samarel et al, 2002 (31) | USA | Physician's offices, hospitals, and the American Cancer Society/NM | N=125 30 to 83 years Age:53.8 ± 10.8 |
| 3 | Pierce et al, 2004 (32) | USA | NM | N=2970 Mean Age:52 Years |
| 4 | Winzelberg et al, 2004 (33) | USA | NM | N=72 Age: 49.5 ± 6.2 |
| 5 | Mishel, 2005 (34) | USA | Cancer centers and hospital based/NM | N=509 Age: 64 ± 8.9 |
| 6 | Owen et al, 2005 (76) | Turkey | NM | N=53 Age: Intervention group: 52.5 ± 8.6; Control group 51.3 ± 10.5 |
| 7 | Aranda et al, 2006 (59) | Australia | Hospital based | N=60 Age (Median/Range)Intervention group:57/ (34–85) Control group: 55/ (36–82) |
| 8 | Gotay et al, 2007 (35) | USA | Hospital based/ 1998-2002 | N=305 Age: (Median/Range)Intervention group:53/ (34–93) Control group: 55/(25–90) |
| 9 | Pierce et al, 2007 (30) | USA | Multi-institutional/2000-2006. | N=3088 Age: Intervention group:53.3 ± 8.9; Control group:53.0 ± 9.0 |
| 10 | Sandgren et al., 2007 (36) | USA | Oncology Clinics/NM | N=218 Age: (Mean) 54.4 years |
| 11 | Budin et al, 2008 (37) | USA | Medical Centers/NM | N=249 Age: 53.8 ± 11.7 |
| 12 | Kathleen et al, 2009 (38) | USA | NM/2002-2004 | N=487 Age-(Mean) Intervention group: 69 (55); Control group: 63 (55) |
| 13 | Beaver et al, 2009 (39) | UK | Outpatient clinic in hospital/ 2003- 2005. | N=374 Age: Intervention group:64.0 ± 11.1; Control group:63.9 ± 10.1 |
| 14 | Marcus et al, 2010 (40) | USA | Hospital and medical Centre/ NM | N=304 Age: <40 to >70 years |
| 15 | Hawkins et al, 2010 (41) | USA | Hospital and University based/ NM | N=323 Age: Internet Access group: 52.3 ± 10.2; CHESS Group: 50.9 ± 9.0 Telephone group: 53.9 ± 10.9; CHESS ± Cancer information group: 52.7 ± 9.4 |
| 16 | Baker et al, 2011 (42) | USA | Hospital/2005-2007 | N=450 Age: Internet only group:52.3 ± 10.2; CHESS information only:52.2 ± 9.8; CHESS information and support:50.6 ± 0.8; Full Chess:50.9 ± 9.0 |
| 17 | David et al., 2011 (74) | Germany | Medical University/2005-2008 | N=235 Age: Intervention group: 48.2± 9.2; Control group:45.9 ± 7.8 |
| 18 | Hawkins, 2011 (43) | USA | Hospital Cancer centres/NM | N=434 Age: Internet Only: 52.3 ± 10.2, Full Chess + Support + coaching: 50.9 ± 9.0; Mentor only: 53.9 ± 10.9; Full chess + Mentor: 52.7 ± 9.4 |
| 19 | Hayes et al, 2011 (60) | Australia | University and hospital based/ NM | N=194 Age: 52.4 ± 8.5 |
| 20 | Hoyer et al, 2011 (69) | Denmark | Hospital/ 2010-2010 | N=140 Age: Intervention group: 59 ± 9; Control group: 61 ± 8 |
| 21 | Kimman et al, 2011 (66) | Netherland | Multi-center trial/NM | N=320 Age: Intervention group 56.2± 10.7 Control group: 55.5± 9.0 |
| 22 | Sherman et al, 2011 (44) | USA | Medical centers and Hospital based/NM | N= 249 Age:53.8 ± 11.7 |

(Continued)

TABLE 2 Continued

| S No. | Author/year/source | Country | Setting/Data Collection | Participants demographics/Age in years (Mean+SD) |
|-------|------------------------------------|-------------|---|--|
| 23 | Crane-Okada et al, 2012 (45) | USA | Medical Institute/NM | N=142 Age: Immediate Contact group 63.4 ± 10.3; Delayed contact group(DC): 60.6 ± 7.4; Usual Contact group: 61.3± 8.7 |
| 24 | Eakin at al, 2013 (61) | Australia | NM/2007-2009 | N=143 Age: Intervention group: 51.7 ± 9.0; Control group: 54.1 ± 8.7 |
| 25 | Hayes et al., 2013 (80) | Australia | University Hospital/2006-2008. | N=194 Age: Face to face group:51.2 ± 8.8; Telephone group: 52.2 ± 8.6 Control group:53.9 ± 7.7 |
| 26 | Pinto et al, 2013 (46) | USA | Hospital-based oncology clinic/2004-2009 | N=192 Age: Intervention group: 56.1 ± 9.9; Control group: 55.9 + 9.9 |
| 27 | Ryhanen et al., 2013 (77) | Finland | University Hospital/2008-2010 | N=90 Age: Intervention group: 54.4; Control group: 55.7 |
| 28 | Ziller et al, 2013 (75) | Germany | University Hospital/2006-2008 | N=181 Age: 63.3 ± 8.8 |
| 29 | Goodwin et al, 2014 (78) | Canada | University based/2007-2010. | N=167: Age: Mail based intervention 60.4 ± 7.8; Individualized Lifestyle Intervention: 61.6 ± 6.7 |
| 30 | Carpenter et al, 2014 (47) | USA | NM | N=115 Age: 50.9 ± 9.9 |
| 31 | Berg et al, 2015 (65) | Netherlands | Multi Centre including University and hospitals/2010-2012 | N=150 Age: Intervention group:51.44± 8.30; Control group: 50.18 + 9.15 |
| 32 | Freeman et al, 2015 (48) | USA | NM | N=118: Age: live-delivery 55.44 ± 8.08; Telemedicine group: 55.57 ± 9.88 Waitlist:55.28± 7.90. |
| 33 | Demark Wahnefried et al, 2015 (47) | USA | University based/2010-2012 | N=697 Age: Intensive intervention group:56.0 ± 9.47; control group: 56.4 + 9.53 |
| 34 | Befort et al, 2016 (49) | USA | Medical University/NM | N=172 Age: Intervention group:58.7 ± 8.2; Control group:57.3 ± 8.0 |
| 35 | Chee et al, 2016 (50) | USA | NM/2014-2015. | N=65 Age: Intervention Group: 46.1 ± 10.6; Control group: 48.0 ± 11.1 |
| 36 | Damholdt et al, 2016 (14) | Denmark | University hospital/2013-2014. | N=157 Age: Intervention group: 54.98± 8.51; Control group: 54.56± 8.74 |
| 37 | Galiano-Castillo et al, 2016 (71) | Spain | Physical therapy lab in Health science faculty/2012-2013, | N=72 Age: Intervention group:47.4 ± 9.6 Control group: 49.2 ± 7.9 |
| 38 | Harrigan et al, 2016 (51) | USA | Cancer institute/NM | N=100 Age: 59.0 ± 7.5 years |
| 39 | Abrahams et al, 2017 (67) | Netherland | Medical Centre 2014-2016 | N=125 Age: Internet-based cognitive behavioral therapy (ICBT) group:52.5 ± 8.2;Care as Usual (CAU): 50.5 ± 7.6 |
| 40 | Han et al, 2017 (52) | USA | Cancer institutions/2010-2014 | N=560 Age: Intervention group: 45.8 ± 68.6 Control group: 46.4± 68.4 |
| 41 | Gordon et al, 2017 (62) | Australia | University Hospital/2006-2008 | N=194 Age: 52 ± 8 |
| 42 | Bruggeman et al, 2017 (68) | Netherland | 2013-2015 | N=167 Age: Intervention group: 51.36 ± 12.04; Control group: 56.54 ± 8.43 |
| 43 | Cox et al, 2017 (53) | USA | University based/NM | N=37 Age: Intervention group: 59.62 + 9.65; Control group: 59.92 ± 10.94 |
| 44 | Zachariae et al, 2018 (70) | Denmark | NM/2011-2013 | N=255 Age: Intervention group: 53.2 ± 8.8; Control group: 52.9 ± 8.9 |
| 45 | Hartman et al, 2018 (55) | USA | 2015- 2016 University based | N=87 Age:57.9+11.3 |
| 46 | Kim et al, 2018 (79) | Korea | 2013-2014/ University based | N=76 Age: Intervention group: 52.1; Control group: 49.8 |

(Continued)

TABLE 2 Continued

| S No. | Author/year/source | Country | Setting/Data Collection | Participants demographics/Age in years (Mean+SD) |
|-------|-----------------------------------|-----------|-------------------------------------|---|
| 47 | Meneses et al, 2018 (22) | USA | Medical University | N=40 Age: 56.63 ± 10.63 |
| 48 | Ferrante et al, 2018 (54) | USA | 2016-2018 University based | N=37 Age: 61.54 ± 8.83 |
| 49 | Sherman et al, 2018 (63) | Australia | 2015- 2015 University based | N=3014 Age: Intervention group: 57.5 ± 8.98; Control group: 57.23 ± 9.97 |
| 50 | Eun-Ok Im et al, 2019 (56) | USA | 2017-2018 | N=91 Age: 51.3 ± 11.31 |
| 51 | Garcia et al, 2019 (72) | Spain | University based/NM | N=68 Age: Intervention group: 48.82 ± 7.68; Control group: 47.32 ± 9.92 |
| 52 | Lynch et al, 2019 (64) | Australia | 2016/NM | N=83 Age: Intervention group: 61.3 ± 5.9; Control group: 61.6 ± 6.4 |
| 53 | Paladino et al, 2019 (57) | USA | 2018-2021/ University based | N=200 Age: NM |
| 54 | Meneses et al, 2020 (58) | USA | NM/University based | N=432 Age: NM |
| 55 | Lleras de Frutos et al, 2020 (73) | Spain | 2016-2019/NM | N=269 Age: Intervention group: 47.34 ± 8.05; Control group: 52.17 ± 8.36 |
| 56 | Hou et al, 2020 (81) | Taiwan | 2017-2018/University Hospital based | N=100 Age: Range (50-64 years) |

breast cancer patients (SMD 0.48, 95% CI 0.03 to 0.92, $p=0.04$) (Figure 2E).

Discussion

In recent decades, medical technology has experienced significant development (82). In addition, breast cancer patients nowadays tend to have better survival rates compared with those in the past. However, during the survival period, these patients' QOL, physical and psychological health need close attention. Psychological symptoms such as sadness, anxiety and perceived stress are common and generally untreated in breast cancer patients, which can have a detrimental impact on their quality of life. Also, physical health issues like weight gain and obesity can result into recurrent risk, poor prognosis and all-cause mortality in breast cancer survivors (30, 83). Lifestyle interventions in form of weight reduction has been recommended to improve health outcomes (84). In comparison to traditional care, telehealth is a highly accessible and effective intervention that may overcome time and location obstacles. Patients can connect with medical professionals about their disease issues and gain more information about disease management through telehealth care. These situations can give patients with continual access to assistance and make them feel that they're not alone and that medical help is always nearby both of which are advantageous to their psychological well-being. The use of telehealth has numerous advantages for breast cancer patients, but there are also many

challenges and issues among patients, healthcare professionals, and service providers. These include patient's unwillingness to use the technology, especially older patients who prefer in-person consultations, inconsistent internet connections in rural regions, patient mistrust because a thorough physical examination cannot be performed remotely, and inadequate insurance coverage. Additional challenges to telehealth include concerns regarding the security of patient health records transmitted electronically, high acquisition and implementation costs, significant maintenance costs, management and training of healthcare professionals to effectively use the various platforms and limited access to technology or low platform literacy. To the best of our knowledge, this study represents the first meta-analysis to examine the effect of telehealth intervention from inception till date on various physical and psychological health parameters in breast cancer patients. The results revealed that compared with usual care, telehealth intervention was associated with higher QOL, with less depression, distress and perceived stress symptoms however no significant effect was seen on anxiety and weight status. Fifty Six RCTs incorporating telehealth modalities for breast cancer women were included in this review. Telephone was found to be the leading telehealth tool in most of the studies. A large number of studies also supported use of web based interventions for various physical and psychological outcomes in cancer survivors. There has been an increasing interest in the use of smart wearable technologies to encourage breast cancer survivors to modify their physical activity (PA) habits. Alternate telehealth technologies like mobile-based apps or other advanced e-Health

TABLE 3 Interventions, outcome measures and results of included trials.

| | Author/ year/ source | Intervention | Outcome measures/Assessment | Result |
|----|-----------------------------|--|---|--|
| 1 | Rock et al, 2001 (29) | Telephone guided diet counseling | Average weight change % change, BMI, waist circumference Assessment: Baseline, 6 month, 12month,18month, 24 month | Diet intervention was not associated with significant weight loss |
| 2 | Samarel et al, 2002 (31) | Combined individual telephone and in person group support and education. | VAS-W, EWBS, a subscale of the Spiritual Well-Being Questionnaire UCLA Loneliness Scale–Version 3, Relationship Change Scale Assessment: Baseline, 13 month | A telephone based support intervention was found to be an effective option to in person support in early stage breast cancer survivors. |
| 3 | Pierce et al, 2004 (32) | Telephone counseling to promote dietary change | Dietary intakes, plasma carotenoid concentrations, Percentage energy from fat Assessment: Baseline,12 month | Telephone based counseling intervention promoted dietary change in breast cancer survivors. |
| 4 | Winzelberg et al, 2004 (33) | Structured, web based support group moderated by a mental health professional | CES –D, PCL-C54,STAI-55, PSS54CBI-55, Mini-MAC-58 Assessment: Baseline, 12 weeks | Web-based support group was found to be effective in reducing depression and cancer-related trauma, as well as perceived stress |
| 5 | Mishel, 2005 (34) | Telephone sessions for the use of audiotapes and self-help manual for behavioral strategies | Cancer Survivor Knowledge Scale, Patient/Provider Communication Scale, Social support satisfaction, CSQ, POMS-SF Assessment: Baseline,10 month | Improvement in cognitive reframing, coping skills, cancer awareness and communication in intervention group was observed |
| 6 | Owen et al, 2005 (76) | Internet-based group was given access to website for coping skills training exercises | QOL (FACT-B), Distress (IES) Assessment: Baseline, 12 week | Self-guided internet based coping technique resulted into improved self-rated health status and reduced distress. |
| 7 | Aranda et al, 2006 (59) | Face to face sessions and telephonic interactions for addressing concerns and coping strategies. | EORTC Q-C30, SCNS Assessment: Baseline,1 month and 3 month | Intervention significantly reduced the psychological and emotional needs of high needs group. However no effect was seen on low needs group |
| 8 | Gotay et al, 2007 (35) | Four to eight Telephonic calls over a 1-month period by trained peer counselors | CARES-S, CES-D Assessment: Baseline, 3 month,6 month | No statistically significant improvement was seen in distress and depression in telephonic counselling group. |
| 9 | Pierce et al, 2007 (30) | Telephone counseling regarding dietary intake. | Invasive breast cancer event (recurrence or new primary) or death from any cause Assessment: Baseline, 1year, 4 year | No significant reductions in cancer events or mortality was seen in telephone counselling group |
| 10 | Sandgren et al., 2007 (36) | Telephone-delivered health education | FACT-G, POMS, Revised PSS Assessment: Baseline, 6 month, 13 month | Telephone delivered sessions improved distress but no significant effect was seen on QOL. |
| 11 | Budin et al, 2008 (37) | Videos delivered psycho-education with telephonic counseling | PAIS, PAL-C, SRHS and the Breast Cancer Treatment Response Inventory Assessment: Baseline, diagnostic phase, 2 days post-surgery, 2 weeks after chemotherapy and 6 months post-surgery. | Intervention group had less distress and better psychological outcomes than standard care group |
| 12 | Kathleen et al, 2009 (38) | Telephone interview assessing adherence barriers; health education, problem-solving, and self-management support. | KPSS, FACT-G, Patient Health Questionnaire 9 Brief Symptom Inventory Assessment: Baseline, 12 month | Overall adherence rates range was good for both groups and no significant differences were noted. |
| 13 | Beaver et al, 2009 (39) | Telephone appointments to address questions related to changes in condition, new symptom development, required information about spread of disease, treatment and side effects, genetic risk, sexual attractiveness, self-care was provided. | STAI, GHQ-12, participants' needs for information, participants' satisfaction, clinical investigations ordered, and time to detection of recurrent disease. Assessment : Baseline,12 month | When compared to those who visited clinics in hospitals, participants in the telephone group showed less anxiety and higher levels of satisfaction. For women with a low to moderate recurrence risk, those with travel and movement issues, and those suffering from sickness with no physical or psychological disadvantage, telephone follow-up was found to be useful. In addition, the pressure on overburdened clinics was lessened. |
| 14 | Marcus et al, 2010 (40) | Telephone counseling program of 16 sessions for improving post treatment psycho social outcomes. | IES,CES-D, The Sexual Dysfunction scale Assessment: Baseline, 3 month,6 month, 12 month and 18 month | Telephone delivered counseling was found to be a viable option for providing psychological support to cancer survivors |

(Continued)

TABLE 3 Continued

| | Author/ year/ source | Intervention | Outcome measures/Assessment | Result |
|----|------------------------------|--|---|--|
| 15 | Hawkins et al, 2010 (41) | Access to the Web-based comprehensive Health Enhancement Support System (CHESS), Telephone-based Cancer information | Health care competence, Cancer Information Competence, Emotional processing, Positive coping using Carver's Brief Cope, FACT-B, Wisconsin social support scale Assessment: Baseline, 6 week | Combination of a computer-based information system and support produced significantly improved quality of life than for patients who were given training with general internet |
| 16 | Baker et al, 2011 (42) | Information, Support, and Coaching: Full CHESS. Training was conducted by telephone. | Cancer information outcomes, Health care competence, Emotional processing, positive coping, functional well-being, breast cancer concerns, satisfaction with professionals Assessment: baseline, 2 week, 6 week, 12 week, 24 week | E health interventions were found to be beneficial for survivors of breast cancer. |
| 17 | David et al., 2011 (74) | Email based individually tailored psycho education | EORTC QLQ-C30, BSI-GSI Assessment: Baseline, 2week | E mail based counseling was found to be beneficial for psycho-educational training of breast cancer survivors who are not being reached by conventional avenues of therapy. However, it may be difficult for patients with high distress level. |
| 18 | Hawkins, 2011 (43) | Access to the Web-based comprehensive Health Enhancement Support System (CHESS),Telephone-based Cancer information and mentorship | Functional well-being, emotional processing, social support and cancer information competence, breast cancer concerns, healthcare competence, satisfaction with professionals and positive coping. Assessment: Baseline, 6 week, 3 month, 6 month | On all the outcomes group with Full CHESS + Mentor group showed better scores than the Full CHESS condition. |
| 19 | Hayes et al, 2011 (60) | Telephone delivered 45 minutes of moderate-intensity physical activities including aerobic-based exercise, Strength-based exercise twice/week. | Breast (FACT-B+4) questionnaire Assessment: Baseline, 6 month,12 month | Participation of women during and after treatment was found to be feasible and acceptable. |
| 20 | Hoyer et al, 2011 (69) | Telephonic session by four experienced nurses for 10 to 30 minutes. | EORTC QLQ-C30 and EORTC QLQ-BR23 Assessment: Baseline, 2 week, 4 week | Telephone sessions did not bring statistically significant improvement in QOL of survivors. |
| 21 | Kimman et al, 2011 (66) | Nurse delivered telephone follow-up care and educational program | EORTC QLQ-C30, STAI Assessment: Baseline, 3 month, 6 month, 12 month | Nurse -led telephone follow-up can be an appropriate way to reduce number of visits to clinics and represents an accepted alternative strategy. |
| 22 | Sherman et al, 2011 (44) | Disease Management, standardized education and Telephone counselling | PAL-C, SRHS, PAIS, BCTRI Assessment: Baseline, 1 week before surgery,72 hours after surgery, 2 weeks, 6 month | The general finding for physical, emotional, and social adjustment is that normal care, which was the standard of treatment for women in both the control and intervention groups, supported their adjustment to breast cancer, with or without extra interventions. |
| 23 | Crane-Okada et al, 2012 (45) | Telephone based counseling sessions | HADS, IPRI, Short form social The Brief COPE Assessment: before surgery, post-intervention, and six months after surgery. | Peer counseling delivered by telephone may affect instrumental support seeking and appears to be differentially received by age group. |
| 24 | Eakin at al, 2013 (61) | Telephone delivered exercise intervention to increase women's self-efficiency for exercise. | Feasibility indicators (recruitment and retention rates, sample representativeness, intervention implementation and participant satisfaction), Effectiveness outcomes were meeting intervention targets for aerobic and resistance training, quality of life, fatigue, anxiety and upper body function. Assessment: Baseline, 6 month,12 month | Results suggest strong support for feasibility and modest support for the efficacy of telephone-delivered interventions. |
| 25 | Hayes et al., 2013 (80) | Face to face and Telephone delivered exercise sessions (16) | FACT-B +4, fitness, functional status Assessment: Baseline, 6 month,12 month | Face to face or telephone delivered exercise intervention can prevent decline in fitness and function during treatment and optimize recovery post-treatment |
| 26 | Pinto et al, 2013 (46) | Telephone based counselling aimed to promote the level of physical activity | 7-day PAR, Motivational Readiness for PA, MOS, SF-36, FACT-F Assessment: Baseline, 3 month, 6 month, 12 month | Telephone delivered counseling in addition to health care advise improved physical activity and readiness for physical activity in breast cancer survivors |

(Continued)

TABLE 3 Continued

| | Author/ year/ source | Intervention | Outcome measures/Assessment | Result |
|----|------------------------------------|--|--|---|
| 27 | Ryhanen et al., 2013 (77) | Internet-based patient educational program for empowerment of breast cancer patients | Instrument-Breast Cancer Patient Version, STAI Assessment: Baseline, 1 year | The internet delivered educational program did not decrease anxiety level or treatment-related side effects among breast cancer patients or improve subscales of quality of life when compared with controls |
| 28 | Ziller et al, 2013 (75) | Telephone delivered sessions to provide individualized information, feedback to questions and problems with medication | Self-reported adherence, MPR Assessment: Baseline, 12 month, 24 month | Groups that received additional information, improved adherence was seen however it was not statistically significant |
| 29 | Goodwin et al, 2014 (78) | Telephone-based intervention programme meant for weight reduction | Disease-free survival, Weight, overall survival, distant disease-free survival, quality of life Assessment: Baseline, 6 month, 12 month, 18 month, 24 month | A telephone based lifestyle intervention led to significant weight loss without adverse effects on QOL. |
| 30 | Carpenter et al, 2014 (47) | Online stress management workbook | IES, Revised CBI Assessment: Baseline, 10 week, 20 week | Internet based stress management therapy was helpful in reducing stress and improving confidence of breast cancer survivors |
| 31 | Berg et al, 2015 (65) | Web-based self-management intervention for reducing distress and improving empowerment. | EORTC QLQC30, IES, SES Assessment: Baseline, 4 month | Access to web based management reduced distress among survivors, but this effect was not sustained during follow-up |
| 32 | Freeman et al, 2015 (48) | Live Delivery (LD) and Telemedicine delivered (TD) sessions (total five) 4-hour weekly group sessions, and received brief weekly phone calls to encourage at-home practice. | SF-36, FACT-B, FACIT-F, FACT-Cog, FACIT-Sp-Ex; version 4, BSGSI, PSQI Assessment: Baseline, 1 month, 3 month | Telemedicine delivered intervention improved QOL and is recommended to be an alternative for cancer survivors specifically in remote areas |
| 33 | Demark Wahnefried et al, 2015 (47) | Weight loss program supplemented with telephone counseling and tailored newsletters. | Weight, IOCV2, SF-36, CES-D Assessment: Baseline, 6 month, 12 month, 2 year | There was improvement in some aspects of QOL in intervention group which diminished with time. |
| 34 | Befort et al, 2016 (49) | Telephone based counseling for weight loss, physical activity and weight loss maintenance. | Weight regain, Measures of weight change and costs. Assessment: Baseline 12 month | A lifestyle based intervention that included group phone-based support improved the intensity of weight loss, maintained and increased the proportion of survivors who maintained clinically significant reductions |
| 35 | Chee et al, 2016 (50) | Internet based Support was provided for emotional support, information and interaction. | FACT-B, CBI Assessment: pre-test, post test | Acceptance and satisfaction improved in intervention group. |
| 36 | Damholdt et al, 2016 (14) | Web-based cognitive training (e-CogT) with telephone support | Paced Auditory Serial Addition Test, Improvement on other measures of cognition. Assessment: Baseline, post-intervention and at 5-month follow-up. | Web-based cognitive therapy didn't result in improvements in any of outcomes. Improved performance was observed on verbal learning and working memory |
| 37 | Galiano-Castillo et al, 2016 (71) | Internet-based exercise intervention, videoconference and telephone calls | EORTC QLQC30 Assessment: Baseline, 6 month | Intervention group had significantly improved scores global health status, physical, role, cognitive functioning, and arm symptoms as well as pain severity and pain interference and muscle strength |
| 38 | Harrigan et al, 2016 (51) | Telephonic counselling regarding weight loss | Height and weight, Waist and hip circumference, Dual-energy x-ray absorptiometry scans, Physical activity, Number of steps walked/day, Change in daily calorie intake, serum biomarkers Assessment: Baseline, 6 month | Both telephonic and in person counseling were effective as weight loss strategy for breast cancer survivors |
| 39 | Abrahams et al, 2017 (67) | 2 face to face sessions followed by online treatment (web modules) for which guidance was provided by cognitive behavioral therapist through e mail, telephone and video consultation. | Fatigue severity, Functional impairment, psychological distress, and quality of life. Assessment: Baseline, 6 month | ICBT can be effective, evidence based and easily accessible treatment options for severely fatigued breast cancer survivors. However no effect was seen on QOL. |

(Continued)

TABLE 3 Continued

| | Author/ year/ source | Intervention | Outcome measures/Assessment | Result |
|----|----------------------------|--|--|--|
| 40 | Han et al, 2017 (52) | An individually designed cancer-screening brochure, skills training, and telephone based counseling. | Psychosocial health outcomes Cancer information competence scale Assessment: Baseline, 6 weeks, 3 month and 6 month | Intervention group promoted cancer-screening behaviors and related cognitive and attitudinal outcomes |
| 41 | Gordon et al, 2017 (62) | Telephonic intervention.16 planned sessions by a trained exercise physiologist. | FACT-B+4 questionnaire; QALY's and intervention costs Assessment: Baseline, 5 week, 6month,12 month | A combination of face to face and telephone based intervention resulted in improved QOL in breast cancer survivors. |
| 42 | Bruggeman et al, 2017 (68) | Web based mindfulness based cognitive therapy, accelerometer for feedback related to activity patterns | Fatigue severity, CIS-FS, HADS Assessment: Baseline, 2 week, 6 months | Both interventions were effective in reducing fatigue severity in both groups compared to group receiving psychoeducational mails |
| 43 | Cox et al, 2017 (53) | Access to online content by logging to website | Body composition, diet, physical activity, aerobic fitness Assessment: Baseline,6 month | Better health outcomes were seen in telephone group compared to internet group |
| 44 | Zachariae et al, 2018 (70) | Online CBTI (tele-education) program and completing sleep diaries | Sleep diary, insomnia severity by Insomnia Severity Index, PSI, and fatigue using FACIT-F Assessment: Baseline, 9 week, 15 week | Tele based CBTI programme resulted in improved sleep outcomes in survivors of breast cancer |
| 45 | Hartman et al, 2018 (55) | Wearable technology (fitbit) for self-monitoring of Physical activity | Physical activity measures Assessment: Baseline, 2 week, 3 week, 12 week | Technology based intervention helped survivors in tracking their physical activity levels |
| 46 | Kim et al, 2018 (79) | Mobile game play group | Time spent for education, compliance to medical treatment, QOL, depression, anxiety Assessment: Baseline, 3 week | Patients who received an app-based intervention had better drug adherence, fewer chemotherapy side effects, and better patient education, but no effect on depression or anxiety, indicating the feasibility and potentiality of using smart phone mobile games for breast cancer patients receiving chemotherapy. |
| 47 | Meneses et al, 2018 (22) | Telephone education sessions, Support and early education | SF-36, CES-D Fatigue, pain Assessment: Baseline, 3 month, 6 month | Telephone based intervention helped in self-management of pain and fatigue |
| 48 | Ferrante et al, 2018 (54) | Physical activity tracking using technology (Fitbit) | Anthropometric measures, diet, Physical activity, cardiopulmonary fitness, QOL, body weight Assessment: Baseline, 1 month, 3 month | There was no significant effect on weight loss however improvement was seen in QOL, weight status, anthropometric measures and calorie intake |
| 49 | Sherman et al, 2018 (63) | Web based intervention to reduce stress | Body image related distress, body appearance scale, psychological distress and self-compassion Assessment: Baseline, 1 week, 1 month, 3 month | Web based intervention was helpful in reducing body image related distress, greater self-compassion and reduced psychological distress |
| 50 | Eun-Ok Im et al, 2019 (56) | Information and support with the help of mobile phones, computer and web based information | CBI-B, MSAS-SF Assessment: Baseline, 1 month, 3 month | Technology based intervention alleviated symptoms in survivors of breast cancer |
| 51 | Garcia et al, 2019 (72) | Web based exercise intervention | 6MWT, Fitness variables Assessment: Baseline, 8 week | A web based intervention helped in preventing decline in functional capacity and strength in breast cancer patients undergoing chemotherapy |
| 52 | Lynch et al, 2019 (64) | Wearable technology to assess physical activity levels as well as telephone delivered behavioral counselling | Physical activity levels and sedentary behavior Assessment: Baseline,12 week | Wearable technology may be a useful approach for breast cancer survivors to maintain an active lifestyle. There was an increase in physical activity and a decrease in sitting time. |
| 53 | Paladino et al, 2019 (57) | Received app based(web or internet) information about adherence to endocrinal treatment and feedback including links regarding coping strategies | Adherence to treatment, symptom management, FACT-ES,SF-12, PROMIS Assessment: Baseline, 6 month, 12 month | Intervention groups showed improved adherence to endocrinal treatment and self-management of symptoms |

(Continued)

TABLE 3 Continued

| | Author/ year/ source | Intervention | Outcome measures/Assessment | Result |
|----|-----------------------------------|---|---|---|
| 54 | Meneses et al, 2020 (58) | Early education and support using telephone and mail | SF-36, CES-D, POMS, MOS-SSS Assessment: Baseline, 6 month | The use of a telephone-based intervention was found to be an effective way of reaching survivors in rural BC who were at risk of not receiving enough care. |
| 55 | Lleras de Frutos et al, 2020 (73) | Positive psychology classes were given via video-conferencing(online group) | HADS, PCL-C31, PTGI-34,CTB-R Assessment: Baseline, immediately after treatment, 3 months | Online positive psychology classes were effective in reducing distress in cancer survivors |
| 56 | Hou et al, 2020 (81) | Subjects received mobile health application based breast cancer self-management support | EORTC, QLQ-C30, QLQ-BR23 | Mobile app based intervention was found to be effective in promoting QoL. |

Center for Epidemiologic Studies Depression Scale (CES-D), Functional Assessment of Chronic Illness Therapy for Fatigue (FACIT-F), quality-adjusted life years (QALYs); The Short Form Health Survey (SF-36), The refined Impact of Cancer Scale (IOCv2), The Breast Cancer Prevention Trial (BCPT) Symptom Scales, Functional Assessment of Cancer Therapy-Breast (FACT-B), FACIT-Fatigue Scale (FACIT-F), FACT-Cog (version 2), Functional Assessment of Chronic Illness Therapy Spiritual Well-Being Expanded Scale (FACIT-Sp-Ex; version 4), 18-item Brief Symptom Inventory (BSI-18) Global Severity Index (BSIGSI), Pittsburgh Sleep Quality Index (PSQI), Medication possession ratio (MPR), Seven-Day Physical Activity Recall (7-day PAR), MOS 36-Item Short Form Health Survey (SF-36), Functional Assessment of Cancer Therapy Scale-Fatigue (FACT-F), Hospital Anxiety and Depression Scale (HADS), Interpersonal Relationship Inventory (IPRI), Functional Assessment of Cancer Therapy, Breast (FACT-B+4) questionnaire, Impact of Event Scale (IES), Epidemiologic Studies Depression Scale (CES-D), Adjustment to Illness Scale (PAIS), Profile of Adaptation to Life Clinical Scale (PAL-C), Self-rated Health subscale (SRHS), Cancer Rehabilitation Evaluation System-Short Form (CARES-SF), cognitive reframing subscale modified version of the cognitive coping strategies questionnaire (CSQ), European Organization of Research and Treatment of Quality of life Q-C30 version (2.0) (EORTC Q-C30) and Supportive Care Needs Survey (SCNS), PCL-C54, STAI-55, PSS54CBI-55, Mini-MAC-58, Visual Analogue Scale-Worry (VAS-W), Well-Being Scale (EWBS), MOS-SSS(Medical outcome study-social support survey, CIS-FS (Check individual strength fatigue scale), PCL-C31(Post traumatic stress disorder checklist version 31, PTGI-34 (Post traumatic growth inventory), CTB-R (Revised cognitive therapy scale, PTGI-34(Post traumatic growth Inventory), FACIT-F(Facit fatigue scale), Functional Assessment of Chronic Illness Therapy Spiritual Well-Being Expanded Scale (FACIT-Sp-Ex; version 4), Brief Symptom Inventory (BSI-18) Global Severity Index (BSIGSI), Refined Impact of Cancer Scale (IOCv2), Cancer Rehabilitation Evaluation System-Short Form [CARES-SF], The European Organization for Research and Treatment of Cancer (EORTC), Quality-of-Life Questionnaire Core 30 (QLQ-C30),The EORTC Breast Cancer-Specific Quality-of-Life Questionnaire (QLQ-BR23), Quality of Life (QoL)

TABLE 4 Risk of bias assessment.

| Trial | Random sequence generation | Allocation concealment | Blinding of patient and personnel | Blinding of outcome assessment | Incomplete outcome data addressed | Selective reporting | Other Bias |
|----------------------------|----------------------------------|---------------------------|--------------------------------------|--------------------------------------|--------------------------------------|------------------------|---------------|
| 1. Rock et al, 2001 | Low | Low | Low | Some concern | Low | Low | Low |
| 2. Samarel et al, 2002 | Low | Low | High | High | Low | Low | Low |
| 3. Pierce et al, 2004 | Low | Low | Low | Some concern | Low | Low | Low |
| 4. Winzelberg et al., 2003 | High | High | High | High | Low | Low | Low |
| 5. Mishel, 2005 | Low | High | High | High | Low | Low | Low |
| 6. Owen. 2005 | Low | High | Some concern | High | Low | Low | Low |
| 7. Aranda et al, 2006 | Low | Some concern | Some concern | Some concern | Low | Low | Low |
| 8. Gotay et al, 2007 | Low | High | High | High | High | Low | Low |
| 9. Pierce et al, 2007 | Low | Low | High | Some concern | Low | Low | Low |
| 10. Sandgren et al, 2003 | Some concern | Some concern | High | High | Low | Some concern | Low |
| 11. Budin et al, 2008 | Some concern | Some concern | Some concern | Some concern | Low | Low | Low |
| 12. Kathleen et al, 2009 | High | Low | Low | Low | Low | Low | Low |
| 13. Beaver et al, 2009 | Low | Low | Some concern | Low | High | Low | Low |
| 14. Marcus, 2010 | Yes | High | High | High | Low | Low | Low |
| 15. Hawkins, 2010 | Low | High | High | High | Low | Low | Low |
| 16. Baker et al, 2011 | Low | High | High | High | Low | Low | Low |
| 17. David et al, 2011 | High | High | High | High | Low | Low | Low |
| 18. Hawkins, 2011 | Low | Some concern | Some concern | High | Low | low | Low |

(Continued)

TABLE 4 Continued

| Trial | Random sequence generation | Allocation concealment | Blinding of patient and personnel | Blinding of outcome assessment | Incomplete outcome data addressed | Selective reporting | Other Bias |
|-----------------------------------|----------------------------|------------------------|-----------------------------------|--------------------------------|-----------------------------------|---------------------|------------|
| 19. Hayes et al, 2011 | Low | Low | Some concern | Low | Low | Low | Low |
| 20. Hoyer, 2011 | Low | Low | High | Low | Low | Low | Low |
| 21. Kimman et al, 2011 | Low | Some concern | High | Some concern | Low | High | Low |
| 22. Sherman et al, 2011 | Low | Low | High | High | Low | Low | Low |
| 23. Crane-Okada et al, 2012 | Low | High | High | Some concern | Low | Low | Low |
| 24. Eakin et al, 2013 | Low | Some concern | Some concern | Some concern | High | Low | Low |
| 25. Hayes, 2013 | Low | Low | Low | Low | Low | Low | Low |
| 26. Pinto et al, 2013 | Low | High | High | High | Low | Low | Low |
| 27. Rhyanen et al, 2013 | Low | Some concern | Some concern | Some concern | Low | Some concern | Low |
| 28. Ziller et al, 2013 | Low | Some concern | Low | Some concern | Low | Low | Low |
| 29. Goodwin et al, 2014 | Low | Some concern | Some concern | High | Low | Low | Low |
| 30. Carpenter, 2014 | Low | High | Some concern | High | Low | Low | Low |
| 31. Berg, 2015 | Low | Low | Some concern | Some concern | Low | Low | Low |
| 32. Freeman et al, 2015 | Low | Some concern | High | Some concern | Low | Low | High |
| 33. Demark Wahnefried et al, 2015 | High | Some concern | Some concern | High | Low | Low | Low |
| 34. Befort et al, 2016 | Low | Some concern | High | Some concern | Low | Low | Low |
| 35. Chee, 2016 | Low | High | High | High | Low | Low | Low |
| 36. Damholdt et al, 2016 | Low | Some concern | Low | Some concern | Some concern | Low | Low |
| 37. Galiano Castillo et al, 2016 | Low | Low | Some concern | Low | Low | Some concern | Low |
| 38. Harrigan et al, 2016 | Low | Low | Low | Low | Some Concern | Low | Low |
| 39. Abrahams et al, 2017 | Low | Low | High | High | Low | Low | Low |
| 40. Han et al, 2017 | Low | Some concern | High | High | Low | Low | Low |
| 41. Gordon et al, 2016 | Low | Some concern | Some concern | Low | High | Low | Low |
| 42. Bruggeman et al, 2017 | Low | High | High | Low | Low | Low | Low |
| 43. Cox et al., 2017 | Low | High | High | High | Low | Low | Low |
| 44. Zachariae et al., 2018 | Low | High | High | High | Low | Low | Low |
| 45. Hartman et al., 2018 | Low | High | High | High | Low | Low | Low |
| 46. Kim et al., 2018 | Low | High | High | High | Low | Low | Low |
| 47. Meneses et al., 2018 | Some concern | High | High | High | Low | Low | Low |
| 48. Ferrante et al., 2020 | Low | Low | High | High | Low | Low | Low |
| 49. Sherman et al., 2018 | Low | Low | Low | Some concern | Low | Low | Low |

(Continued)

TABLE 4 Continued

| Trial | Random sequence generation | Allocation concealment | Blinding of patient and personnel | Blinding of outcome assessment | Incomplete outcome data addressed | Selective reporting | Other Bias |
|-----------------------------------|----------------------------|------------------------|-----------------------------------|--------------------------------|-----------------------------------|---------------------|------------|
| 50. Eun-Ok Im et al, 2019 | Some concern | High | High | High | High | Low | Low |
| 51. Garacia et al., 2019 | Low | Low | Low | Low | Low | Low | Low |
| 52. Lynch et al., 2019 | Low | Low | Low | Low | Low | Low | Low |
| 53. Paladino et al., 2021 | Low | High | High | High | Low | Low | Low |
| 54. Meneses et al., 2020 | Some concern | Some concern | High | High | Low | Low | Low |
| 55. Lleras de Frutos et al., 2020 | Low | Low | High | High | High | Low | Low |
| 56. Hou et al., 2020 | Low | Low | Low | Low | Low | Low | Low |

systems have also seen an upsurge in last few years. A precise, reproducible, trustworthy, and affordable diagnosis of breast cancer lymphedema can be made using augmented reality techniques, such as 3DLS, in the clinical setup (84). However, more number of RCTs are needed to evaluate their efficacy on weight status, QOL and mental health parameters. Majority of telehealth interventions were related to awareness using educational/supportive material based on scheduled phone calls aimed at improving physical and psychological health of study populations. To enhance the quality of this systematic review, only randomized controlled trials were included and quality was assessed using the Cochrane risk of bias tool. Timely information and consultation with experts is a crucial aspect for women suffering from breast cancer. Technological advancements have improved the survival rates of these patients. But, during the survival period, their health parameters need to be vigilantly monitored. Our findings are consistent with previous studies that show that breast cancer patients need continuous consultation that would help them in understanding their condition better so that they can cope with the treatment process more confidently (83, 85, 86). The results of this systematic review indicate that telehealth technologies could considerably improve quality of life, physiological and psychological parameters of breast cancer patients.

The increasing enthusiasm for tele health is determined not only by its established benefits, but also by the extensive accessibility of mobile phones, and the comparatively low levels of education required to use them (1). In comparison to traditional care, telehealth is a highly accessible and effective intervention that may overcome time and location obstacles (65). Patients can conveniently interact with health professionals about their medical conditions and get more information about disease management through telehealth care (87). Results of our review also show majority of trials used telephone based interventions. The dominance of telephone based and Web-based telehealth interventions makes participant recruitment easy and facilitates

timely data collection. Also the risk of missing information is reduced and follow up becomes easy. Furthermore, eHealth interventions are relatively more cost effective and provide wide geographical coverage overcoming mobility issues. But researchers have less control over respondents (77, 88). The COVID-19 pandemic has significantly transformed how healthcare is provided. In order to sustain patient care while reducing the danger of nosocomial SARS-COV-2 infection, decentralization measures such as telehealth visits, home-based care, and remote patient monitoring should be quickly adopted. These techniques can be used to relieve the burden of treatment and lower the risk of exposure for patients and medical staff across the entire spectrum of care, from prevention to palliation (89–92). Moreover, our findings also divulge that telehealth interventions are primarily used in developed nations while their use in developing countries is still less. This may be due to inappropriate resource allocation, dearth of technical expertise, high initial investment and deficient healthcare infrastructure in developing countries.

The large scale search conducted in multiple databases, inclusion of exclusive randomized controlled trials, methodological quality assessment are the strengths of this review. Studies that had only telehealth interventions were included thus making comparison of studies feasible. Another strength is inclusion of wide range of physical, physiological and psychological outcome measures. There are some limitations also. Differences between duration of interventions, outcomes measures and varied control groups in trials led to heterogeneity. Also, inclusion of trials written in English language only was another limitation that may introduce publication bias.

Conclusion

This systematic review concludes that telehealth care is a quick, convenient and assuring approach to breast cancer care in

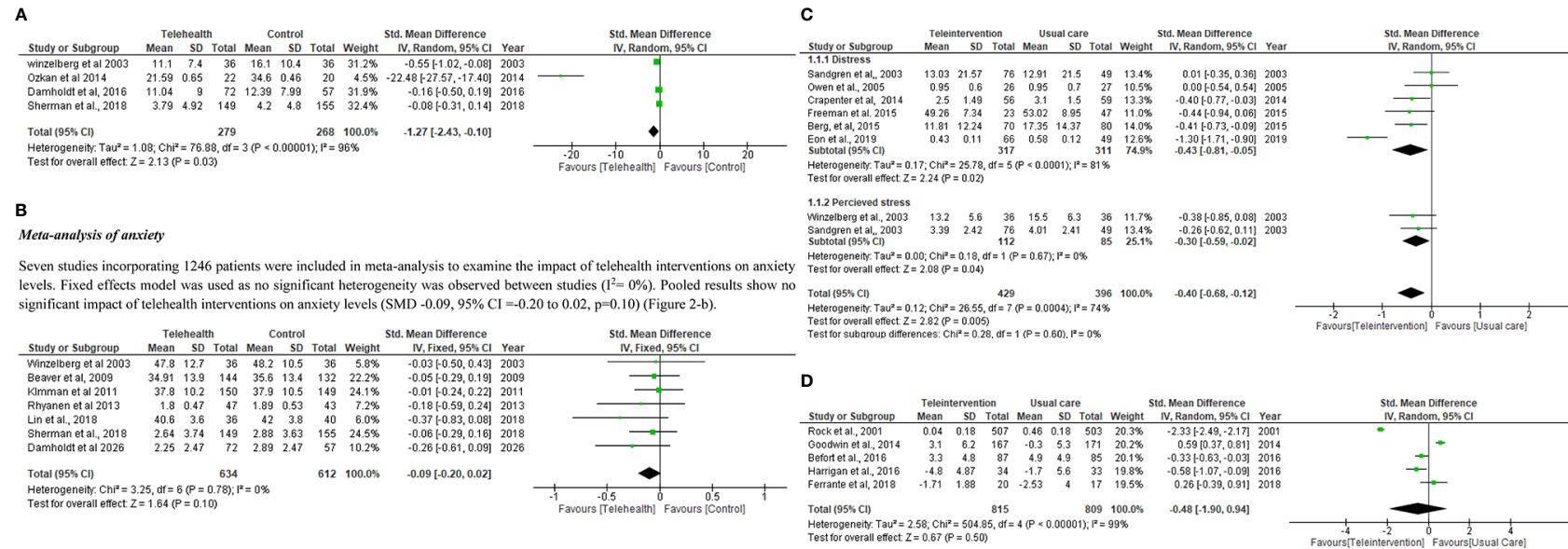


FIGURE 2

(A) Meta-analysis of depression. (B) Meta-analysis of anxiety. (C) Meta-analysis of (A) Distress (B) perceived stress. (D) Meta-analysis of weight change. (E) Meta-analysis of Quality of life.

women that can reduce treatment burden and subsequent disturbance to the lives of breast cancer survivors. Telehealth interventions are worthy of clinical consideration and should be used as part of a holistic breast cancer treatment plans. We suggest that additional resources should be placed in the development of telehealth care and more high-quality randomized controlled trials should be conducted to investigate the worth of telehealth care in the management of breast cancer patients. It is also important to tailor and develop telehealth interventions according to survivor's needs, possibly by involving them in the early stages of intervention design to curtail perception of impersonal care and attain benefits of remote monitoring.

Data availability statement

The original contributions presented in the study are included in the article/supplementary material. Further inquiries can be directed to the corresponding author.

Author contributions

Conceptualization: Done by PA, SK, RG. Designing the study: RG, VC, RS. Data collection: PA, MA, AA, MAI, SM, SP. Compilation, analysis and interpretation of data: PA, RA, VM, MM. Manuscript writing and review: MM, PA, SK, VM. All the drafts were reviewed by PA, MM, SK, RG, VC, RS, MA, AA,

MAI, SM. All authors contributed to the article and approved the submitted version.

Funding

The authors are grateful to the Deanship of Scientific Research, Majmaah University, for funding through Deanship of Scientific Research vide Project No. RGP-2019-35. The authors are also thankful to AlMareefa and Saudi Electronic University, Riyadh, Saudi Arabia, for providing support to do this research.

Conflict of interest

The authors declare that the research was conducted in the absence of any commercial or financial relationships that could be construed as a potential conflict of interest.

Publisher's note

All claims expressed in this article are solely those of the authors and do not necessarily represent those of their affiliated organizations, or those of the publisher, the editors and the reviewers. Any product that may be evaluated in this article, or claim that may be made by its manufacturer, is not guaranteed or endorsed by the publisher.

References

- Torre LA, Bray F, Siegel RL, Ferlay J, Lortet-Tieulent J, Jemal A. Global cancer statistics, 2012. *CA Cancer J Clin* (2015) 65(2):87–108. doi: 10.3322/caac.21262
- Bray F, Ferlay J, Soerjomataram I, Siegel RL, Torre LA, Jemal A. Global cancer statistics 2018: GLOBOCAN estimates of incidence and mortality worldwide for 36 cancers in 185 countries. *CA Cancer J Clin* (2018) 68(6):394–424. doi: 10.3322/caac.21492
- Henson KE, Elliss-Brookes L, Coupland VH, Payne E, Vernon S, Rous B, et al. Data resource profile: National cancer registration dataset in England. *Int J Epidemiol* (2020) 49(1):16–h. doi: 10.1093/ije/dyz076
- Reich RR, Lengacher CA, Alinat CB, Kip KE, Paterson C, Ramesar S, et al. Mindfulness-based stress reduction in post-treatment breast cancer patients: immediate and sustained effects across multiple symptom clusters. *J Pain Symptom Manage* (2017) 53(1):85–95. doi: 10.1016/j.jpainsymman.2016.08.005
- Akram M, Iqbal M, Daniyal M, Khan AU. Awareness and current knowledge of breast cancer. *Biol Res* (2017) 50(1):1–23. doi: 10.1186/s40659-017-0140-9
- Park BW, Hwang SY. Unmet needs of breast cancer patients relative to survival duration. *Yonsei Med J* (2012) 53(1):118–25. doi: 10.3349/ymj.2012.53.1.118
- Sanchez L, Fernandez N, Calle AP, Ladera V, Casado I, Sahagun AM. Long-term treatment for emotional distress in women with breast cancer. *Eur J Oncol Nurs* (2019) 42:126–33. doi: 10.1016/j.ejon.2019.09.002
- Khan F, Amatya B, Pallant JF, Rajapaksa I. Factors associated with long-term functional outcomes and psychological sequelae in women after breast cancer. *Breast* (2012) 21(3):314–20. doi: 10.1016/j.breast.2012.01.013
- Amatya B, Khan F, Galea MP. Optimizing post-acute care in breast cancer survivors: A rehabilitation perspective. *J Multidiscip healthcare*. (2017) 10:347. doi: 10.2147/JMDH.S117362
- Kalra S, Yadav J, Ajmera P, Sindhu B, Pal S. Impact of physical activity on physical and mental health of postmenopausal women: A systematic review. *J Clin Diagn Res* (2022) 16(2):YE01–YE08. doi: 10.7860/JCDR/2022/52302.15974
- Gustafson DH, McTavish FM, Stengle W, Ballard D, Hawkins R, Shaw BR, et al. Use and impact of eHealth system by low-income women with breast cancer. *J Health communicat* (2005) 10(S1):195–218. doi: 10.1080/10810730500263257
- Abrahams HJ, Gielissen MF, Donders RR, Goedendorp MM, van der Wouw AJ, Verhagen CA, et al. The efficacy of Internet-based cognitive behavioral therapy for severely fatigued survivors of breast cancer compared with care as usual: A randomized controlled trial. *Cancer* (2017) 123(19):3825–34. doi: 10.1002/cncr.30815
- Chen Y-Y, Guan B-S, Li Z-K, Li X-Y. Effect of telehealth intervention on breast cancer patients' quality of life and psychological outcomes: a meta-analysis. *J Telemed Telecare*. (2018) 24(3):157–67. doi: 10.1177/1357633X16686777
- Damholdt M, Mehlsen M, O'Toole M, Andreassen R, Pedersen A, Zachariae R. Web-based cognitive training for breast cancer survivors with cognitive complaints—a randomized controlled trial. *Psycho-Oncology* (2016) 25(11):1293–300. doi: 10.1002/pon.4058
- Ashing K, Rosales M. A telephonic-based trial to reduce depressive symptoms among latina breast cancer survivors. *Psycho-Oncology* (2014) 23(5):507–15. doi: 10.1002/pon.3441

16. Badger TA, Segrin C, Hepworth JT, Pasvogel A, Weihs K, Lopez AM. Telephone-delivered health education and interpersonal counseling improve quality of life for latinas with breast cancer and their supportive partners. *Psycho-Oncology* (2013) 22(5):1035–42. doi: 10.1002/pon.3101
17. Senanayake B, Wickramasinghe SI, Eriksson L, Smith AC, Edirippulige S. Telemedicine in the correctional setting: a scoping review. *J Telemed Telecare*. (2018) 24(10):669–75. doi: 10.1177/1357633X18800858
18. Cox A, Lucas G, Marcu A, Piano M, Grosvenor W, Mold F, et al. Cancer survivors' experience with telehealth: a systematic review and thematic synthesis. *J Med Internet Res* (2017) 19(1):e11. doi: 10.2196/jmir.6575
19. Hancock S, Preston N, Jones H, Gadoud A. Telehealth in palliative care is being described but not evaluated: a systematic review. *BMC Palliat Care* (2019) 18(1):1–15. doi: 10.1186/s12904-019-0495-5
20. Ghosh A, Chakraborty D, Law A. Artificial intelligence in Internet of things. *CAAI Trans Intell Technol* (2018) 3(4):208–18. doi: 10.1049/trit.2018.1008
21. Ashing KT, Miller AM. Assessing the utility of a telephonically delivered psychoeducational intervention to improve health-related quality of life in African American breast cancer survivors: a pilot trial. *Psychooncology* (2016) 25(2):236–8. doi: 10.1002/pon.3823
22. Meneses K, Gisiger-Camata S, Benz R, Raju D, Bail JR, Benitez TJ, et al. Telehealth intervention for latina breast cancer survivors: A pilot. *Womens Health* (2018) 14:1745506518778721. doi: 10.1177/1745506518778721
23. Hung Y, Bauer J, Horsely P, Coll J, Bashford J, Isenring E. Telephone-delivered nutrition and exercise counselling after auto-SCT: a pilot, randomised controlled trial. *Bone Marrow Transplant*. (2014) 49(6):786–92. doi: 10.1038/bmt.2014.52
24. Hatcher JB, Oladeru O, Chang B, Malhotra S, McLeod M, Shulman A, et al. Impact of high-Dose-Rate brachytherapy training via telehealth in low-and middle-income countries. *JCO Global Oncol* (2020) 6:1803–12. doi: 10.1200/GO.20.00302
25. Lopez AM. Telemedicine, telehealth, and e-health technologies in cancer prevention. *Fundament Cancer Prevent: Springer*; (2019), 333–52. doi: 10.1007/978-3-030-15935-1_10
26. Shamseer L, Moher D, Clarke M, Ghersi D, Liberati A, Petticrew M, et al. Preferred reporting items for systematic review and meta-analysis protocols (PRISMA-p) 2015: elaboration and explanation. *BMJ* (2016) 350:354. doi: 10.1136/bmj.g7647
27. Page MJ, McKenzie JE, Bossuyt PM, Boutron I, Hoffmann TC, Mulrow CD, et al. The PRISMA 2020 statement: an updated guideline for reporting systematic reviews. *BMJ* (2021) 372:n71372. doi: 10.1136/bmj.n71
28. Sterne J, Savović J, Page M, Elbers R, Blencowe N, Boutron I, et al. RoB 2: a revised tool for assessing risk of bias in randomised trials. *BMJ* (2019) 366:l4898. doi: 10.1136/bmj.l4898
29. Rock CL, Thomson C, Caan BJ, Flatt SW, Newman V, Ritenbaugh C, et al. Reduction in fat intake is not associated with weight loss in most women after breast cancer diagnosis: evidence from a randomized controlled trial. *Cancer* (2001) 91(1):25–34. doi: 10.1002/1097-0142(20010101)91:1<25::AID-CNCR4>3.0.CO;2-G
30. Pierce JP, Natarajan L, Caan BJ, Parker BA, Greenberg ER, Flatt SW, et al. Influence of a diet very high in vegetables, fruit, and fiber and low in fat on prognosis following treatment for breast cancer: the women's healthy eating and living (WHEL) randomized trial. *JAMA* (2007) 298(3):289–98. doi: 10.1001/jama.298.3.289
31. Samarel N, Tulman L, Fawcett J. Effects of two types of social support and education on adaptation to early-stage breast cancer. *Res Nurs Health* (2002) 25(6):459–70. doi: 10.1002/nur.10061
32. Pierce JP NV, Flatt SW, et al. Telephone counseling intervention increases intakes of micronutrient-and phytochemical-rich vegetables, fruit and fiber in breast cancer survivors. *J Nutr* (2004) 134(2):452–8. doi: 10.1093/jn/134.2.452
33. Winzelberg AJ, Classen C, Alpers GW, Roberts H, Koopman C, Adams RE, et al. Evaluation of an internet support group for women with primary breast cancer. *Cancer: Interdiscip Int J Am Cancer Society*. (2003) 97(5):1164–73. doi: 10.1002/cncr.11174
34. Mishel MH, Germino BB, Gil KM, Belyea M, LaNey IC, Stewart J, et al. Benefits from an uncertainty management intervention for African-American and Caucasian older long-term breast cancer survivors. *Psycho-Oncol: J Psychol Soc Behav Dimensions Canc* (2005) 14(11):962–78. doi: 10.1002/pon.909
35. Gotay CC, Moynour CM, Unger JM, Jiang CS, Coleman D, Martino S, et al. Impact of a peer-delivered telephone intervention for women experiencing a breast cancer recurrence. *J Clin Oncol* (2007) 25(15):2093–9. doi: 10.1200/JCO.2006.07.4674
36. Sandgren AK, McCaul KD. Long-term telephone therapy outcomes for breast cancer patients. *Psycho-Oncol: J Psychol Soc Behav Dimensions Canc* (2007) 16(1):38–47. doi: 10.1002/pon.1038
37. Budin WC, Hoskins CN, Haber J, Sherman DW, Maislin G, Cater JR, et al. Breast cancer: education, counseling, and adjustment among patients and partners: a randomized clinical trial. *Nurs Res* (2008) 57(3):199–213. doi: 10.1097/01.NNR.0000319496.67369.37
38. Ell K, Vourlekis B, Xie B, Nedjat-Haiem FR, Lee PJ, Munderspach L, et al. Cancer treatment adherence among low-income women with breast or gynecologic cancer: a randomized controlled trial of patient navigation. *Cancer: Interdiscip Int J Am Cancer Society*. (2009) 115(19):4606–15. doi: 10.1002/cncr.24500
39. Beaver K, Tysver-Robinson D, Campbell M, Twomey M, Williamson S, Hindley A, et al. Comparing hospital and telephone follow-up after treatment for breast cancer: randomised equivalence trial. *BMJ* (2009) 338:a3147. doi: 10.1136/bmj.a3147
40. Marcus AC, Garrett KM, Cella D, Wenzel L, Brady MJ, Fairclough D, et al. Can telephone counseling post-treatment improve psychosocial outcomes among early stage breast cancer survivors? *Psycho-oncology* (2010) 19(9):923–32. doi: 10.1002/pon.1653
41. Hawkins RP, Pingree S, Shaw B, Serlin RC, Swoboda C, Han J-Y, et al. Mediating processes of two communication interventions for breast cancer patients. *Patient Educ Couns*. (2010) 81:S48–53. doi: 10.1016/j.pec.2010.10.021
42. Baker TB, Hawkins R, Pingree S, Roberts LJ, McDowell HE, Shaw BR, et al. Optimizing eHealth breast cancer interventions: which types of eHealth services are effective? *Transl Behav Med* (2011) 1(1):134–45. doi: 10.1007/s13142-010-0004-0
43. Hawkins RP, Pingree S, Baker TB, Roberts LJ, Shaw BR, McDowell H, et al. Integrating eHealth with human services for breast cancer patients. *Transl Behav Med* (2011) 1(1):146–54. doi: 10.1007/s13142-011-0027-1
44. Sherman DW, Haber J, Hoskins CN, Budin WC, Maislin G, Shukla S, et al. The effects of psychoeducation and telephone counseling on the adjustment of women with early-stage breast cancer. *Appl Nurs Res* (2012) 25(1):3–16. doi: 10.1016/j.apnr.2009.10.003
45. Crane-Okada R, Freeman E, Kiger H, Ross M, Elashoff D, Deacon L, et al. Senior peer counseling by telephone for psychosocial support after breast cancer surgery: effects at six months. *Oncol Nurs Forum* (2012) 39(1):78–89. doi: 10.1188/12.ONF.78-89
46. Pinto BM, Papandonatos GD, Goldstein MG. A randomized trial to promote physical activity among breast cancer patients. *Health Psychol* (2013) 32(6):616. doi: 10.1037/a0029886
47. Carpenter KM, Stoner SA, Schmitz K, McGregor BA, Doorenbos AZ. An online stress management workbook for breast cancer. *J Behav Med* (2014) 37(3):458–68. doi: 10.1007/s10865-012-9481-6
48. Freeman LW, White R, Ratcliff CG, Sutton S, Stewart M, Palmer JL, et al. A randomized trial comparing live and telemedicine deliveries of an imagery-based behavioral intervention for breast cancer survivors: reducing symptoms and barriers to care. *Psycho-oncology* (2015) 24(8):910–8. doi: 10.1002/pon.3656
49. Befort CA, Klemp JR, Sullivan DK, Shireman T, Diaz FJ, Schmitz K, et al. Weight loss maintenance strategies among rural breast cancer survivors: the rural women connecting for better health trial. *Obesity* (2016) 24(10):2070–7. doi: 10.1002/oby.21625
50. Chee W, Lee Y, Im E-O, Chee E, Tsai H-M, Nishigaki M, et al. A culturally tailored Internet cancer support group for Asian American breast cancer survivors: a randomized controlled pilot intervention study. *J Telemed Telecare*. (2017) 23(6):618–26. doi: 10.1177/1357633X16658369
51. Harrigan M, Cartmel B, Loffield E, Sanft T, Chagpar AB, Zhou Y, et al. Randomized trial comparing telephone versus in-person weight loss counseling on body composition and circulating biomarkers in women treated for breast cancer: the lifestyle, exercise, and nutrition (LEAN) study. *J Clin Oncol* (2016) 34(7):669. doi: 10.1200/JCO.2015.61.6375
52. Han H-R, Song Y, Kim M, Hedlin HK, Kim K, Ben Lee H, et al. Breast and cervical cancer screening literacy among Korean American women: A community health worker-led intervention. *Am J Public Health* (2017) 107(1):159–65. doi: 10.2105/AJPH.2016.303522
53. Cox M, Basen-Engquist K, Carmack CL, Blalock J, Li Y, Murray J, et al. Comparison of internet and telephone interventions for weight loss among cancer survivors: randomized controlled trial and feasibility study. *JMIR cancer*. (2017) 3(2):e7166. doi: 10.2196/cancer.7166
54. Ferrante JM, Devine KA, Bator A, Rodgers A, Ohman-Strickland PA, Bandera EV, et al. Feasibility and potential efficacy of commercial mHealth/eHealth tools for weight loss in African American breast cancer survivors: pilot randomized controlled trial. *Transl Behav Med* (2020) 10(4):938–48. doi: 10.1093/tbm/iby124
55. Hartman SJ, Nelson SH, Weiner LS. Patterns of fitbit use and activity levels throughout a physical activity intervention: exploratory analysis from a randomized controlled trial. *JMIR mHealth uHealth*. (2018) 6(2):e8503. doi: 10.2196/mhealth.8503
56. Im EO, Kim S, Yang YL, Chee W. The efficacy of a technology-based information and coaching/support program on pain and symptoms in Asian

American survivors of breast cancer. *Cancer* (2020) 126(3):670–80. doi: 10.1002/cncr.32579

57. Paladino AJ, Anderson JN, Krukowski RA, Waters T, Kocak M, Graff C, et al. THRIVE study protocol: a randomized controlled trial evaluating a web-based app and tailored messages to improve adherence to adjuvant endocrine therapy among women with breast cancer. *BMC Health Serv Res* (2019) 19(1):1–12. doi: 10.1186/s12913-019-4588-x

58. Meneses K, Pisu M, Azuero A, Benz R, Su X, McNees P. A telephone-based education and support intervention for rural breast cancer survivors: a randomized controlled trial comparing two implementation strategies in rural Florida. *J Cancer survivorship: Res practice* (2020) 14(4):494–503. doi: 10.1007/s11764-020-00866-y

59. Aranda S, Schofield P, Weih L, Milne D, Yates P, Faulkner R. Meeting the support and information needs of women with advanced breast cancer: a randomised controlled trial. *Br J Cancer* (2006) 95(6):667–73. doi: 10.1038/sj.bjc.6603320

60. Hayes S, Rye S, Battistutta D, Yates P, Pyke C, Bashford J, et al. Design and implementation of the exercise for health trial—a pragmatic exercise intervention for women with breast cancer. *Contemp Clin Trials*. (2011) 32(4):577–85. doi: 10.1016/j.cct.2011.03.015

61. Eakin EG, Lawler SP, Winkler EA, Hayes SC. A randomized trial of a telephone-delivered exercise intervention for non-urban dwelling women newly diagnosed with breast cancer: exercise for health. *Ann Behav Med* (2012) 43(2):229–38. doi: 10.1007/s12160-011-9324-7

62. Gordon LG, DiSipio T, Battistutta D, Yates P, Bashford J, Pyke C, et al. Cost-effectiveness of a pragmatic exercise intervention for women with breast cancer: results from a randomized controlled trial. *Psycho-oncology* (2017) 26(5):649–55. doi: 10.1002/pon.4201

63. Sherman KA, Przedziecki A, Alcorso J, Kilby CJ, Elder E, Boyages J, et al. Reducing body image-related distress in women with breast cancer using a structured online writing exercise: Results from the my changed body randomized controlled trial. *J Clin Oncol* (2018) 36(19):1930–40. doi: 10.1200/JCO.2017.76.3318

64. Lynch BM, Nguyen NH, Moore MM, Reeves MM, Rosenberg DE, Boyle T, et al. A randomized controlled trial of a wearable technology-based intervention for increasing moderate to vigorous physical activity and reducing sedentary behavior in breast cancer survivors: The ACTIVATE trial. *Cancer* (2019) 125(16):2846–55. doi: 10.1002/cncr.32143

65. van den Berg SW, Gielissen MF, Custers JA, van der Graaf WT, Ottevanger PB, Prins JB. BREATHE: web-based self-management for psychological adjustment after primary breast cancer—results of a multicenter randomized controlled trial. *J Clin Oncol* (2015) 33(25):2763–71. doi: 10.1200/JCO.2013.54.9386

66. Kimmman N, Dirksen C, Voogd A, Falger P, Gijzen B, Thuring M, et al. Nurse-led telephone follow-up and an educational group programme after breast cancer treatment: results of a 2 × 2 randomised controlled trial. *Eur J Cancer* (2011) 47(7):1027–36. doi: 10.1016/j.ejca.2010.12.003

67. Abrahams N, Jewkes R, Lombard C, Mathews S, Campbell J, Meel B. Impact of telephonic psycho-social support on adherence to post-exposure prophylaxis (PEP) after rape. *AIDS Care* (2010) 22(10):1173–81. doi: 10.1080/09540121003692185

68. Bruggeman-Everts FZ, Wolvers MD, Van de Schoot R, Vollenbroek-Hutten MM, van der Lee ML. Effectiveness of two web-based interventions for chronic cancer-related fatigue compared to an active control condition: results of the “Fitter na kanker” randomized controlled trial. *J Med Internet Res* (2017) 19(10):e336. doi: 10.2196/jmir.7180

69. Høyer BB, Toft GV, Debess J, Ramlau-Hansen CH. A nurse-led telephone session and quality of life after radiotherapy among women with breast cancer: A randomized trial. *Open Nurs J* (2011) 5:31. doi: 10.2174/1874434601105010031

70. Zachariae R, Amidi A, Damholdt MF, Clausen CD, Dahlgaard J, Lord H, et al. Internet-Delivered cognitive-behavioral therapy for insomnia in breast cancer survivors: a randomized controlled trial. *JNCI: J Natl Cancer Institute*. (2018) 110(8):880–7. doi: 10.1093/jnci/djx293

71. Galiano-Castillo N, Cantarero-Villanueva I, Fernández-Lao C, Ariza-García A, Díaz-Rodríguez L, Del-Moral-Ávila R, et al. Telehealth system: A randomized controlled trial evaluating the impact of an internet-based exercise intervention on quality of life, pain, muscle strength, and fatigue in breast cancer survivors. *Cancer* (2016) 122(20):3166–74. doi: 10.1002/cncr.30172

72. Ariza-García A, Lozano-Lozano M, Galiano-Castillo N, Postigo-Martin P, Arroyo-Morales M, Cantarero-villanueva i. a web-based exercise system (e-cuidatechemo) to counter the side effects of chemotherapy in patients with breast cancer: randomized controlled trial. *J Med Internet Res* (2019) 21(7):e14418. doi: 10.2196/14418

73. Lleras de Frutos M, Medina JC, Vives J, Casellas-Grau A, Marzo JL, Borrás JM, et al. Video conference vs face-to-face group psychotherapy for distressed cancer survivors: A randomized controlled trial. *Psycho-Oncology* (2020) 29(12):1995–2003. doi: 10.1002/pon.5457

74. David N, Schlenker P, Prudlo U, Larbig W. Online counseling via e-mail for breast cancer patients on the German internet: preliminary results of a

psychoeducational intervention. *GMS Psycho-Social-Med* (2011) 8. doi: 10.3205/psm000074

75. Ziller V, Kyvernitis I, Knöll D, Storch A, Hars O, Hadji P. Influence of a patient information program on adherence and persistence with an aromatase inhibitor in breast cancer treatment—the COMPAS study. *BMC Canc* (2013) 13(1):1–9. doi: 10.1186/1471-2407-13-407

76. Owen JE, Klapow JC, Roth DL, Shuster JL, Bellis J, Meredith R, et al. Randomized pilot of a self-guided internet coping group for women with early-stage breast cancer. *Ann Behav Med* (2005) 30(1):54–64. doi: 10.1207/s15324796abm3001_7

77. Ryhänen AM, Rankinen S, Siekkinen M, Saarinen M, Korvenranta H, Leino-Kilpi H. The impact of an empowering Internet-based breast cancer patient pathway program on breast cancer patients’ clinical outcomes: a randomised controlled trial. *J Clin Nurs* (2013) 22(7–8):1016–25. doi: 10.1111/jocn.12007

78. Goodwin PJ, Segal RJ, Vallis M, Ligibel JA, Pond GR, Robidoux A, et al. Randomized trial of a telephone-based weight loss intervention in postmenopausal women with breast cancer receiving letrozole: the LISA trial. *J Clin Oncol* (2014) 32(21):2231–9. doi: 10.1200/JCO.2013.53.1517

79. Kim HJ, Kim SM, Shin H, Jang J-S, Kim YI, Han DH. A mobile game for patients with breast cancer for chemotherapy self-management and quality-of-life improvement: randomized controlled trial. *J Med Internet Res* (2018) 20(10):e273. doi: 10.2196/jmir.9559

80. Hayes SC, Rye S, DiSipio T, Yates P, Bashford J, Pyke C, et al. Exercise for health: a randomized, controlled trial evaluating the impact of a pragmatic, translational exercise intervention on the quality of life, function and treatment-related side effects following breast cancer. *Breast Cancer Res Treat* (2013) 137(1):175–86. doi: 10.1007/s10549-012-2331-y

81. Hou I-C, Lin H-Y, Shen S-H, Chang K-J, Tai H-C, Tsai A-J, et al. Quality of life of women after a first diagnosis of breast cancer using a self-management support mHealth app in Taiwan: randomized controlled trial. *JMIR mHealth uHealth*. (2020) 8(3):e17084. doi: 10.2196/17084

82. Lippi L, D’Abrosca F, Folli A, Dal Molin A, Moalli S, Maconi A, et al. Closing the gap between inpatient and outpatient settings: Integrating pulmonary rehabilitation and technological advances in the comprehensive management of frail patients. *Int J Environ Res Public Health* (2022) 19(15):9150. doi: 10.3390/ijerph19159150

83. Invernizzi M, Runza L, De Sire A, Lippi L, Blundo C, Gambini D, et al. Integrating augmented reality tools in breast cancer related lymphedema prognostication and diagnosis. *JoVE (Journal Visualized Experiments)*. (2020) 156:e60093. doi: 10.3791/60093

84. Kalra S, Miraj M, Ajmera P, Shaik RA, Seyam MK, Shawky GM, et al. Effects of yogic interventions on patients diagnosed with cardiac diseases: a systematic review and meta-analysis. *Front Cardiovasc Med* (2022) 9. doi: 10.3389/fcvm.2022.942740

85. Smith TJ, Dow LA, Virago EA, Khatcheressian J, Matsuyama R, Lyckholm LJ. A pilot trial of decision aids to give truthful prognostic and treatment information to chemotherapy patients with advanced cancer. *J supportive Oncol* (2011) 9(2):79. doi: 10.1016/j.suponc.2010.12.005

86. Vogel RI, Petzel SV, Cragg J, McClellan M, Chan D, Dickson E, et al. Development and pilot of an advance care planning website for women with ovarian cancer: a randomized controlled trial. *Gynecol Oncol* (2013) 131(2):430–6. doi: 10.1016/j.ygyno.2013.08.017

87. Leon N, Schneider H, Daviaud E. Applying a framework for assessing the health system challenges to scaling up mHealth in south Africa. *BMC Med Inform Decis Mak*. (2012) 12(1):1–12. doi: 10.1186/1472-6947-12-123

88. Loubani K, Kizony R, Milman U, Schreuer N. Hybrid tele and in-clinic occupation based intervention to improve women’s daily participation after breast cancer: A pilot randomized controlled trial. *Int J Environ Res Public Health* (2021) 18(11):5966. doi: 10.3390/ijerph18115966

89. Eysenbach G, Group C-E. CONSORT-EHEALTH: improving and standardizing evaluation reports of web-based and mobile health interventions. *J Med Internet Res* (2011) 13(4):e1923. doi: 10.2196/jmir.1923

90. Palmqvist B, Carlbring P, Andersson G. Internet-Delivered treatments with or without therapist input: does the therapist factor have implications for efficacy and cost? *Expert Rev Pharmacoecon Outcomes Res* (2007) 7(3):291–7. doi: 10.1586/14737167.7.3.291

91. Binder AF, Handley NR, Wilde L, Palmisiano N, Lopez AM. Treating hematologic malignancies during a pandemic: utilizing telehealth and digital technology to optimize care. *Front Oncol* (2020) 10:1183. doi: 10.3389/fonc.2020.01183

92. Demark-Wahnefried W, Colditz GA, Rock CL, Sedjo RL, Liu J, Wolin KY, et al. Quality of life outcomes from the exercise and nutrition enhance recovery and good health for you (ENERGY)-randomized weight loss trial among breast cancer survivors. *Breast Cancer Res Treat* (2015) 154(2):329–37. doi: 10.1007/s10549-015-3627-5



OPEN ACCESS

EDITED BY
Dayanidhi Raman,
University of Toledo, United States

REVIEWED BY
Liu Yiqiang,
Beijing Cancer Hospital, China
Ekta Khattar,
SVKM's Narsee Monjee Institute of
Management Studies, India

*CORRESPONDENCE
Li Zhu
✉ zhuli8@yeah.net

[†]These authors have contributed
equally to this work

SPECIALTY SECTION
This article was submitted to
Breast Cancer,
a section of the journal
Frontiers in Oncology

RECEIVED 17 July 2022

ACCEPTED 14 December 2022

PUBLISHED 12 January 2023

CITATION
Chen W, Wu J, Zhu Y, Huang J,
Chen X, Huang O, He J, Li Y, Chen W,
Shen K and Zhu L (2023) Impact of
clinicopathological factors on
extended endocrine therapy
decision making in estrogen
receptor-positive breast cancer.
Front. Oncol. 12:996522.
doi: 10.3389/fonc.2022.996522

COPYRIGHT
© 2023 Chen, Wu, Zhu, Huang, Chen,
Huang, He, Li, Chen, Shen and Zhu. This
is an open-access article distributed
under the terms of the [Creative
Commons Attribution License \(CC BY\)](#).
The use, distribution or reproduction
in other forums is permitted, provided
the original author(s) and the
copyright owner(s) are credited and
that the original publication in this
journal is cited, in accordance with
accepted academic practice. No use,
distribution or reproduction is
permitted which does not comply with
these terms.

Impact of clinicopathological factors on extended endocrine therapy decision making in estrogen receptor-positive breast cancer

Weilin Chen^{1†}, Jiayi Wu^{1†}, Yifei Zhu¹, Jiahui Huang¹,
Xiaosong Chen¹, Ou Huang¹, Jianrong He¹, Yafen Li¹,
Weiguo Chen¹, Kunwei Shen¹ and Li Zhu^{2*}

¹Department of General Surgery, Comprehensive Breast Health Center, Ruijin Hospital, Shanghai Jiaotong University School of Medicine, Shanghai, China, ²Department of Thyroid and Breast Surgery, Shanghai General Hospital, Shanghai Jiaotong University School of Medicine, Shanghai, China

Purpose: In our study, we aim to analyze the impact of clinicopathological factors on the recommendation of extended endocrine therapy (EET) in patients with ER+ breast cancer and to retrospectively validate the value of CTS5 in EET decision making.

Patients and methods: The retrospective analysis was performed in patients with ER+ breast cancer who have finished 4.5–5 years of adjuvant endocrine therapy and undergone MDT discussion from October 2017 to November 2019. Multivariate logistic regression was used to identify the independent factors for treatment recommendation. CTS5 was calculated for retrospective validation of the EET decision making.

Results: Two hundred thirty-five patients were received; 4.5–5 years of adjuvant endocrine therapy were included in the study. Multivariate analysis suggested that age (OR 0.460, 95% CI 0.219–0.965, $p = 0.04$), pN (OR 39.350, 95% CI 9.831–157.341, $P < 0.001$), and receipt of chemotherapy (OR 3.478, 95% CI 1.336–9.055, $p = 0.011$) were independent predictors for the recommendation of EET. In the previously selective estrogen receptor modulator (SERM)-treated subgroup, pN and receipt of chemotherapy were independent predictors for the recommendation of EET. In the previously AI-treated subgroup, age, pN, and receipt of chemotherapy were independent predictors. Adverse events did not affect the recommendation in patients previously treated with adjuvant endocrine treatment nor in the previously SERM or AI-treated subgroups. CTS5 (OR 21.887, 95% CI 2.846–168.309, $p = 0.003$) remained an independent predictor for the recommendation of EET.

Conclusions: Our study indicated that age, lymph nodal status, and receipt of chemotherapy were independent predictors for the recommendation of EET. The application of the CTS5 on EET decision making might be valuable among ER+ breast cancer patients.

KEYWORDS

breast malignancy, extended endocrine therapy, multidisciplinary team, estrogen receptor positive (ER+), CTS5

Introduction

For decades, breast cancer has been the most frequently diagnosed malignant tumor in women globally. According to the latest global epidemiological cancer survey, 2.1 million new cases of breast cancer were diagnosed worldwide in 2018 (1). In estrogen receptor (ER)-positive early breast cancer, endocrine therapy plays an important role in its comprehensive treatment, and 5 years of treatment was considered the standard treatment duration traditionally (2–4).

However, recent studies have shown that among women with ER-positive breast cancer who were scheduled to receive 5 years of endocrine therapy, distant recurrences still have a steady rate for at least another 15 years after the end of the 5-year treatment (5–7). According to the results of several clinical trials regarding extended adjuvant endocrine therapy (ATLAS, aTTom, MA-17R, and NSABP B-42), the effect of extended endocrine therapy (EET) beyond 5 years to reduce the risk of late recurrence for ER+ breast cancer has been demonstrated (8–13). An EBCTCG meta-analysis also showed the efficacy of extending AI therapy compared with stopping AI after about 5 years of endocrine therapy in preventing disease recurrence and death from breast cancer (14). In the American Society of Clinical Oncology (ASCO) clinical practice guideline in 2018, EET was included among node-positive and some node-negative breast cancer patients with co-existing high-risk factors (15). However, controversies remain about the target population who may benefit from EET in clinical decision making.

In our study, we aim to analyze the impact of clinicopathological factors on the choice of follow-up treatment after 5 years of endocrine therapy in patients with ER-positive breast cancer and to retrospectively validate the value of CTS5 in EET decision making.

Abbreviations: EET, extended endocrine therapy; ER, estrogen receptor; PR, progesterone receptor; HER-2, human epidermal growth factor receptor 2; SERM, selective estrogen receptor modulators; AI, aromatase inhibitors; OFS, ovarian function suppression; MDT, Multiple Disciplinary Team.

Patients and methods

Study population

The retrospective analysis was performed in patients who met the following eligibility criteria: (1) female gender; (2) post-surgery; (3) have received adjuvant endocrine therapy for 4.5–5 years; (4) have undergone Multiple Disciplinary Team (MDT) discussion regarding the use of EET in Comprehensive Breast Health Center, Ruijin Hospital, Shanghai Jiao Tong University School of Medicine, Shanghai, China, between October 2017 and November 2019; (5) ER-positive. Patient information was extracted from Shanghai Jiao Tong University Breast Cancer Database (SJTU-BCDB).

Histopathological evaluation

Tumor histopathologic result was independently performed by two experienced pathologists, including estrogen receptor (ER), progesterone receptor (PR), human epidermal growth factor receptor 2 (HER-2) status, Ki-67 status, histological grade, and pathological type. ER-positivity (ER+) and PR-positivity (PR+) were defined as more than 1% positive invasive tumor cells with nuclear staining (16). HER-2 status was identified according to the 2013 ASCO/CAP guidelines (17) (the minority of patients' HER-2 status diagnosed before 2013 was evaluated according to 2007 ASCO/CAP guidelines (18)). The median Ki-67 value for hormone receptor-positive disease in SJTU-BCDB was 15.0%, so we defined Ki-67 high as more than 15% positive invasive tumor cells with nuclear staining. TNM stage was based on the 7th edition of the American Joint Committee on Cancer (AJCC) (19). CTS5 was calculated for retrospective validation of the EET decision making, and patients were divided into two risk groups according to CTS5 score: low (< 3.13) and high (≥ 3.13) groups (20). $CTS5 = 0.438 \times \text{nodes} + 0.988 \times (0.093 \times \text{size(mm)} - 0.001 \times \text{size}) + 0.375 \times \text{grade} + 0.017 \times \text{age}$.

Treatment decision

After the completion of 4.5–5 years of adjuvant endocrine therapy, the MDT meeting would be held to recommend extending the endocrine treatment regimen based on patients' clinicopathological features and other related factors such as adverse events. Treatment choices on whether or not to extend endocrine therapy were decided through MDT meetings including surgical oncologists, medical oncologists, radiation oncologists, ultrasound physicians, pathologists, breast cancer specialized nurses, and other related specialists. The recommendation was first determined by each physician in the MDT team and then finally determined after MDT discussion and comprehensive opinions. The standard regimens for recommendation include stopping endocrine therapy, treating with aromatase inhibitors (AIs) for 3 or 5 years, and treating with selective estrogen receptor modulators (SERMs) for 5 years, with or without applying ovarian function suppression (OFS).

Statistical analysis

All clinicopathological characteristics were analyzed as categorical variables by using logistic regression. Multivariate logistic regression was used to identify the independent factors for treatment recommendation. The chi-square test was used to evaluate the adverse events. Fisher's exact tests were carried out if necessary. Data were analyzed using IBM SPSS statistics software version 23 (SPSS, Inc. Chicago, IL). Two-sided $P < 0.05$ were considered statistically significant.

Results

Clinical characteristics

A total of 252 patients participated in the multidisciplinary discussion, 235 patients who had received 4.5–5 years of adjuvant endocrine therapy were included in the study, and 17 patients were excluded because of information loss. One hundred forty-three patients (60.9%) were suggested to receive EET, and 92 patients (39.1%) were suggested to stop EET. The mean age of patients was 60 years old, and 136 (57.9%) patients were older than 50 years. There were 140 (59.6%) patients with T1 stage tumors and 105 (44.7%) patients with positive lymph nodes. The proportion of patients with PR-positive, Ki-67 $\geq 15\%$, or HER-2 positive was 81.3, 51.1, and 18.7%, respectively. The baseline characteristics of the participants are presented in Table 1.

Impact factors on decision making in all patients

In univariate analysis, age (OR 5.19, 95% CI 0.301–0.895, $p = 0.018$), pT (OR 3.042, 95% CI 1.713–5.404, $P < 0.001$), pN (OR 26.444, 95% CI 1.713–5.404, $p < 0.001$), HER-2 (OR 2.989, 95% CI 1.361–6.562, $p = 0.006$), Ki-67 status (OR 2.574, 95% CI 1.500–4.415, $p = 0.001$), Grade (GII vs. GI: OR 1.994, 95% CI 0.828–4.802, $p = 0.0124$; and GIII vs. GI: OR 6.416, 95% CI 2.506–20.016, $p = 0.001$), receipt of chemotherapy (OR 9.288, 95% CI 5.042–17.108, $p < 0.001$), receipt of target therapy (OR 3.089, 95% CI 1.292–7.387, $p = 0.011$), and receipt of radiotherapy (OR 2.510, 95% CI 1.463–4.307, $p = 0.001$) were correlated with the recommendation of EET (Table 2).

Multivariate analysis suggested that age (OR 0.460, 95% CI 0.219–0.965, $p = 0.04$), pN (OR 39.350, 95% CI 9.831–157.341, $p < 0.001$), and receipt of chemotherapy (OR 3.478, 95% CI 1.336–9.055, $p = 0.011$) were independent predictors for the recommendation of EET (Table 3).

Impact factors of decision making in previously SERM/AI-treated subgroups

In univariate analysis of the previously SERM-treated group, pT (OR 4.000, 95% CI 1.136–14.085, $p = 0.031$), pN (OR 18.692, 95% CI 13.760–92.926, $p < 0.001$), Ki-67 index (OR 4.846, 95% CI 1.515–15.504, $p = 0.008$), receipt of chemotherapy (OR 16.333, 95% CI 4.281–62.310, $p < 0.001$) were correlated with EET (Table 4). Multivariate analysis suggested that pN (OR 10.811, 95% CI 1.937–60.346, $p = 0.007$) and receipt of chemotherapy (OR 9.396, 95% CI 2.155–40.980, $p = 0.003$) were independent predictors for the recommendation of EET (Table 3).

In univariate analysis of the previously-AI-treated group, age (OR 0.400, 95% CI 0.186–0.860, $p = 0.019$), pT (OR 2.844, 95% CI 1.483–5.454, $p = 0.002$), pN (OR 29.731, 95% CI 10.939–80.809, $p < 0.001$), HER-2 (OR 2.670, 95% CI 1.078–6.613, $p = 0.034$), Ki-67 status (OR 2.107, 95% CI 1.140–3.893, $p = 0.017$), Grade (GIII vs. GI: OR 7.778, 95% CI 2.032–29.773, $p = 0.003$), receipt of chemotherapy (OR 7.802, 95% CI 3.920–15.528, $p < 0.001$), and receipt of radiotherapy (OR 2.596, 95% CI 1.389–4.852, $p = 0.003$) were correlated with EET (Table 5). Multivariate analysis suggested that age (OR 0.315, 95% CI 0.117–0.848, $p = 0.022$), pN (OR 20.533, 95% CI 7.249–58.158, $p < 0.001$), and receipt of chemotherapy (OR = 4.387, 95% CI 1.893–10.169, $p = 0.001$) were independent predictors for the recommendation of EET (Table 3).

TABLE 1 Baseline characteristics of study participants and impact factors for extended endocrine therapy decision.

| | Number | Percent % |
|--------------------------|--------|-----------|
| Recommend | 235 | |
| No-EET | 92 | 39.1 |
| EET | 143 | 60.9 |
| Age, years | | |
| ≤ 60 | 99 | 42.1 |
| > 60 | 136 | 57.9 |
| Menopause status | | |
| Pre | 55 | 23.4 |
| Post | 180 | 76.6 |
| pT | | |
| pT1 | 140 | 59.6 |
| pT2+ | 95 | 40.4 |
| pN | | |
| pN0 | 130 | 55.3 |
| pN1+ | 105 | 44.7 |
| PR status | | |
| Negative | 44 | 18.7 |
| Positive | 191 | 81.3 |
| HER-2 status | | |
| Negative | 191 | 81.3 |
| Positive | 44 | 18.7 |
| Ki67 status | | |
| < 15 | 115 | 48.9 |
| ≥ 15 | 120 | 51.1 |
| Grade | | |
| N/A | 37 | 15.7 |
| I | 24 | 10.2 |
| II | 129 | 54.9 |
| III | 45 | 19.1 |
| Operation methods | | |
| Lumpectomy | 77 | 32.8 |
| Mastectomy | 158 | 67.2 |
| Chemotherapy | | |
| No | 86 | 36.6 |
| Yes | 149 | 63.4 |
| Target therapy | | |
| (Continued) | | |

TABLE 1 Continued

| | Number | Percent % |
|-------------------|--------|-----------|
| No | 199 | 84.7 |
| Yes | 36 | 15.3 |
| Radiotherapy | | |
| No | 96 | 40.9 |
| Yes | 139 | 59.1 |
| CTS5 (N = 198) | | |
| < 3.13 | 156 | 78.8 |
| ≥ 3.13 | 42 | 21.2 |
| RS (N = 21) | | |
| Low risk | 2 | 9.5 |
| Intermediate risk | 15 | 71.4 |
| High risk | 4 | 19 |

PR, progesterone receptor; CTS5, the Clinical Treatment Score post-5 years.

The retrospective validation of CTS5 for EET decision making

In this study, 198 patients had data on CTS5. The distribution of CTS5 was 78.8% and 21.2% for the low (< 3.13) and high-risk (≥ 3.13) groups, respectively. Overall, CTS5 (OR 36.865, 95% CI 2.846–168.309, $p = 0.001$) was correlated with EET in univariate analysis (Table 2). After excluding the factors involved in the CTS5 formula, CTS5 (OR 21.887, 95% CI 2.846–168.309, $p = 0.003$) remained an independent predictor for the recommendation of EET in multivariate analysis (Table 3).

For patients previously SERM-treated, all patients were suggested to extend the endocrine therapy when their CTS5 status was indicated as high risk (Table 4).

For patients previously AI-treated, 35 (97.2%) patients were recommended EET in the previously AI-treated group when their CTS5 status was indicated as high risk. In the univariate analysis of the previously AI-treated group, CTS5 (OR 34.375, 95% CI 4.550–259.724, $p = 0.001$) was correlated with EET (Table 5). In multivariate analysis, CTS5 (OR 25.191, 95% CI 3.240–195.841, $p = 0.002$) remained an independent predictor for the recommendation of EET (Table 3).

Impact of adverse events on decision making

In our study, the following common adverse events after endocrine therapy were recorded and analyzed: endometrial thickening, endometrial cancer, musculoskeletal symptoms,

T-score < -2, fracture, hot flash (≥ G3), libido decreased (≥ G2), depression or anxiety, and dyslipidemia.

Of all patients who participated in the multidisciplinary discussion ($n = 235$), 14 patients had endometrial thickening (6%), one patient had endometrial cancer (0.4%), 19 patients had musculoskeletal symptoms (8.1%), 46 patients had osteoporosis (19.6%), 14 patients had fracture (6%), nine patients had hot flash (3.8%), six patients had libido decreased (≥ G2) (2.6%), 43 patients had depression or anxiety (18.3%), and 58 patients had dyslipidemia (24.7%) (Table 6). None of these AEs were significantly correlated with the recommendation of EET in univariate analysis. In patients previously treated with SERM or AI, similar results were found that none of these adverse events were correlated with treatment decisions (Table 6).

Discussion

Extending the duration of the endocrine therapy to 10 years has now proved to reduce the risk of late recurrence in selected ER+ breast cancer patients (4, 5, 10, 21). However, controversies remain about the target population who may benefit from the EET in clinical decision making. In our study, there were 235 ER-positive patients participated in the multidisciplinary discussion, and we found that age, lymph node status, and receipt of chemotherapy were independently associated with the recommendation of EET.

Among classic clinicopathological factors, nodal status is the strongest predictor of early recurrence (22). The study by HongChao and colleagues included 62,923 ER+ breast cancer

TABLE 2 Univariate analysis of impact factors for extended endocrine therapy recommendation in the whole-patients group.

| N = 235 | EET recommendation | | OR | p | CI 95% |
|-------------------|--------------------|-------------|--------|---------|---------------|
| | No-EET | EET | | | |
| Age, years | | | 0.519 | 0.018 | 0.301–0.895 |
| ≤ 60 | 30 (30.3%) | 69 (68.7%) | | | |
| > 60 | 62 (45.6%) | 74 (54.4%) | | | |
| Menopause status | | | 0.774 | 0.425 | 0.412–1.453 |
| Pre | 19 (34.5%) | 36 (65.5%) | | | |
| Post | 73 (40.6%) | 107 (59.4%) | | | |
| pT | | | 3.042 | < 0.001 | 1.713–5.404 |
| pT1 | 69 (49.3%) | 71 (50.7%) | | | |
| pT2+ | 23 (24.2%) | 72 (75.8%) | | | |
| pN | | | 26.444 | < 0.001 | 11.329–61.726 |
| pN0 | 85 (65.4%) | 45 (34.6%) | | | |
| PN1+ | 7 (6.7%) | 98 (93.3%) | | | |
| PR status | | | 0.974 | 0.938 | 0.497–1.908 |
| Negative | 17 (38.6%) | 27 (61.4%) | | | |
| Positive | 75 (39.3%) | 116 (60.7%) | | | |
| HER-2 status | | | 2.989 | 0.006 | 1.361–6.562 |
| Negative | 83 (43.5%) | 108 (56.5%) | | | |
| Positive | 9 (20.5%) | 35 (79.5%) | | | |
| Ki67 status | | | 2.574 | 0.001 | 1.500–4.415 |
| < 15 | 58 (50.4%) | 57 (49.6%) | | | |
| ≥ 15 | 34 (28.3%) | 86 (71.7%) | | | |
| Grade | | | | 0.004 | |
| I | 13 (54.2%) | 11 (45.8%) | | | |
| II | 48 (37.2%) | 81 (62.8%) | 1.994 | 0.124 | 0.828–4.802 |
| III | 7 (15.6%) | 38 (84.4%) | 6.416 | 0.001 | 2.056–20.016 |
| Operation methods | | | 1.477 | 0.168 | 0.849–2.569 |
| Lumpectomy | 35 (45.5%) | 42 (54.5%) | | | |
| Mastectomy | 57 (36.1%) | 101 (63.9%) | | | |
| Chemotherapy | | | 9.288 | < 0.001 | 5.042–17.108 |
| No | 61 (70.9%) | 25 (29.1%) | | | |
| Yes | 31 (20.8%) | 118 (79.2%) | | | |
| Target therapy | | | 3.089 | 0.011 | 1.292–7.387 |
| No | 85 (42.7%) | 114 (57.3%) | | | |
| Yes | 7 (19.4%) | 29 (80.6%) | | | |
| Radiotherapy | | | 2.510 | 0.001 | 1.463–4.307 |
| No | 50 (52.1%) | 46 (47.9%) | | | |

(Continued)

TABLE 2 Continued

| N = 235 | EET recommendation | | OR | p | CI 95% |
|-------------------|--------------------|------------|--------|-------|---------------|
| | No-EET | EET | | | |
| Yes | 42 (30.2%) | 97 (69.8%) | | | |
| CTS5 | | | 30.865 | 0.001 | 4.140–230.102 |
| < 3.13 | 67 (42.9%) | 89 (57.1%) | | | |
| ≥ 3.13 | 1 (2.4%) | 41 (97.6%) | | | |
| RS | | | | | 0.622 |
| Low risk | 2 (100%) | 0 (0) | | | |
| Intermediate risk | 8 (53.3%) | 7 (46.7%) | – | 1 | – |
| High risk | 1 (25.0%) | 3 (75.0%) | – | 1 | – |

PR, progesterone receptor; CTS5, the Clinical Treatment Score post-5 years. The bold values provided for making meaningful result ($p < 0.05$) stand out.

patients and reported that the annual risk of distant recurrence was strongly related to nodal status ($P < 0.001$), and recurrence increased with the number of metastatic lymph nodes (20-year risk with N0, N1, and N2: 22%, 31%, and 52%) (5). 2018 ASCO guideline also recommended that women with node-positive breast cancer receive extended therapy, including AI, for up to a total of 10 years of adjuvant endocrine treatment (11). In our study, lymph node status turned out to be the strongest factor associated with therapy recommendation in all clinicopathological indicators. This indicated that clinicians would pay more attention to lymph node status when they make a recommendation on whether to use EET or not.

In our study, we found that age did not affect the recommendation for extended SERMs in the previously SERM-treated group, but it was the independent predictor for recommendation in the previously AI-treated group and older patients are less likely to be recommended for extended AIs.

At present, there is no evidence that age is related to the risk of recurrence (2). A meta-analysis in 2017 shows that there was no statistically significant benefit from extended therapy in the age subgroup (23). Therefore, for those who were previously treated with SERMs, age will not affect the choice of doctors. However, in patients previously treated with AI, the proportion of elderly patients (age > 60) is relatively large (75%) in our data. In the face of those patients, considering the physical condition, tolerance, and the lack of evidence to prove the validity of EET, clinicians tend to make the relatively conservative decision.

CTS5 (ATAC), including tumor size, number of positive nodes, histologic grade, and age, is a simple tool that was validated as highly prognostic for late recurrence (7, 24). In Dowsett's research, the prognostic value of CTS5 was tested using data from the ATAC trial and validated with data from the BIG 1-98 trial (20). Furthermore, populations of those clinical trials are all postmenopausal patients and may behave differently

TABLE 3 Multivariate analysis of impact factors for extended endocrine therapy recommendation in whole-patients group and previously SERM or AI-treated subgroups.

| | | OR | 95%CI | p |
|----------------|--------------|--------|---------------|--------|
| Whole patients | Age | 0.460 | 0.219–0.965 | 0.04 |
| | pN | 20.695 | 8.099–52.882 | <0.001 |
| | Chemotherapy | 5.652 | 2.696–11.850 | <0.001 |
| | CTS5 | 21.887 | 2.846–168.309 | 0.003 |
| SERM | pN | 10.811 | 1.937–60.346 | 0.007 |
| | Chemotherapy | 9.396 | 2.155–40.980 | 0.003 |
| AI | Age | 0.315 | 0.117–0.848 | 0.022 |
| | pN | 20.533 | 7.249–58.158 | <0.001 |
| | Chemotherapy | 4.387 | 1.893–10.169 | 0.001 |
| | CTS5 | 25.191 | 3.240–195.841 | 0.002 |

CTS5, the Clinical Treatment Score post-5 years.

TABLE 4 Univariate analysis of impact factors for extended endocrine therapy recommendation in SERM group.

| SERM(<i>n</i> = 60) | EET recommendation | | OR | <i>p</i> | CI 95% |
|----------------------|--------------------|-------------------|---------------|-------------------|----------------------|
| | No-EET | EET | | | |
| Age, years | | | 1.541 | 0.716 | 0.150–15.930 |
| ≤ 60 | 19 (33.9%) | 27 (66.1%) | | | |
| > 60 | 1 (25.0%) | 3 (75.0%) | | | |
| Menopause status | | | 2.154 | 0.238 | 0.603–7.699 |
| Pre | 16 (38.1%) | 26 (61.9%) | | | |
| Post | 4 (22.2%) | 14 (77.8%) | | | |
| pT | | | 4.000 | 0.031 | 1.136–14.085 |
| pT1 | 16 (44.4%) | 20 (55.6%) | | | |
| pT2+ | 4 (16.7%) | 20 (83.3%) | | | |
| pN | | | 18.692 | < 0.001 | 13.760–92.929 |
| pN0 | 18 (58.1%) | 13 (41.9%) | | | |
| pN1+ | 2 (6.9%) | 27 (93.1%) | | | |
| PR status | | | 0.778 | 0.777 | 0.137–4.412 |
| Negative | 2 (28.6%) | 5 (71.4%) | | | |
| Positive | 18 (34.0%) | 35 (66.0%) | | | |
| HER-2 status | | | 3.857 | 0.100 | 0.771–19.293 |
| Negative | 18 (39.1%) | 28 (60.9%) | | | |
| Positive | 2 (14.3%) | 12 (85.7%) | | | |
| Ki67 status | | | 4.846 | 0.008 | 1.515–15.504 |
| < 15 | 14 (51.9%) | 13 (48.1%) | | | |
| ≥ 15 | 6 (18.2%) | 27 (81.8%) | | | |
| Grade | | | | 0.374 | |
| I | 3 (37.5%) | 5 (62.5%) | | | |
| II | 8 (25.0%) | 24 (75.0%) | 1.800 | 0.482 | 0.349–9.278 |
| III | 1 (9.1%) | 10 (90.9%) | 6.000 | 0.161 | 0.490–73.452 |
| Operation methods | | | 1.420 | 0.551 | 0.449–4.490 |
| Lumpectomy | 7 (38.9%) | 11 (61.1%) | | | |
| Mastectomy | 13 (31.0%) | 29 (69.0%) | | | |
| Chemotherapy | | | 16.333 | < 0.001 | 4.281–62.310 |
| No | 14 (73.7%) | 5 (26.3%) | | | |
| Yes | 6 (14.6%) | 35 (85.4%) | | | |
| Target therapy | | | 6.333 | 0.090 | 0.749–53.531 |
| No | 19 (38.8%) | 30 (61.2%) | | | |
| Yes | 1 (9.1%) | 10 (90.9%) | | | |
| Radiotherapy | | | 2.500 | 0.103 | 0.832–7.511 |
| No | 12 (44.4%) | 15 (55.6%) | | | |

(Continued)

TABLE 4 Continued

| SERM(<i>n</i> = 60) | EET recommendation | | OR | <i>p</i> | CI 95% |
|----------------------|--------------------|------------|----|----------|--------|
| | No-EET | EET | | | |
| Yes | 8 (24.2%) | 25 (75.8%) | | | |
| CTS5 | | | – | – | – |
| < 3.13 | 12 (26.7%) | 33 (73.3%) | | | |
| ≥ 3.13 | 0 (0) | 6 (100%) | | | |

PR, progesterone receptor; CTS5, the Clinical Treatment Score post-5 years. The bold values provided for making meaningful result (*p*<0.05) stand out.

TABLE 5 Univariate analysis of impact factors for extended endocrine therapy recommendation in AI group.

| AI(<i>n</i> = 175) | EET recommendation | | OR | <i>p</i> | CI 95% |
|---------------------|--------------------|-------------------|---------------|-------------------|----------------------|
| | No-EET | EET | | | |
| Age, years | | | 0.400 | 0.019 | 0.186–0.860 |
| ≤ 60 | 11 (25.6%) | 32 (74.4%) | | | |
| > 60 | 61 (46.2%) | 71 (53.8%) | | | |
| Menopause status | | | 0.404 | 0.181 | 0.107–1.525 |
| Pre | 3 (23.1%) | 10 (76.9%) | | | |
| Post | 69 (42.6%) | 93 (57.4%) | | | |
| pT | | | 2.844 | 0.002 | 1.483–5.454 |
| pT1 | 53 (51.0%) | 51 (49.0%) | | | |
| pT2+ | 19 (26.8%) | 52 (73.2%) | | | |
| pN | | | 29.731 | < 0.001 | 10.939–80.809 |
| pN0 | 67 (67.7%) | 32 (32.3%) | | | |
| PN1+ | 5 (6.6%) | 71 (93.4%) | | | |
| PR status | | | 0.969 | 0.933 | 0.463–2.028 |
| Negative | 15 (40.5%) | 22 (59.5%) | | | |
| Positive | 57 (41.3%) | 81 (58.7%) | | | |
| HER-2 status | | | 2.670 | 0.034 | 1.078–6.613 |
| Negative | 65 (44.8%) | 80 (55.2%) | | | |
| Positive | 7 (23.3%) | 23 (76.7%) | | | |
| Ki67 status | | | 2.107 | 0.017 | 1.140–3.893 |
| < 15 | 44 (50.0%) | 44 (50.0%) | | | |
| ≥ 15 | 28 (32.2%) | 59 (69.8%) | | | |
| Grade | | | | 0.008 | |
| I | 10 (62.5%) | 6 (37.5%) | | | |
| II | 40 (41.2%) | 57 (58.8%) | 2.375 | 0.120 | 0.799–7.063 |
| III | 6 (17.6%) | 28 (82.4%) | 7.778 | 0.003 | 2.032–29.773 |
| Operation methods | | | 1.478 | 0.227 | 0.784–2.786 |
| Lumpectomy | 28 (47.5%) | 31 (52.5%) | | | |

(Continued)

TABLE 5 Continued

| AI(<i>n</i> = 175) | EET recommendation | | OR | <i>p</i> | CI 95% |
|-----------------------|--------------------|-------------------|---------------|-------------------|----------------------|
| | No-EET | EET | | | |
| Mastectomy | 44 (37.9%) | 72 (62.1%) | | | |
| Chemotherapy | | | 7.802 | < 0.001 | 3.920–15.528 |
| No | 47 (70.1%) | 20 (29.9%) | | | |
| Yes | 25 (23.1%) | 83 (76.9%) | | | |
| Target therapy | | | 2.488 | 0.066 | 0.941–6.582 |
| No | 66 (44.0%) | 84 (56.0%) | | | |
| Yes | 6 (24.0%) | 19 (76.0%) | | | |
| Radiotherapy | | | 2.596 | 0.003 | 1.389–4.852 |
| No | 38 (55.1%) | 31 (44.9%) | | | |
| Yes | 34 (32.1%) | 72 (69.7%) | | | |
| CTS5 | | | 34.375 | 0.001 | 4.550–259.724 |
| < 3.13 | 55 (49.5%) | 56 (50.5%) | | | |
| ≥ 3.13 | 1 (2.8%) | 35 (97.2%) | | | |

PR, progesterone receptor; CTS5, the Clinical Treatment Score post-5 years. The bold values provided for making meaningful result (*p*<0.05) stand out.

TABLE 6 The distribution of side effects in enrolled breast cancer patients and the correlation between AEs and extended endocrine therapy in whole patients enrolled and patients previously treated with SERM or AI.

| | All patients enrolled (<i>N</i> = 235) | | | Post-treatment with SERM (<i>N</i> = 60) | | | Posttreatment with AI (<i>N</i> = 175) | | |
|---|---|-------------|----------|---|------------|----------|---|-------------|----------|
| | No-EET | EET | <i>p</i> | No-EET | EET | <i>p</i> | No-EET | EET | <i>p</i> |
| Endometrial Thickening (<i>n</i> = 14, 6%) | | | | | | | | | |
| No | 78 (40.2%) | 116 (59.8%) | 0.164 | 18 (36.7%) | 31 (63.3%) | 0.476 | 60 (41.4%) | 85 (58.6%) | 0.649 |
| Yes | 3 (21.4%) | 11 (78.6%) | | 2 (22.2%) | 7 (77.8%) | | 1 (20.0%) | 4 (80.0%) | |
| Endometrial cancer (<i>n</i> = 1, 0.4%) | | | | | | | | | |
| No | 91 (38.9%) | 143 (61.1%) | 0.374 | 20 (26.7%) | 40 (73.3%) | – | 72 (41.4%) | 102 (58.6%) | 1 |
| Yes | 1 (100%) | 0 (0) | | 0 (0) | 0 (0) | | 0 (0) | 1 (100%) | |
| Musculoskeletal symptoms (> G2) (<i>n</i> = 19, 8.1%) | | | | | | | | | |
| No | 87 (40.3%) | 129 (59.7%) | 0.114 | 20 (34.5%) | 38 (65.5%) | 0.548 | 64 (40.5%) | 94 (59.5%) | 0.602 |
| Yes | 5 (26.3%) | 14 (73.7%) | | 0 (0) | 2 (100%) | | 6 (75%) | 2 (25%) | |
| T-score ≤ -2 (<i>n</i> = 46, 19.6%) | | | | | | | | | |
| No | 79 (42.7%) | 106 (57.3%) | 0.059 | 19 (35.8%) | 34 (64.2%) | 0.161 | 52 (39.1%) | 81 (60.9%) | 0.344 |
| Yes | 11 (23.9%) | 35 (76.1%) | | 0 (0) | 5 (100%) | | 19 (47.5%) | 21 (52.5%) | |
| Fracture (<i>n</i> = 14, 6%) | | | | | | | | | |
| No | 86 (38.9%) | 135 (61.1%) | 0.769 | 25 (42.3%) | 34 (57.6%) | / | 68 (42.0%) | 94 (58.0%) | 0.430 |
| Yes | 6 (42.9%) | 8 (57.1%) | | 0 (0) | 1 (100%) | | 4 (30.8%) | 9 (69.2%) | |
| Hot flash (≥ G3) (<i>n</i> = 9, 3.8%) | | | | | | | | | |
| No | 89 (39.4%) | 137 (60.6%) | 0.503 | 19 (33.3%) | 38 (66.7%) | 1 | 70 (41.4%) | 99 (58.6%) | 1 |

(Continued)

TABLE 6 Continued

| | All patients enrolled (N = 235) | | | Post-treatment with SERM (N = 60) | | | Posttreatment with AI (N = 175) | | |
|---|---------------------------------|-------------|-------|-----------------------------------|------------|-------|---------------------------------|-------------|-------|
| | No-EET | EET | p | No-EET | EET | p | No-EET | EET | p |
| Yes | 3 (33.3%) | 6 (66.7%) | | 1 (33.3%) | 2 (66.7%) | | 2 (33.3%) | 4 (66.7%) | |
| Libido decreased (\geq G2) (n = 6, 2.6%) | | | | | | | | | |
| No | 89 (38.9%) | 140 (61.1%) | 0.681 | 18 (32.1%) | 38 (67.9%) | 0.595 | 72 (41.6%) | 101 (58.4%) | 0.513 |
| Yes | 3 (50%) | 3 (50%) | | 2 (50.0%) | 2 (50.0%) | | 0 (0) | 2 (100%) | |
| Depression (n = 43, 18.3%) or anxiety | | | | | | | | | |
| No | 73 (38.0%) | 119 (62.0%) | 0.454 | 16 (33.3%) | 32 (66.7%) | 1 | 60 (41.7%) | 84 (58.3%) | 0.762 |
| Yes | 19 (44.2%) | 24 (55.8%) | | 4 (33.3%) | 8 (66.7%) | | 12 (38.7%) | 19 (61.3%) | |
| Dyslipidemia (n = 58, 24.7%) | | | | | | | | | |
| No | 72 (40.7%) | 105 (59.3%) | 0.402 | 18 (34.6%) | 34 (65.4%) | 0.707 | 57 (45.6%) | 68 (54.4%) | 0.058 |
| Yes | 20 (34.5%) | 38 (65.5%) | | 2 (25%) | 6 (75%) | | 15 (30.0%) | 35 (70.0%) | |

to real-life patients. In their follow-up study, CTS5 demonstrated clinical validity for predicting late recurrence in unselected postmenopausal patients but less so in premenopausal patients (25). In our study, CTS5 was used for retrospective validation of the physician's clinical recommendations about EET. Consistent with the experimental conclusion mentioned previously, we found that CTS5 was strongly associated with clinician recommendations, especially in the previously AI-treated group, and the higher the value, the more likely EET would be recommended. In addition, from the perspective of the OR values in the multivariate analysis, the CTS5 score was a more valuable guiding factor for the EET recommendation than lymph nodes and other independent clinicopathological factors.

Endocrine therapy causes some side effects, most of which were non-life threatening. In the IBIS-II trial, John et al. reported the side-effect profiles in breast cancer patients who had completed 5 years of endocrine therapy, including fractures (9%), arthralgia (57%), and osteoporosis (7%) with anastrozole and gynecological cancers (1.9%), vaginal symptoms (28%), and deep vein thromboses (1%) with tamoxifen (26). There are also some studies showing a possible side effect of tamoxifen with raise in the triglycerides level (27, 28). In our study, the side effects we counted were mainly T -score < -2 (26.7%), musculoskeletal symptoms (5.3%), and fracture (8.7%) with AI and endometrial thickening (15.5%) and dyslipidemia (13.3%) with tamoxifen.

EET would also increase the incidence of some side effects. In the NSABP B-14 trial, the risk of endometrial cancer was raised in the extended tamoxifen group [RR:2.0 (0.7–6.6)]. As reported by MA-17R, extended letrozole significantly increased

the risk of osteoporosis (12%:9%, $p = 0.01$) and fracture (14%:9%, $p = 0.001$) (10, 29, 30). In our study, there was no influence of adverse events on the treatment decision. First, this might be related to the fact that the population enrolled in this study was able to tolerate 5 years of basic adjuvant endocrine therapy and was likely to endure further EET. Secondly, we consider that if complications would occur, priority would be given to the change of treatment or to treat complications aggressively rather than stopping EET.

There are some limitations to our study: one is that it was a retrospective analysis, which needs further validation. Next in importance, our data included cases from October 2017 to December 2019. Since then, the publication of clinical trial results and the update of clinical guidelines would lead to a change in decision making.

Conclusions

Our study indicated that age, lymph nodal status, and receipt of chemotherapy were independent predictors for the recommendation of EET. The application of the CTS5 on EET decision making might be valuable among ER+ breast cancer patients.

Data availability statement

The raw data supporting the conclusions of this article will be made available by the authors, without undue reservation.

Author contributions

WLC: Conceptualization, Writing - Original Draft, Formal analysis, Statistical Analysis. JW: Methodology, Visualization. YZ, JHH: Investigation. XC: Data Curation. OH, JRH: Validation. YL, WGC, KS: Project administration, Supervision. LZ: Writing- Reviewing and Editing. All authors contributed to the article and approved the submitted version.

Acknowledgments

We would like to thank the assistant from Yidong Du for her significant contribution during the follow-up. Special thanks should be given to the Shanghai Jiaotong University Breast Cancer Database (SJTU-BCDB).

References

- Bray F, Ferlay J, Soerjomataram I, Siegel RL, Torre LA, Jemal A. Global cancer statistics 2018: GLOBOCAN estimates of incidence and mortality worldwide for 36 cancers in 185 countries. *CA Cancer J Clin* (2018) 68(6):394–424. doi: 10.3322/caac.21492
- Burstein HJ, Lacchetti C, Anderson H, Buchholz TA, Davidson NE, Gelmon KE, et al. Adjuvant endocrine therapy for women with hormone receptor-positive breast cancer: American society of clinical oncology clinical practice guideline update on ovarian suppression. *J Clin Oncol* (2016) 34(14):1689–701. doi: 10.1200/JCO.2015.65.9573
- NCCN Breast Cancer Clinical Practice Guidelines in Oncology. (2006). Available at: <http://www.nccn.org/profess>.
- Goldhirsch A, Wood WC, Gelber RD, Coates AS, Thürlimann B, Senn HJ, et al. Meeting highlights: updated international expert consensus on the primary therapy of early breast cancer. *J Clin Oncol* (2003) 21:3357–65. doi: 10.1200/JCO.2003.04.576
- Pan H, Gray R, Braybrooke J, Davies C, Taylor C, McGale P, et al. 20-year risks of breast-cancer recurrence after stopping endocrine therapy at 5 years. *Engl J Med* (2017) 377:1836–46. doi: 10.1056/NEJMoa1701830
- Early Breast Cancer Trialists' Collaborative Group (EBCTCG). Aromatase inhibitors versus tamoxifen in early breast cancer: patient-level meta-analysis of the randomised trials. *Lancet* (2015) 386(10001):1341–52. doi: 10.1016/S0140-6736(15)61074-1
- Cuzick J, Sestak I, Baum M, Buzdar A, Howell A, Dowsett M, et al. Effect of anastrozole and tamoxifen as adjuvant treatment for early-stage breast cancer: 10-year analysis of the ATAC trial. *Lancet Oncol* (2010) 11(12):1135e41. doi: 10.1016/S1470-2045(10)70257-6
- Davies C, Pan H, Godwin J, Gray R, Arriagada R, Raina V, et al. Long-term effects of continuing adjuvant tamoxifen to 10 years versus stopping at 5 years after diagnosis of oestrogen receptor-positive breast cancer: ATLAS, a randomised trial. *Lancet* (2013) 381(9869):805–16. doi: 10.1016/S0140-6736(12)61963-1
- Gray RG, Rea D, Handley K, Bowden SJ, Perry P, Earl HM, et al. aTTom: Long-term effects of continuing adjuvant tamoxifen to 10 years versus stopping at 5 years in 6,953 women with early breast cancer. *J Clin Oncol* (2013) 31(suppl; abstr5). doi: 10.1200/jco.2013.31.15_suppl.5
- Goss PE, Ingle JN, Pritchard KI, Robert NJ, Muss H, Gralow J, et al. Extending aromatase-inhibitor adjuvant therapy to 10 years. *N Engl J Med* (2016) 375(3):209–19. doi: 10.1056/NEJMoa1604700
- Mamounas EP, Bandos H, Lembersky BC, Jeong JH, Geyer CE Jr, Rastogi P, et al. Use of letrozole after aromatase inhibitor-based therapy in postmenopausal breast cancer (NRG Oncology/NSABP b-42): a randomised, double-blind, placebo-controlled, phase 3 trial. *Lancet Oncol* (2019) 20(1):88–99. doi: 10.1016/S1470-2045(18)30621-1
- Cardoso F, Kyriakides S, Ohno S, Penault-Llorca F, Poortmans P, Rubio IT, et al. Early breast cancer: ESMO clinical practice guidelines for diagnosis, treatment and follow-up. *Ann Oncol* (2009) 30(10):1674. doi: 10.1093/annonc/mdz189

Conflict of interest

The authors declare that the research was conducted in the absence of any commercial or financial relationships that could be construed as a potential conflict of interest.

Publisher's note

All claims expressed in this article are solely those of the authors and do not necessarily represent those of their affiliated organizations, or those of the publisher, the editors and the reviewers. Any product that may be evaluated in this article, or claim that may be made by its manufacturer, is not guaranteed or endorsed by the publisher.

- NCCN. *NCCN clinical practice guidelines in oncology: Breast cancer*. Available at: <http://www.nccn.org>.
- Gray R. Early Breast Cancer Trialists' Collaborative Group. Effects of prolonging adjuvant aromatase inhibitor therapy beyond five years on recurrence and cause-specific mortality: An EBCTCG meta-analysis of individual patient data from 12 randomized trials including 24,912 women. *J. Cancer research* (2019) 79(4_Supplement):GS3-03-GS3-03.
- Burstein HJ, Lacchetti C, Anderson H, Buchholz TA, Davidson NE, Gelmon KA, et al. Adjuvant endocrine therapy for women with hormone receptor-positive breast cancer: ASCO clinical practice guideline focused update. *J Clin Oncol* (2019) 37(5):423–38. doi: 10.1200/JCO.18.01160
- Hammond ME, Hayes DF, Dowsett M, Allred DC, Haggerty KL, Badve S, et al. American society of clinical oncology/college of American pathologist's guideline recommendations for immunohistochemical testing of estrogen and progesterone receptors in breast cancer. *J Clin Oncol* (2010) 28(16):2784–95. doi: 10.1200/JCO.2009.25.6529
- Wolff AC, Hammond ME, Hicks DG, Dowsett M, McShane LM, Allison KH, et al. Recommendations for human epidermal growth factor receptor 2 testing in breast cancer: American society of clinical Oncology/College of America pathologists clinical practice guideline update. *J Clin Oncol* (2013) 31(31):3997–4013. doi: 10.1200/JCO.2013.50.9984
- Harris L, Fritzsche H, Mennel R, Norton L, Ravdin P, Taube S, et al. American Society of clinical oncology 2007 update of recommendations for the use of tumor markers in breast cancer. *J Clin Oncol* (2007) 25(33):5287–312. doi: 10.1200/JCO.2007.14.2364
- Edges B, Compton CC. The American joint committee on cancer: The 7th edition of the ajcc cancer staging manual and the future of TNM. *Ann Surg Oncol* (2010) 17(6):1471–14 174. doi: 10.1245/s10434-010-0985-4
- Dowsett M, Sestak I, Regan MM, Dodson A, Viale G, Thürlimann B, et al. Integration of clinical variables for the prediction of late distant recurrence in patients with estrogen receptor-positive breast cancer treated with 5 years of endocrine therapy: CTS5. *J Clin Oncol* (2018) 36:1941–8. doi: 10.1200/JCO.2017.76.4258
- Goss PE, Ingle JN, Martino S, Robert NJ, Muss HB, Piccart MJ, et al. Randomized trial of letrozole following tamoxifen as extended adjuvant therapy in receptor-positive breast cancer: updated findings from NCIC CTG MA.17. *J Natl Cancer Inst* (2005) 97(17):1262–71. doi: 10.1093/jnci/dji250
- Khoshnoud MR, Fornander T, Johansson H, Rutqvist LE. Long-term pattern of disease recurrence among patients with early-stage breast cancer according to estrogen receptor status and use of adjuvant tamoxifen. *Breast Cancer Res Treat* (2008) 107(1):71–8. doi: 10.1007/s10549-007-9520-0
- Goldvaser H. Efficacy of extended adjuvant therapy with aromatase inhibitors in early breast cancer among common clinicopathologically-defined subgroups: A systematic review and meta-analysis. *Cancer Treat Rev* (2017) 60:53–7. doi: 10.1016/j.ctrv.2017.08.008

24. Baum M, Budzar AU, Cuzick J, Forbes J, Houghton JH, Klijn JG, et al. Anastrozole alone or in combination with tamoxifen versus tamoxifen alone for adjuvant treatment of postmenopausal women with early breast cancer: first results of the ATAC randomised trial. *Lancet* (2002) 359(9324):2131–9. doi: 10.1016/S0140-6736(02)09088-8
25. Richman J, Ring A, Dowsett M, Sestak I. Clinical validity of clinical treatment score 5 (CTS5) for estimating risk of late recurrence in unselected, non-trial patients with early oestrogen receptor-positive breast cancer. *Breast Cancer Res Treat* (2021) 186(1):115–23. doi: 10.1007/s10549-020-06013-6
26. Forbes JF, Sestak I, Howell A, Bonanni B, Bundred N, Levy C, et al. Anastrozole versus tamoxifen for the prevention of locoregional and contralateral breast cancer in postmenopausal women with locally excised ductal carcinoma *in situ* (IBIS-II DCIS): a double-blind, randomized controlled trial. *Lancet* (2016) 387(10021):866–73. doi: 10.1016/S0140-6736(15)01129-0
27. Hozumi Y, Kawano M, Saito T, Miyata M. Effect of tamoxifen on serum lipid metabolism. *J Clin Endocrinol Metab* (1998) 83(5):1633–5. doi: 10.1210/jcem.83.5.4753
28. Liu CL, Yang TL. Sequential changes in serum triglyceride levels during adjuvant tamoxifen therapy in breast cancer patients and the effect of dose reduction. *Breast Cancer Res Treat* (2003) 79(1):11–6. doi: 10.1023/A:1023348021773
29. Goldvaser H, Barnes TA, Seruga B, Cescon DW, Ocaña A, Ribnikar D, et al. Toxicity of extended adjuvant therapy with aromatase inhibitors in early breast cancer: a systematic review and meta-analysis. *J Natl Cancer Inst* (2018) 110(1):31–9. doi: 10.1093/jnci/djx141
30. Fisher B, Dignam J, Bryant J, Wolmark N. Five versus more than five years of tamoxifen for lymph node-negative breast cancer: updated findings from the national surgical adjuvant breast and bowel project b-14 randomized trial. *J Natl Cancer Inst* (2001) 93(9):684–90. doi: 10.1093/jnci/93.9.684



OPEN ACCESS

EDITED BY

Dayanidhi Raman,
University of Toledo, United States

REVIEWED BY

Gail Lewis,
Genentech Inc., United States
Francesco Pepe,
University of Naples Federico II, Italy

*CORRESPONDENCE

Zhaosheng Ma
✉ mzs@enzemed.com

SPECIALTY SECTION

This article was submitted to
Breast Cancer,
a section of the journal
Frontiers in Oncology

RECEIVED 28 June 2022

ACCEPTED 14 December 2022

PUBLISHED 19 January 2023

CITATION

Chen M-L, Yu W, Cui B, Yu Y and Ma Z
(2023) HER2-positive metastatic breast
cancer with brain metastases responds
favorably to pyrotinib and
trastuzumab-based treatment: A case
report and literature review.
Front. Oncol. 12:980635.
doi: 10.3389/fonc.2022.980635

COPYRIGHT

© 2023 Chen, Yu, Cui, Yu and Ma. This
is an open-access article distributed
under the terms of the [Creative
Commons Attribution License \(CC BY\)](#).
The use, distribution or reproduction
in other forums is permitted, provided
the original author(s) and the
copyright owner(s) are credited and
that the original publication in this
journal is cited, in accordance with
accepted academic practice. No use,
distribution or reproduction is
permitted which does not comply with
these terms.

HER2-positive metastatic breast cancer with brain metastases responds favorably to pyrotinib and trastuzumab-based treatment: A case report and literature review

Min-long Chen, Wenjie Yu, Binbin Cui, Yijian Yu
and Zhaosheng Ma*

Department of Oncological Surgery, Taizhou Hospital, Wenzhou Medical University,
Zhejiang, China

For HER2-positive metastatic breast cancer patients with the brain involved at initial diagnosis, there was no standard regimen before 2022 when the HER2CLIMB trial published its final overall survival analysis, and the prognosis is relatively poor under the current treatment strategy. We herein reported a case of a female patient who was initially diagnosed with HER2-positive metastatic breast cancer with brain metastases, receiving pyrotinib and trastuzumab-based systematic therapy after palliative craniocerebral radiotherapy as the first-line systematic therapy. During the treatment, the tumor lesions showed obvious regression, and chemotherapy drugs were gradually removed from the regimen. The patient continued receiving trastuzumab and pyrotinib for HER2-targeted therapy. She had achieved more than 26 months of progression-free survival and the disease was stable during the evaluation in April 2022. Radiotherapy followed by dual HER2-targeted therapy of macromolecular monoclonal antibodies trastuzumab and micromolecular TKI pyrotinib plus chemotherapy could be an alternative option for this subtype of patients and need to be further verified by future clinical trials.

KEYWORDS

breast cancer, brain metastase, pyrotinib, trastuzumab, treatment

Introduction

Breast cancer (BC) with overexpression of human epidermal growth factor receptor 2 (HER2) occurs in approximately 15% to 20% of all primary breast cancers, which were indicated to be more aggressive, easily metastasized, and to have poor prognosis (1). With the development of anti-HER2 systemic treatments, patients with HER2-positive breast cancer achieve long-term survival benefits, which also increase the incidence of brain metastases (BMs). BC with central nervous system (CNS) metastases has been reported in 15%–25% of BC patients, and BMs occur in 30%–55% of HER2-positive metastatic breast cancer (MBC) patients, which is much higher than other BC subtypes (2, 3). The median overall survival (OS) after the initial diagnosis of CNS metastases is poor, at 13.0 months (4).

Currently, locally directed therapy, such as surgical resection, stereotactic radiosurgery, and whole-brain radiation are initially considered for BMs. Dual-targeted therapy of pertuzumab and trastuzumab plus docetaxel or paclitaxel is the first line recommendation for HER2-positive MBC by National Comprehensive Cancer Network (NCCN) guidelines (5). In the HER2CLIMB trial, tucatinib together with trastuzumab and capecitabine significantly improved OS and PFS in HER2-positive MBC, including those with BMs (6).

Pyrotinib is a novel oral pan-ErbB receptor tyrosine kinase inhibitor (TKI), which potently inhibits EGFR/HER1, HER2, and HER4 (7). It was approved for use in combination with capecitabine for the treatment of patients with HER2-positive metastatic BC in August 2018 in China. We herein reported a case of a female patient, who was initially diagnosed with HER2-positive metastatic BC with BMs, receiving pyrotinib and trastuzumab-based systematic therapy after palliative craniocerebral radiotherapy as the first-line systematic therapy. To the best of our knowledge, this is the first case reporting pyrotinib and trastuzumab-based systematic therapy as the first-line systematic therapy for HER2-positive metastatic BC with BMs.

Case report

A 56-year-old Chinese female patient presented to our outpatient department in March 2020, complaining of endurable headache and palpable nodules in the right axilla and supraclavicular region. A 5*6 cm hard tumor in the outer upper quadrant of the right breast and multiple enlarged lymph nodes in the right axilla and supraclavicular region were found in the physical examination. The pathological biopsy results of the maximal mass showed invasive ductal carcinoma (Figure 1A). Immunohistochemistry (IHC) analysis revealed ER (-), PR (-), HER2 (3+), GCDEF-15(+) (Figures 1B-E). Head magnetic resonance imaging (MRI) revealed multiple masses in brain

parenchyma, the diameter of the maximal mass was 2 cm, located in the left frontal lobe of the brain (Figure 2A). Her serum cancer antigen 15-3 (CA15-3) was 126.1 U/ml (normal, <31 U/ml) while serum carcinoembryonic antigen (CEA) and serum cancer antigen 12-5 (CA12-5) were both in the normal level. Imaging assessment including chest computed tomography (CT) scan, and abdominal ultrasound indicated a negative result. PET-CT was then recommended and revealed multiple masses in the right axilla, right supraclavicular region, spleen, and brain (Figure 3). This patient was finally diagnosed with a metastatic breast cancer, T3N3M1, stage IV, HER2-positive.

This patient received palliative craniocerebral radiotherapy for 2 weeks in our hospital and the process was smooth. She then received systemic therapy of paclitaxel (175 mg/m², d1, 1/21 d) and capecitabine (1000 mg/m², bid, d1–d14/21 d) for chemotherapy plus trastuzumab (loading 8 mg/kg, then 6 mg/kg, d1, 1/21 d) and pyrotinib (400 mg, po, qd) for HER2-targeted therapy since April 2020. During the first course of systemic therapy, she had nausea, diarrhea, and loss of appetite, which could be recovered after symptomatic treatment, and chemotherapy-related hand-foot syndrome, which was endurable. Efficacy evaluation of the systemic therapy was performed at the beginning of the second course. Ultrasound revealed that all the enlarged lymph nodes in the axilla and supraclavicular region disappeared and the maximal mass in the breast was reduced to 2.1*0.8 cm. Head MRI revealed that the diameter of the maximal mass in the left frontal lobe of the brain was reduced to 1.2 cm (Figure 2B). CA15-3 also dropped back to normal level. Because of the excellent therapeutic effect, she continued the second course of previous systemic therapy.

During the second course of systemic therapy, the side effects of the drugs progressed. The patient complained most of insufferable loss in strength and acroanesthesia. At the beginning of the third course, ultrasound revealed a 1.8*1.0 cm mass in the breast and the mass in the left frontal lobe of the brain was similar with that of the last course in head MRI. CA15-3 was also in the normal level. Because of the severe side-effects of the drugs, capecitabine was first eliminated from the regimen since the third course. She continued another six courses of paclitaxel for chemotherapy plus trastuzumab and pyrotinib for HER2-targeted therapy. During this treatment, her breast mass showed continuous reduction and disappeared since the seventh course in ultrasound; the diameter of the maximal mass in the left frontal lobe of the brain reduced to 1.0 cm (Figure 2C) since the sixth course and the other small masses in the brain were completely relieved. Meanwhile, her strength quickly recovered, but she still felt the acroanesthesia even though symptomatic treatment was given. She stopped chemotherapy since the ninth course and continued trastuzumab and pyrotinib for HER2-targeted therapy. The latest treatment evaluation was carried out in April 2022, the mass in brain was stable, and no new lesion was discovered (Figure 2D). The patient was still receiving trastuzumab and pyrotinib for HER2-targeted therapy up to now. To now, the

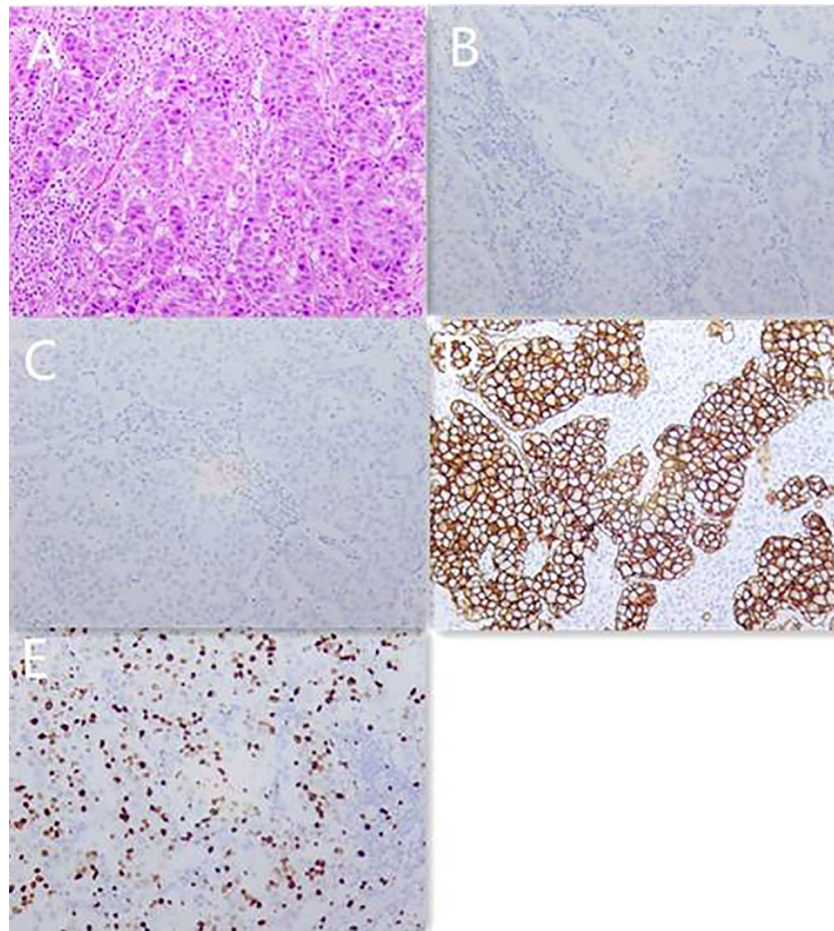


FIGURE 1

Pathology images and immunotherapy staining images of this patient in March 2020. (A) Pathology images of core needle biopsy. (B) ER immunotherapy staining image of core needle biopsy. (C) PR immunotherapy staining image of core needle biopsy. (D) HER2 immunotherapy staining image of core needle biopsy. (E) Ki-67 immunotherapy staining image of core needle biopsy.

patient had received as long as 26 months of progression-free survival and the disease was still controlled well (Table 1).

Discussion

Nowadays, patients with breast cancer brain metastasis are still lacking effective treatment and associated with poor outcomes, although substantial improvements have been achieved in the diagnosis and treatment (8, 9). Due to the existence of blood-brain barrier (BBB) and limited permeability, many chemotherapeutic drugs and macromolecular anti-HER2 targeted drugs exhibit restricted efficacy for intracranial lesions, such as paclitaxel, anthracyclines, trastuzumab, pertuzumab, and T-DM1 (10). Meanwhile, the good control of extracranial lesions by systemic treatment leads to long-term survival and also more

BM occurrence. Thus, there is an urgent need for clinical strategies targeting BM for this type of breast cancer.

Radiotherapy is a common option for local control of brain lesions, reported to be able to change the permeability of the BBB (11). In the TBCRC 022 trial, neratinib plus capecitabine was considered to have synergistic effects with radiotherapy for HER2-positive breast cancer brain metastasis (12). In real world data, patients with BM could benefit in PFS and OS when receiving systemic therapy in combination with radiotherapy, compared with those not receiving radiotherapy (13, 14). In this case, the patient was recommended to receive palliative craniocerebral radiotherapy before systemic treatment.

Up to now, the anti-HER2 drugs are divided into three categories, including monoclonal antibodies, such as trastuzumab and pertuzumab; antibody-drug conjugates (ADC), such as T-DM1 and DS8201; and tyrosine kinase inhibitors (TKI), such as lapatinib, neratinib, tucatinib and

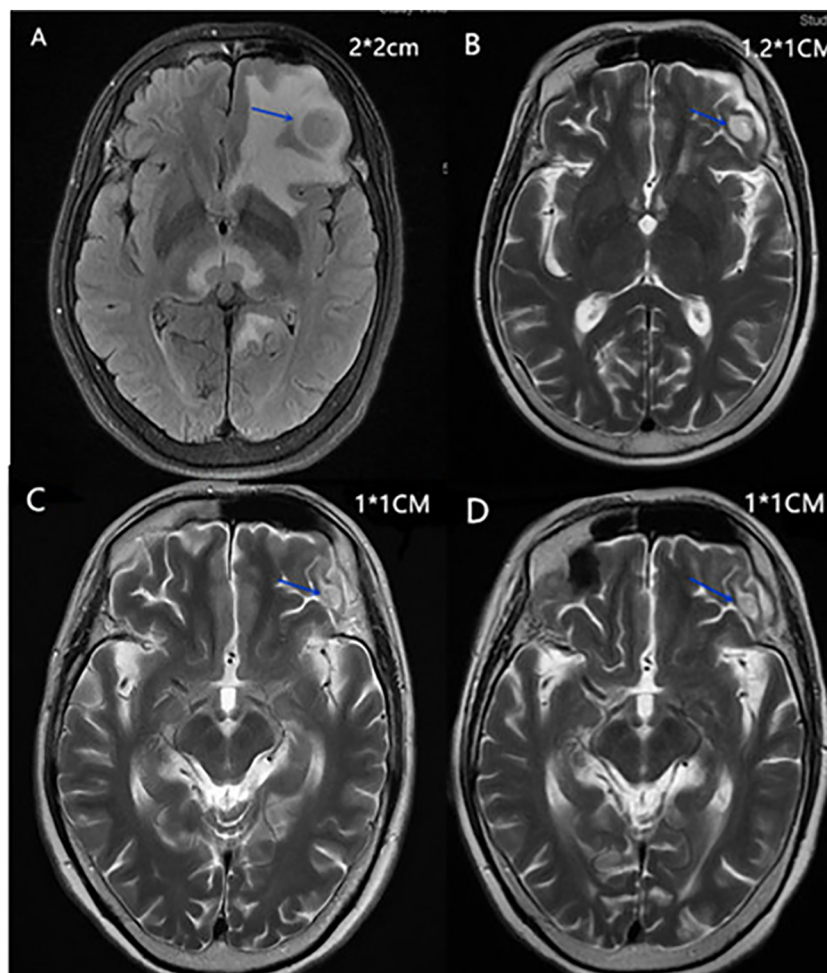


FIGURE 2

(A) Head MRI of the maximal mass in the left frontal lobe of the brain in April 2020. (B) Head MRI of the maximal mass in the left frontal lobe of the brain in May 2020. (C) Head MRI of the maximal mass in the left frontal lobe of the brain in August 2020. (D) Head MRI of the maximal mass in the left frontal lobe of the brain in April 2022.

pyrotinib. Trastuzumab-based therapy is still the standard regimen for the treatment of HER2-positive locally advanced or metastatic breast cancer recommended by the NCCN guidelines and Chinese Society of Clinical Oncology (CSCO) guidelines (5, 15). However, trastuzumab often shows primary or acquired resistance during or post treatment, and patients with BM were excluded from the criteria in the CLEOPATRA trial, which laid the foundation for dual-targeted therapy of pertuzumab and trastuzumab plus chemotherapy as the first-line treatment for HER2-positive metastatic breast cancer (16).

T-DM1 only contributed approximately 5.5 months of median PFS for patients with BM while it was confirmed to have an advantage for the PFS and OS for HER2-positive MBC in the EMILIA trial (17). Several studies reported that anti-HER2 monoclonal antibodies and HER2-directed antibody drug conjugates could improve survival in BC patients with BM,

but considering the limited permeability into the BBB, their intracranial effects remain controversial (4, 16).

Compared with monoclonal antibodies, the physical features of small-molecule TKIs play an important role in allowing them to cross the BBB, thereby improving drug concentrations in the brain, indicating that TKIs could be a rational therapeutic approach to treat CNS metastases (18, 19). Tucatinib, a small-molecule oral tyrosine kinase inhibitor (TKI) that is highly selective for HER2, was approved by the FDA in April 2020 for use in patients who have received one or more prior anti-HER2-based regimens in the metastatic setting. In the HER2CLIMB study, compared with placebo, the addition of tucatinib to trastuzumab and capecitabine reduced the risk of intracranial progression by 68% (hazard ratio [HR], 0.32; 95% CI, 0.22–0.48; $p = .0001$), and reduced the risk of death by 42% (OS HR, 0.58; 95% CI, 0.40–0.85; $p = .005$) among BMs group,

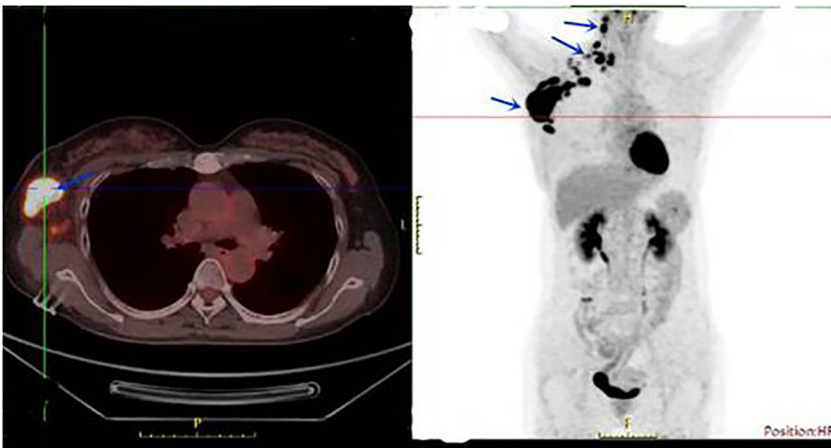


FIGURE 3
PET-CT showed multiple masses in the right axilla, right supraclavicular region, and spleen in March 2020.

providing a clinically meaningful survival benefit (6, 20). Unfortunately, tucatinib was not available in China in 2020 and not even nowadays.

Pyrotinib is another novel micromolecular oral pan-ErbB receptor TKI, inhibiting HER1, HER2, and HER4 (7), which was first approved in China for use in combination with capecitabine for the treatment of patients with HER2-positive MBC who had previously received anthracycline or taxane chemotherapy. An open-label phase II study organized in China demonstrated that pyrotinib plus capecitabine had a significantly longer PFS (18.1 vs. 7.0 months, $p < 0.001$) and higher objective response rate (ORR) (78.5% vs. 57.1%, $p < 0.05$) than lapatinib plus capecitabine in MBC patients (21). The PHOEBE study conducted a similar result for those patients who had been previously treated with trastuzumab and taxane and/or anthracycline (22). Furthermore, neratinib plus capetabine achieved 8.8 months of median PFS as a third or later line therapy, and neratinib plus paclitaxel achieved 12.9 months of median PFS as a first-line treatment, suggesting the potentially

comparable efficacy of pyrotinib to neratinib (23, 24). Among patients with brain metastases, pyrotinib was reported to have a better PFS benefit than monoclonal antibodies in real-world study (25, 26).

For this patient, there is no standard regimen, considering the heavy tumor burden and the metastases in the brain; dual HER2-targeted therapy plus chemotherapy was preferentially recommended in the purpose to rapidly contract the tumor. In the 2020 CSCO guidelines, the regimen of TXH (taxel, capecitabin, trastuzumab) or THP (taxel, trastuzumab, pertuzumab) was first recommended for those HER2-positive MBC patients without trastuzumab pretreated. Furthermore, the unavailability of TDM-1 and neratinib in China at that time and the high price of Pertuzumab prevent the patient from considering the clinical application of these drugs. Pyrotinib was finally added in the regimen of TXH. During the treatment, the tumor showed obvious regression, especially the extracranial lesions, which disappeared after six cycles of treatment.

TABLE 1 The brief course of treatment.

| Date | Treatment | Maximal head mass (cm) | Mass in right axilla (cm) |
|----------------|---|------------------------|---------------------------|
| 2020.3 | Diagnosed | 2*2 | 5*6 |
| 2020.4 | Palliative craniocerebral radiotherapy for 2 weeks | 2*2 | 5*6 |
| 2020.4- | Two cycles of Paclitaxel, capecitabine plus trastuzumab and pyrotinib | 2*2 | 5*6 |
| 2020.6- | Six cycles of paclitaxel, trastuzumab and pyrotinib | 1.2*1 | 1.8*1 |
| 2020.11-2022.4 | Trastuzumab and pyrotinib | 1*1 | none |

The maximal head mass was evaluated by MRI; the mass in right axilla was evaluated by ultrasonography.

Chemotherapy drugs were gradually removed from the regimen because of the progressed side effects. Till now, the patient is still receiving trastuzumab and pyrotinib for HER2-targeted therapy and the disease is stable during evaluation.

Conclusion

For HER2-positive MBC patients with brain involved at initial diagnosis, the current treatment strategy results in relatively poor prognosis. Radiotherapy followed by dual HER2-targeted therapy of macromolecular monoclonal antibodies trastuzumab and micromolecular TKI pyrotinib plus chemotherapy could be an alternative option for this subtype of patients and needs to be further verified by future clinical trials.

Data availability statement

The original contributions presented in the study are included in the article/supplementary material. Further inquiries can be directed to the corresponding author.

References

1. Waks AG, Winer EP. Breast cancer treatment: A review. *JAMA* (2019) 321(3):288–300. doi: 10.1001/jama.2018.19323
2. Custodio-Santos T, Videira M, Brito MA. Brain metastasization of breast cancer. *Biochim Biophys Acta Rev Cancer* (2017) 1868(1):132–47. doi: 10.1016/j.bbcan.2017.03.004
3. Lin NU, Amiri-Kordestani L, Palmieri D, Liewehr DJ, Steeg PS. CNS metastases in breast cancer: old challenge, new frontiers. *Clin Cancer Res* (2013) 19(23):6404–18. doi: 10.1158/1078-0432.CCR-13-0790
4. Brufsky AM, Mayer M, Rugo HS, Kaufman PA, Tan-Chiu E, Tripathy D, et al. Central nervous system metastases in patients with HER2-positive metastatic breast cancer: incidence, treatment, and survival in patients from registHER. *Clin Cancer Res* (2011) 17(14):4834–43. doi: 10.1158/1078-0432.CCR-10-2962
5. Gradishar WJ, Moran MS, Abraham J, Aft R, Agnese D, Allison KH, et al. NCCN Guidelines(R) insights: Breast cancer, version 4.2021. *J Natl Compr Cancer Network JNCCN* (2021) 19(5):484–93. doi: 10.6004/jnccn.2021.0023
6. Curigliano G, Mueller V, Borges V, Hamilton E, Hurvitz S, Loi S, et al. Tucatinib versus placebo added to trastuzumab and capecitabine for patients with pretreated HER2+ metastatic breast cancer with and without brain metastases (HER2CLIMB): final overall survival analysis. *Ann Oncol* (2022) 33(3):321–9. doi: 10.1016/j.annonc.2021.12.005
7. Li X, Yang C, Wan H, Zhang G, Feng J, Zhang L, et al. Discovery and development of pyrotinib: A novel irreversible EGFR/HER2 dual tyrosine kinase inhibitor with favorable safety profiles for the treatment of breast cancer. *Eur J Pharm Sci* (2017) 110:51–61. doi: 10.1016/j.ejps.2017.01.021
8. Ording AG, Heide-Jorgensen U, Christiansen CF, Norgaard M, Acquavella J, Sorensen HT. Site of metastasis and breast cancer mortality: a Danish nationwide registry-based cohort study. *Clin Exp Metastasis* (2017) 34(1):93–101. doi: 10.1007/s10585-016-9824-8
9. Patil A, Sherbet GV. Therapeutic approach to the management of HER2-positive breast cancer metastatic to the brain. *Cancer Lett* (2015) 358(2):93–9. doi: 10.1016/j.canlet.2014.12.026
10. Yao JH, Xie ZY, Li M, Zhang ML, Ci HF, Yang Y. Metastatic brain tumors respond favorably to pyrotinib in a HER2-positive breast cancer following failure using trastuzumab. *Am J Transl Res* (2020) 12(9):5874–81.

Author contributions

MC, WY, BC and ZM acquired the data and prepared the manuscript. YY performed histological examinations. MC and ZM performed data analysis and interpretation. All authors contributed to the article and approved the submitted version.

Conflict of interest

The authors declare that the research was conducted in the absence of any commercial or financial relationships that could be construed as a potential conflict of interest.

Publisher's note

All claims expressed in this article are solely those of the authors and do not necessarily represent those of their affiliated organizations, or those of the publisher, the editors and the reviewers. Any product that may be evaluated in this article, or claim that may be made by its manufacturer, is not guaranteed or endorsed by the publisher.

11. Bouchet A, Potez M, Coquery N, Rome C, Lemasson B, Brauer-Krisch E, et al. Permeability of brain tumor vessels induced by uniform or spatially microfractionated synchrotron radiation therapies. *Int J Radiat Oncol Biol Phys* (2017) 98(5):1174–82. doi: 10.1016/j.ijrobp.2017.03.025
12. Freedman RA, Gelman RS, Anders CK, Melisko ME, Parsons HA, Cropp AM, et al. TBCRC 022: A phase II trial of neratinib and capecitabine for patients with human epidermal growth factor receptor 2-positive breast cancer and brain metastases. *J Clin Oncol* (2019) 37(13):1081–9. doi: 10.1200/JCO.18.01511
13. Anwar M, Chen Q, Ouyang D, Wang S, Xie N, Ouyang Q, et al. Pyrotinib treatment in patients with HER2-positive metastatic breast cancer and brain metastasis: Exploratory final analysis of real-world, multicenter data. *Clin Cancer Res* (2021) 27(16):4634–41. doi: 10.1158/1078-0432.CCR-21-0474
14. Lin Y, Lin M, Zhang J, Wang B, Tao Z, Du Y, et al. Real-world data of pyrotinib-based therapy in metastatic HER2-positive breast cancer: Promising efficacy in lapatinib-treated patients and in brain metastasis. *Cancer Res Treat* (2020) 52(4):1059–66. doi: 10.4143/crt.2019.633
15. Huang X, Yin YM. [Updates of Chinese society of clinical oncology (CSCO) guideline for breast cancer in 2018]. *Zhonghua Yi Xue Za Zhi* (2018) 98(16):1213–7. doi: 10.3760/cma.j.issn.0376-2491.2018.16.005
16. Swain SM, Kim SB, Cortes J, Ro J, Semiglazov V, Campone M, et al. Pertuzumab, trastuzumab, and docetaxel for HER2-positive metastatic breast cancer (CLEOPATRA study): overall survival results from a randomised, double-blind, placebo-controlled, phase 3 study. *Lancet Oncol* (2013) 14(6):461–71. doi: 10.1016/S1470-2045(13)70130-X
17. Dieras V, Miles D, Verma S, Pegram M, Welslau M, Baselga J, et al. Trastuzumab emtansine versus capecitabine plus lapatinib in patients with previously treated HER2-positive advanced breast cancer (EMILIA): a descriptive analysis of final overall survival results from a randomised, open-label, phase 3 trial. *Lancet Oncol* (2017) 18(6):732–42. doi: 10.1016/S1470-2045(17)30312-1
18. Wang W, He H, Marin-Ramos NI, Zeng S, Swenson SD, Cho HY, et al. Enhanced brain delivery and therapeutic activity of trastuzumab after blood-brain barrier opening by NEO100 in mouse models of brain-metastatic breast cancer. *Neuro Oncol* (2021) 23(10):1656–67. doi: 10.1093/neuonc/noab041

19. Chien AJ, Rugo HS. Tyrosine kinase inhibitors for human epidermal growth factor receptor 2-positive metastatic breast cancer: Is personalizing therapy within reach? *J Clin Oncol* (2017) 35(27):3089–91. doi: 10.1200/JCO.2017.73.5670
20. Lin NU, Borges V, Anders C, Murthy RK, Paplomata E, Hamilton E, et al. Intracranial efficacy and survival with tucatinib plus trastuzumab and capecitabine for previously treated HER2-positive breast cancer with brain metastases in the HER2CLIMB trial. *J Clin Oncol* (2020) 38(23):2610–9. doi: 10.1200/JCO.20.00775
21. Ma F, Ouyang Q, Li W, Jiang Z, Tong Z, Liu Y, et al. Pyrotinib or lapatinib combined with capecitabine in HER2-positive metastatic breast cancer with prior taxanes, anthracyclines, and/or trastuzumab: A randomized, phase II study. *J Clin Oncol* (2019) 37(29):2610–9. doi: 10.1200/JCO.19.00108
22. Xu B, Yan M, Ma F, Hu X, Feng J, Ouyang Q, et al. Pyrotinib plus capecitabine versus lapatinib plus capecitabine for the treatment of HER2-positive metastatic breast cancer (PHOEBE): a multicentre, open-label, randomised, controlled, phase 3 trial. *Lancet Oncol* (2021) 22(3):351–60. doi: 10.1016/S1470-2045(20)30702-6
23. Saura C, Oliveira M, Feng YH, Dai MS, Chen SW, Hurvitz SA, et al. Neratinib plus capecitabine versus lapatinib plus capecitabine in HER2-positive metastatic breast cancer previously treated with ≥ 2 HER2-directed regimens: Phase III NALA trial. *J Clin Oncol* (2020) 38(27):3138–49. doi: 10.1200/JCO.20.00147
24. Awada A, Colomer R, Inoue K, Bondarenko I, Badwe RA, Demetriou G, et al. Neratinib plus paclitaxel vs trastuzumab plus paclitaxel in previously untreated metastatic ERBB2-positive breast cancer: The NEfERT-T randomized clinical trial. *JAMA Oncol* (2016) 2(12):1557–64. doi: 10.1001/jamaoncol.2016.0237
25. Zhang L, Wu X, Zhou J, Zhu M, Yu H, Zhang Y, et al. Pyrotinib in the treatment of women with HER2-positive advanced breast cancer: A multicenter, prospective, real-world study. *Front Oncol* (2021) 11:699323. doi: 10.3389/fonc.2021.699323
26. Li Y, Gong C, Lu Q, Zhou Z, Luo T, Li W, et al. Real-world data of triplet combination of trastuzumab, lapatinib, and chemotherapy in HER2-positive metastatic breast cancer: A multicenter retrospective study. *Front Oncol* (2020) 10:271. doi: 10.3389/fonc.2020.00271



OPEN ACCESS

EDITED BY

Dayanidhi Raman,
University of Toledo, United States

REVIEWED BY

Carlos Martinez-Perez,
Medical Research Council Institute of
Genetics and Molecular Medicine (MRC),
United Kingdom
Arnold H. Zea,
Louisiana State University, United States

*CORRESPONDENCE

Lina Prasmickaite
✉ linap@rr-research.no

SPECIALTY SECTION

This article was submitted to
Breast Cancer,
a section of the journal
Frontiers in Oncology

RECEIVED 09 September 2022

ACCEPTED 07 February 2023

PUBLISHED 22 February 2023

CITATION

Pettersen S, Øy GF, Egeland EV, Juell S,
Engebråten O, Mælandsmo GM and
Prasmickaite L (2023) Breast cancer
patient-derived explant cultures
recapitulate *in vivo* drug responses.
Front. Oncol. 13:1040665.
doi: 10.3389/fonc.2023.1040665

COPYRIGHT

© 2023 Pettersen, Øy, Egeland, Juell,
Engebråten, Mælandsmo and Prasmickaite.
This is an open-access article distributed
under the terms of the [Creative Commons
Attribution License \(CC BY\)](#). The use,
distribution or reproduction in other
forums is permitted, provided the original
author(s) and the copyright owner(s) are
credited and that the original publication in
this journal is cited, in accordance with
accepted academic practice. No use,
distribution or reproduction is permitted
which does not comply with these terms.

Breast cancer patient-derived explant cultures recapitulate *in vivo* drug responses

Solveig Pettersen¹, Geir Frode Øy¹, Eivind Valen Egeland¹,
Siri Juell¹, Olav Engebråten^{1,2,3}, Gunhild Mari Mælandsmo^{1,4}
and Lina Prasmickaite^{1*}

¹Department of Tumor Biology, Radium Hospital, Oslo University Hospital, Oslo, Norway,

²Department of Oncology, Oslo University Hospital, Oslo, Norway, ³Institute for Clinical Medicine,
University of Oslo, Oslo, Norway, ⁴Department of Medical Biology, Faculty of Health Sciences,
University of Tromsø/the Arctic University of Norway, Tromsø, Norway

Assessment of drug sensitivity in tumor tissue *ex vivo* may significantly contribute to functional diagnostics to guide personalized treatment of cancer. Tumor organoid- and explant-cultures have become attractive tools towards this goal, although culturing conditions for breast cancer (BC) tissue have been among the most challenging to develop. Validation of possibilities to detect concordant responses in individual tumors and their respective cultures *ex vivo* is still needed. Here we employed BC patient-derived xenografts (PDXs) with distinct drug sensitivity, to evaluate different conditions for tissue dissociation, culturing and monitoring of treatment efficacy *ex vivo*, aiming to recapitulate the *in vivo* drug responses. The common challenge of discriminating between tumor and normal cells in the cultured tissue was also addressed. Following conventional enzymatic dissociation of BC tissue, the tumor cells stayed within the non-disrupted tissue fragments, while the single cells represented mostly normal host cells. By culturing such fragments as explants, viable tumor tissue could be maintained and treated *ex vivo*, providing representative indications on efficacy of the tested treatment. Thus, drug sensitivity profiles, including acquired chemoresistance seen in the PDXs, were recapitulated in the respective explants. To detect the concordant responses, however, the effect monitoring had to be harmonized with the characteristics of the cultured tissue. In conclusion, we present the feasibility of BC explants *ex vivo* to capture differences in drug sensitivity of individual tumors. The established protocols will aid in setting up an analogous platform for BC patient biopsies with the aim to facilitate functional precision medicine.

KEYWORDS

breast cancer, patient-derived xenografts, *ex vivo* cultures, organoids, explants, drug sensitivity

Abbreviations: BC, Breast cancer; IF, Immunofluorescent; I.V., Intravenous; PDE, Patients-derived explant; PDO, Patients-derived organoid, PDX, Patients-derived xenograft; PDXC, Patients-derived xenograft culture; PI, Propidium iodide; PR, Paclitaxel resistant; TNBC, Triple-negative breast cancer; 3D, Three-dimensional.

Introduction

Patient-proximal models hold promise as a drug screening platform for personalized cancer therapy. Patient-derived xenografts (PDXs) in mice have long been considered among the most important models, although their use is limited due to low throughput, high costs and ethical issues (1, 2). More recently, cultures of patient-derived organoids (PDOs) and patient-derived explants (PDEs) have become attractive tools for assessing drug sensitivity *ex vivo* in a personalized manner (3, 4). The term “organoids” describes stem-cell derived self-organizing three-dimensional (3D) structures that recapitulate features of the tissue of origin and have the ability to be expanded *in vitro* for long-term (5, 6). PDOs of colorectal, pancreatic and prostate cancers were among the first successfully developed and employed for assessing drug sensitivity *ex vivo* (7–9). This, on the other hand, has been challenging for breast cancer (BC). Currently, PDOs for most cancer forms, also BC have been developed (3, 10–13). In contrast to PDOs, PDEs represent short-term cultures of small fragments of tumor tissue (4, 14). Since PDEs partially maintain the heterogeneity and the microenvironment of the tumor of origin, they provide an opportunity to explore drug responses within the authentic context (15, 16).

Access to patient biopsies, particularly throughout the course of treatment (i.e. at the start, when the tumors are sensitive, and later, when they develop resistance) is often limited. Thus, precious patient material is seldom available for testing experimental drugs, developing new assays or performing mechanistic studies on treatment response or resistance. Such studies still have to rely on model systems, and PDX-derived cultures (PDXCs) *ex vivo* are attractive alternatives. It has been demonstrated that PDXCs can predict responses to targeted drugs in the matching PDXs (10, 13). However, discrepancies in response between *in vivo* and *ex vivo* models have also been observed (17).

The protocols used for tumor tissue processing, culturing and read-out of drug sensitivity vary between different studies (10–13), suggesting that individual optimization might be needed. Here we aimed to establish conditions for evaluation of drug responses *ex vivo* by using tumor tissue from triple-negative breast cancer (TNBC) PDXs with distinct drug sensitivity. The goal was to recapitulate *ex vivo* the drug sensitivity profile of the parental PDXs.

Materials and methods

PDXs maintenance and treatment

MAS98.12 PDX was established in-house and described previously (18). The paclitaxel resistant sub-line MAS98.12PR was established from a mouse bearing MAS98.12 tumor that was treated with 15 mg/kg paclitaxel twice per week for three weeks and after the initial response developed resistance as shown in Figure 1A. HBCx39 PDX was established at the Institute Curie (Paris, France) (19, 20) and was obtained through collaboration with Dr. Elisabetta Marangoni. All xenografts were maintained by

serial passaging, implanting 1–3 mm³ pieces of the parental tumors into thoracic mammary glands of 6–8 week-old female HSD : Athymic Nude Foxn1nu mice locally bred at the Department of Comparative Medicine at the Norwegian Radium Hospital (Oslo, Norway). Before implantation, the mice were placed under anesthesia with sevoflurane (Baxter, Deerfield, IL, USA).

The treatments were initiated when tumor volume reached 60–200 mm³ and lasted for three weeks. Paclitaxel (Hospira UK Ltd, Hurley, UK or Sandoz, Basel, Switzerland) diluted in 0.9% saline was given intravenously (i.v), while capecitabine (Accord-UK, Barnstaple, UK) diluted in 40 mM citric buffer/5% gummi arabicum and everolimus (LC Laboratories, Woburn, MA, US) diluted in 0.5% methyl cellulose solution were given orally. Tumor growth was followed by measuring their size (length L and width W) using a caliper, and the tumor volume was calculated as: $W^2 \times L \times 0.5$.

This study is compliant with all relevant ethical regulations regarding animal research and was conducted according to the recommendations of the European Laboratory Animals Science Association. All experiments involving animals were approved by the Norwegian Food Safety Authority (FOTS id 15499).

PDX tissue dissociation and isolation of tissue fragments

Freshly resected or thawed cryopreserved (0.5 g tissue as 3–4 mm pieces/cryotube with 1 ml Recovery Cell Culture Freezing Medium (Gibco, Grand Island, NY, US)) tumors were minced with a scalpel and digested with 2 mg/ml collagenase IV and 100 µg/ml DNase (both from Sigma-Aldrich, St. Louis, MO, USA) dissolved in advanced DMEM/F12 supplemented with Glutamax, HEPES and Penicillin/Streptomycin (concentrations/producers specified in Supplementary Table S1). The digestion was performed at 37°C on rotation for up to 1 h. Where indicated, additional mechanical dissociation using the gentleMACS dissociator (Miltenyi Biotec, Bergisch Gladbach, Germany) at “m-imp Tumor 03” settings were applied. The dissociated tissue suspension was diluted with phosphate-buffered saline (PBS)/1% bovine serum albumin (BSA) (both Sigma-Aldrich) and centrifuged at 18g for 4 min. The pellet was re-suspended and centrifuged again first at 32g, then at 200g for 4 min. The cell viability was monitored by staining aliquots with 0.2% trypan blue (NanoEntek, Seoul, Korea). Majority of dead cells remained in the supernatants, while the final pellet consists of a mixture of viable single cells and small non-disrupted tissue fragments. The final pellet was re-suspended in breast cancer organoid medium (OM) described by Sachs et al. (12) (specified in Supplementary Table S1).

Additional steps to remove normal mouse cells included plating re-suspended pellet in 24-well plates treated with anti-adherence Rinsing Solution (Stemcell Technologies, Cambridge, UK) and culturing in OM supplemented with 5 µM of the MDM2 inhibitor Nutlin-3 (Cayman, Ann Arbor, MI, USA), further called OM+. Nutlin-3 induces death in cells with wild-type TP53 i.e. normal cells, while tumor cells with lost/mutated TP53 stay viable (11). The PDXs used in this study harbor a mutation of the TP53

gene (18, 19). Therefore, the tumor tissue can be subjected to Nutlin-3 selection for enrichment of cancer cells. Subsequently, the tissue suspension was filtered through a 100 µm cell strainer to collect fragments below this size that were further sedimented for 2–5 min. The resulting fragment-enriched pellet was used for establishment of PDXCs.

PDXCs in Matrigel and treatment with drugs

The fragment-enriched pellet was resuspended in OM+ to a concentration of approximately 7–9 fragments/µl. Fragment counting was performed manually in a 10 µl droplet of suspension by using a light microscope. After addition of 30% Matrigel (Corning, New York, USA), a droplet of 10 µl containing approximately 50–60 fragments was added to each well in a 48-well plate, and the domes were allowed to solidify at 37°C for 30 min before addition of 190 µl of OM+. The next day, 200 µl of OM+ with the desired concentration of the drug was added. Half of the medium (+/- drug) was replaced twice per week.

Scoring of treatment response in PDXCs

Analysis of fragment growth by measuring their total area

Each well was analyzed in real-time by using Incucyte® S3 equipped with the organoid analysis software module (Sartorius, Gottingen, Germany). The module automatically detects fragment total area providing growth curves for control- and treated-explants.

Live/dead staining and calculation of a proportion of live cells in the fragments

The treated PDXCs and the respective untreated controls were stained with 2 µM calcein-AM (Sigma- Aldrich) for 30 min at 37°C followed by staining with 350 nM propidium iodide (PI) (Invitrogen, Waltham, MA, USA) for 30 min to distinguish live (green) and dead (red) cells, respectively. The stained cultures were analyzed by Olympus IX81 microscope equipped with a 4x objective and filters 488/527 (for calcein) and 540/590 (for PI) (Olympus, Tokyo, Japan). Three images per well together covering whole area of the dome were captured. Fiji/ImageJ (21), an open-source software for image processing was used to measure the calcein- and PI-signal area in pixels in each fragment. Proportion of live cells in the fragments was calculated in each well based on the equation “calcein-signal”/[“calcein-signal” + “PI-signal”].

Metabolic activity measurements by CellTiter-Glow assay

The PDXCs were prepared as above but in white 96-well plates with clear bottom (Corning, New York, NY, USA). After one week of treatment, CellTiter-Glo 3D reagent (Promega, Madison, WI, USA) was added at a ratio 1:2, and luminescence was measured by the Victor X3 plate reader (PerkinElmer, Waltham, MA, USA).

Evaluation of the proliferative ability *ex vivo*

The proliferative ability of the dissociated PDX tissue *ex vivo* was evaluated by scoring EdU incorporation using the Click-iT™ EdU kit (Invitrogen), according to the manufacturer protocol. In brief, 2 µM of EdU labeling solution was added to the cultures and incubated for 2 days before the cultures were fixed with 4% paraformaldehyde (PFA) (Electron Microscopy Sciences, Hatfield, PA, USA) for 15 min. After washing and permeabilization with 0.5% Triton® X-100 (Sigma-Aldrich) for 20 min, the Click-iT® reaction cocktail was added, and after 30 min the proliferating cells were identified by imaging using Olympus IX81 microscope equipped with a 4x objective and a 488/527 filter.

Immunofluorescent staining

Cultures were fixed with 4% PFA for 15 min followed by 1 h blocking in 10% horse serum (Gibco, Grand Island, NY, USA) in IF buffer (PBS with 0.1% BSA, 0.2% Triton X-100 and 0.05% Tween-20 (Merck, Darmstadt, Germany)). The samples were incubated with primary antibodies (diluted in the IF-buffer as specified in the [Supplementary Table S2](#)) overnight at 4°C. After washing with IF buffer 3x10 min, the samples were incubated with secondary antibody and DAPI (as specified in [Supplementary Table S2](#)) in IF buffer for 2 h at room temperature, followed by washing with PBS 4x10 min. Imaging was performed using a Zeiss LSM 710 laser-scanning confocal microscope equipped with a Zeiss plan-Apochromat 20x NA/0.8 air objective (Carl Zeiss, Jena, Germany).

Assessment of multidrug transporter functionality *ex vivo*

The fragments cultured in suspension for one week were collected and incubated with/without 10 µM verapamil (Sigma-Aldrich), an inhibitor of a multidrug transporter, for 30 min followed by incubation with 1 µM doxorubicin (Pfizer, New York, NY, USA) for 24 h at 37°C. The accumulation of doxorubicin in the fragments was analyzed by Olympus IX81 microscope equipped with a 10x objective and a 540/590 filter, and quantification was performed using an Olympus software Cell P, which separately measures mean color intensity per fragment within the image.

Quantification of human/mouse DNA content and ABCB1 mRNA level by real-time qPCR

Up to 30 mg of fresh frozen tumor tissue or 1x10⁷ cells were lysed in 600 µl RLT Plus buffer w/2 mM DTT using the QIAshredder homogenizer (Qiagen, Hilden, Germany). The instrument was operated for 2x4 min at a frequency of 30Hz.

Homogenized lysate was passed through a QIAshredder spin column at 20000g for 30 s to remove debris. Genomic DNA and total RNA were simultaneously extracted from the lysates using the QIAcube instrument and the AllPrep DNA/RNA/miRNA Universal kit (all Qiagen).

To estimate the content of human and mouse DNA in each sample, we use the assay described previously (22). It is based on real-time qPCR using species-specific TaqMan probes conjugated with different fluorescent tags (human: tgctgcttcattgtctcg (FAM) and mouse: cctgctgcttatcgtggctg (VIC)) along with common human/mouse forward (tacctgcagctgtacgccac) and reverse (gaccacctcattctcctgc) primers. The primer/probes detect the prostaglandin E receptor 2 (*PTGER2*) gene region, which is highly homologous between the two species and known not to be duplicated/deleted in disease. The standard curve (Ct values as a function of known amount of human and mouse DNA) were generated employing serially diluted DNA isolated from the human melanoma cell line WM115 and the mouse colon carcinoma cell line CT26. Real-time PCR was carried out on an BioRad CFX connect Real time System (Bio-Rad, Hercules, CA, USA) using 50 ng of total genomic DNA in 25 µl reaction mix containing 200 nM of each primer/probe (Applied Biosystems, Waltham, MA, USA) and 1x PerfeCTa qPCR ToughMix (Quanta Biosciences, Gaithersburg, MD, USA). The qPCR conditions were as follows: 5 min 95°C initial denaturation, 40 cycles of 15 s denaturation at 95°C and 30 s annealing/extension at 60°C. Quantifications were performed taking into account that one haploid mouse genome is approximately 2.9 pg, whereas one human haploid genome is approximately 3.33 pg. “Percent human (or mouse) DNA” was estimated as follows: [number of human (or mouse) genome]*100/[sum human+mouse genome].

To detect *ABCB1* gene mRNA level, extracted total RNA was converted into cDNA using the qScript cDNA Synthesis Kit (Quanta Biosciences). PCR was carried out as specified above using 50 ng cDNA, *ABCB1* forward (5'gaaattagaagatctgatgcaaca'3) and reverse (5'actgtaataataggcatacctggta'3) primers (Integrated DNA Technologies, Leuven, Belgium) and 10 µM probe #65 from Universal Probe Library (Roche Applied Science, Penzberg, Germany). The reference gene *TBP* was detected using the commercially available Applied BioSystems TaqMan Assay. Relative gene expression was calculated using the $\Delta\Delta$ Ct method.

Results

Isogenic PDXs with distinct sensitivity to paclitaxel

To establish *ex vivo* models that recapitulate treatment responses seen in individual tumors, we have utilized the previously described TNBC PDX, MAS98.12 (18) and its chemoresistant derivative, MAS98.12PR. *In vivo*, MAS98.12 was highly sensitive to paclitaxel (Figure 1). One of the regressed tumors, however, started to re-grow after ten weeks (Figure 1A, dashed line) and was unresponsive to repeated treatment with paclitaxel. This tumor was the origin of the paclitaxel-resistant

sub-line, MAS98.12PR. Later generations of MAS98.12PR tumors retained resistance to paclitaxel (Figure 1B). This pair of isogenic PDXs has been used as a source of human tumor tissue that originates from the same patient but differs with respect to paclitaxel sensitivity. We aimed to establish tissue cultures that recapitulate this difference *ex vivo*.

Ex vivo proliferative capacity of the dissociated PDX tissue

To dissociate BC tissue for subsequent culturing, we tested two methods used in similar studies: the conventional enzymatic digestion using collagenase IV/DNase for up to 1 h (11–13), and the additional mechanical homogenization using gentleMACS dissociator, as used by Guillen et al. (10). Regardless of the dissociation method and the PDX model, the resulting tissue suspension consisted of single cells and small non-disrupted tissue fragments as shown in Figure 2. Trypan blue staining revealed lower viability among single cells than fragments, which mostly harbored trypan blue-negative viable cells (Figure 2A). GentleMACS increased the recovery of single cells (data not shown), though the non-disrupted tissue fragments were still present at significant amounts. To note, enzymatic digestion overnight disrupted the fragments to single cells, but cell viability was very low (data not shown).

The proliferative capacity of the cells isolated by the two methods was further compared by measuring incorporation of EdU. The dissociated tissue was cultured in suspension and, at different time points, stained with EdU. On day 1, no obvious difference with respect to EdU-incorporation was observed between the two methods, indicating a similar proliferative capacity of the dissociated tissue. With time, however, cultures prepared with gentleMACS lost their proliferative capacity, while the cultures processed by the enzymatic digestion only, kept proliferating for at least 11 days (Figure 2B). The proliferative capacity was also maintained when the dissociated tissue was cultured within Matrigel (Figure 2C). In both suspension and Matrigel cultures, the EdU positive cells were primarily found in the tissue fragments, although there was substantial heterogeneity between and within the fragments (Figures 2B, C).

The tissue fragments harbor human tumor cells

To analyze the composition of the dissociated PDX tissue, we performed immunostaining using species-specific antibodies. To identify mammary cells of human origin, we stained for the human epithelial markers: epithelial cell adhesion molecule EpCAM, myoepithelial/basal cytokeratin CK14 and luminal cytokeratin CK19. In both PDX models, the fragments were positive for these markers, while the single cells outside the fragments were negative, suggesting their mouse origin (Figure 3A). Staining with the mouse-specific MHC class-I molecule H-2Kd/Dd validated that majority of the cells outside the fragments are H-2Kd/Dd-positive mouse cells

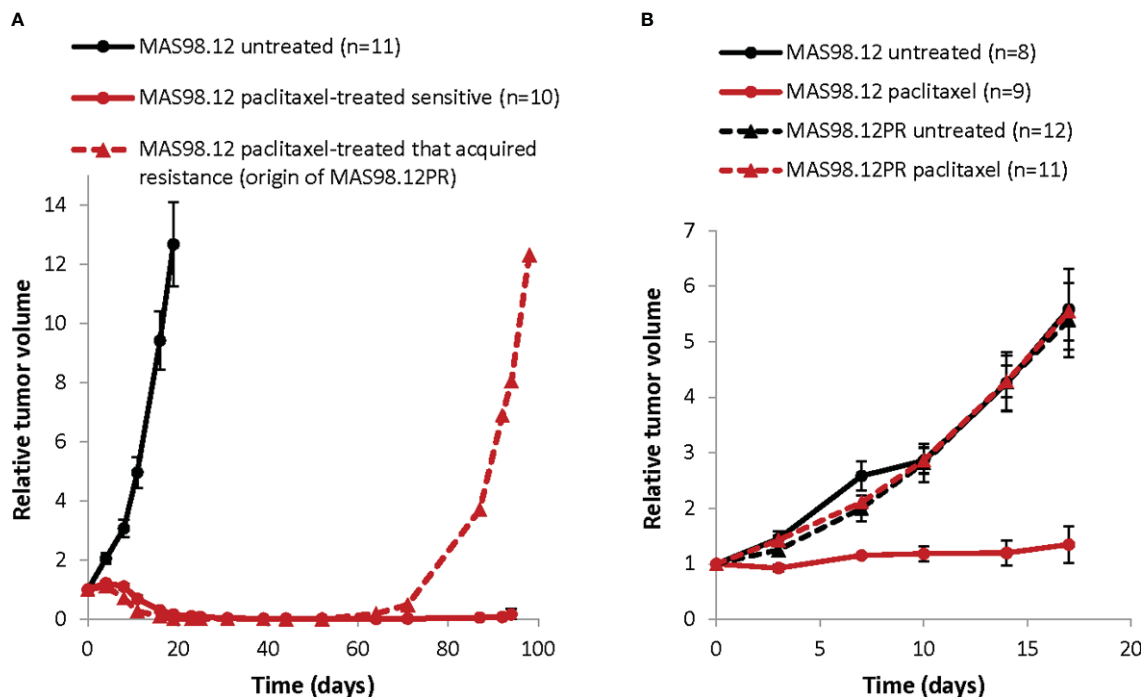


FIGURE 1

Growth of TNBC PDXs: paclitaxel sensitive MAS98.12 and the resistant sub-line MAS98.12PR with/without treatment. (A) Relative tumor volume (normalized to the volume at the day when the treatment was started) of the non-treated and the paclitaxel-treated (15 mg/kg, 2x/week for 3 weeks) MAS98.12. One of the treated tumors acquired resistance and re-grew, being the origin of the resistant sub-line MAS98.12PR; average \pm SEM (n indicated in the legend). (B) Validation of the distinct sensitivity to paclitaxel (10 mg/kg, 2x/week) in the MAS98.12 and the daughter sub-line MAS98.12PR; average \pm SEM (n indicated in the legend).

(Figure 3A). Based on this data, we introduced additional steps (multiple low-speed centrifugations and size-based separation as specified in Materials and Methods) to separate the fragments. The fragment-enriched fraction was embedded in Matrigel for further culturing as explants *ex vivo*. In such cultures, the fragment size did not change significantly over time (Figure 3B upper panel, blue arrows). However, we observed single cell-derived structures that increased notably in diameter during culturing (Figure 3B upper panel, red arrows), similar to what has been reported for normal- or BC-organoids (11, 12). Immunostaining with human EpCAM, CK14, CK19 and mouse H-2Kd/Dd validated that the fragments consisted of human epithelial tumor cells. In contrast, the single-cell derived structures consisted of mouse cells surrounding the cavity (Figure 3B, lower panel), suggesting that they were organoids of mouse origin. To eliminate mouse cells forming such structures, we applied Nutlin-3 selection. As shown previously, treatment with Nutlin-3 eliminates normal organoids, but does not affect cancer organoids with *TP53* mutation (11), and MAS98.12 harbors mutation in the *TP53* gene (18). In Nutlin-3 pre-treated explants, we observed reduced amount of mouse cells and the absence of mouse organoids. Such explants are further called PDXCs.

To further validate the origin of the different samples along the PDXCs preparation (specified in Figure 3C), we quantified human and mouse DNA content by qPCR using species-specific probes for the *PTGER2* gene. As expected, in single-cell derived structures only mouse *PTGER2* was detected (Ct values around 26) (Figure 3D). In the isolated fragment-enriched fraction and the eventual PDXCs,

human DNA was clearly dominant, though some contamination with mouse DNA should be noted (Figure 3D). For comparison, the original PDX tissue contained approximate equal amounts of human and mouse DNA. Altogether, this data indicates that fragments are the main source of human tumor cells in the dissociated tissue from the investigated PDXs.

The resistant PDXs and PDXCs over-express ABCB1 transporter that is functional *ex vivo*

To investigate whether PDXCs from MAS98.12 and MAS98.12PR retain the molecular properties of the parental PDXs, we measured the expression of the characteristic genes. Previously performed gene expression profiling of this PDX pair identified *ABCB1* (*MDR1*), which encodes a multidrug ABC transporter, as the most differentially expressed gene, with approximately 16-fold up-regulation in MAS98.12PR compared to MAS98.12 (data not shown). Correspondingly, we detected a significantly higher level of *ABCB1* mRNA in the cultures from MAS98.12PR compared to MAS98.12 cultures (Figure 4A).

Up-regulation of ABC transporters is a well-described mechanism of chemoresistance that reduces cellular accumulation of drugs (23). To investigate whether the over-expressed transporter encoded by *ABCB1* was functional *ex vivo*, we analyzed cellular accumulation of a fluorescent drug doxorubicin. Cultures from

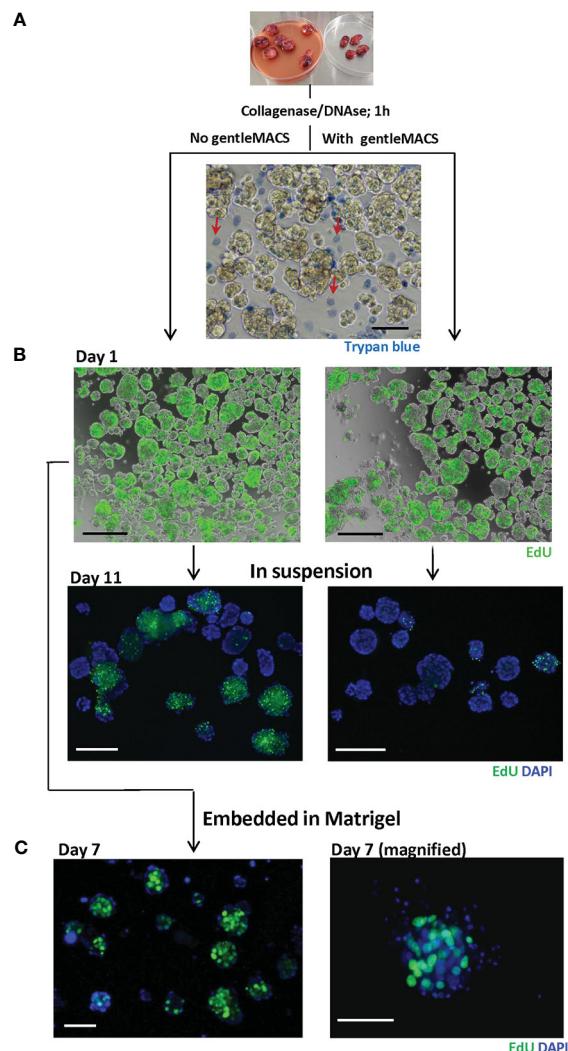


FIGURE 2

Dissociated MAS98.12/MAS98.12PR PDX tissue; appearance and proliferative capacity *ex vivo*. Tumors were disintegrated using collagenase/DNase with/without gentleMACS. The resulting tissue suspension was stained with trypan blue (A) to identify dead cells and EdU (B) to evaluate the proliferative capacity. The EdU staining was also performed on 7/11 day-cultures either in suspension (B) or in Matrigel (C); DAPI stains the nucleus; scale bars, 100 μ m.

MAS98.12PR accumulated notably less doxorubicin compared to the cultures from MAS98.12 (Figures 4B, C). In the presence of verapamil, the inhibitor of ABC transporters, the accumulation of doxorubicin was increased in the cultures from MAS98.12PR and reached the same levels as in the MAS98.12 cultures (Figures 4B, C). Altogether, this indicates that *ABCB1* expression difference seen in the PDXs is retained in the respective cultures, and that the transporter is active *ex vivo*.

PDXCs recapitulate paclitaxel-resistance of the PDXs

To assess whether the difference in paclitaxel sensitivity seen in the PDXs (Figure 1B) can be recapitulated in the respective PDXCs, we treated the explants with increasing concentrations of paclitaxel for one week. The treatment efficacy was evaluated by three different

read-out strategies. First, we attempted to automatically monitor fragment size/total area by the Incucyte equipped with the organoid module. Unfortunately, this approach was unsuitable for the cultures from the MAS98.12/MAS98.12PR PDXs (to note, it was useful for cultures from other PDXs, such as HBCx39 as shown below. After treatment, high numbers of dead cells were found in the periphery of the fragments; this contributed to the fragment size, impairing correlation between size and viability/growth (Figure 5A, left panel). Therefore, we employed another read-out based on live and dead staining with calcein and PI, respectively (Figure 5A middle/right panel), followed by microscopy-based quantification of the proportion of live cells in the fragments. As shown in Figure 5B, the PDXCs from MAS98.12 demonstrated a paclitaxel dose-dependent decrease in the proportion of viable cells. In concordance, the extent of dead, PI-positive cells was increased as illustrated in Figure 5A. On the contrary, the PDXCs from MAS98.12PR showed no decrease in the proportion of viable cells

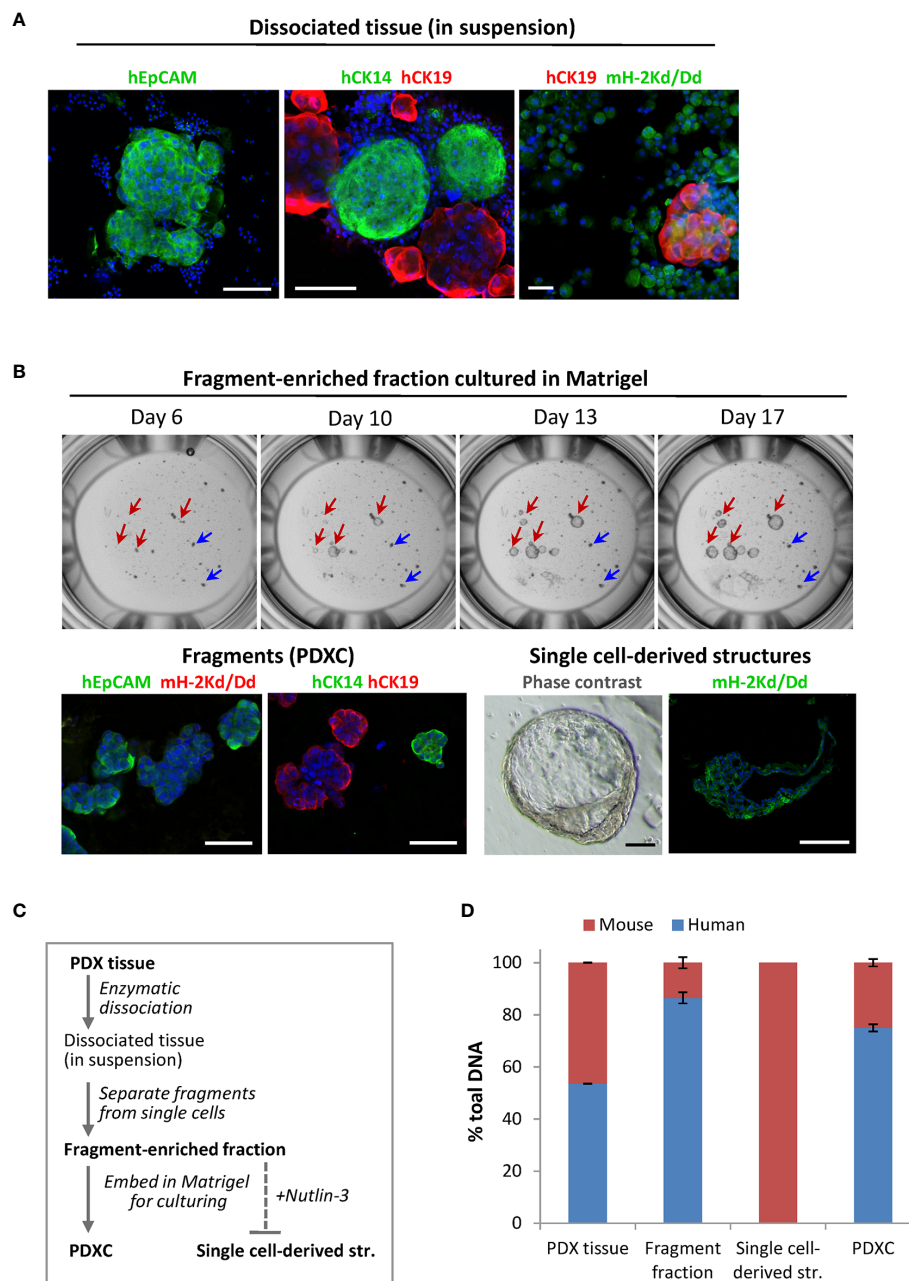


FIGURE 3

The composition of the dissociated MAS98.12/MAS98.12PR PDXs and the *ex vivo* cultures. **(A)** IF staining of the dissociated PDX tissue suspension with human EpCAM, CK14 and CK19, and mouse H-2Kd/Dd; scale bars, 100 μ m. **(B)** Cultures established from fragment-enriched fraction embedded in Matrigel. Upper panel: phase contrast pictures taken over time, where fragments and single cell-derived structures are shown by blue and red arrows, respectively. Lower panel: IF staining with human EpCAM, CK14 and CK19 and mouse H-2Kd of fragments and single cell-derived structures; DAPI stains the nucleus; scale bars, 100 μ m. **(C)** The scheme indicating preparation of the samples discussed in the figure; bold indicates the samples whose DNA composition was analyzed by species-specific qPCR and presented in **(D)**; **(D)** Quantitative assessment of human and mouse DNA content in the different samples; average \pm StDv ($n=2$, here represented by one sample from each PDX).

(Figure 5B) and no increased staining with PI (Figure 5A), indicating their insensitivity to paclitaxel. Importantly, similar differences in sensitivity were observed in both cultures from fresh and cryopreserved tumor tissue (Supplementary Figure S1). Finally, we applied the conventional CTG assay that measures bulk metabolic activity in the cultures. The results matched the live-dead staining (except at the highest dose of paclitaxel), revealing the paclitaxel resistance in cultures from MAS98.12PR (Supplementary

Figure S2A). However, we noted big variation between parallel wells. Furthermore, it was not possible to discriminate the impact from the contaminating mouse cells, which could explain equal drop in metabolic activity in both PDXCs at the highest dose of paclitaxel.

Further, we compared the PDXCs sensitivity to another chemotherapeutic agent, capecitabine (a 5-FU pro-drug). This drug is commonly used as a salvage therapy in patients with

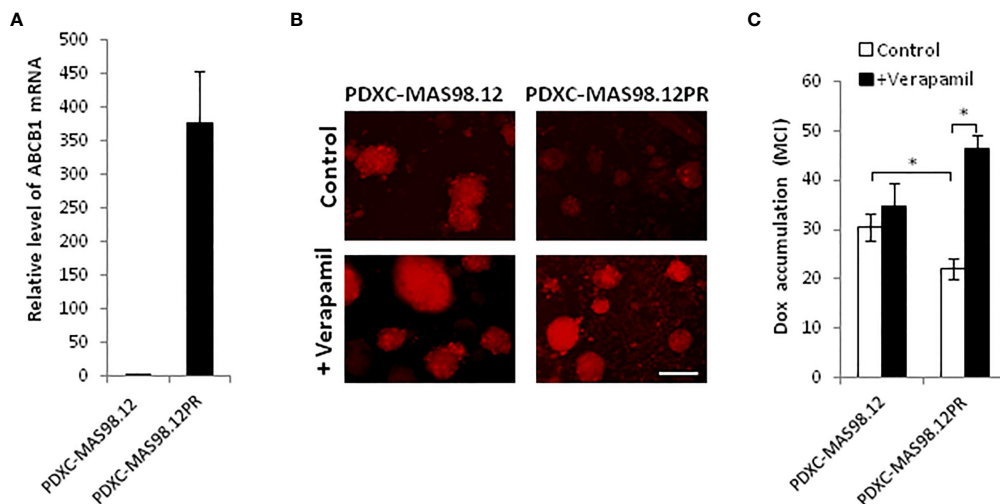


FIGURE 4

MAS98.12PR-derived cultures over-express ABCB1 that is functionally active *ex vivo*. (A) Relative expression of ABCB1 gene in 10 d-cultures from MAS98.12PR compared to MAS98.12 (set to 1); average \pm SEM (n=4 (2 for suspension and 2 for Matrigel cultures)). (B, C) Accumulation of doxorubicin (Dox) in 10d-cultures from MAS98.12 and MAS98.12PR after 24h-incubation with 1 μ M Dox in the presence or absence of 10 μ M verapamil. Representative fluorescence pictures (B) and quantified Dox accumulation presented as mean color intensity (MCI) in the fragments (average \pm SEM (n \geq 7) (C); scale bar, 200 μ m; *, p < 0.05 by unpaired t-test. (C).

remaining TNBC after pre-operative chemotherapy (24). *In vivo*, capecitabine treatment notably inhibited tumor growth in both MAS98.12 and MAS98.12PR, and the latter even showed a slightly better response (Figure 6A). In line with the *in vivo* data, both PDXCs showed good dose-dependent response to capecitabine as quantified by live-dead staining and the CTG assay (Figures 6B, C and Supplementary Figure S2B). Furthermore, PDXC-MAS98.12PR showed a tendency for a slightly better response than PDXC-MAS98.12 (Figure 6C).

HBCx39-derived PDXCs recapitulate the drug sensitivity profile of the parental PDX

To investigate PDXCs from another patient, we employed HBCx39 PDX, which also represent TNBC. Similar to MAS98.12, the dissociated HBCx39 consisted of non-disrupted tissue fragments positive for human epithelial markers, EpCAM, CK14 and CK19 (Supplementary Figure S3A). The HBCx39-derived fragments were effectively growing *ex vivo* (Supplementary Figure S3BA). The explants

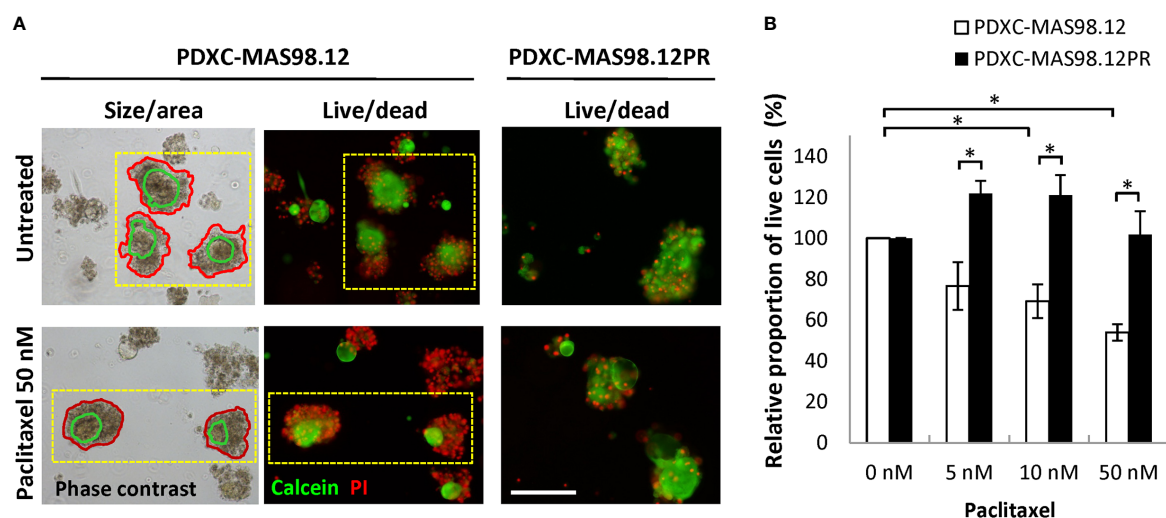


FIGURE 5

Sensitivity of MAS98.12- and MAS98.12PR-derived PDXCs to paclitaxel. Untreated and paclitaxel treated for one week PDXCs in Matrigel were stained with calcein/PI and a proportion of viable cells was quantified. (A) Representative pictures, where the red lines in the phase contrast pictures (left) mark the automatically detected fragment area, and the green line marks the "live" part, as validated by the fluorescence pictures (middle); scale bar, 200 μ m. (B) A proportion of viable cells in the treated cultures presented as a percentage of the respective untreated controls; average \pm SEM (n=4; where either fresh (n=2) or cryopreserved (n=2) PDX tissue was used to establish PDXCs, see Supplementary Figure S1); *, p < 0.05 by unpaired t-test.

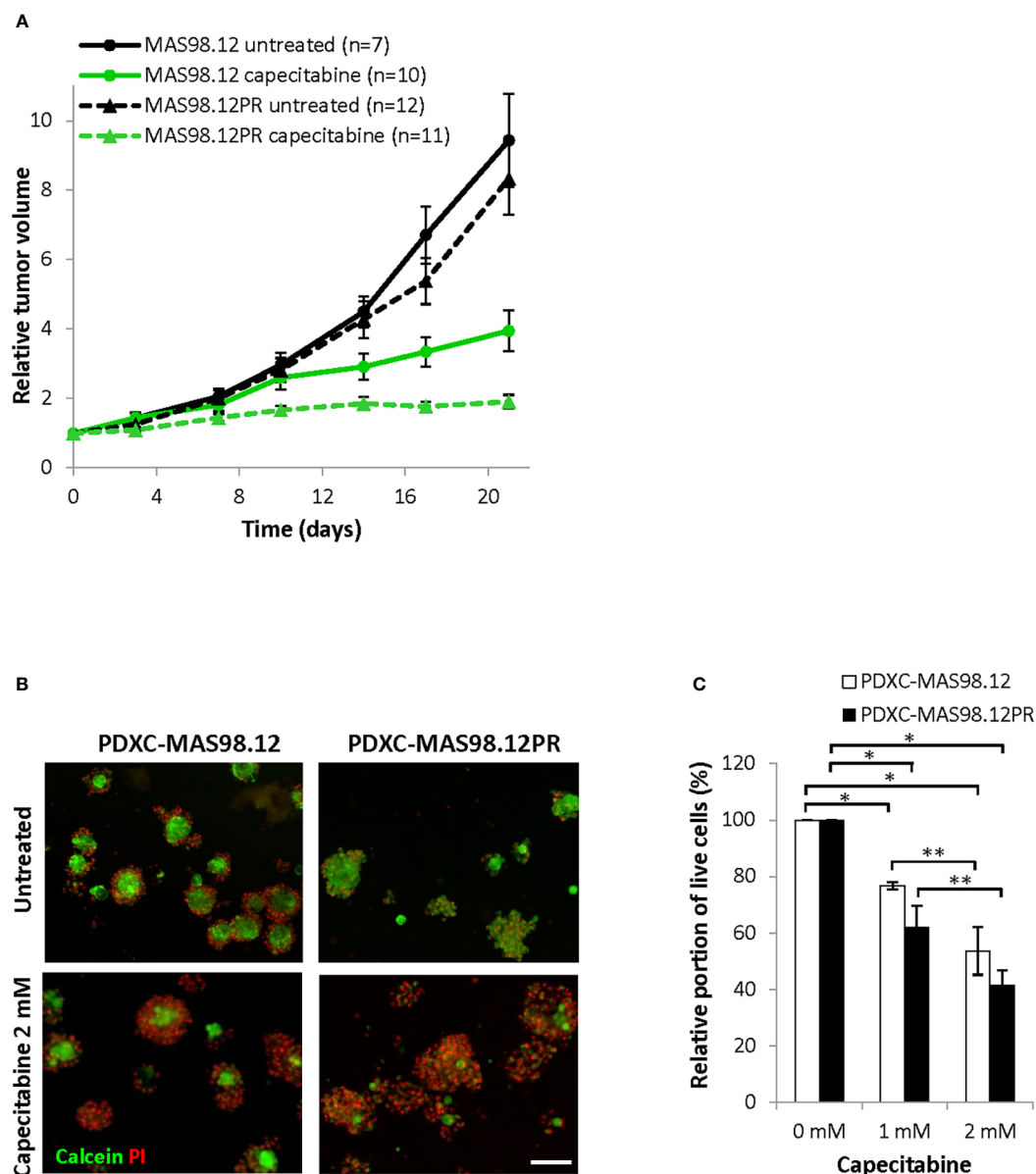


FIGURE 6

Sensitivity of MAS98.12/MAS98.12PR PDXs and the respective PDXCs to capecitabine. (A) Relative tumor volume (normalized to the volume at the day when the treatment was started) of non-treated and capecitabine-treated (540 mg/kg, 5x/week) MAS98.12 and MAS98.12PR PDX; average \pm SEM (n indicated in the legend). (B, C) PDXCs in Matrigel with/without capecitabine treatment for one week followed by calcein/PI staining (representative pictures in (B)) to quantify the proportion of viable cells among all cells (C). (B) Representative fluorescent pictures; scale bar, 200 μ m. (C) A proportion of viable cells in the treated cultures presented as a percentage of the respective untreated controls; average \pm SEM (n=3); * and **, $p < 0.05$ by unpaired and paired t-test, respectively.

showed high viability as revealed by calcein/PI staining (Supplementary Figure S3BB) and represented human tumor tissue as they stained with human-specific mitochondria and panCK antibodies and were mostly negative for mouse H-2Kd/Dd (Supplementary Figure S3C). Due to efficient growth, high viability and well-defined periphery of the fragments, PDXCs from HBCx39 could be easily analyzed by monitoring fragment size as a read-out of treatment efficacy.

In vivo HBCx39 PDXs showed high sensitivity to paclitaxel and particularly capecitabine, and lower sensitivity to the mTOR inhibitor everolimus (Figure 7A and Supplementary Figure S4). To investigate whether such sensitivity differences are recapitulated

ex vivo, we treated HBCx39-derived PDXCs with these drugs and followed changes in fragment size over time by the Incucyte organoid module. As expected, a time-dependent increase in the total fragment area was detected in the untreated controls (Figure 7B). Everolimus (20 nM) induced a low growth inhibitory effect, while paclitaxel significantly reduced and capecitabine completely abrogated the fragment growth (Figures 7B, C and Supplementary Figures S5A, B). Similar difference in sensitivity was registered also by the CTG assay (Supplementary Figure S5C) and further validated by live/dead staining (Figure 7D). The latter also revealed substantial cell death at day 19 upon capecitabine

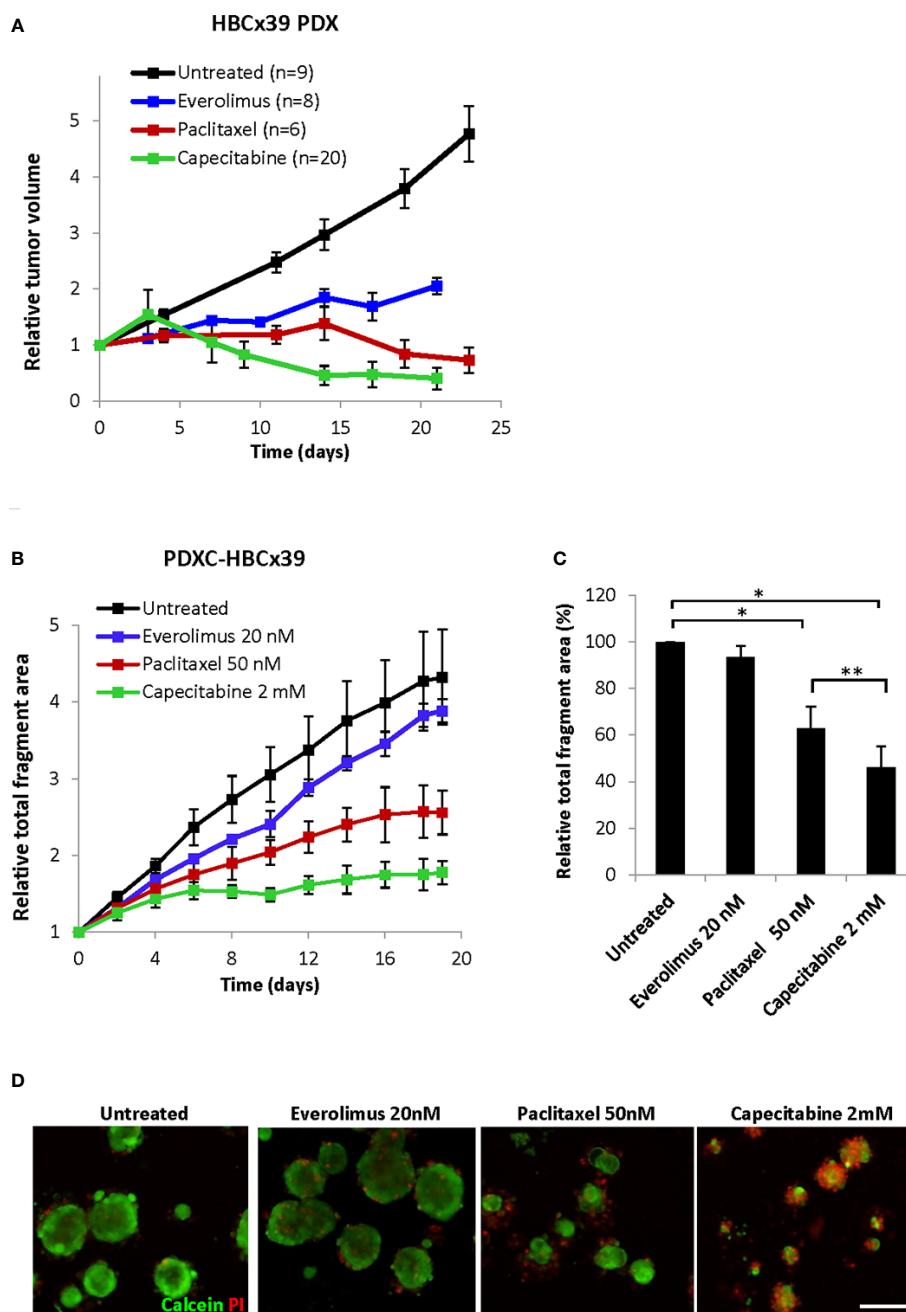


FIGURE 7

Response of HBCx39 PDX and PDXC to paclitaxel, capecitabine and everolimus. (A) Relative tumor volume (normalized to the volume at the day when the treatment was started) of non-treated and treated HBCx39 PDX; the treatment was as follows: paclitaxel (15 mg/kg, 2x/week), capecitabine (755 mg/kg, 5x/week) and everolimus (5 mg/kg, 5x/week). (B) Relative total fragment area normalized to the area at the start of the treatment; average \pm StDv (3-4 parallels for each condition in one representative experiment). (C) The total fragment area in the treated cultures (day 19) shown as a percentage of the untreated controls; average \pm SEM (n=3 for paclitaxel and capecitabine) and \pm StDv (n=2 for everolimus); * and **, $p < 0.05$ by unpaired and paired t-test, respectively. (D) Representative fluorescence pictures of PDXCs treated with/without the indicated drugs for 19 days before staining with calcein and PI; scale bar, 200 μ m.

treatment, while the effect of paclitaxel was strongly cytostatic with much fewer dead cells observed (Figure 7D). These observations correlated nicely to the *in vivo* results of long follow-up, where on week 7 we observed complete regression of all tumors in the capecitabine group, while the paclitaxel group carried small residual tumors (Supplementary Figure S4).

Discussion

In this study, we have recapitulated *in vivo* drug responses using patient-derived tissue cultures from BC. With the applied “know-how” reported in the previous publications (10–13), short-term explants from PDXs with distinct drug sensitivity were established, and

possibilities to detect concordant responses were validated. BC PDOs and PDEs are being considered as attractive tools for predicting drug sensitivity in individual tumors, though their application has not been straightforward. Although we succeeded in demonstrating matching differences in drug responsiveness between PDXs and PDXCs, several challenges were encountered. First, conventional enzymatic dissociation of BC tissue resulted in a mix of single cells and difficult-to-disrupt tissue fragments. Many applications, including generation of organoids, single-cell RNAseq or cytometric analyses, require single cells. However, in the dissociated PDX tissue, the single cells showed low viability. Furthermore, they represented mostly normal host cells, including mammary progenitors able to generate organoid-like structures of mouse origin. Viable human tumor cells were retained within the non-disrupted tissue fragments, indicating the possibility to maintain tumor tissue *ex vivo* by culturing such fragments as explants. The “behavior” of the fragments in culture, however, depended on the characteristics of the PDX tissue. In this study, one of the aims was to recapitulate sensitivity and resistance to paclitaxel as found in the isogenic pair of PDXs, MAS98.12 and MAS98.12PR. However, tissue from these PDXs appeared to be challenging to culture. Although we confirmed the presence of viable and proliferating tumor cells, the MAS98.12/MAS98.12PR-derived fragments demonstrated limited growth, in contrast to the fragments from the other PDX, HBCx39. Furthermore, a notable number of dead cells were associated with the cultured fragments from MAS98.12/MAS98.12PR, which was not the case for HBCx39 cultures. Those features influenced the choice of a method for monitoring treatment efficacy. Tracking changes in fragment size was a suitable and easy read-out for cultures from HBCx39, but not MAS98.12/MAS98.12PR. For cultures from MAS98.12/MAS98.12PR, estimation of the proportion of live cells based on imaging was a suitable approach, allowing to capture the cytotoxic influence of the drug. Since this method estimates the ratio between two signals (live and dead) and not a total signal in a well (like e.g. CTG), it is not obstructed by the different amount/size of the fragments in individual wells. The latter has been difficult to avoid due to heterogeneity of the dissociated tissue, which affected the CTG measurements, where we noted big variations between parallels. Furthermore, the CTG assay gives no possibility to discriminate the fragment-signal from the signal of the “contaminating” normal cells, which was possible by the imaging-based approaches. Despite those limitations, the CTG assay generally recapitulated the effects registered by other methods, where the mentioned concerns could be controlled. In conclusion, the choice of an optimal read-out method might depend on the cultured tissue characteristics and might require individual adjustment.

Despite those technical challenges, we succeeded in recapitulating paclitaxel-resistance and -sensitivity in the PDXCs from the resistant and the sensitive PDXs, respectively. This has been demonstrated in cultures from both fresh and cryopreserved tissue, and the latter might be advantageous when collecting tissue directly from a patient. The difference in response was not an artifact associated with the tissue, but was drug-dependent i.e. observed for paclitaxel, but not capecitabine, as in the matching PDXs. Furthermore, we recapitulated drug sensitivity

profile of another PDX, HBCx39, where superior responses to capecitabine, compared to paclitaxel or everolimus, were observed also in the PDXCs. Finally, we addressed a common technical challenge of the PDX cultures i.e. contamination with normal host cells, which could be reduced by the treatment with the MDM2 inhibitor Nutlin-3. This, however, is a suitable approach only for tumors with lost/mutated *TP53* (25), which is commonly observed among TNBC. For tumors with wild-type *TP53*, alternative approaches are needed, and one of such is separation based on physical parameters, like size. We have employed size-based filtering combined with low-speed centrifugation and thereby facilitated separation of tumor fragments from contaminating normal single cells.

Taken together, the presented data demonstrates the feasibility of employing tissue explants to “capture” drug sensitivity of individual tumors, which supports the predictive potential of the *ex vivo* platform. The established protocols will facilitate setting up an analogous platform for BC patient biopsies with the aim to facilitate functional precision medicine. It would be highly useful to determine *ex vivo* the sensitivity to e.g. salvage therapy as recommended for TNBC and HER2⁺ patients that have shown less-than-optimal response to neo-adjuvant chemotherapy (24, 26).

Data availability statement

The raw data supporting the conclusions of this article will be made available by the authors, without undue reservation.

Ethics statement

The animal study was reviewed and approved by the Norwegian Food Safety Authority (FOTS id 15499).

Author contributions

SP performed all *ex vivo* experiments and immunostaining, data analysis and interpretation, and contributed to making the respective figures and writing the manuscript; GØ performed all *in vivo* work and PCR analysis; EE performed gene expression profiling of the PDXs and contributed to the revision of the manuscript; SJ contributed to establishment of tissue dissociation conditions; OE and GM participated in study design, result interpretation, drawing the conclusions, and contributed to writing the manuscript; LP designed the study, contributed to the data analysis, result interpretation, preparation of the figures, and wrote the manuscript. All authors critically evaluated the results and reviewed the manuscript. All authors contributed to the article and approved the submitted version.

Funding

This work was supported by the Norwegian Cancer Society (grant # 190257), South-Eastern Norway Health Authority (grant # 2022069) and the European Union's Horizon 2020 Research and Innovation Program (grant # 847912).

Acknowledgments

We thank Dr. Alexander Kristian (Oslo University Hospital) for contribution establishing the MAS98.12PR PDX and Dr. Elisabetta Marangoni (The Institute Curie, Paris, France) for providing HBCx39 PDX. We are grateful to Prof. Juha Klefström and Dr. Pauliina Munne (University of Helsinki, Finland) for sharing their experiences on PDE cultures, and Dr. Mads H. Haugen (Oslo University Hospital) for fruitful discussions on the project. We also thank Dr. Nirma Skrbø (Oslo University Hospital) and the Genomics Core Facility (Oslo University Hospital) for assistance in analysis of gene expression in the PDX. The Core Facility for Advanced Light Microscopy at Oslo University Hospital is acknowledged for providing access to confocal microscope.

References

- Byrne AT, Alferez DG, Amant F, Annibaldi D, Arribas J, Biankin A, et al. Interrogating open issues in cancer precision medicine with patient-derived xenografts. *Nat Rev Cancer* (2017) 17:254. doi: 10.1038/nrc.2016.140
- Whittle JR, Lewis MT, Lindeman GJ, Visvader JE. Patient-derived xenograft models of breast cancer and their predictive power. *Breast Cancer Res* (2015) 17:17. doi: 10.1186/s13058-015-0523-1
- Driehuis E, Kretschmar K, Clevers H. Establishment of patient-derived cancer organoids for drug-screening applications. *Nat Protoc* (2020) 15:3380. doi: 10.1038/s41596-020-0379-4
- Powley IR, Patel M, Miles G, Pringle H, Howells L, Thomas A, et al. Patient-derived explants (PDEs) as a powerful preclinical platform for anti-cancer drug and biomarker discovery. *Br J Cancer* (2020) 122:735. doi: 10.1038/s41416-019-0672-6
- Clevers H. Modeling development and disease with organoids. *Cell* (2016) 165:1586. doi: 10.1016/j.cell.2016.05.082
- Tuveson D, Clevers H. Cancer modeling meets human organoid technology. *Science* (2019) 364:952. doi: 10.1126/science.aaw6985
- van de Wetering M, Francies HE, Francis JM, Bounova G, Iorio F, Pronk A, et al. Prospective derivation of a living organoid biobank of colorectal cancer patients. *Cell* (2015) 161:933. doi: 10.1016/j.cell.2015.03.053
- Boj SF, Hwang CI, Baker LA, Chio II, Engle DD, Corbo V, et al. Organoid models of human and mouse ductal pancreatic cancer. *Cell* (2015) 160:324. doi: 10.1016/j.cell.2014.12.021
- Gao D, Vela I, Sboner A, Jaquinta PJ, Karthaus WR, Gopalan A, et al. Organoid cultures derived from patients with advanced prostate cancer. *Cell* (2014) 159:176. doi: 10.1016/j.cell.2014.08.016
- Guillen KP, Fujita M, Butterfield AJ, Scherer SD, Bailey MH, Chu Z, et al. A human breast cancer-derived xenograft and organoid platform for drug discovery and precision oncology. *Nat Cancer* (2022) 3:232. doi: 10.1038/s43018-022-00337-6
- Dekkers JF, van Vliet EJ, Sachs N, Rosenbluth JM, Kopper O, Rebel HG, et al. Long-term culture, genetic manipulation and xenotransplantation of human normal and breast cancer organoids. *Nat Protoc* (2021) 16:1936. doi: 10.1038/s41596-020-00474-1
- Sachs N, de Ligti J, Kopper O, Gogola E, Bounova G, Weeber F, et al. A living biobank of breast cancer organoids captures disease heterogeneity. *Cell* (2018) 172:373. doi: 10.1016/j.cell.2017.11.010
- Bruna A, Rueda OM, Greenwood W, Batra AS, Callari M, Batra RN, et al. A biobank of breast cancer explants with preserved intra-tumor heterogeneity to screen anticancer compounds. *Cell* (2016) 167:260. doi: 10.1016/j.cell.2016.08.041
- Templeton AR, Jeffery PL, Thomas PB, Perera MPJ, Ng G, Calabrese AR, et al. Patient-derived explants as a precision medicine patient-proximal testing platform informing cancer management. *Front Oncol* (2021) 11:76797. doi: 10.3389/fonc.2021.76797

Conflict of interest

The authors declare that the research was conducted in the absence of any commercial or financial relationships that could be construed as a potential conflict of interest.

Publisher's note

All claims expressed in this article are solely those of the authors and do not necessarily represent those of their affiliated organizations, or those of the publisher, the editors and the reviewers. Any product that may be evaluated in this article, or claim that may be made by its manufacturer, is not guaranteed or endorsed by the publisher.

Supplementary material

The Supplementary Material for this article can be found online at: <https://www.frontiersin.org/articles/10.3389/fonc.2023.1040665/full#supplementary-material>

- Majumder B, Baraneedharan U, Thiyagarajan S, Radhakrishnan P, Narasimhan H, Dhandapani M, et al. Predicting clinical response to anticancer drugs using an ex vivo platform that captures tumour heterogeneity. *Nat Commun* (2015) 6:6169. doi: 10.1038/ncomms7169
- Haikala HM, Anttila JM, Marques E, Raatikainen T, Ilander M, Hakanen H, et al. Pharmacological reactivation of MYC-dependent apoptosis induces susceptibility to anti-PD-1 immunotherapy. *Nat Commun* (2019) 10:620. doi: 10.1038/s41467-019-08541-2
- Duarte AA, Gogola E, Sachs N, Barazas M, Annunziato S, de Ruiter JR, et al. BRCA-deficient mouse mammary tumor organoids to study cancer-drug resistance. *Nat Methods* (2018) 15:134. doi: 10.1038/nmeth.4535
- Bergamaschi A, Hjortland GO, Triulzi T, Sorlie T, Johnsen H, Ree AH, et al. Molecular profiling and characterization of luminal-like and basal-like *in vivo* breast cancer xenograft models. *Mol Oncol* (2009) 3:469. doi: 10.1016/j.molonc.2009.07.003
- Marangoni E, Laurent C, Coussy F, El-Botty R, Château-Joubert S, Servely JL, et al. Capecitabine efficacy is correlated with TYMP and RB1 expression in PDX established from triple-negative breast cancers. *Clin Cancer Res* (2018) 24:2605. doi: 10.1158/1078-0432.CCR-17-3490
- Marangoni E, Vincent-Salomon A, Auger N, Degeorges A, Assayag F, de Cremoux P, et al. A new model of patient tumor-derived breast cancer xenografts for preclinical assays. *Clin Cancer Res* (2007) 13:3989. doi: 10.1158/1078-0432.CCR-07-0078
- Schneider CA, Rasband WS, Eliceiri KW. NIH Image to ImageJ: 25 years of image analysis. *Nat Methods* (2012) 9:671. doi: 10.1038/nmeth.2089
- Alcoser SY, Kimmel DJ, Borgel SD, Carter JP, Dougherty KM, Hollingshead MG, et al. Real-time PCR-based assay to quantify the relative amount of human and mouse tissue present in tumor xenografts. *BMC Biotechnol* (2011) 11:124. doi: 10.1186/1472-6750-11-124
- Gottesman MM, Fojo T, Bates SE. Multidrug resistance in cancer: role of ATP-dependent transporters. *Nat Rev Cancer* (2002) 2:48. doi: 10.1038/nrc706
- Masuda N, Lee SJ, Ohtani S, Im YH, Lee ES, Yokota I, et al. Adjuvant capecitabine for breast cancer after preoperative chemotherapy. *N Engl J Med* (2017) 376:2147. doi: 10.1056/NEJMoa1612645
- Saito Y, Muramatsu T, Kanai Y, Ojima H, Sukeda A, Hiraoka N, et al. Establishment of patient-derived organoids and drug screening for biliary tract carcinoma. *Cell Rep* (2019) 27:1265. doi: 10.1016/j.celrep.2019.03.088
- von Minckwitz G, Huang CS, Mano MS, Loibl S, Mamounas EP, Untch M, et al. Trastuzumab emtansine for residual invasive HER2-positive breast cancer. *N Engl J Med* (2019) 380:617. doi: 10.1056/NEJMoa1814017



OPEN ACCESS

EDITED BY

Gianluca Franceschini,
Agostino Gemelli University Polyclinic
(IRCCS), Italy

REVIEWED BY

Zaixiang Tang,
Soochow University Medical College, China
Fenglin Dong,
The First Affiliated Hospital of Soochow
University, China
Zhenyu Shu,
Zhejiang Provincial People's Hospital, China

*CORRESPONDENCE

Yong Gao
✉ 21412066@qq.com

SPECIALTY SECTION

This article was submitted to
Breast Cancer,
a section of the journal
Frontiers in Oncology

RECEIVED 05 November 2022

ACCEPTED 17 February 2023

PUBLISHED 07 March 2023

CITATION

Huang Q, Nong W, Tang X and Gao Y
(2023) An ultrasound-based radiomics
model to distinguish between sclerosing
adenosis and invasive ductal carcinoma.
Front. Oncol. 13:1090617.
doi: 10.3389/fonc.2023.1090617

COPYRIGHT

© 2023 Huang, Nong, Tang and Gao. This is
an open-access article distributed under the
terms of the [Creative Commons Attribution
License \(CC BY\)](#). The use, distribution or
reproduction in other forums is permitted,
provided the original author(s) and the
copyright owner(s) are credited and that
the original publication in this journal is
cited, in accordance with accepted
academic practice. No use, distribution or
reproduction is permitted which does not
comply with these terms.

An ultrasound-based radiomics model to distinguish between sclerosing adenosis and invasive ductal carcinoma

Qun Huang, Wanxian Nong, Xiaozhen Tang and Yong Gao*

Department of Ultrasound, First Affiliated Hospital of Guangxi Medical University, Nanning, Guangxi, China

Objectives: We aimed to develop an ultrasound-based radiomics model to distinguish between sclerosing adenosis (SA) and invasive ductal carcinoma (IDC) to avoid misdiagnosis and unnecessary biopsies.

Methods: From January 2020 to March 2022, 345 cases of SA or IDC that were pathologically confirmed were included in the study. All participants underwent pre-surgical ultrasound (US), from which clinical information and ultrasound images were collected. The patients from the study population were randomly divided into a training cohort ($n = 208$) and a validation cohort ($n = 137$). The US images were imported into MaZda software (Version 4.2.6.0) to delineate the region of interest (ROI) and extract features. Intragroup correlation coefficient (ICC) was used to evaluate the consistency of the extracted features. The least absolute shrinkage and selection operator (LASSO) logistic regression and cross-validation were performed to obtain the radiomics score of the features. Based on univariate and multivariate logistic regression analyses, a model was developed. 56 cases from April 2022 to December 2022 were included for independent validation of the model. The diagnostic performance of the model and the radiomics scores were evaluated by performing the receiver operating characteristic (ROC) analysis. The calibration curve and decision curve analysis (DCA) were used for calibration and evaluation. Leave-One-Out Cross-Validation (LOOCV) was used for the stability of the model.

Results: Three predictors were selected to develop the model, including radiomics score, palpable mass and BI-RADS. In the training cohort, validation cohort and independent validation cohort, AUC of the model and radiomics score were 0.978 and 0.907, 0.946 and 0.886, 0.951 and 0.779, respectively. The model showed a statistically significant difference compared with the radiomics score ($p < 0.05$). The Kappa value of the model was 0.79 based on LOOCV. The Brier score, calibration curve, and DCA showed the model had a good calibration and clinical usefulness.

Conclusions: The model based on radiomics, ultrasonic features, and clinical manifestations can be used to distinguish SA from IDC, which showed good stability and diagnostic performance. The model can be considered a potential candidate diagnostic tool for breast lesions and can contribute to effective clinical diagnosis.

KEYWORDS

sclerosing adenosis, invasive ductal carcinoma, ultrasound, radiomics, model

Introduction

Sclerosing adenosis (SA) is a common benign lesion that may mimic breast malignancy clinically, radiologically, and pathologically (1–4). SA is usually asymptomatic or palpated with a mass, which is unexpectedly found in premenopausal women who have been examined using imaging or histopathology for other reasons (2). SA is often radiologically evaluated as a malignancy. Pathologically, SA is a complex proliferative change consisting of enlarged and twisted nodules and containing repeated and crowded acini accompanied by significant myoepithelial and interstitial fibrosis (5). SA often imitates malignancy, leading to misdiagnosis and excessive biopsies, which have a negative influence on women's physical and mental health. As the most common breast cancer, IDC may coexist with SA, making it difficult to distinguish between them (6). However, surgical resection is the main treatment for IDC due to its invasiveness and metastasis, whereas follow-up procedures are performed for SA (7).

The conventional breast ultrasound (US) plays a key role in screening, diagnostic imaging, and interventional breast surgery for breast lesions. For patients, US is relatively quicker, more comfortable, less expensive, and radiation-free. The American College of Radiology Breast Imaging Report and Data System (ACR BI-RADS) has developed a standardized vocabulary to describe the findings of US examinations, and has established a system to classify these findings and the probability of malignant tumors (8, 9). However, US and BI-RADS both depend on the subjective observations of radiologists. Therefore, exploring the use of a non-invasive and objective method to differentiate between benign and malignant lesions is crucial.

Texture analysis technology extracts texture feature parameters by certain image processing systems, which can objectively and quantitatively provide information about the lesions that cannot be identified by the naked eye (10, 11). MaZda is a software package used for 2D and 3D image texture analyses, and it provides a complete path for the quantitative analysis of image textures. It is effective in its use for various imaging analyses, including X-rays, US, and magnetic resonance imaging. It has been proven to be an efficient and reliable tool for quantitative image analyses, providing more accurate and objective medical diagnoses (12–15).

A logistic regression model is based on a multivariate regression analysis, integrating multiple predictors and using multiple indicators to diagnose or predict the occurrence or progress of diseases (16, 17). To our knowledge, there is no model based on an ultrasonic texture analysis used to distinguish between SA and IDC. We aimed to develop and validate an ultrasound-based radiomics model to differentiate between SA and IDC, which could be a potential candidate diagnostic tool for breast lesions and could help to avoid misdiagnosis and unnecessary biopsies.

Materials and methods

Study population

This retrospective study was approved by the Research Ethics Committee of the First Affiliated Hospital of Guangxi Medical University. We retrospectively reviewed the medical records of 345 consecutive female patients (345 lesions) in our hospital from January 2020 to March 2022, including 76 cases of SA and 269 cases of IDC. Patients from the study population were randomly divided into a training cohort ($n=208$, mean age: 51.3 ± 12.2 years) and a validation cohort ($n=137$, mean age: 51.5 ± 10.2 years). The consistency between the two cohorts was tested. In addition, patients from our hospital from April 2022 to December 2022, including 26 cases of SA and 30 cases of IDC, were included for independent validation ($n = 56$, mean age: 48.3 ± 13.6 years).

The inclusion criteria were as follows: (1) a breast US was performed before biopsy or surgery; (2) US images were available for qualitative and radiomic analysis; (3) all participants were confirmed as SA or IDC by biopsy or surgical pathology; (4) all patients had not received systemic hormone therapy or neoadjuvant chemotherapy; (5) the clinical information and US images were complete; and (6) only a lesion in the largest or highest BI-RADS category was included for patients with multiple lesions.

The exclusion criteria were as follows: (1) the poor quality of ultrasonic images affected the texture analysis; (2) the pathological result was indefinite; (3) patients had received systemic hormone therapy or neoadjuvant chemotherapy; (4) clinical information and

US images were lacking; and (5) the lesion was too large to delineate the ROI.

The flow chart of the study was shown in Figure 1.

Breast ultrasound technology

All patients underwent a pre-surgical US examination. The patients were in a supine position with their hands raised above their heads to fully expose the breast. Color Doppler ultrasound instruments included GE LOGIQ E9, VOLUSON E9 (General Electric Company, Boston, USA), or HITACHI ARIETTA 70 (HITACHI Ltd., Tokyo, Japan) with a linear array probe and a frequency of 9–12 MHz.

The standard store images of breast lesion included at least two vertical sections, one of which showing the maximum diameter of the lesion. The images with the clearest and most complete demonstration of lesions were chosen. The focus was located slightly below the lesion, and the frequency range was 9–12 MHz. Each lesion was classified into a category (3, 4A, 4B, 4C, or 5) according to the 5th edition of ACR BI-RADS US. According to ACR BI-RADS classification, BI-RADS 4A means that the degree of malignancy is very low, and the possibility of benign lesions is far greater than that of malignant lesions. According to relevant literature, lesions of BI-RADS 3 or 4A were considered to be negative, and lesions of BI-RADS 4B, 4C or 5 were considered to be malignant in our study (18). The ultrasonic features of the breast lesions were recorded, including maximum size, shape, echo pattern, echo distribution, boundary, orientation, posterior feature, calcification, vascularity distribution, and associated features. All lesions were examined and evaluated by two ultrasound doctors with more than five years of experience with breast US. In the case of a disagreement, a final consensus was reached through a discussion.

The maximum size was the largest diameter of the tumor. The shape was defined as regular or irregular. The echo pattern was divided into hypoechoic, or complex echo. The echo distribution

was divided into uniform or non-uniform types. The boundary was interpreted as well-circumscribed or obscure. The orientation was depicted as whether or not the breast lesion was parallel to the chest wall. The posterior acoustic features were classified as attenuated or not. The vascularity distribution was recorded as absent or internal (1). Associated features included duct ectasia, and palpable mass.

Pathological findings

The histopathological results of all lesions were obtained from the surgical resection report. Each specimen was placed in a formalin solution, and then histopathological treatment was carried out using the standard procedures. The final pathological results were evaluated by experienced pathologists.

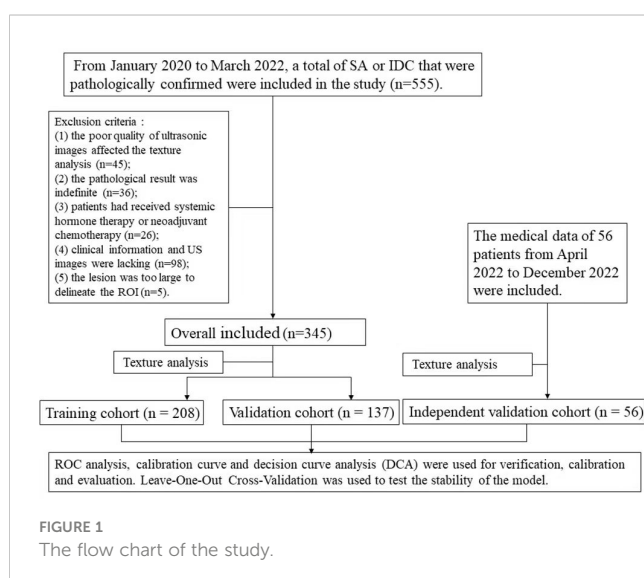
Radiomic analysis

The section of the largest diameter of the lesion was selected to draw ROI by one ultrasound doctor with more than ten years experience of breast US. ROI was set to be 0.1–0.2 cm along the inner edge of the lesion. The ultrasound gray-scale images were imported into MaZda software (Version 4.2.6.0), and the ROI results were then delineated manually (Figure 2). After normalization, a total of 279 descriptors were used to characterize the gray-scale image texture using MaZda software, including nine texture features based on the histogram, 11 features based on the co-occurrence matrix (derived from 20 co-occurrence matrices produced for four directions and five inter-pixel distances), five features based on the run-length matrix (each in four different directions), five features based on a gradient map, five features based on an autoregressive model, and up to 20 features based on the Haar wavelet transform (12).

In order to select the features with good reproducibility and stability to build the model, 30 ultrasound images of breast lesions were randomly selected. The ROI was drawn by another ultrasound doctor with more than ten years experience of breast US and the features were extracted again. Intragroup correlation coefficient (ICC) was used to evaluate the consistency between the ROI extraction features, which was drawn by two ultrasound doctors. The features with ICC greater than or equal to 0.75 were considered to have good reproducibility and stability. The least absolute shrinkage and selection operator (LASSO) logistic regression and cross-validation were performed to select the significant features. The selected features were used to establish the radiomics score.

Development and validation of the model

We conducted univariate and multivariate logistic regression analyses to explore the influencing factors. The candidate factors included clinical information, ultrasonic features, BI-RADS, and the radiomics score. In the training cohort, variables selected by the univariate analysis ($p < 0.05$) were used for the multivariate logistic regression to determine the independent risk factors for the model. On



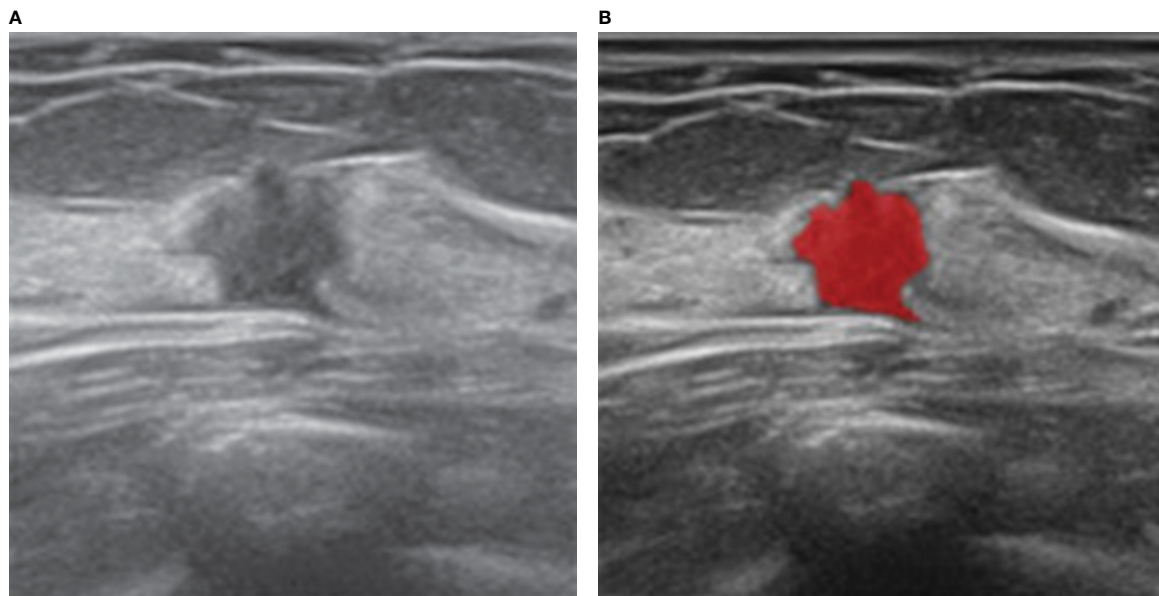


FIGURE 2

Ultrasound and histopathologic findings of a 35-year-old woman with SA. (A) The ultrasound image showed a hypoechoic lesion with irregular shape. The lesion was classified as BI-RADS 4C and considered malignant, which was considered benign by our model. (B) ROI was manually drawn in red by MaZda software along the edge of the lesion.

the basis of the validation cohort, the discrimination, calibration, and clinical usefulness of the model were evaluated. In addition, the logistic score of each patient in the independent validation cohort was calculated using our model. The ROC curves were plotted to assess the diagnostic performance of the model (19). The area under the ROC curve (AUC) was used to quantify discrimination. The calibration curve was used to examine the model's predictive accuracy. To determine the clinical usefulness of the model, a decision curve analysis (DCA) was performed (20). Leave-One-Out Cross-Validation (LOOCV) was used to test the stability of the model, which was graded as very good (Kappa value of 0.80 to 1.00), good (Kappa value of 0.60 to 0.80), fair (Kappa value of 0.40 to 0.60), moderate (Kappa value of 0.20 to 0.40) or poor (Kappa value < 0.20).

Statistical analysis

The statistical analysis was conducted using R software (version 4.1.3) and SPSS 26.0 (Chicago, IL). For the categorical variables, the Chi-square test was used, although when necessary, Fisher's exact test was used. The Student's t-test was used to compare the continuous variables with a normal distribution. The reported statistical significance levels were all two-sided, and a P value < 0.05 was considered significant.

The "caret" package of R software was used to randomly split the total data, 60% of which was included in the training cohort and the remaining 40% in the verification cohort. At the same time, the package was also used for cross-validation. The "glmnet" package was used for the LASSO regression. The "glm" function of R

software was used for the logistic regression analysis. The "Cairo" package was used to plot the model. The "pROC" package was used to plot the ROC curves and to measure the AUCs, which were compared using DeLong's test. The "calibrate" function was used for the calibration curves. The "decision_curve" function was used to perform the DCA.

Results

Study population

A total of 401 lesions from 401 female patients (mean age: 50.9 ± 11.8 years, age range: 21–89 years) were recruited, including 102 SA (mean age: 47.1 ± 12.7 years, age range: 21–83 years) and 299 IDC (mean age: 52.2 ± 11.2 years, age range: 23–89 years). There were 208 patients with 208 lesions in the training cohort (mean age: 51.3 ± 12.2 years), 137 patients with 137 lesions in the validation cohort (mean age: 51.5 ± 10.2 years), and 56 patients with 56 lesions in the independent validation cohort (mean age: 48.3 ± 13.6 years).

Clinical and ultrasonic characteristics

The clinical and ultrasonic characteristics of the training cohort and the verification cohort were shown in Table 1. There were no statistical differences in 14 observation indexes ($p > 0.05$) between the training cohort and the verification cohort, which indicated that the consistency between the two cohorts was good.

Radiomic analysis

Based on the training cohort, we extracted 279 texture features for each ROI. According to the result of reproducibility analysis by

TABLE 1 The clinical and ultrasonic characteristics in the training and validation cohorts.

| | Training cohort (n=208) | Validation cohort (n=137) | P- value |
|--------------------------|----------------------------|------------------------------|-------------|
| Age (years) | 51.3 ± 12.2 | 51.5 ± 10.2 | 0.863 |
| Pathology | | | 0.962 |
| SA | 46 (22.1%) | 30 (21.9%) | |
| IDC | 162 (77.9%) | 107 (78.1%) | |
| BI-RADS | | | 0.509 |
| 3-4A | 44 (21.2%) | 25 (18.2%) | |
| 4B-5 | 164 (78.8%) | 112 (81.8%) | |
| Tumor Size (cm) | 2.3 ± 1.3 | 2.3 ± 1.1 | 0.867 |
| Duct Ectasia | | | 0.981 |
| None | 199 (95.7%) | 131 (95.6%) | |
| Ectasia | 9 (4.3%) | 6 (4.4%) | |
| Palpable Mass | | | 0.217 |
| None | 36 (17.3%) | 17 (12.4%) | |
| Palpable | 172 (82.7%) | 120 (87.6%) | |
| Echo Pattern | | | 1.000 |
| Hypoechoic | 202 (97.1%) | 133 (97.1%) | |
| Complex Echo | 6 (2.9%) | 4 (2.9%) | |
| Echo Distribution | | | 0.053 |
| Uniform | 21 (10.1%) | 6 (4.4%) | |
| Non-Uniform | 187 (89.9%) | 131 (95.6%) | |
| Boundary | | | 0.630 |
| Well- | 92 (44.2%) | 57 (41.6%) | |
| Circumscribed | 116 (55.8%) | 80 (58.4%) | |
| Obscure | | | |
| Shape | | | 0.455 |
| Regular | 20 (9.6%) | 10 (7.3%) | |
| Irregular | 188 (90.4%) | 127 (92.7%) | |
| Orientation | | | 0.478 |
| Parallel | 170 (81.7%) | 116 (84.7%) | |
| Not Parallel | 38 (18.3%) | 21 (15.3%) | |
| Posterior Feature | | | 0.993 |
| None | 173 (83.2%) | 114 (83.2%) | |
| Attenuation | 35 (16.8%) | 23 (16.8%) | |
| Calcification | | | 0.828 |
| None | 89 (42.8%) | 57 (41.6%) | |
| Calcification | 119 (57.2%) | 80 (58.4%) | |
| Vascularity Distribution | | | 0.994 |
| Absent | 76 (36.5%) | 50 (36.5%) | |
| Internal | 132 (63.5%) | 87(63.5%) | |

two ultrasound doctors, 250 radiomic features had good consistency (ICC ≥ 0.75). Through the LASSO regression (Figure 3), the following six optimal variables were selected: Skewness, Horzl_RLNonUni, Horzl_GLevNonU, WavEnLL_s.3, WavEnLH_s.3, and WavEnLH_s.4. Based on these six features, the radiomics score was calculated using the following formula:

$$\begin{aligned} \text{Radiomics score} = & -3.675163 - \text{Skewness} \times 2.24776 \times 10^{-1} \\ & - \text{Horzl_RLNonUni} \times 9.498166 \times 10^{-6} \\ & - \text{Horzl_GLevNonU} \times 3.05807 \times 10^{-4} \\ & + \text{WavEnLL_s.3} \times 6.213542 \times 10^{-5} \\ & + \text{WavEnLH_s.3} \times 6.650157 \times 10^{-3} \\ & + \text{WavEnLH_s.4} \times 1.14583 \times 10^{-3} \end{aligned}$$

Development and validation of the model

In the training cohort, a univariate analysis was performed on 14 observation indexes (Table 2). A multivariate logistic regression was used to analyze the selected variables ($p < 0.05$) to determine the independent risk factors for the model (Table 2). Based on radiomics score, BI-RADS and palpable mass as independent risk variables ($p < 0.05$), the logistic regression model was established by the following function (Table 3):

$$\begin{aligned} \text{Logit}(P) = & -5.880236 + 3.996762X_1 + 3.130755X_2 \\ & - 1.603437X_3 \end{aligned}$$

The nomogram was developed based on the logistic regression model (Figure 4) (21, 22).

The diagnostic performances of the model and the radiomics scores were verified by the ROC analysis (Figure 5). The AUC was used to quantify discrimination. In the training cohort, the AUC of the model and the radiomics score were 0.978 (95% confidence interval [CI: 0.960-0.997]) and 0.907 (95% confidence interval [CI:

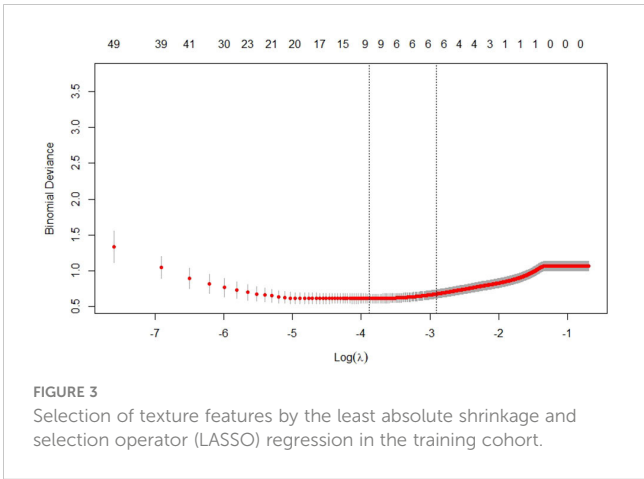


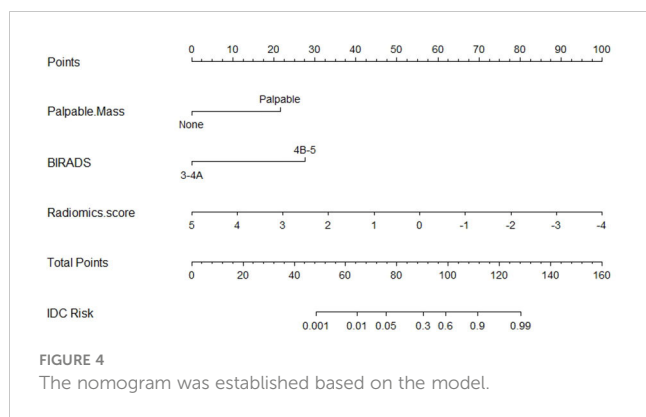
TABLE 2 Results of the univariate and multivariate logistic regression analysis in the training cohort.

| | Univariate logistic regression analysis | | Multivariate logistic regression analysis | |
|-------------------------------|--|---------|--|---------|
| | OR (95% CI) | P-value | OR (95% CI) | P-value |
| Age | 0.97 (0.87-1.07) | 0.559 | | |
| BI-RADS | | | | |
| 3-4A 4B-5 | Ref. 79.78 (4.81-3889.12) | 0.007 | Ref. 54.42 (12.98-308.27) | <0.001 |
| Tumor Size (cm) | 2.87 (0.86-11.72) | 0.100 | | |
| Duct Ectasia | | | | |
| None Ectasia | Ref. 0.02 (0.00-1.19) | 0.055 | | |
| Palpable Mass | | | | |
| None Palpable | Ref. 68.03 (5.04-2661.21) | 0.006 | Ref. 22.89 (4.33-144.54) | <0.001 |
| Echo Pattern | | | | |
| Hypoechoic Complex Echo | Ref. 0.06 (0.00-36.89) | 0.539 | | |
| Echo Distribution | | | | |
| Uniform Non-Uniform | Ref. 13.98 (0.72-659.76) | 0.112 | | |
| Boundary | | | | |
| Well-Circumscribed Obscure | Ref. 7.85 (0.77-154.81) | 0.109 | | |
| Shape | | | | |
| Regular Irregular | Ref. 5.83 (0.18-215.56) | 0.316 | | |
| Orientation | | | | |
| Parallel Not Parallel | Ref. 0.67 (0.02-32.58) | 0.819 | | |
| Posterior Feature | | | | |
| None Attenuation | Ref. 0.48 (0.02-15.15) | 0.642 | | |
| Calcification | | | | |
| None Calcification | Ref. 0.14 (0.00-2.01) | 0.184 | | |
| Vascularity Distribution | | | | |
| Absent Internal | Ref. 8.28 (0.84-146.54) | 0.088 | | |
| Radiomics Score | 0.13 (0.02-0.54) | 0.019 | 0.20 (0.07-0.46) | 0.001 |

TABLE 3 Variable assignment table in the logistic regression model.

| Variable | Code | Variable assignment |
|-----------------|----------------|---------------------|
| BI-RADS | X ₁ | 3-4A=0, 4B-5 = 1 |
| Palpable Mass | X ₂ | None=0, Palpable=1 |
| Radiomics Score | X ₃ | Score |

0.854-0.960)), respectively. In the validation cohort, the AUC of the model and the radiomics score were 0.946 (95% confidence interval [CI: 0.903-0.990]) and 0.886 (95% confidence interval [CI: 0.821-0.951]), respectively. In the total dataset, the AUC of the model and the radiomics score were 0.965 (95% confidence interval [CI: 0.943-0.986]) and 0.899 (95% confidence interval [CI: 0.858-0.939]), respectively. In the independent validation cohort, the AUCs of



the model and the radiomics score were 0.951 (95% confidence interval [CI: 0.891-1]) and 0.779 (95% confidence interval [CI: 0.650-0.909]), respectively. (Table 4) According to DeLong's test, there were statistically significant differences ($p < 0.05$) between the model and radiomics scores.

The specificity, sensitivity, accuracy, Youden index, negative predictive value, positive predictive value, false positive rate, true positive rate, true negative rate and false negative rate of the model and the radiomics score in the training cohort, the validation cohort, the total dataset and in the independent validation cohort were shown in Table 5, respectively. The Brier score of 0.066 suggested a

high accuracy of the model. The calibration curve demonstrated good agreement between the prediction and the pathological results (Figure 6). The DCA was plotted for the model (Figure 7). It demonstrated that if the threshold probability is more than 5%, using the model to predict SA and IDC will be more beneficial than either the treat-all-patients scheme (assuming all lesions are IDC) or the treat-none scheme (assuming all lesions are SA). Based on Leave-One-Out Cross-Validation, the Kappa value of this model was 0.79, which proved that the model had good stability.

According to the model, the lower the radiomics score, the higher the BI-RADS classification, the more palpable the mass, and the greater the possibility of IDC.

Discussion

We developed and validated an ultrasound-based radiomics model, which included the radiomics score, BI-RADS and palpable mass, to distinguish between SA and IDC. Although the radiomics score we created was proved to have a high AUC value, the model showed a better diagnostic efficacy and clinical utility than the radiomics score alone, which indicates the superiority of the model in disease identification.

SA is an IDC-mimicking benign proliferative breast lesion, which is usually asymptomatic or only palpated with a mass. In previous

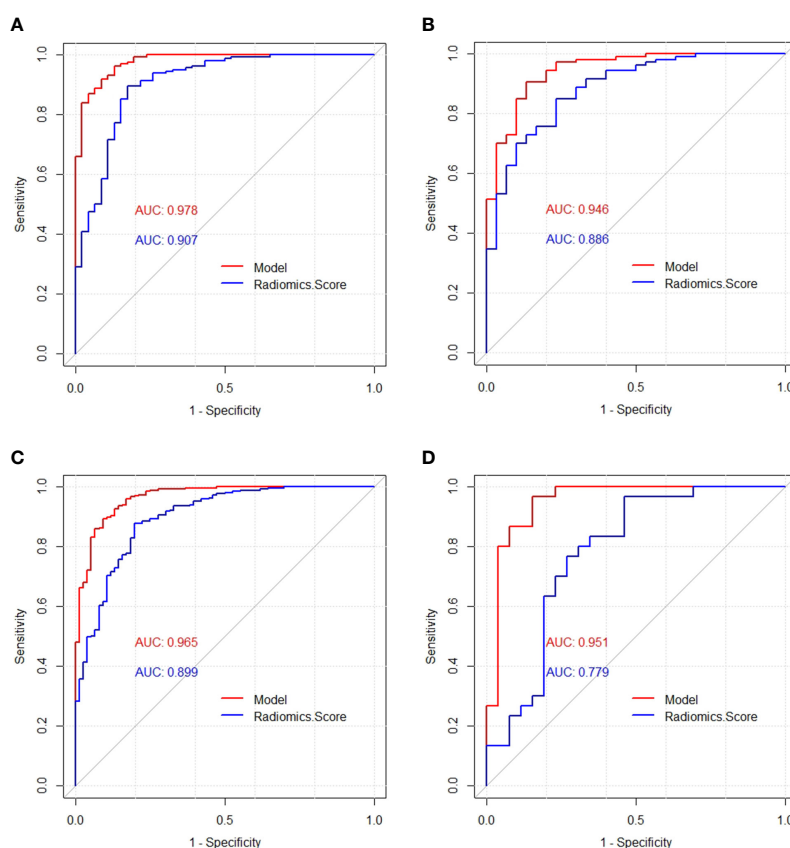


TABLE 4 AUCs of the radiomics score and model.

| | Training cohort (n=208) | P- value | Validation cohort (n=137) | P- value | Total dataset (n=345) | P- value | Independent validation cohort (n=56) | P- value |
|---------------------------------|----------------------------|-------------|------------------------------|-------------|--------------------------|-------------|---|-------------|
| | AUC (95% CI) | | AUC (95% CI) | | AUC (95% CI) | | AUC (95% CI) | |
| Model | 0.978 (0.960-0.997) | | 0.946 (0.903-0.990) | | 0.965 (0.943-0.986) | | 0.951 (0.891-1) | |
| Radiomics score | 0.907 (0.854-0.960) | | 0.886 (0.821-0.951) | | 0.899 (0.858-0.939) | | 0.779 (0.650-0.909) | |
| Model vs. Radiomics score | | 0.005 | | 0.025 | | <0.001 | | 0.002 |

studies, it has been confirmed that SA can imitate IDC clinically, radiologically, and pathologically, so it is necessary to distinguish between SA and IDC (1–5, 7). As a convenient, affordable, and radiation-free imaging examination, the US is a most widely used breast screening technique. Liu et al. found that US BI-RADS atlas and elastography are powerful tools in diagnosing SA (1). Shao et al. asserted that an enhanced US could improve the diagnostic accuracy of SA (23). However, these researchers used a subjective analysis or expensive inspections. The texture analysis is a new computer-aided technology used for quantitative analyses of image information through algorithms, which can prevent the subjectivity of ultrasonic examinations and BI-RADS classifications (10, 11). To our knowledge, no research has focused on ultrasonic omics to distinguish between SA and IDC using a texture analysis.

We selected six radiomic features based on a regression analysis, including one histogram parameter (Skewness), two grey level run-length matrix (RLM) parameters (Horzl_RLNonUni and Horzl_GLevNonU), and three Haar wavelet transform parameters (WavEnLL_s.3, WavEnLH_s.3, and WavEnLH_s.4). The texture analysis was normalized by MaZda software. According to the coefficients, Skewness, Horzl_RLNonUni, and Horzl_GLevNonU were negatively correlated with the radiomics score. That is, the larger the Skewness, Horzl_RLNonUni, and Horzl_GLevNonU, the

lower the radiomics score and the higher the probability of IDC. In addition, the three Haar wavelet transform parameters were all positively correlated with the radiomics score, which indicates that when these three parameters are larger, the radiomics score is higher and the probability of IDC is lower. Furthermore, skewness seemed to contribute most to the radiomics score.

The histogram is computed based on the intensity of the pixels without considering any spatial relations between the pixels within the image (12). As one characteristic variable of a histogram, a high skewness means an asymmetrical distribution with a long right tail. A tumor with a high skewness of signal intensity is mainly composed of fibrosis or stroma. In this study, skewness was positively correlated with the malignant degree of the tumor, which may be related to the high gray intensity of the image caused by hyperplasia, fibrosis, calcification, and tumor cell accumulation in the IDC glands. Previous studies have shown that a high mammographic density independently predicts the risk of breast cancer and that a high skewness of a tumor might be related to poor survival (24–26). Our observations were consistent with these previous reports. On a gray-level image, the RLM quantifies the coarseness of a texture in a specific direction. When runs are equally distributed throughout the gray levels, the function of gray-level non-uniformity reaches its lowest values. If the runs are equally distributed throughout the lengths, the

TABLE 5 The evaluation index of the radiomics score and model.

| | Training cohort (n=208) | | Validation cohort (n=137) | | Total dataset (n=345) | | Independent validation cohort (n=56) | |
|--------------|-------------------------|-----------------|---------------------------|-----------------|-----------------------|-----------------|--------------------------------------|-----------------|
| | Model | Radiomics score | Model | Radiomics score | Model | Radiomics score | Model | Radiomics score |
| specificity | 0.913 | 0.826 | 0.867 | 0.767 | 0.908 | 0.803 | 0.846 | 0.538 |
| sensitivity | 0.920 | 0.895 | 0.907 | 0.850 | 0.892 | 0.877 | 0.967 | 0.967 |
| accuracy | 0.918 | 0.880 | 0.898 | 0.832 | 0.896 | 0.861 | 0.911 | 0.768 |
| Youden index | 0.833 | 0.721 | 0.774 | 0.617 | 0.800 | 0.680 | 0.813 | 0.505 |
| npv | 0.764 | 0.691 | 0.722 | 0.590 | 0.704 | 0.649 | 0.957 | 0.933 |
| ppv | 0.974 | 0.948 | 0.960 | 0.929 | 0.972 | 0.940 | 0.879 | 0.707 |
| fpr | 0.087 | 0.174 | 0.133 | 0.233 | 0.092 | 0.197 | 0.154 | 0.462 |
| tpr | 0.920 | 0.895 | 0.907 | 0.850 | 0.892 | 0.877 | 0.967 | 0.967 |
| tnr | 0.913 | 0.826 | 0.867 | 0.767 | 0.908 | 0.803 | 0.846 | 0.538 |
| fnr | 0.080 | 0.105 | 0.093 | 0.150 | 0.108 | 0.123 | 0.033 | 0.033 |

(npv,negative predictive value; ppv,positive predictive value; fpr,false positive rate; tpr,true positive rate; tnr,true negative rate; fnr,false negative rate).

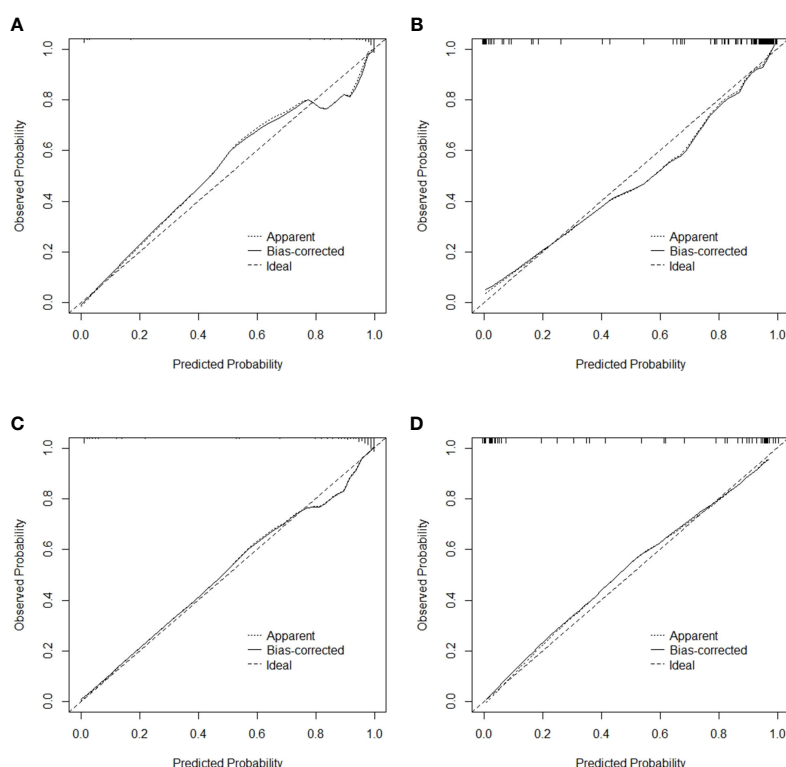


FIGURE 6

Calibration curve for the model in the training cohort (A), validation cohort (B), total dataset (C) and independent validation cohort (D), respectively.

function of run length non-uniformity has a low value (27). In our study, *HorzL_RLNonUni* and *HorzL_GLevNonU* were negatively correlated with the radiomics score, which meant that the gray levels and the lengths of IDC were nonuniform. This is consistent with our observation of the IDC ultrasonic features. The wavelet transform provides time/space and frequency (or scale) resolution information of the signal/image and the details of the image at different frequencies, which reflects the detailed features of the image. When the image is clearer or the frequency is richer, the parameter value is higher. The Haar wavelet has mainly been used for the feature extraction of breast cancer diagnoses in many studies (28). In this study, the selected three Haar wavelet transform parameters were all positively correlated with the radiomics score, which meant that the IDC texture images were

blurred. This may be due to the heterogeneity of IDC cells and the proliferation of tumor blood vessels, which are prone to necrosis and make the tumor image blurry.

Despite the promising performance of the radiomics score, the model of our study, which combined ultrasonic characteristics, BI-RADS, clinical information, and radiomic features, had the advantages of being affordable and objective, suggesting that it is beneficial to combine a texture analysis with ultrasonic features and clinical manifestations in future medical work. Based on the univariate logistic regression, each index was gradually fitted, and three characteristics were screened out as indicators to distinguish between SA and IDC. Soo-Yeon Kim et al. proposed that BI-RADS 4B or 5 was independently related to malignant tumors, and had a high upgrade rate (29). Based on our findings, BI-RADS 3 or 4A suggests that SA is possible, and a higher classification tends to be malignant. A palpable mass with a lower radiomics score further suggests IDC. The results were basically consistent with previous research conclusions (1, 29, 30). In addition, based on the multivariate logistic regression analysis, the influence of confounding factors was eliminated, and the final three variables were obtained, including the radiomics score, BI-RADS and palpable mass, which were used as independent influence factors and were selected to develop the model.

There are some limitations of the current study that need to be further investigated. (1) This study was a retrospective analysis, therefore it was difficult to completely overcome the operator dependency of the initial examination, making a bias error inevitable. (2) This study was a single-center research study, so the

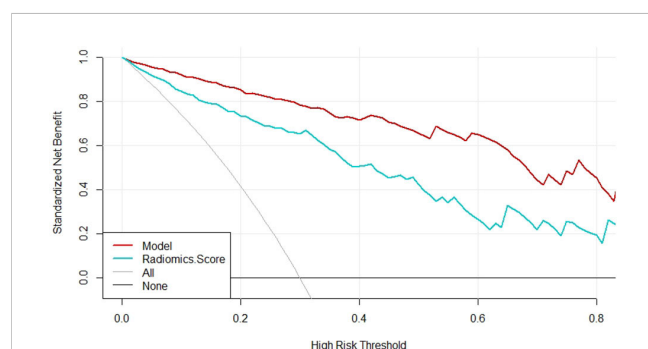


FIGURE 7

Decision curve analysis for the model and radiomics score.

number of SA and IDC cases was limited. The performance of this model needs to be verified by other centers and a larger cohort in the future. (3) We only included patients with SA and IDC, though the differences in the texture features for the pathological subtypes of breast cancer and adenosis can be analyzed in the future.

Conclusion

The model in our study based on radiomics, ultrasonic features, and clinical manifestations can be used to distinguish SA from IDC, which showed good stability and diagnostic performance. The model can be considered a potential candidate diagnostic tool for breast lesions and can contribute to effective clinical diagnosis and treatment.

Data availability statement

The original contributions presented in the study are included in the article/Supplementary Material. Further inquiries can be directed to the corresponding author.

Ethics statement

The study was conducted in accordance with the principles of the Declaration of Helsinki, and the study protocol was approved by

the First Affiliated Hospital of Guangxi Medical University ethics committee. The study is of the retrospective nature, patient consent for inclusion was waived.

Author contributions

QH wrote the main manuscript text. WN and XT prepared tables and figures. YG was fully responsible for the design of this study and data processing. All authors contributed to the article and approved the submitted version.

Conflict of interest

The authors declare that the research was conducted in the absence of any commercial or financial relationships that could be construed as a potential conflict of interest.

Publisher's note

All claims expressed in this article are solely those of the authors and do not necessarily represent those of their affiliated organizations, or those of the publisher, the editors and the reviewers. Any product that may be evaluated in this article, or claim that may be made by its manufacturer, is not guaranteed or endorsed by the publisher.

References

1. Liu W, Li W, Li Z, Shi L, Zhao P, Guo Z, et al. Ultrasound characteristics of sclerosing adenosis mimicking breast carcinoma. *Breast Cancer Res Tr* (2020) 181:127–34. doi: 10.1007/s10549-020-05609-2
2. Tan H, Zhang H, Lei Z, Fu F, Wang M. Radiological and clinical findings in sclerosing adenosis of the breast. *Medicine* (2019) 98:e17061. doi: 10.1097/MD.00000000000017061
3. Sharma T, Chaurasia JK, Kumar V, Mukhopadhyay S, Joshi D. Cytological diagnosis of sclerosing adenosis of breast: Diagnostic challenges and literature review. *Cytopathology* (2021) 32:827–30. doi: 10.1111/cyt.13041
4. Zhang J, Yu Z, Dong A, Zhu Y. FDG-avid sclerosing adenosis of the breast mimicking malignancy. *Clin Nucl Med* (2022) 47:192–94. doi: 10.1097/RLU.00000000000003849
5. Visscher DW, Nassar A, Degnim AC, Frost MH, Vierkant RA, Frank RD, et al. Sclerosing adenosis and risk of breast cancer. *Breast Cancer Res Tr* (2014) 144:205–12. doi: 10.1007/s10549-014-2862-5
6. Watkins EJ. Overview of breast cancer. *Jaapa-J Am Acad Phys* (2019) 32:13–7. doi: 10.1097/01.JAA.0000580524.95733.3d
7. Yan P, DeMello L, Baird GL, Lourenco AP. Malignancy upgrade rates of radial sclerosing lesions at breast cancer screening. *Radiol Imaging Cancer* (2021) 3:e210036. doi: 10.1148/rycan.2021210036
8. Malherbe K, Tafti D. Breast ultrasound. In: *StatPearls*. Treasure Island (FL: StatPearls Publishing (2022).
9. Magny SJ, Shikhan R, Keppke AL. Breast imaging reporting and data system. In: *StatPearls*. Treasure Island (FL: StatPearls Publishing (2022).
10. Scalco E, Rizzo G. Texture analysis of medical images for radiotherapy applications. *Brit J Radiol* (2017) 90:20160642. doi: 10.1259/bjr.20160642
11. Corrias G, Micheletti G, Barberini L, Suri JS, Saba L. Texture analysis imaging “what a clinical radiologist needs to know”. *Eur J Radiol* (2022) 146:110055. doi: 10.1016/j.ejrad.2021.110055
12. Szczypinski PM, Strzelecki M, Materka A, Klepaczek A. MaZda—a software package for image texture analysis. *Comput Meth Prog Bio* (2009) 94:66–76. doi: 10.1016/j.cmpb.2008.08.005
13. Ge S, Yixing Y, Jia D, Ling Y. Application of mammography-based radiomics signature for preoperative prediction of triple-negative breast cancer. *BMC Med Imaging* (2022) 22:166. doi: 10.1186/s12880-022-00875-6
14. Marino MA, Leithner D, Sung J, Avendano D, Morris EA, Pinker K, et al. Radiomics for tumor characterization in breast cancer patients: A feasibility study comparing contrast-enhanced mammography and magnetic resonance imaging. *Diagnostics* (2020) 10:492. doi: 10.3390/diagnostics10070492
15. Chen Q, Xia J, Zhang J. Identify the triple-negative and non-triple-negative breast cancer by using texture features of medical ultrasonic image: A STROBE-compliant study. *Medicine* (2021) 100:e25878. doi: 10.1097/MD.00000000000025878
16. Wang QQ, Yu SC, Qi X, Hu YH, Zheng WJ, Shi JX, et al. [Overview of logistic regression model analysis and application]. *Zhonghua Yu Fang Yi Xue Za Zhi* (2019) 53:955–60. doi: 10.3760/cma.j.issn.0253-9624.2019.09.018
17. Meurer WJ, Tolles J. Logistic regression diagnostics: Understanding how well a model predicts outcomes. *Jama-J Am Med Assoc* (2017) 317:1068–69. doi: 10.1001/jama.2016.20441
18. Su X, Lin Q, Cui C, Xu W, Wei Z, Fei J, et al. Non-calcified ductal carcinoma *in situ* of the breast: Comparison of diagnostic accuracy of digital breast tomosynthesis, digital mammography, and ultrasonography. *Breast Cancer-Tokyo* (2017) 24:562–70. doi: 10.1007/s12282-016-0739-7
19. Obuchowski NA, Bullen JA. Receiver operating characteristic (ROC) curves: review of methods with applications in diagnostic medicine. *Phys Med Biol* (2018) 63:1T–7T. doi: 10.1088/1361-6560/aab4b1
20. Liang T, Cong S, Yi Z, Liu J, Huang C, Shen J, et al. Ultrasound-based nomogram for distinguishing malignant tumors from nodular sclerosing adenosis in solid breast lesions. *J Ultras Med* (2021) 40:2189–200. doi: 10.1002/jum.15612
21. Balachandran VP, Gonen M, Smith JJ, DeMatteo RP. Nomograms in oncology: more than meets the eye. *Lancet Oncol* (2015) 16:e173–80. doi: 10.1016/S1470-2045(14)71116-7
22. Bandini M, Fossati N, Briganti A. Nomograms in urologic oncology, advantages and disadvantages. *Curr Opin Urol* (2019) 29:42–51. doi: 10.1097/MOU.0000000000000541

23. Shao S, Yao M, Li X, Li C, Chen J, Li G, et al. Conventional and contrast-enhanced ultrasound features in sclerosing adenosis and correlation with pathology. *Clin Hemorheol Micro* (2021) 77:173–81. doi: 10.3233/CH-200943
24. Marta R, Javier L, Margarita P, Rodrigo A, Lupe P, Maria S, et al. Breast density, benign breast disease, and risk of breast cancer over time. *Eur Radiol* (2021) 31:4839–47. doi: 10.1007/s00330-020-07490-5
25. Poussaint TY, Vajapeyam S, Ricci KI, Panigrahy A, Kocak M, Kun LE, et al. Apparent diffusion coefficient histogram metrics correlate with survival in diffuse intrinsic pontine glioma: A report from the pediatric brain tumor consortium. *Neuro-Oncology* (2016) 18:725–34. doi: 10.1093/neuonc/nov256
26. Jin K, Rao S, Sheng R, Zeng M. Skewness of apparent diffusion coefficient (ADC) histogram helps predict the invasive potential of intraductal papillary neoplasms of the bile ducts (IPNBs). *Abdominal Radiol (New York)* (2019) 44:95–103. doi: 10.1007/s00261-018-1716-8
27. Ito K, Kurasawa M, Sugimori T, Muraoka H, Hirahara N, Sawada E, et al. Risk assessment of external apical root resorption associated with orthodontic treatment using computed tomography texture analysis. *Oral Radiol* (2022) 39:75–82. doi: 10.1007/s11282-022-00604-3
28. Vidya KS, Muthu RKM, Acharya RA, Vinod C, Filippo M, Hamido F, et al. Application of wavelet techniques for cancer diagnosis using ultrasound images: A review. *Comput Biol Med* (2016) 69: 97–111. doi: 10.1016/j.compbiomed.2015.12.006
29. Kim SY, Kim EK, Lee HS, Kim MJ, Yoon JH, Koo JS, et al. Asymptomatic benign papilloma without atypia diagnosed at ultrasonography-guided 14-gauge core needle biopsy: Which subgroup can be managed by observation? *Ann Surg Oncol* (2016) 23:1860–66. doi: 10.1245/s10434-016-5144-0
30. Villegas-Carlos F, Andino-Araque V, Valverde-Quintana M, Larios-Cruz KY, Perez-Gonzalez Y, Solano-Perez JJ, et al. Predictive factors of invasion in ductal carcinoma *in situ* diagnosed by core-needle biopsy. *Cir Cir* (2022) 90:41–9. doi: 10.24875/CIRU.21000136



OPEN ACCESS

EDITED BY

Dayanidhi Raman,
University of Toledo, United States

REVIEWED BY

Jiehui Cai,
Second Affiliated Hospital of Shantou
University Medical College, China
Emir Çapkinoğlu,
Acıbadem University, Türkiye

*CORRESPONDENCE

Jianming Ying
✉ jmying@cicams.ac.cn

SPECIALTY SECTION

This article was submitted to
Breast Cancer,
a section of the journal
Frontiers in Oncology

RECEIVED 12 November 2022

ACCEPTED 16 February 2023

PUBLISHED 10 March 2023

CITATION

Lei H, Yuan P, Guo C
and Ying J (2023) Development
and validation of nomograms for
predicting axillary non-SLN
metastases in breast cancer
patients: A retrospective analysis.
Front. Oncol. 13:1096589.
doi: 10.3389/fonc.2023.1096589

COPYRIGHT

© 2023 Lei, Yuan, Guo and Ying. This is an
open-access article distributed under the
terms of the [Creative Commons Attribution
License \(CC BY\)](#). The use, distribution or
reproduction in other forums is permitted,
provided the original author(s) and the
copyright owner(s) are credited and that
the original publication in this journal is
cited, in accordance with accepted
academic practice. No use, distribution or
reproduction is permitted which does not
comply with these terms.

Development and validation of nomograms for predicting axillary non-SLN metastases in breast cancer patients: A retrospective analysis

Huizi Lei, Pei Yuan, Changyuan Guo and Jianming Ying*

National Cancer Center/National Clinical Research Center for Cancer/Cancer Hospital, Chinese Academy of Medical Sciences and Peking Union Medical College, Beijing, China

Purpose: The aim of this study was to develop a nomogram for predicting positive non-sentinel lymph nodes (non-SLNs) in positive SLN breast cancer patients and validate the Memorial Sloan-Kettering Cancer Center (MSKCC) nomogram for non-SLN metastasis in Chinese patients.

Methods: The pathological features of 2,561 breast cancer patients were retrospectively reviewed, and the patients were divided into training and validation cohorts. Positive non-SLN predictors were identified using univariate and multivariate analyses and used to construct the nomogram. In patients with positive SLNs, the MSKCC nomogram was used to calculate the probability of non-SLN metastasis. The area under the receiver operating characteristic curve (AUC) was calculated to assess the accuracy of this model and the MSKCC nomogram.

Results: According to multivariate logistic regression analysis, the number of positive and negative SLNs, tumor stage, lymphovascular invasion, perineural invasion, and extracapsular extension were independent predictive factors for non-SLN metastasis and were selected to establish the nomogram for predicting positive non-SLNs. This nomogram performed favorably in predicting positive non-SLNs, with AUCs of 0.765 and 0.741 for the training and validation cohorts, respectively. The MSKCC nomogram predicted non-SLN metastasis with an AUC of 0.755.

Conclusion: A nomogram was developed and validated to assist clinicians in evaluating the likelihood of positive non-SLN. For Chinese patients with a known ER status before surgery, the MSKCC nomogram can be used to predict non-SLN metastases.

KEYWORDS

breast cancer, sentinel lymph nodes, MSKCC, nomogram, metastasis

Introduction

Axillary lymph node metastasis is an important prognostic factor in breast cancer patients. Since its introduction in the 1990s, sentinel lymph node biopsy (SLNB) has revolutionized surgeries for predicting ALN status, especially for those with clinically negative nodes. Axillary lymph node dissection (ALND) is no longer necessary when there is no metastasis in the SLNs, and thus, its surgical-associated complications can be avoided. In contrast, patients with positive SLNs require ALND. The Z0011 designed by the American College of Surgeons Oncology Group (ACOSOG) demonstrated that ALND does not prolong survival in patients with T1 to T2 breast cancer who have ≤ 2 positive SLNs. However, ALND is highly recommended when metastatic disease is found in more than two SLNs or when metastatic lymph nodes are identified intraoperatively (1, 2). The Z0011 trial suggested that some positive SLN patients failed to experience benefits. This result was also confirmed in China; a prospective single-arm study showed that ALND could be avoided for patients eligible for Z0011 in China (3). Therefore, unnecessary ALND may be minimized by analyzing the factors influencing non-SLN status among patients with positive SLNs.

In recent years, several prediction models have been developed using a combination of statistically significant factors, such as the Memorial Sloan-Kettering Cancer Center (MSKCC) nomogram (4), the Tenon scoring system (5), the Louisville scoring system (6), and the Stanford nomogram (7). The MSKCC nomogram is most commonly used to predict non-SLN status. However, the application range of the MSKCC nomogram is restricted because it has not yet been widely validated in Chinese populations, and the ER status of most Chinese patients is unknown at the time of surgery because diagnostic methods are different from those in other countries.

In the present study, we aimed to use a large number of patients to assess the predictive accuracy of the MSKCC nomogram and to establish a separate nomogram to identify the predictors of non-SLN status in patients with positive SLNs and use it to subsequently predict which patient subgroups might avoid ALND.

Materials and methods

Case selection

A total of 2,561 patients diagnosed with breast cancer between 2011 and 2022 were selected from Cancer Hospital, Chinese Academy of Medical Sciences (CAMS). The inclusion criteria were as follows: (i) diagnosis of invasive ductal carcinoma and invasive lobular carcinoma; (ii) previous lumpectomy or mastectomy; (iii) positive SLNs (macrometastases) and previous ALND; and (iv) confirmed T1–T2 stage cancer. Patients who had undergone primary systemic therapy were excluded.

The patients were divided into two cohorts, the training cohort (70%, 1,792/2,561) and the validation cohort (30%, 768/2,561), with the R function “createDataPartition” to ensure that outcome events were distributed randomly between the two cohorts. The prognostic

risk model was constructed based on the training cohort and confirmed in the validation cohort. Thirteen variables were included: number of positive and negative SLNs, age (at diagnosis), pathological patterns, tumor stage, molecular subtype, lymphovascular invasion, perineural invasion, extracapsular extension, number of tumors, human epidermal growth factor receptor (HER2), estrogen receptor (ER), and progesterone receptor (PR). The flowchart illustrating the establishment and validation of the nomograms for predicting non-SLN metastases in patients with SLN metastases is shown in Figure 1.

SLN biopsy

SLNs can be identified with nanocarbon dyes or technetium-99 m colloids. All lymph nodes detected based on radioactivity or that were dyed black were excised as SLNs for histopathological evaluation. Eight-micrometer-thick frozen sections of tumor tissue were prepared. The remaining tissue was fixed in 10% neutral buffered formalin and embedded in paraffin. Hematoxylin and eosin (H&E) staining was performed on frozen sections or on 4- μ m-thick paraffin sections.

Testing the Memorial Sloan-Kettering Cancer Center nomogram

To assess the performance of the MSKCC nomogram in predicting non-SLN metastasis, we applied it to all patients in this study. We input eight variables to the website (<https://nomograms.mskcc.org/breast/BreastAdditionalNonSLNMetastasesPage.aspx>) to produce an estimate of the risk of non-SLN metastasis: method of SLN metastasis detection [frozen section, routine or serial H&E, or immunohistochemistry (IHC)], pathological tumor size, tumor type and grade (ductal grade I or ductal grade II or ductal grade III or lobular), number of positive SLNs, number of negative SLNs, lymphatic or vascular structure involvement (positive or negative), multifocality (positive or negative), and ER status (positive or negative).

Statistical analysis

Univariate analysis was performed with the Pearson chi-square test for categorical variables and independent samples *t*-tests for quantitative data. Variables with a *p*-value < 0.05 in the univariate analysis were included in binary multivariable logistic regression analysis, and multicollinearity between variables was assessed to build the clinical factor model. The potential for multicollinearity was tested using the variance inflation factor (VIF); variables with a VIF >10 were excluded from the model. Receiver operating characteristic (ROC) curves and area under the curve (AUC) values were computed using the “pROC” R package. The predicted and actual observed outcomes of the nomogram were plotted to create a calibration curve, where the 45° line represents the best prediction. The proposed nomogram was validated in an independent external validation cohort. Variables or differences

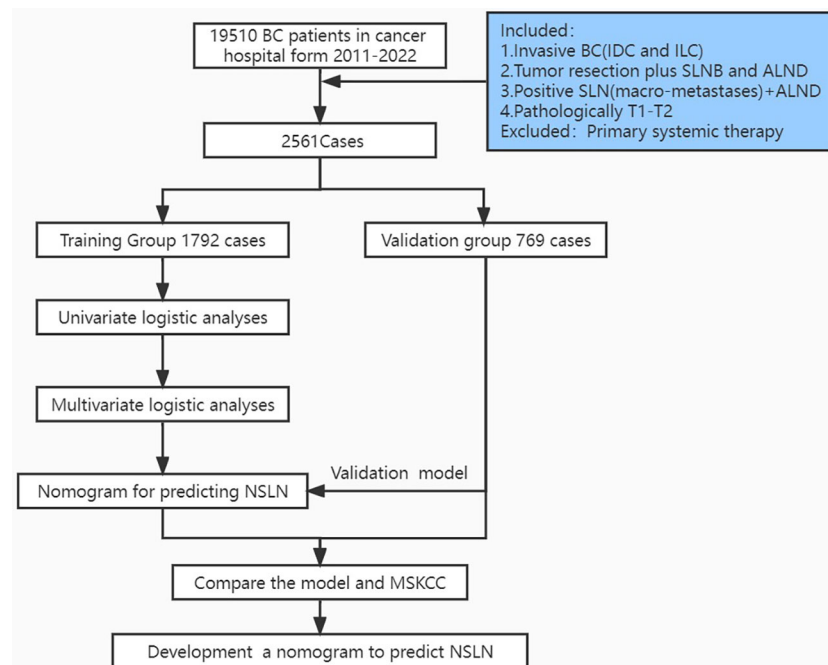


FIGURE 1
Flowchart illustrating the establishment and validation of nomograms for predicting non-SLN metastases in patients with SLN metastases.

with two-tailed p -values < 0.05 were considered statistically significant. Statistical analysis was performed using SPSS version 23.0 (IBM SPSS Statistics for Windows) and R programming language and environment (<https://www.r-project.org>).

Results

Clinical factors of the patients

The clinical characteristics of the patients are summarized in Table 1. The median ages were similar in the training and validation groups (50.63 ± 10.34 vs. 51.11 ± 10.66). A total of 12,434 SLNs were detected in 2,561 patients, with an average of 4.86 ± 2.00 SLNs per patient; of these, 4,616 sentinel nodes were positive, with an average of 1.80 ± 1.22 per patient. A total of 1,586 patients (61.9%) had positive axillary lymph nodes after completion of ALND, and 975 patients (38.1%) had negative lymph nodes.

Clinicopathological feature selection and nomogram building

Univariate analysis demonstrated that non-SLN metastasis was significantly correlated with the number of positive and negative SLNs, tumor size, tumor stage, molecular subtype, lymphovascular invasion, perineural invasion, extracapsular extension, and HER2 status (Table 2). The VIF values were all < 10 , indicating that no collinearity existed between the predictor variables. In multivariate logistic regression analysis, the number of positive and negative

SLNs ($p < 0.001$), tumor stage ($p = 0.039$), lymphovascular invasion ($p < 0.001$), perineural invasion ($p < 0.001$), and extracapsular extension ($p = 0.003$) were identified as independent predictive factors for non-SLN metastasis (Figure 2). These six independently predictive factors were used to create a predictive nomogram.

Internal performance and independent validation of the nomogram

The outstanding discriminability of the nomogram gave an AUC of 0.765 (95% CI: 0.738–0.793) in the training group and 0.741 (95% CI: 0.695–0.787) in the validation group (Figure 3A). In addition, the calibration curve of the nomogram showed good agreement between the predicted and actual observations in the training group (Figure 3B, $p = 0.960$) and validation group (Figure 3C, $p = 0.993$). In conclusion, the predictive model had good discriminative and calibration abilities. Figure 4 shows an example of using the nomogram to predict the risk of non-SLN metastasis in a given patient. The total score was derived from the individual scores calculated using the nomogram; most patients in the training group had total risk points ranging from 260 to 380.

This patient had T1 stage breast cancer, perineural and vascular invasion, one positive surgical lymph node, and three negative surgical lymph nodes but no extracapsular extension. The density plot of total points and tumor stages shows their distribution. For category variables, their distributions are reflected by the size of the box (for perineural invasion, the smaller box represents positive, and the larger one represents negative). The importance of each variable is ranked according to the standard deviation along the

TABLE 1 Clinical and pathological characteristics of the training cohort and the validation cohort.

| Characteristics | Training cohort | Validation cohort |
|----------------------------|-----------------|-------------------|
| Cases | 1,792 | 768 |
| Positive SLN number | 1.84 ± 1.28 | 1.71 ± 1.08 |
| Negative SLN number | 3.08 ± 2.06 | 2.98 ± 1.97 |
| Age | | |
| <50 | 870 (48.5) | 361 (47.0) |
| ≥50 | 922 (51.5) | 407 (53.0) |
| IDC histological grade | | |
| I | 147 (8.4) | 52 (7.1) |
| II | 1,172 (67.1) | 479 (65.0) |
| III | 418 (23.9) | 204 (27.7) |
| Unknown | 10 (0.6) | 2 (0.3) |
| Pathological patterns | | |
| IDC | 1,747 (97.5) | 737 (96.0) |
| Invasive lobular carcinoma | 45 (2.5) | 31 (4.0) |
| pT stage | | |
| T1 | 1,010 (56.4) | 423 (55.1) |
| T2 | 782 (43.6) | 345 (44.9) |
| Molecular subtype | | |
| Luminal A | 718 (40.1) | 290 (37.8) |
| Luminal B | 705 (39.3) | 309 (40.2) |
| HER2 | 120 (6.7) | 46 (6.0) |
| TNBC | 104 (5.8) | 49 (6.4) |
| Unknown | 145 (8.1) | 74 (9.6) |
| Lymphovascular invasion | | |
| Negative | 582 (32.5) | 254 (33.1) |
| Positive | 796 (44.4) | 330 (43.0) |
| Unknown | 414 (23.1) | 184 (24.0) |
| Perineural invasion | | |
| Negative | 929 (51.8) | 399 (52.0) |
| Positive | 457 (25.5) | 186 (24.2) |
| Unknown | 406 (22.7) | 183 (23.8) |
| Extracapsular extension | | |
| Negative | 1,692 (94.4) | 733 (95.4) |
| Positive | 100 (5.6) | 35 (4.6) |
| Mutifocal | | |
| No | 1,574 (87.8) | 683 (88.9) |
| Yes | 218 (12.2) | 85 (11.1) |

(Continued)

TABLE 1 Continued

| Characteristics | Training cohort | Validation cohort |
|---------------------------------------|-----------------|-------------------|
| HER2 IHC | | |
| 0 | 380 (21.2) | 184 (24.0) |
| 1+ | 492 (27.5) | 180 (23.4) |
| 2+ | 557 (31.1) | 246 (32.0) |
| 3+ | 279 (15.6) | 119 (15.5) |
| Unknown | 84 (4.7) | 39 (5.1) |
| HER2 | | |
| IHC 0,1+,2+(FISH-) | 1,256 (70.1) | 533 (69.4) |
| ICH 3+,2+(FISH+) | 351 (19.6) | 141 (18.4) |
| IHC 2+(FISH Unknown) and HER2 Unknown | 185 (10.3) | 94 (12.2) |
| ER | | |
| Negative | 259 (14.5) | 129 (16.8) |
| Positive | 1,451 (81.0) | 600 (78.1) |
| Unknown | 82 (4.6) | 39 (5.1) |
| PR | | |
| Negative | 306 (17.1) | 172 (22.4) |
| Positive | 1,402 (78.2) | 557 (72.5) |
| Unknown | 84 (4.7) | 39 (5.1) |

IDC, invasive ductal carcinoma; TNBC, triple-negative breast cancer. All values are *n* (%).

nomogram scales. An individual patient’s score (black dot) is placed on each variable axis. Red lines and dots are drawn upward to determine the points received by each variable; the sum (308) of these points is located on the total points axis, and a line is drawn downward to the NSLN axes to predict the risk of non-SLN metastasis, which for this patient is 36.1%.

Performance of the MSKCC nomogram in our cohort of SLN-positive patients

The MSKCC nomogram was used to estimate non-SLN metastasis risk in all patient groups (training and validation), with an AUC of 0.755 (95% CI: 0.732–0.778) (Figure 3A).

Discussion

This study used data from 2,561 early breast cancer patients in two cohorts and presented a simple nomogram that demonstrated strong discriminability for axillary non-SLN metastases. The current trends in surgery for breast cancer are toward more conservative management, which aims to avoid the complications of ALND, such as lymphedema of the arm and restriction of arm

mobility. If metastasis is not found in the SLN, further ALND is generally not needed; otherwise, the standard management is completion of the ALND. This study found that 61.66% (1,579/2,611) of patients with positive SLNs had no further non-SLN metastases. By extension, the percentage of negative non-SLNs in patients with one or two SLN metastases was 74.64% (1,077/1,443) and 57% (350/614), respectively, while in patients with three or more SLN metastases, 30.16% (152/504) did not have non-SLN metastasis. Therefore, completing ALND would have no therapeutic value in more than half of patients with SLN metastasis; this would require identifying the non-SLN low-risk subgroup to avoid unnecessary treatment. Univariate and multivariate analyses were used to assess the association between the clinical pathologic variables and non-SLN metastasis. The results showed that the number of positive and negative SLNs, tumor stage, lymphovascular invasion, perineural invasion, and

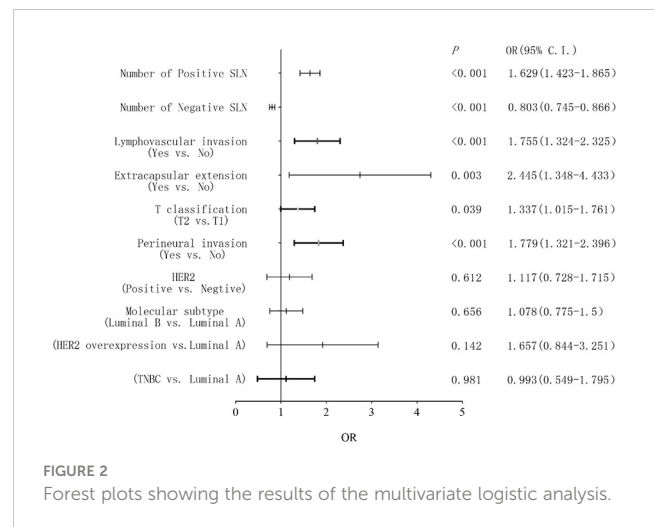


TABLE 2 Univariate analyses of positive non-sentinel lymph nodes in the training group.

| Characteristics | Training cohort (N = 1792) | | Univariable |
|----------------------------|----------------------------|---------------|-------------|
| | Negative NSLN | Positive NSLN | p |
| Tumor size | 2.03 ± 0.99 | 2.26 ± 0.63 | <0.001 |
| Positive SLN number | 1.48 ± 0.82 | 2.41 ± 1.60 | <0.001 |
| Negative SLN Number | 3.53 ± 2.0 | 2.38 ± 1.95 | <0.001 |
| Age | | | 0.911 |
| <50 | 529 (48.4) | 341 (48.7) | |
| ≥50 | 563 (51.6) | 359 (51.3) | |
| IDC histological grade | | | 0.118 |
| I | 99 (9.3) | 48 (7.1) | |
| II | 720 (67.9) | 452 (66.9) | |
| III | 242 (22.8) | 176 (26.0) | |
| Pathological patterns | | | 0.896 |
| IDC | 1065 (97.5) | 682 (97.4) | |
| Invasive lobular carcinoma | 27 (2.5) | 18 (2.6) | |
| pT stage | | | <0.001 |
| T1 | 670 (61.4) | 340 (48.6) | |
| T2 | 422 (38.6) | 360 (51.4) | |
| Molecular subtype | | | 0.005 |
| Luminal A | 471 (46.6) | 247 (43.6) | |
| Luminal B | 403 (39.9) | 302 (47.5) | |
| HER2 | 68 (6.7) | 52 (8.2) | |
| TNBC | 69 (6.8) | 35 (5.5) | |
| Lymphovascular invasion | | | <0.001 |
| Negative | 422 (51.0) | 160 (29) | |

(Continued)

TABLE 2 Continued

| Characteristics | Training cohort (N = 1792) | | Univariable |
|-------------------------|----------------------------|---------------|-------------|
| | Negative NSLN | Positive NSLN | p |
| Positive | 405 (49.0) | 391 (71) | |
| Perineural invasion | | | <0.001 |
| Negative | 622 (72.1) | 307 (58.7) | |
| Positive | 241 (27.9) | 216 (41.3) | |
| Extracapsular extension | | | <0.001 |
| Negative | 1055 (96.6) | 637 (91.0) | |
| Positive | 37 (3.4) | 63 (9.0) | |
| Multifocal | | | 0.387 |
| No | 965 (88.4) | 609 (87.0) | |
| Yes | 127 (11.6) | 91 (13.0) | |
| HER2 IHC | | | 0.028 |
| 0 | 234 (22.3) | 146 (22.2) | |
| 1+ | 328 (31.2) | 164 (24.9) | |
| 2+ | 327 (31.1) | 230 (35.0) | |
| 3+ | 161 (15.3) | 118 (17.9) | |
| HER2 | | | 0.037 |
| IHC 0,1+,2+(FISH-) | 789 (79.9) | 467 (75.4) | |
| ICH 3+,2+(FISH+) | 199 (20.1) | 152 (24.6) | |
| ER | | | |
| Negative | 158 (15.0) | 101 (15.3) | 0.886 |
| Positive | 892 (85.0) | 559 (84.7) | |
| PR | | | |
| Negative | 183 (17.4) | 123 (18.7) | 0.507 |
| Positive | 867 (82.6) | 535 (81.3) | |

extracapsular extension were independent risk factors for non-SLN metastasis. While some research has shown that non-SLN metastasis is associated with the number of tumor lesions in breast cancer, no association was observed in our study (8). In the MSKCC nomogram, the effect of ER status was only borderline significant ($p = 0.08$), but ER status was included in the MSKCC nomogram to improve the overall predictive capacity (4). Therefore, only the patients with known ER status can use the MSKCC nomogram. However, our study did not observe significant associations between ER status and NSLN metastasis ($p = 0.886$), similar to the result shown by other studies (8–10). Thus, we did not include ER status to establish the nomogram for predicting positive non-SLNs. The results of this study can not only help guide clinicians in predicting the risk of axillary non-SLN metastases and selecting appropriate treatment strategies but also provide a basis for guiding clinical decision-making in the radiation field.

SLN biopsy requires the collaboration of a multidisciplinary team of doctors to integrate and interpret clinical information. Chemotherapy and radiotherapy can be used instead of ALND in T1–T2 stage patients

who have not undergone neoadjuvant chemotherapy, are clinically node negative, and have fewer than or equal to two positive SLNs (11). The number of studies on breast cancer patients with three or more positive SLNs is limited at present. Whether patients with three or more positive SLNs could receive ALND still requires confirmation with a large prospective, randomized controlled trial. Two studies randomizing patients with micrometastatic SLN to complete ALND or clinical follow-up included patients who had undergone mastectomy. Neither study showed significant effects on survival between groups, suggesting that ALND and radiotherapy are unnecessary for these patients (12, 13). ALND is also not recommended for patients with isolated tumor cells in lymph nodes (14, 15).

The MSKCC nomogram is the most widely used nomogram to predict the likelihood of non-SLN disease, using nine identified risk factors to achieve AUCs of 0.76 (retrospective group) and 0.77 (prospective group) (4). There is a great deal of variation in its predictive value among different populations. The MSKCC nomogram has been tested in many studies; some reported that the MSKCC nomogram had an AUC ranging from 0.73 to 0.80 (16, 17),

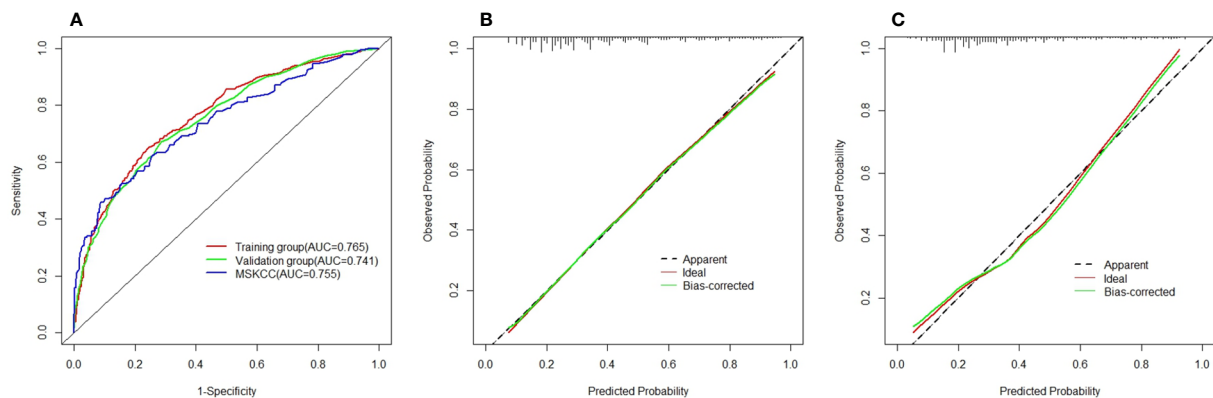


FIGURE 3

(A) Area under the receiver–operator characteristic curve for the training group (red) and validation group (green) and the Memorial Sloan-Kettering Cancer Center (MSKCC) nomogram (blue). (B) Calibration curves for the nomogram in the training group. (C) Calibration curves for the nomogram in the validation group.

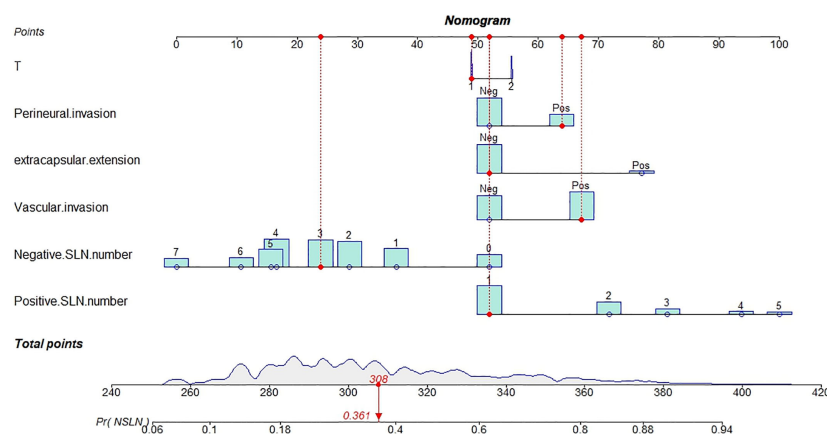


FIGURE 4

Constructed nomogram for predicting the risk of non-SLN metastasis in a patient.

but research from China reported values ranging from 0.677 to 0.688 (18–20). Likely due to the smaller validated sample size, these Chinese studies showed predictive abilities that were lower than those of the original research study. In this study, the MSKCC nomogram was applied to 1,760 patients with a positive SLN who subsequently completed ALND. The AUC value was 0.755, which is basically consistent with the original study. Although there are differences in race, age of onset, and staining methods, the prediction of metastasis in non-SLNs is also feasible with the MSKCC nomogram. A limitation of this approach is that limited pathologic information is available at the time of mastectomy. We observed a similar AUC value between our research and the initial MSKCC nomogram study, but the MSKCC nomogram cannot be widely applied to Chinese patients since the patient's ER status is often unknown before surgery.

Of course, there were still several limitations to our study. First, only routine pathological examination and H&E-stained SLNs and non-SLNs were examined. Multisection analysis and IHC in lymph node staging may help increase the accuracy of lymph node analysis. Second, patients with lymph node micrometastases were not included in the study. Furthermore, the size of the metastatic foci in the node was unknown.

In conclusion, the nomogram we proposed uses six variables: the number of positive and negative SLNs, tumor stage, lymphovascular invasion, perineural invasion, and extracapsular extension. This nomogram can be used to estimate the likelihood of having at least one positive non-SLN in patients with positive SLNs during the surgery. An evaluation of the model showed good predictiveness, suggesting that it can be used by the surgeon in determining which surgical modality will be used. The MSKCC nomogram can be applied to Chinese breast cancer patients with known ER status before surgery, and its predictive ability was similar to that of a previous study predicting non-SLN metastases.

Data availability statement

The original contributions presented in the study are included in the article/supplementary material. Further inquiries can be directed to the corresponding author/s.

Ethics statement

This study involving human participants was reviewed and approved by the NCC Ethics Committee/Institution Review Board. Written informed consent for participation was not required for this study in accordance with the national legislation and the institutional requirements.

Author contributions

HL: data curation, formal analysis, writing—original draft, and methodology. PY: data curation, writing—original draft, and formal analysis. CG: data curation, writing—original draft, and formal analysis. JY: conceptualization, resources, formal analysis, supervision, funding acquisition, investigation, methodology, writing—original draft, project administration, and writing—review and editing. All authors contributed to the article and approved the submitted version.

References

- Giuliano AE, Ballman KV, McCall L, Beitsch PD, Brennan MB, Kelemen PR, et al. Effect of axillary dissection vs no axillary dissection on 10-year overall survival among women with invasive breast cancer and sentinel node metastasis: The ACOSOG Z0011 (Alliance) randomized clinical trial. *JAMA* (2017) 318(10):918–26. doi: 10.1001/jama.2017.11470
- Giuliano AE, Hunt KK, Ballman KV, Beitsch PD, Whitworth PW, Blumencranz PW, et al. Axillary dissection vs no axillary dissection in women with invasive breast cancer and sentinel node metastasis: A randomized clinical trial. *JAMA* (2011) 305(6):569–75. doi: 10.1001/jama.2011.90
- Peng Y, Liu M, Li X, Tong F, Cao Y, Liu P, et al. Application of the ACOSOG Z0011 criteria to Chinese patients with breast cancer: a prospective study. *World J Surg Oncol* (2021) 19(1):128. doi: 10.1186/s12957-021-02242-1
- Van Zee KJ, Manasseh DM, Bevilacqua JL, Boolbol SK, Fey JV, Tan LK, et al. A nomogram for predicting the likelihood of additional nodal metastases in breast cancer patients with a positive sentinel node biopsy. *Ann Surg Oncol* (2003) 10(10):1140–51. doi: 10.1245/aso.2003.03.015
- Barranger E, Coutant C, Flahault A, Delpach Y, Darai E, Uzan S. An axilla scoring system to predict non-sentinel lymph node status in breast cancer patients with sentinel lymph node involvement. *Breast Cancer Res Treat* (2005) 91(2):113–9. doi: 10.1007/s10549-004-5781-z
- Chagpar AB, Scoggins CR, Martin RC2nd, Carlson DJ, Laidley AL, El-Eid SE, et al. Prediction of sentinel lymph node-only disease in women with invasive breast cancer. *Am J Surg* (2006) 192(6):882–7. doi: 10.1016/j.amjsurg.2006.08.063
- Kohrt HE, Olshen RA, Bermas HR, Goodson WH, Wood DJ, Henry S, et al. New models and online calculator for predicting non-sentinel lymph node status in sentinel lymph node positive breast cancer patients. *BMC Cancer* (2008) 8:66. doi: 10.1186/1471-2407-8-66
- Yu Y, Wang Z, Wei Z, Yu B, Shen P, Yan Y, et al. Development and validation of nomograms for predicting axillary non-SLN metastases in breast cancer patients with 1-2 positive sentinel lymph node macro-metastases: A retrospective analysis of two independent cohorts. *BMC Cancer* (2021) 21(1):466. doi: 10.1186/s12885-021-08178-9
- Padmanabhan N, Ayub MF, Hussain K, Kurien A, Radhakrishna S. Factors influencing non-sentinel node involvement in sentinel node positive patients and validation of MSKCC nomogram in Indian breast cancer population. *Indian J Surg Oncol* (2015) 6(4):337–45. doi: 10.1007/s13193-015-0431-y
- Malter W, Hellmich M, Badian M, Kirn V, Mallmann P, Kramer S. Factors predictive of sentinel lymph node involvement in primary breast cancer. *Anticancer Res* (2018) 38(6):3657–62. doi: 10.21873/anticancer.12642
- Donker M, van Tienhoven G, Straver ME, Meijnen P, van de Velde CJ, Mansel RE, et al. Radiotherapy or surgery of the axilla after a positive sentinel node in breast cancer (EORTC 10981-22023 AMAROS): A randomised, multicentre, open-label, phase 3 non-inferiority trial. *Lancet Oncol* (2014) 15(12):1303–10. doi: 10.1016/S1470-2045(14)70460-7
- Galimberti V, Cole BF, Zurrada S, Viale G, Luini A, Veronesi P, et al. Axillary dissection versus no axillary dissection in patients with sentinel-node micrometastases (IBCSG 23-01): A phase 3 randomised controlled trial. *Lancet Oncol* (2013) 14(4):297–305. doi: 10.1016/S1470-2045(13)70035-4
- Sola M, Alberro JA, Fraile M, Santesteban P, Ramos M, Fabregas R, et al. Complete axillary lymph node dissection versus clinical follow-up in breast cancer patients with sentinel node micrometastasis: final results from the multicenter clinical trial AATRM 048/13/2000. *Ann Surg Oncol* (2013) 20(1):120–7. doi: 10.1245/s10434-012-2569-y
- China anti-cancer Association. Guidelines on diagnosis and treatment for breast cancer (2021 version). *China Oncol* (2021) 31(10):954–1040. doi: 10.19401/j.cnki.1007-3639.2021.10.013
- Morrow M. Management of the node-positive axilla in breast cancer in 2017: Selecting the right option. *JAMA Oncol* (2018) 4(2):250–1. doi: 10.1001/jamaoncol.2017.3625
- Gruber I, Henzel M, Schonfisch B, Stabler A, Taran FA, Hahn M, et al. Prediction of non-sentinel lymph node metastases after positive sentinel lymph nodes using nomograms. *Anticancer Res* (2018) 38(7):4047–56. doi: 10.21873/anticancer.12694
- Ceylan C, Pehlevan Ozel H, Agackiran I, Altun Ozdemir B, Atas H, Menekse E. Preoperative predictive factors affecting sentinel lymph node positivity in breast cancer and comparison of their effectiveness with existing nomograms. *Med (Baltimore)* (2022) 101(48):e32170. doi: 10.1097/MD.00000000000032170
- Chao Y, Liu M, Zhou B. Comparative validation of MSKCC and SOC models for predicting non-sentinel lymph node metastasis in Chinese breast cancer patients. *Chin J Clin Oncol* (2014) 8:508–12. doi: 10.3969/j.issn.1000-8179.21031009
- Huang J, Chen X, Fei X, Huang O. Risk factors of non-sentinel lymph node metastasis and performance of MSKCC nomogram in breast cancer patients with metastatic sentinel lymph node. *Chin J Surg* (2015) 53(12):941–6. doi: 10.3760/cma.j.issn.0529-5815.2015.12.011
- Wu P, Zhao K, Liang Y, Ye W, Liu Z, Liang C. Validation of breast cancer models for predicting the nonsentinel lymph node metastasis after a positive sentinel lymph node biopsy in a Chinese population. *Technol Cancer Res Treat* (2018) 17:1533033818785032. doi: 10.1177/1533033818785032

Conflict of interest

The authors declare that the research was conducted in the absence of any commercial or financial relationships that could be construed as a potential conflict of interest.

Publisher's note

All claims expressed in this article are solely those of the authors and do not necessarily represent those of their affiliated organizations, or those of the publisher, the editors and the reviewers. Any product that may be evaluated in this article, or claim that may be made by its manufacturer, is not guaranteed or endorsed by the publisher.



OPEN ACCESS

EDITED BY

Gianluca Franceschini,
Agostino Gemelli University Polyclinic
(IRCCS), Italy

REVIEWED BY

Qian Xiaoqin,
Jiangsu University Affiliated People's
Hospital, China
Simona Ruxandra Volovat,
Grigore T. Popa University of Medicine and
Pharmacy, Romania

*CORRESPONDENCE

Sonia Silipigni
✉ s.silipigni@policlinicocampus.it

SPECIALTY SECTION

This article was submitted to
Breast Cancer,
a section of the journal
Frontiers in Oncology

RECEIVED 05 October 2022

ACCEPTED 08 March 2023

PUBLISHED 17 March 2023

CITATION

Ippolito E, Silipigni S, Pantano F,
Matteucci P, Carrafiello S, Marrocco M,
Alaimo R, Palumbo V, Fiore M, Orsaria P,
D'Angelillo RM, Altomare V, Tonini G and
Ramella S (2023) BOMB trial: First results of
stereotactic radiotherapy to primary breast
tumor in metastatic breast cancer patients.
Front. Oncol. 13:1062355.
doi: 10.3389/fonc.2023.1062355

COPYRIGHT

© 2023 Ippolito, Silipigni, Pantano,
Matteucci, Carrafiello, Marrocco, Alaimo,
Palumbo, Fiore, Orsaria, D'Angelillo,
Altomare, Tonini and Ramella. This is an
open-access article distributed under the
terms of the [Creative Commons Attribution
License \(CC BY\)](https://creativecommons.org/licenses/by/4.0/). The use, distribution or
reproduction in other forums is permitted,
provided the original author(s) and the
copyright owner(s) are credited and that
the original publication in this journal is
cited, in accordance with accepted
academic practice. No use, distribution or
reproduction is permitted which does not
comply with these terms.

BOMB trial: First results of stereotactic radiotherapy to primary breast tumor in metastatic breast cancer patients

Edy Ippolito^{1,2}, Sonia Silipigni^{2*}, Francesco Pantano^{3,4},
Paolo Matteucci², Sofia Carrafiello², Maristella Marrocco⁵,
Rita Alaimo², Vincenzo Palumbo², Michele Fiore^{1,2},
Paolo Orsaria^{6,7}, Rolando Maria D'Angelillo⁸,
Vittorio Altomare^{6,7}, Giuseppe Tonini^{3,4} and Sara Ramella^{1,2}

¹Department of Radiation Oncology (Medicine and Surgery), Università Campus Bio-Medico di Roma, Rome, Italy, ²Radiation Oncology, Fondazione Policlinico Universitario Campus Bio-Medico, Rome, Italy, ³Department of Medical Oncology (Medicine and Surgery), Università Campus Bio-Medico di Roma, Rome, Italy, ⁴Medical Oncology, Fondazione Policlinico Universitario Campus Bio-Medico, Rome, Italy, ⁵Department of Radiation Oncology, Azienda Sanitaria Locale (ASL) Frosinone, Hospital of Sora, Sora, Italy, ⁶Department of Breast Surgery (Medicine and Surgery), Università Campus Bio-Medico di Roma, Rome, Italy, ⁷Breast Surgery, Fondazione Policlinico Universitario Campus Bio-Medico, Rome, Italy, ⁸Radiation Oncology, Department of Biomedicine and Prevention University of Rome "Tor Vergata", Rome, Italy

Aim: A prospective dose escalation trial was developed to evaluate the maximum tolerated dose of stereotactic body radiotherapy (SBRT) to primary breast cancer in stage IV disease. The aim of the present report was to describe safety and outcome of the first dose level cohort of patients.

Material and methods: Patients with histologically confirmed diagnosis of invasive breast carcinoma (biological immuno-histochemical profile: luminal and/or HER2 positive) and distant metastatic disease not progressing after 6 months of systemic therapy with a tumor CT or 5FDG-PET detectable were deemed eligible. The starting dose was 40 Gy in 5 fractions (level 1) because this dose proved to be safe in previous dose-escalation trial on adjuvant stereotactic body radiotherapy. The maximum dose level was chosen as 45 Gy in 5 fractions. Dose limiting toxicity was any grade 3 or worse toxicity according to CTCAE v.4. Time-to-event Keyboard (TITE-Keyboard) design (Lin and Yuan, Biostatistics 2019) was used to find the maximum tolerated dose (MTD). MTD was the dose of radiotherapy associated with a $\leq 20\%$ rate pre-specified treatment-related dose-limiting toxicity (DLT).

Results: To date 10 patients have been treated at the starting dose level. Median age was 80 years (range 50–89). 7 patients had a luminal disease, while 3 patients had an HER2 positive disease. No patient suspended ongoing systemic treatment. No protocol defined DLTs were observed. Grade 2 skin toxicity occurred in 4 patients with diseases located close to or involving the skin. Median follow-up was 13 months and all 10 patients were evaluable for response: 5 achieved a complete response, 3 achieved a partial response and 2 showed a stable disease, all with a clinical benefit (resolution of skin retraction,

bleeding and pain). The mean reduction in the sum of the largest diameters of target lesions was of 61.4% (DS=17.0%).

Conclusions: SABR to primary breast cancer seems feasible and is associated with symptoms reduction. Continued accrual to this study is needed to confirm the safety and assess the MTD.

Clinical trial registration: [ClinicalTrials.gov](https://clinicaltrials.gov), identifier NCT05229575.

KEYWORDS

stereotactic radiation (SBRT), breast cancer, metastatic patients, safety, outcome

Introduction

Approximately 5-10% of women present *de novo* metastatic breast cancer (MBC). This is still an incurable disease even if in the last decades several advances in the treatment of MBC patients have significantly prolonged survival over time (1).

Loco-regional treatment in these patients is highly debatable and its role is not yet established.

It appears that preclinical studies could justify the addition of local treatment to systemic therapy. In fact, the primary breast tumor can be a reservoir of cancer stem cells (2), and can secrete growth factors involved in implantation and growth of metastatic sites (3). Moreover, studies in animal models suggest that resection of the primary breast tumor in mice can restore the immunocompetence of the host (4).

On the other hand, clinical trials results are controversial. A Cochrane systematic review on this topic was recently published, including two randomized studies. Breast surgery showed improved local progression-free survival (HR 0.22, 95% CI 0.08 to 0.57; 2 studies; 607 women), but worsened distant progression-free survival (HR 1.42, 95% CI 1.08 to 1.86) in one study. The authors concluded that with the available data, the decision to perform breast surgery on these women should be individualized and shared between the physician and the patient, carefully considering the potential risks, benefits, and costs (5). More recently, results from EA2108 randomized trials were published showing that early loco-regional therapy for the primary site was associated with improved loco-regional control, but did not improve survival (6).

However, even if current data does not support loco-regional treatment, some of the results of randomized trials, together with the findings of several retrospective studies, suggest that there could be a subset of patients presenting long progression-free survival who might benefit from radical loco-regional treatment. Moreover, treatment of primary breast cancer may provide clinical benefits eventually reducing related symptoms such as pain, bleeding, and skin retraction (7).

There is not much data available on radiotherapy alone for the primary tumor in metastatic breast cancer patients.

A French study retrospectively evaluated the impact of loco-regional treatment (mostly radiotherapy) in a well-selected stage IV breast cancer patients group (33% single metastatic site, 49% without visceral metastases). With a median follow-up of 6.5 years, loco-regional treatment obtained a durable local control of 85%. Particularly, radiotherapy alone compared with surgery followed by radiotherapy provided similar outcomes in terms of overall survival and metastatic-free survival after adjustments for prognostic factors (8).

Stereotactic ablative body radiotherapy (SABR) is a safe and effective treatment modality in several tumor sites, including lung, brain and liver (9, 10). In breast cancer treatment, SABR has been mainly studied in the neoadjuvant and adjuvant settings (11–13). To date, SABR to intact primary tumors without subsequent surgery has not been investigated, even in palliation setting in metastatic patients. However, SABR has many potential advantages such as the radio-biological advantage of a short and highly effective schedule, the possibility of preventing lesions from becoming symptomatic, as well as the possibility of not interrupting systemic therapy.

Taking into consideration the aforementioned, we started an ongoing phase I trial (see [ClinicalTrials.gov](https://clinicaltrials.gov) Identifier: NCT05229575) to assess the maximum tolerated dose of SABR to primary breast cancer tumors in stage IV patients. The present report aimed to describe the outcome of the first dose-level patients.

Material and methods

All women 18 years of age or older presenting with a histologically confirmed diagnosis of invasive breast carcinoma (biological immuno-histochemical profile: luminal and/or HER2 positive) and stage IV disease not experiencing extra-mammary disease progression after 6 months of systemic therapy, primary unifocal tumor < 5 cm detectable at either CT or FDG PET-CT scans, were eligible for inclusion. All patients recommended for surgery were excluded. Our institutional ethics committee approved the trial, and informed consent was obtained from all participants.

Simulation and treatment were performed with the patient in the supine position using a breast board (Civco Medical Solutions, Orange City, IA, U.S.A.). The gross tumor volume (GTV) was defined as the primary breast lesion seen on CT scan or 5-FDG PET-CT scan. The clinical target volume was defined as the GTV plus a 3 mm margin. The planning target volume (PTV) was defined as the clinical target volume plus an internal margin as defined by 4a DCT scan or plus a 3 mm margin if breath hold was employed. Critical structures included the heart, lungs, skin, both breasts, and the chest wall.

The dose was prescribed at the edge of the PTV. To be approved, the 80% isodose line prescription needed to encompass 100% of the PTV volume.

The trial's primary endpoint was to establish the maximum tolerated dose (MTD) of stereotactic body radiotherapy for breast primary tumors. The MTD was considered as the dose of radiotherapy associated with a $\leq 20\%$ rate of pre-specified treatment-related dose-limiting toxicity (DLT) occurring within 6 months from the start of treatment. DLT was defined as any grade 3 or worse toxicity according to CTCAE v.4.02. If no DLT occurs, the trial aims to recruit a total of 30 patients. The goal of the present interim analysis was to assess with a minimum follow-up of 6 months toxicity experienced by the first dose level cohort of patients. The radiological response was also assessed.

Patients received 5 fractions of radiation, on a 2-day basis. The starting dose level was 40 Gy in 5 fractions (level 1) as this dose was deemed safe in a previous dose-escalation trial on adjuvant stereotactic body radiotherapy (13), which corresponds to a 2 Gy equivalent dose of 76 Gy (biologically equivalent dose- BED 110 Gy, α/β 4.6 Gy). The highest dose level was set at 45 Gy in 5 fractions, equivalent to 93 Gy delivered in 2 Gy fractions ($BED_{4.6Gy} = 133$ Gy). According to older studies on radiotherapy as the definitive treatment in breast cancer (14, 15), this dose should be associated with very low local recurrence risk rate ($<15\%$).

Ipsilateral breast and axillary ultrasonography and a chest CT scan were performed 45 days after rt and thereafter according to the physician's prerogative. The radiologic response was evaluated according to the Response Evaluation Criteria in Solid Tumors.

NCI CTCAE v 4.02 scale for radiation dermatitis, breast pain, breast infection, breast asymmetry, fibrosis, skin atrophy, rib fracture, or chest wall pain was used. Photographic documentation was carried out at each clinical evaluation.

Results

Between August 2019 and June 2021, 10 patients were enrolled and treated at the starting dose level. The median age was 80 years (range 50–89). Seven patients had a luminal disease, while 3 patients had HER2-positive disease. No patient suspended ongoing systemic treatment (see Table 1 for details), median tumor diameter, measured on pre-treatment ultrasonography was 20 mm (range: 10 mm–46 mm). Before starting radiotherapy 3 patients showed skin retraction, 1 patient skin ulceration and bleeding and 2 patients presented breast pain. All patients received radiotherapy course as planned. Planning data is listed in Table 2.

No protocol-defined DLTs were observed. There were 6 acute grade 1 toxicity events (breast pain, hyperpigmentation, radiation dermatitis) and 4 acute grade 2 skin dermatitis. All of the latter occurred in 4 patients with diseases located next to the skin and showing clinical retraction. In these patients, the medium maximum dose delivered to 10 cc of skin was 30.1 Gy. In all of these patients, bolus was employed. To date, no grade ≥ 2 late toxicity events occurred; 1 patient developed grade 1 lung fibrosis, and 2 patients G1 breast induration. See Table 2 for details.

The median follow-up of the entire cohort was 13 months (7–24 months). To date, 7 patients are alive (2 died due to brain progression and 1 for cardiovascular disease). The median largest tumor diameter, measured on post-treatment ultrasonography was 10.5 mm (range: 5 mm–41 mm). The mean reduction in the sum of the largest diameters of target lesions was 61.4% ($DS=17.0\%$).

At 1 year, the local control was 100%. All 10 patients were evaluable for response: 5 achieved a complete response, 3 achieved a partial response and 2 showed stable disease. The 2 patients showing stable disease presented with skin retraction. In both patients, skin retraction disappeared after treatment.

TABLE 1 Patients' clinical characteristics.

| Patient | Age | Laterality (right/left) | Molecular subtype | Concurrent systemic treatment | Site of Metastatic disease |
|---------|-----|-------------------------|-------------------|--------------------------------------|----------------------------|
| 1 | 80 | left | HER2 Luminal | Capecitabine/Lapatinib | bone |
| 2 | 53 | left | Luminal | Palbociclib + Aromatase inhibitors | bone, liver, lung |
| 3 | 89 | right | Luminal | Aromatase inhibitors | lung |
| 4 | 80 | left | Luminal | Palbociclib + Aromatase inhibitors | liver |
| 5 | 84 | left | Luminal | Aromatase inhibitors | lung |
| 6 | 85 | left | Luminal | Aromatase inhibitors | lung |
| 7 | 56 | right | HER2 Luminal | Capecitabine/Lapatinib | brain, liver |
| 8 | 82 | left | Luminal | Aromatase inhibitors | lung |
| 9 | 50 | right | Luminal | Ribociclib + Aromatase inhibitors | bone, lung |
| 10 | 76 | left | HER2 | Trastuzumab/pertuzumab dual blockade | bone |

TABLE 2 Planning data and toxicity description.

| Patient | GTV (cc) | PTV (cc) | Uninvolved ipsilateral breast (dose to 50% of volume) | Maximum point dose contralateral breast (Gy) | Skin dose (10 cc) | Chest wall dose (10 cc) | Lung D10% (Gy) | Heart Dmean (Gy) | Toxicity (CTCAE v 4.02) |
|---------|----------|----------|---|--|-------------------|-------------------------|----------------|------------------|--|
| 1 | 16.9 | 38.8 | 1.2 | 0.3 | 1.7 | 16.8 | 4.0 | 0.4 | – |
| 2 | 12.4 | 24.8 | 3.1 | 1.2 | 2.0 | 21.7 | 5.1 | 1.5 | – |
| 3 | 3.30 | 24.2 | 2.5 | 0.7 | 26.7 | 11.2 | 3.0 | 0.4 | Grade 2 radiation dermatitis Grade 1 hyperpigmentation |
| 4 | 27.5 | 75.2 | 1.9 | 1.1 | 9.9 | 29.8 | 5.3 | 0.2 | Grade 1 breast induration, Grade 1 breast pain |
| 5 | 15.4 | 33.2 | 4.5 | 1.2 | 40.3 | 9.6 | 1.5 | 0.8 | Grade 2 radiation dermatitis Grade 1 hyperpigmentation |
| 6 | 14.7 | 44.8 | 1.2 | 13.8 | 27.6 | 37.4 | 0.2 | 1.5 | Grade 2 radiation dermatitis Grade 1 hyperpigmentation |
| 7 | 18.5 | 32.3 | 2.5 | 1.5 | 22.6 | 5.8 | 2.4 | 0.7 | Grade 1 radiation dermatitis Grade 2 hyperpigmentation |
| 8 | 12.8 | 61.2 | 1.1 | 9.4 | 13.9 | 29.3 | 4.5 | 0.3 | Grade 1 radiation dermatitis |
| 9 | 16.2 | 46.8 | 1.2 | 2.4 | 18.5 | 13.0 | 5.6 | 1.5 | Grade 1 lung fibrosis |
| 10 | 15.7 | 39.3 | 1.3 | 3.0 | 22.6 | 29.1 | 7.0 | 0.7 | Grade 2 radiation dermatitis, Grade 1 breast induration Grade 2 hyperpigmentation |

Overall, patients achieved a resolution of pre-radiotherapy clinical symptoms (skin retraction, bleeding and pain).

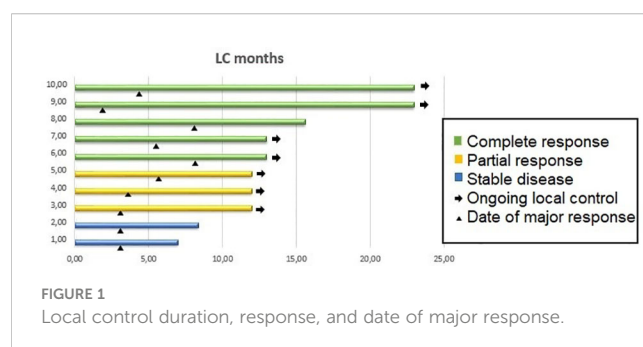
Figure 1 shows local control duration, response, and date of major response.

Discussion

In this ongoing pilot study, we are looking to find the MTD of stereotactic body radiotherapy for luminal and/or HER 2 positive breast primary tumors in stage IV disease patients, delivered during systemic treatment. To the best of our knowledge, no study has investigated the use of SABRT in this setting, consequently, we needed to undergo a dose-finding study.

Historical series on conventionally fractionated radiotherapy alone as definitive breast cancer treatment demonstrated tumor dose as being significantly related to local disease control (14). Arriagada et al. evaluated 463 breast cancer patients treated with radiotherapy alone at the Princess Margaret Hospital and at the Institut Gustave-Roussy. Analysis of local control showed that a radiation dose increase of 15 Gy can lower the relative risk of tumor

or lymph node recurrence twofold (14). Van Limbergen et al. (15), reviewing data on 221 breast cancer patients treated with radiotherapy alone reported that a 10 Gy higher dose for T1 tumors and 35 Gy higher dose for T2 tumors was needed to provide local control rates similar to a combination of surgery and radiation. The rate of local control ranged from 70 to 80% when doses higher than 70 Gy were applied. However, higher doses were associated with poorer cosmetic results, with only 15% of patients who received more than 80 Gy having good cosmetic results (15).



More recently, Shibamoto et al, reported the results of a study investigating a curative radiotherapy treatment for patients with primary operable breast cancer who refused surgery. Radiotherapy doses delivered were 50 Gy/25 fractions to the whole breast +/- regional nodes followed by a tumor boost of 21 Gy/3 fractions (equivalent dose delivered in 2 Gy= 86.9 Gy) by means of SABR or 20 Gy/8 fractions by means of IMRT (equivalent dose delivered in 2 Gy= 71.5 Gy). In this study, despite substantial heterogeneity in treatment delivery (some patients received also hyperthermia and concurrent chemotherapy), stage and biological subtype of disease included, with a median follow-up of 50 months, the 5-year local control was 93.4% (16).

The first level dose (40 Gy in 5 fractions, delivered every other day) was tested in the adjuvant setting and was deemed safe. Rahimi et al. in a phase 1 trial investigating a dose-escalated 5-fraction stereotactic body radiation therapy for partial-breast irradiation delivered in 75 patients after partial mastectomy reported only 1 DLT, which consisted of an acute grade 3 dermatitis in the intermediate dose level cohort. No DLT was observed at the highest dose of 40 Gy (13).

In this paper, we report the outcome of the first 10 patients treated to a total dose of 40 Gy in 5 fraction. All patients completed the treatment in 2 weeks without suspending the systemic treatment they were on, consisting of both hormone therapy and anti CDK4/6 inhibitors, capecitabine plus lapatinib and anti-HER2 therapy. The greatest toxicity was grade 2 moist desquamation occurring in 4 patients, which healed after appropriate treatment.

All patients with clinical symptoms experienced a clinical benefit, and were not excluded from the protocol as the SABR metastatic setting can have a palliative utility. In patients experiencing moist desquamation we recorded a medium maximum dose delivered to 10 cc of skin of 30.1 Gy. Similarly, Rahimi et al. showed that an average maximum dose to the skin of 38 Gy was related to the occurrence of radiation dermatitis (13).

Furthermore, the rate of response appears encouraging, even if the length of follow-up is still inadequate, especially for luminal patients. Also it can be influenced by the different biology of the disease included (HER2 + disease and luminal) as well as by the concomitant systemic therapy delivered.

After treatment of this first cohort of patients, no DLT occurred. Due to the high incidence of grade 2 skin toxicity in patients with tumors infiltrating the skin or located close to the skin (within

5 mm), we decided to expand this particular cohort to an additional 10 patients. The dose is being escalated in all other patients.

Data availability statement

The raw data supporting the conclusions of this article will be made available by the authors, without undue reservation.

Ethics statement

The studies involving human participants were reviewed and approved by Ethics committee Fondazione Campus Biomedico. The patients/participants provided their written informed consent to participate in this study.

Author contributions

Conceptualization: SR. Data curation: SS, PM, and FP. Handle database: SC and VP. Formal analysis: RA and MM. Methodology: PO. Supervision: RD'A, VA, and GT. Writing: original draft EL. Writing: review and editing MF. All authors contributed to the article and approved the submitted version.

Conflict of interest

The authors declare that the research was conducted in the absence of any commercial or financial relationships that could be construed as a potential conflict of interest.

Publisher's note

All claims expressed in this article are solely those of the authors and do not necessarily represent those of their affiliated organizations, or those of the publisher, the editors and the reviewers. Any product that may be evaluated in this article, or claim that may be made by its manufacturer, is not guaranteed or endorsed by the publisher.

References

1. Iqbal J, Ginsburg O, Rochon PA, Sun P, Narod SA. Differences in breast cancer stage at diagnosis and cancer-specific survival by race and ethnicity in the United States. *JAMA*. (2015) 313(2):165–73. doi: 10.1001/jama.2014.17322
2. Perez CB, Khan SA. Local therapy for the primary breast tumor in women with metastatic disease. *Clin Adv Hematol Oncol* (2011) 9(2):112–9.
3. Karnoub AE, Dash AB, Vo AP, Sullivan A, Brooks MW, Bell GW, et al. Mesenchymal stem cells within tumor stroma promote breast cancer metastasis. *Nature*. (2007) 449(7162):557–63. doi: 10.1038/nature06188
4. Danna EA, Sinha P, Gilbert M, Clements VK, Pulaski BA, Ostrand-Rosenberg S. Surgical removal of primary tumor reverses tumor-induced immunosuppression despite the presence of metastatic disease. *Cancer Res* (2004) 64(6):2205–11. doi: 10.1158/0008-5472.can-03-2646
5. Tosello G, Torloni MR, Mota BS, Neeman T, Riera R. Breast surgery for metastatic breast cancer. *Cochrane Database Syst Rev* (2018) 3(3). doi: 10.1002/14651858.CD011276.pub2
6. Khan SA, Zhao F, Goldstein LJ, Cella D, Basik M, Golshan M, et al. Early local therapy for the primary site in *De novo* stage IV breast cancer: Results of a randomized clinical trial (EA2108). *J Clin Oncol* (2022) 40(9):978–87. doi: 10.1200/JCO.21.02006
7. Poggio F, Lambertini M, de Azambuja E. Surgery of the primary tumour in patients presenting with *de novo* metastatic breast cancer: to do or not to do? *ESMO Open* (2018) 3(1):e000324. doi: 10.1136/esmoopen-2018-000324
8. Merino T, Tran WT, Czarnota GJ. Re-irradiation for locally recurrent refractory breast cancer. *Oncotarget*. (2015) 6(33):35051–62. doi: 10.18632/oncotarget.6036

9. Yoon SM, Lim YS, Park MJ, Kim SY, Cho B, Shim JH, et al. Stereotactic body radiation therapy as an alternative treatment for small hepatocellular carcinoma. *PLoS One* (2013) 8(11):e79854. doi: 10.1371/journal.pone.0079854
10. Timmerman R, Paulus R, Galvin J, Michalski J, Straube W, Bradley J, et al. Stereotactic body radiation therapy for inoperable early stage lung cancer. *JAMA*. (2010) 303(11):1070–6. doi: 10.1001/jama.2010.261
11. Bondiau PY, Courdi A, Bahadoran P, Chamoire E, Queille-Roussel C, Lallemand M, et al. Phase 1 clinical trial of stereotactic body radiation therapy concomitant with neoadjuvant chemotherapy for breast cancer. *Int J Radiat Oncol Biol Phys* (2013) 85(5):1193–9. doi: 10.1016/j.ijrobp.2012.10.034
12. Guidolin K, Yaremko B, Lynn K, Gaede S, Kornecki A, Muscedere G, et al. Stereotactic image-guided neoadjuvant ablative single-dose radiation, then lumpectomy, for early breast cancer: the SIGNAL prospective single-arm trial of single-dose radiation therapy. *Curr Oncol* (2019) 26(3):e334–40. doi: 10.3747/co.26.4479
13. Rahimi A, Thomas K, Spangler A, Rao R, Leitch M, Wooldridge R, et al. Preliminary results of a phase 1 dose-escalation trial for early-stage breast cancer using 5-fraction stereotactic body radiation therapy for partial-breast irradiation. *Int J Radiat Oncol Biol Phys* (2017) 98(1):196–205.e2. doi: 10.1016/j.ijrobp.2017.01.020
14. Arriagada R, Mouniesse H, Sarrazin D, Clark RM, Deboer G. Radiotherapy alone in breast cancer. i. analysis of tumor parameters, tumor dose and local control: the experience of the gustave-rousseau institute and the princess Margaret hospital. *Int J Radiat Oncol Biol Phys* (1985) 11(10):1751–7. doi: 10.1016/0360-3016(85)90027-6
15. Van Limbergen E, van der Schueren E, Van den Bogaert W, Van Wing J. Local control of operable breast cancer after radiotherapy alone. *Eur J Cancer*. (1990) 26(6):674–9. doi: 10.1016/0277-5379(90)90115-a
16. Shibamoto Y, Takano S, Iida M, Urano M, Ohta K, Oguri M, et al. Definitive radiotherapy with stereotactic or IMRT boost with or without radiosensitization strategy for operable breast cancer patients who refuse surgery. *J Radiat Res* (2022) 63(6):849–55. doi: 10.1093/jrr/rrac047



OPEN ACCESS

EDITED BY

Anders Wallqvist,
United States Army Medical Research and
Development Command, United States

REVIEWED BY

James Cheung,
Hong Kong Polytechnic University,
Hong Kong SAR, China
Jaidip Jagtap,
Mayo Clinic, United States
Rong Wu,
Shanghai General Hospital, China

*CORRESPONDENCE

Yulan Peng
✉ yulanpeng520@126.com

RECEIVED 12 November 2022

ACCEPTED 18 April 2023

PUBLISHED 09 May 2023

CITATION

Wang S, Wen W, Zhao H, Liu J, Wan X,
Lan Z and Peng Y (2023) Prediction of
clinical response to neoadjuvant therapy in
advanced breast cancer by baseline B-
mode ultrasound, shear-wave
elastography, and pathological information.
Front. Oncol. 13:1096571.
doi: 10.3389/fonc.2023.1096571

COPYRIGHT

© 2023 Wang, Wen, Zhao, Liu, Wan, Lan and
Peng. This is an open-access article
distributed under the terms of the [Creative
Commons Attribution License \(CC BY\)](#). The
use, distribution or reproduction in other
forums is permitted, provided the original
author(s) and the copyright owner(s) are
credited and that the original publication in
this journal is cited, in accordance with
accepted academic practice. No use,
distribution or reproduction is permitted
which does not comply with these terms.

Prediction of clinical response to neoadjuvant therapy in advanced breast cancer by baseline B-mode ultrasound, shear-wave elastography, and pathological information

Siyu Wang, Wen Wen, Haina Zhao, Jingyan Liu, Xue Wan, Zihan Lan and Yulan Peng*

Department of Medical Ultrasound, West China Hospital, Sichuan University, Chengdu, Sichuan, China

Background: Neoadjuvant therapy (NAT) is the preferred treatment for advanced breast cancer nowadays. The early prediction of its responses is important for personalized treatment. This study aimed at using baseline shear wave elastography (SWE) ultrasound combined with clinical and pathological information to predict the clinical response to therapy in advanced breast cancer.

Methods: This retrospective study included 217 patients with advanced breast cancer who were treated in West China Hospital of Sichuan University from April 2020 to June 2022. The features of ultrasonic images were collected according to the Breast imaging reporting and data system (BI-RADS), and the stiffness value was measured at the same time. The changes were measured according to the Response evaluation criteria in solid tumors (RECIST1.1) by MRI and clinical situation. The relevant indicators of clinical response were obtained through univariate analysis and incorporated into a logistic regression analysis to establish the prediction model. The receiver operating characteristic (ROC) curve was used to evaluate the performance of the prediction models.

Results: All patients were divided into a test set and a validation set in a 7:3 ratio. A total of 152 patients in the test set, with 41 patients (27.00%) in the non-responders group and 111 patients (73.00%) in the responders group, were finally included in this study. Among all unitary and combined mode models, the Pathology + B-mode + SWE model performed best, with the highest AUC of 0.808 (accuracy 72.37%, sensitivity 68.47%, specificity 82.93%, $P < 0.001$). HER2+, Skin invasion, Post mammary space invasion, Myometrial invasion and Emax were the factors with a significant predictive value ($P < 0.05$). 65 patients were used as an external validation set. There was no statistical difference in ROC between the test set and the validation set ($P > 0.05$).

Conclusion: As the non-invasive imaging biomarkers, baseline SWE ultrasound combined with clinical and pathological information can be used to predict the clinical response to therapy in advanced breast cancer.

KEYWORDS

advanced breast cancer, B-mode ultrasound, shear-wave elastography, neoadjuvant therapy, clinical response prediction

1 Introduction

Breast cancer has now surpassed lung cancer as the world's largest cancer, ranking first globally and fourth in China in the spectrum of cancer deaths in women (1, 2). Advanced breast cancer (ABC), including locally advanced breast cancer (LABC), and metastatic breast cancer, which cannot undergo radical surgery at present, are related to the high incidence of metastasis and poor prognosis (3, 4). Therefore, the main goal of its treatment is to delay the progress of the disease, prolong the survival time, and improve the quality of life of patients. Neoadjuvant therapy (NAT) and salvage therapy for M1 stage breast cancer, instead of surgical resection at diagnosis, are recommended as the preferred treatment to ABC to provide more surgical opportunities and improve the survival rate according to the National Comprehensive Cancer Network (NCCN) guidelines (5). Therefore, the accurate evaluation of the curative effect is of particular significance. At present, the evaluation of clinical response is mainly carried out through pathological and clinical methods, that is, preoperative Response Evaluation Criteria in Solid Tumors (RECIST1.1) (6) and postoperative Miller–Payne (MP) Grading Criteria classification (7). In clinical application, the timing of surgery and intraoperative tumor resection volume are based on clinical response (8), which should be predicted as early as possible and focused on during treatment.

Studies have proven that breast images can provide tumor biology behavior from multiple aspects but focus more on the changes during disease treatment. In the initial stage, the tumor baseline images can better reflect the original characteristics of the tumor. Ultrasonography is a low-cost imaging modality that increases cancer sensitivity and detection rates in dense breast populations. China has a relatively higher proportion of dense breast lesions than other countries (9), which explains the popularity and importance of ultrasound for Chinese breast screening. Moreover, with the continuous innovation of technology, multimodal ultrasound technology is more and more advocated because of its multiparameter and all-around evaluation ability. Shear wave elastography (SWE), a new technology in clinical applications in recent years, can provide quantitative information by measuring the stiffness of breast masses (10, 11). Adding quantitative SWE parameters to the BI-RADS feature in breast masses has been applied in clinical use to differentiate benign and malignant tumors, improving the specificity of breast US mass assessment without loss of sensitivity, especially in characterizing a complex lesion (12, 13). Furthermore, the deep learning model,

convolutional neural network (CNN) based on SWE parameters, greatly improves the accuracy and reliability of computer-aided diagnosis, which can be used for the detection and management of breast cancer (14, 15). Studies have shown that tumors with high stiffness are more likely to be associated with metastasis and poor prognosis (16, 17). The decrease in tumor stiffness during treatment is related to the curative effect (8). Nevertheless, the establishment of relevant models still needs more experiments, especially the application at the early stage.

This study aims to add imaging information to the traditional clinical and pathological indicators and predict the clinical response to therapy for advanced breast cancer through the tumor baseline situation, moving the prediction period forward to provide critical information for clinical treatment.

2 Materials and method

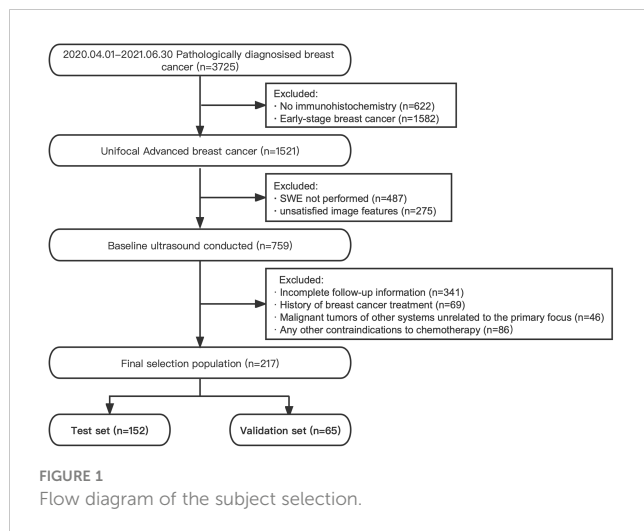
2.1 Patient characteristic

This retrospective, single-center study was conducted by the Declaration of Helsinki and approved by the West China Hospital of Sichuan University Biomedical Research Ethics Committee. All participants provided informed consent for inclusion before participation in the study.

The subjects were collected at West China Hospital of Sichuan University from April 2020 to June 2022. The inclusion criteria were as follows: (I) unifocal advanced breast cancer (T0~2N2M0, T3N0~2M0, T0~4N3M0, and T0~4N0~3M1) (18), (II) B-mode and SWE ultrasound examinations performed within 30 days before intervention, and (III) followed up for clinical response evaluation. The exclusion criteria were as follows: (I) previous treatment history, (II) primary malignancy in other organs, (III) any contraindications to therapeutic drugs, and (IV) pregnant women. All participants received standard cycle treatment according to standard protocols mentioned in the NCCN guidelines (5). The flow diagram of subject selection is shown in Figure 1.

2.2 Pathology information

Immunohistochemistry (IHC) and fluorescence *in situ* hybridization (FISH) tests were conducted for receptor expression estimate. Estrogen receptor (ER) and progesterone receptor (PR)



were recorded in the form of positive (+) or negative (–) and percentage (%) expression according to the American Society of Clinical Oncology/College of American Pathologists (ASCO/CAP) guideline (19). HER2+ was defined as HER2 3+ or FISH+, and the others were defined as HER2– (5). Ki-67 was directly reported as the percentage of positively stained nuclei. All tumors were divided into four IHC subtypes according to the St. Gallen criteria (20).

2.3 Ultrasound examinations

All patients underwent B-mode and SWE ultrasound examinations within 30 days before intervention (baseline), using Siemens OXANA2 ABVS ultrasonic device (Siemens Healthineers, Munich, Germany) equipped with 18L6 high frequency (15 MHz) and 9L4 linear-array (8 MHz) transducers. Radiologists have more than 5 years of breast diagnosis experience and, as one of the multi-center units, have unified requirements and training on operation

technology according to the Chinese Guidelines and Recommendations on the Clinical Use of Ultrasound Elastography (21).

First, to obtain the best B-mode ultrasound image, the major axis plane and plane vertical to it were acquired for each mass for measuring tumor size. Three diameters were recorded, and volume was calculated according to them. Images of each breast mass were interpreted according to ACR BI-RADS Atlas Fifth Edition (22) and documented the ultrasound imaging features, including maximum diameter (dmax), volume, orientation (parallel, not parallel), margin (regular, indistinct, angular, micro-lobulated, and spiculated), calcifications (absence or presence of suspicious calcifications), echo pattern (hypoechoic, isoechoic, and heterogeneous), posterior features (no posterior features, enhancement, shadowing, and combined pattern), peripheral tissue involvement (architectural distortion, duct changes, skin thickening, and skin edema), and invasion layers (skin, subcutaneous fat, gland, posterior mammary space, and muscle). The blood supply of the tumor was evaluated by Adler grades, and lymph node involvement was evaluated at the same time.

Then, the depth, focus, gain, local amplification, and other conditions were optimized and switched to SWE mode. The range scale is uniformly selected at 10 m/s. The patient was asked to hold his breath to reduce the impact of breathing movement on the image. After holding the probe until the elastic image remains stable for several seconds, the image was collected and played back, and the image was taken with the best color signal filling for quantitative measurement. The square region of interest (ROI) used for SWE acquisition was adjusted to include the entire mass and surrounding normal tissue observed in B-mode, excluding the skin and chest wall. In ROI, the default stiffness range was from blue to red (soft to hard). The examiner selected five points in the hardest area for elastic value collection (Site1) and one point in peripheral normal adipose tissue (Site2) (Figure 2). The system calculated the maximum lesion stiffness (E_{max}), minimum (E_{min}), median (E_{median}), mean

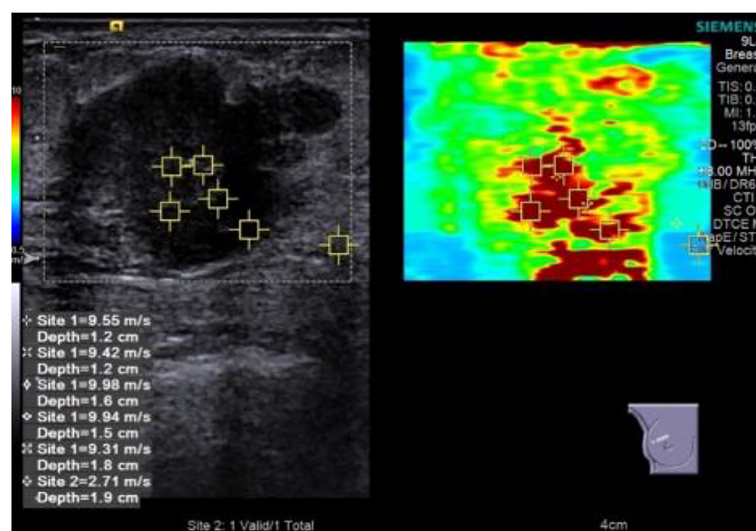


FIGURE 2
Elastic value acquisition: five points in the tumor's hard (red) area and one point in the peripheral normal adipose tissue.

(Emean), and standard deviation (Estd) automatically. Given that the system displays “High” when lesions velocity is higher than 10 m/s, these cases were set equivalent to the maximum value of 10 m/s for analysis.

2.4 Outcome

After completing the standard adjuvant treatment process, the oncologist conducted a comprehensive clinical and image evaluation (by MRI) on the curative effect according to RECIST1.1 guidelines (6) as follows:

- Progressive disease (PD): (I) at least a 20% increase in the sum of diameters of target lesions and demonstrating an absolute increase of at least 5 mm, (II) the appearance of new malignant lesions, and (III) a lesion identified on a follow-up study in an anatomical location that was not scanned at baseline.
- Stable disease (SD): (I) the smallest sum diameters of target lesion, neither sufficient shrinkage to qualify for PR nor sufficient increase to qualify for PD and (II) non-target lesions not all evaluated.
- Partial response (PR): (I) at least a 30% decrease in the sum of diameters of target lesions, taking as reference the baseline sum diameters and (II) persistence of one or more non-target lesion(s) and/or maintenance of tumor marker level above the normal limits.
- Complete response (CR): (I) disappearance of all target lesions, (II) any pathological lymph nodes (whether target or non-target) reduction in short axis to <10 mm, and (III) disappearance of all non-target lesions and normalization of tumor marker level.

We defined PD and SD as non-responders while PR and CR as responders.

2.5 Statistical analysis

Our final selection population was split into a test set for model development and a validation set in a 7:3 ratio. Univariate analyses were performed in the test set using Student's t-test, Mann-Whitney U-test, Pearson's chi-squared test, or Fisher's exact test to examine the factors associated with tumor response. For the multivariable analysis, we selected those covariates with p -values < .2 in the univariate analysis. The odd ratio (OR) and 95% confidence interval [CI] value of significant predictors were determined by the single or combined regression model. A receiver operating characteristic (ROC) curve and the area under the curve (AUC) were generated to assess the discriminative ability of the prediction model. Sensitivity and specificity were calculated using the best cutoff score for the clinical prediction rule and the Youden index for the ROC. In the validation set, the application effectiveness of the combined model was evaluated with AUC and Z-test. In all the

analyses, $p < 0.05$ were considered significant. Data were analyzed using SPSS v26.0 (SPSS, Inc., IMB Company Chicago, IL, USA).

3 Result

3.1 Clinical and pathological indicators

A total of 152 patients were finally included in the test set, with an average age of 47.98 ± 9.36 years at diagnosis. The initial clinical stages were T stages 1, 2, 3, and 4 (4.61%, 30.92%, 19.74%, and 44.74%); N stages 0, 1, 2, and 3 (3.29%, 22.37%, 36.84%, and 37.50%); and M stages 0 and 1 (84.21% and 15.79%). Invasive ductal carcinoma accounted for 81.58%, and other histological types accounted for 18.42%. According to the outcome indicators, 41 patients (27.00%) were divided into the non-responders group and 111 patients (73.00%) into the responders group. Age, T, N, and M stage, and histological type were not significantly correlated with the clinical response after NAT ($p = 0.831, 0.580, 0.905, 0.444$, and 0.464 , respectively) (Supplementary Appendix Table A1).

It showed that HER2+ was a significantly predictive indicator of clinical response, with 50.45% in responders group and 17.07% in non-responders group ($p < 0.001$). There were no differences in the expression of ER%, ER+/-, PR%, PR+/-, Ki-67%, and IHC subtypes between responders and non-responders groups ($p > 0.05$). In the pathology regression model, the factor with a significant predictive value was HER2+ (OR, 4.945; 95% CI, 2.022–12.098; $p < 0.001$). The prediction performance of one modality (Pathology) is listed in Table 1, with an AUC of 0.667 ($p = 0.002$), an accuracy of 59.21%, a sensitivity of 50.45%, and a specificity of 82.93%.

3.2 B-Mode ultrasound features

For size, we measured for responders and non-responders group; dmax was mean of 42.63 ± 21.64 vs. 50.88 ± 25.13 mm ($p = 0.060$), and volume was mean of $37,894.73 \pm 57,625.57$ vs. $71,956.78 \pm 112,500.60$ mm³ ($p = 0.105$). For features, mass without micro-lobulated margin (43.24% [48 of 111] vs. 21.95% [9 of 41]; $p = 0.016$), mass without spiculated margin (80.18% [89 of 111] vs. 60.97% [25 of 41]; $p = 0.015$), mass without skin thickening (79.28% [88 of 111] vs. 63.41% [26 of 41]; $p = 0.045$), mass without skin invasion (81.98% [91 of 111] vs. 63.41% [26 of 41]; $p = 0.016$), and mass without posterior mammary space invasion (19.81% [22 of 111] vs. 4.88% [2 of 41]; $p = 0.025$) were more frequently observed in the responders group than in the non-responders group. Furthermore, 1.80% (2 of 111) of BI-RADS 4b, 16.22% (18 of 111) of BI-RADS 4c, 81.98% (91 of 111) of BI-RADS 5 obtained the response also with statistical differences ($p = 0.034$). However, we found no significant differences in the proportions of regular margin (0 of 152), angular margin ($p = 0.291$), parallel ($p = 0.262$), calcifications ($p = 0.517$), posterior enhancement ($p = 0.144$), posterior shadowing ($p = 0.381$), posterior combined pattern ($p = 0.155$), duct change ($p = 1.000$), skin edema ($p = 0.053$), subcutaneous fat invasion ($p = 0.460$), myometrial invasion ($p =$

TABLE 1 AUC-ROC, sensitivity and specificity of one modality, two modalities, and three modalities and validation set.

| | AUC-ROC | 95% CI | Accuracy (%) | Sensitivity (%) | Specificity (%) | p-value |
|--------------------------|---------|-------------|--------------|-----------------|-----------------|---------|
| 1 modality | | | | | | |
| Pathology | 0.667 | 0.575-0.759 | 59.21 | 50.45 | 82.93 | 0.002 |
| B-mode | 0.712 | 0.623-0.801 | 58.55 | 48.65 | 85.37 | <0.001 |
| SWE | 0.585 | 0.493-0.676 | 57.24 | 47.75 | 82.93 | 0.110 |
| 2 modalities | | | | | | |
| Pathology + B-mode | 0.796 | 0.721-0.870 | 68.42 | 62.16 | 85.37 | <0.001 |
| Pathology + SWE | 0.712 | 0.622-0.801 | 73.68 | 74.77 | 70.73 | <0.001 |
| B-mode + SWE | 0.674 | 0.586-0.763 | 63.16 | 57.66 | 78.05 | 0.001 |
| 3 modalities | | | | | | |
| Pathology + B-mode + SWE | 0.808 | 0.586-0.763 | 72.37 | 68.47 | 82.93 | <0.001 |
| Validation Set | 0.755 | 0.655-0.870 | 72.31 | 70.00 | 80.00 | <0.001 |

AUCs, areas under the curve; ROC, receiver operating characteristic curve; CI, confidence interval; SWE, shear wave elastography. $p < 0.05$, the difference is statistically significant.

0.053), nipple invasion ($p=1.000$), lymph nodes ($p=0.294$), and Adler grads ($p=0.802$) between the responders group and non-responders group (Supplementary Appendix Table A2).

In the B-mode model, volume (OR, 1.000; 95% CI, 1.000–1.000; $p=0.008$), spiculated margin (OR, 0.431; 95% CI, 0.191–0.976; $p=0.043$), and myometrial invasion (OR, 0.353; 95% CI, 0.136–0.914; $p=0.032$) were the factors with a significant predictive value. The AUC under ROC was 0.712, with an accuracy of 58.55%, a sensitivity of 48.65%, and a specificity of 85.37% ($p<0.001$) (Table 1).

3.3 SWE parameters

Table 2 summarizes the relationship between SWE parameters and tumor response. The comparison of Emin and Emean was statistically significant with 8.31 ± 1.62 vs. 7.47 ± 2.11 m/s ($p=0.043$) and 8.97 ± 1.29 vs. 8.13 ± 1.93 m/s ($p=0.046$). No significant difference was found in Emax (9.54 ± 1.15 vs. 8.74 ± 1.80 m/s, $p=0.109$), Emedian (8.98 ± 1.34 vs. 8.17 ± 2.03 m/s, $p=0.098$), and Estd (0.52 ± 0.04 vs. 0.58 ± 0.46 , $p=0.602$) between the two groups. The AUC of ROC made by regression logistic (SWE model) was 0.585, with an accuracy of 57.24%, a sensitivity of 47.75%, and a specificity of 82.93% ($p=0.110$) (Table 1).

3.4 Predictive models development

All multivariate regression models are summarized in Table 1. Among the one-, two-, and three-modalities combined prediction models, the Pathology + B-mode + SWE model performed best, with the highest AUC of 0.808 (95% CI, 0.737–0.879; accuracy, 72.37%; sensitivity, 68.47%; specificity, 82.93%, $p<0.001$). The second is the Pathology + B-mode model with an AUC of 0.796

(95% CI, 0.721–0.870; accuracy, 68.42%; sensitivity, 62.16%; specificity, 85.37%; $p<0.001$). B-mode and Pathology + SWE models show the same AUC of 0.712, and the remaining prediction models were lower than the above, with an AUC < 0.700 (Figure 3).

In the optimal prediction model (three modalities), HER2+ (OR, 8.541; 95% CI, 2.966–24.595; $p<0.001$), skin invasion (OR, 0.236; 95% CI, 0.085–0.654; $p=0.006$), post-mammary space invasion (OR, 0.178; 95% CI, 0.036–0.886; $p=0.035$), myometrial invasion (OR, 0.284; 95% CI, 0.096–0.842; $p=0.023$), and Emax (OR, 0.672; 95% CI, 0.471–0.959; $p=0.028$) were the factors with a significant predictive value (Table 3).

Based on the data in Table 3, we established the following logistic model:

$$p = 1 / 1 + \exp \sum_{\text{mammary space invasion on US}} [6.123 + 2.145 \times (\text{if HER2+}) - 1.443 \times (\text{if skin invasion on US}) - 1.725 \times (\text{if post-mammary space invasion on US}) - 1.259 \times (\text{if myometrial invasion on US}) - 0.397 \times (\text{Emax})]$$

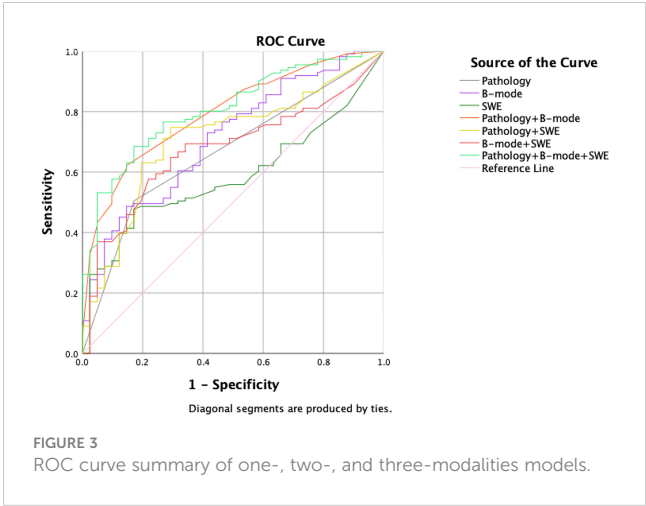
3.5 Validation of predictive model

The calculated p-value was compared with the probability value of the cutoff point of the final combined model. Greater than means a response, and less than means no response. The distribution of all the variables were statistically not different between test and validation sets (all, $p>0.05$) (Supplementary Appendix Tables B1–3). The outcomes are grouped according to the cutoff value in the validation set and then validated. There were 35 true positives, 3 false positives and 15 false negatives, 12 true negatives. The AUC of the validation set was 0.775 (95% CI, 0.655–0.870, $p<0.001$) (Table 1). Compared with the three-modalities model, the AUC was 0.775 vs. 0.808, the accuracy was 72.31% vs. 72.37%, the sensitivity was 70.00% vs. 68.47%, and the specificity was 80.00% vs. 82.93%. After Z-test, there was no statistical difference in ROC between the test set and the validation set ($p>0.05$).

TABLE 2 Summary of the SWE parameters for the 152 patients.

| Parameters | Mean ± SD | | Minimum | | Maximum | | Median | | p-value |
|---------------------|-----------------------|--------------------|-----------------------|--------------------|-----------------------|--------------------|-----------------------|--------------------|---------|
| | Non-responders (n=41) | Responders (n=111) | Non-responders (n=41) | Responders (n=111) | Non-responders (n=41) | Responders (n=111) | Non-responders (n=41) | Responders (n=111) | |
| E _{max} | 9.54 ± 1.15 | 8.74 ± 1.80 | 3.07 | 3.28 | 10.00 | 10.00 | 9.87 | 9.76 | 0.109 |
| E _{min} | 8.31 ± 1.62 | 7.47 ± 2.11 | 1.94 | 2.77 | 10.00 | 10.00 | 8.67 | 8.05 | 0.043 |
| E _{median} | 8.98 ± 1.34 | 8.17 ± 2.03 | 2.68 | 2.85 | 10.00 | 10.00 | 9.41 | 9.22 | 0.098 |
| E _{mean} | 8.97 ± 1.29 | 8.13 ± 1.93 | 2.63 | 2.97 | 10.00 | 10.00 | 9.31 | 8.92 | 0.046 |
| E _{std} | 0.52 ± 0.40 | 0.58 ± 0.46 | 0.00 | 0.00 | 1.59 | 2.47 | 0.46 | 0.48 | 0.602 |

Data are mean ± standard deviation. p-values for difference were determined by Mann-Whitney U test; p<0.05, the difference is statistically significant.



4 Discussion

In this study, the clinical and ultrasonic characteristics and SWE parameters of 152 patients with advanced breast cancer were analyzed to obtain efficacy predictors and establish prediction models, which were well-validated in 65 validation sets. The research results show that histological characteristics, baseline B-mode characteristics, and SWE parameters are all related to the clinical response of adjuvant therapy. The combined prediction model of the three can improve the prediction ability to a certain extent.

We observed that there is no statistical significance in the clinical TNM stage. At the same time, it is not consistent with the results of recent studies, which pointed out that cT1/cT2 can be associated with a good prognosis (23), and high lymph node burden (N stage) will indicate adverse prognosis (24). The main reason may be the generally large tumor diameter and volume of advanced breast cancer and the high proportion of T4 (44.74%), and 96.05% of them are accompanied by lymph node metastasis, resulting in no significant difference in statistical analysis.

In our study, the expression of HER2 is significantly correlated with tumor response, which is in agreement with the subjects and results of a retrospective study by Zheng et al. They confirmed that the response of adjuvant therapy is equivalent to that of NAT in patients with HER2+ and emphasized that patients with cT3/4 or those with positive clinical nodal status were more likely to benefit from NAT (25). Because of the overexpression of the oncogene ERBB2, HER2+ promotes the growth of cancer cells, which results in positive progress and a worse prognosis (26). However, as a therapeutic target, HER2+ BC has been proven to be more sensitive to targeted therapy than other IHC subtypes (27, 28). In each prediction model, HER2+ showed a great contribution that reemphasized its importance. However, the correlation between other biomarkers or IHC subtypes and clinical response is not found in our study, which differs from the report of ER+ and Ki-67% as diagnostic predictors proposed by some previous studies (29–32). It may be the deviation caused by sample size and different proportions of IHC subtypes, and the above studies are mostly focused on a certain subtype.

TABLE 3 Independent influencing factors in three modalities (Pathology + B-mode US + SWE) model.

| Factors | B | OR | 95% CI | p-values |
|-----------------------------|--------|-------|--------------|----------|
| HER2+ | 2.145 | 8.541 | 2.966-24.595 | <0.001 |
| Skin invasion | -1.443 | 0.236 | 0.085-0.654 | 0.006 |
| Post mammary space invasion | -1.725 | 0.178 | 0.036-0.886 | 0.035 |
| Myometrial invasion | -1.259 | 0.284 | 0.096-0.842 | 0.023 |
| Emax | -0.397 | 0.672 | 0.471-0.959 | 0.028 |

OR, odds ratio; HER2+, human epidermal growth factor receptor-2 positive; Emax, maximum lesion stiffness. $p < 0.05$, the difference is statistically significant.

The association between baseline US images and adjuvant treatment outcomes was also demonstrated. Some studies have shown that tumors with larger dmax or metabolic volume are more likely to have a poor response (33, 34); dmax and volume of lesions in non-responders group were also relatively larger in this study, although $p > 0.05$. As discussed above, the recognized relationship between tumor size and prognosis may have been lost for relatively large tumors in the late stage. On the other hand, the image measurement error is large, and the vertical aspect ratio judgment may be inaccurate to a certain extent.

Studies of baseline image features of breast cancer at mammography and MRI have demonstrated that the tumor response is more likely in well-defined, oval or round lesions than in diffuse or irregular ones (33, 35). As we concluded, micro-lobulated and spiculated margins were negatively correlated with the response, which is also one of the common imaging features of all malignant tumors but may be more significant in advanced breast cancer. Additionally, skin, post-mammary space, and myometrial invasion were factors negatively correlated with treatment response in our models. Breast cancer generally occurs in the glandular layer, invading surrounding layers with its invasion and growth, which can be distinguished on ultrasonic images. Our results suggest that the tumor longitudinal, instead of the overall size for advanced breast cancer, is a dependently predictive prognostic factor. Results also showed that patients with non-skin thickening achieved more treatment response, which is proven to be tumor involving the skin, resulting in lymphatic and venous obstruction, massive invasion of subdermal connective tissue, and systemic metastasis (36). Evans and Wen reported that skin thickening (>2.5 mm) revealed by ultrasound imaging was independently related to lymph node load, and the 6-year metastasis-free survival (MFS) of women with skin thickening was worse ($p = 0.032$, 6-year MFS 52% vs. 68%) (37, 38). Not parallel to the skin, calcifications and posterior features described by ultrasound were usually related to malignant tumors in histopathology (39, 40), which are not in this study. Such differences may indicate that in advanced breast cancer, these image features were common or difficult to distinguish due to fusion, resulting in decreased sensitivity of the prompt and not providing better prognostic information.

Emean and Emin were significantly correlated with NAT response in this study. Because all the elastic values come from the hard areas of the tumor, they reflect the elastic characteristics of the tumor to a greater extent. We can find no significant difference in tumor homogeneity between the two groups before treatment. However, there was a trend for the averaged stiffness in the responders group

to be lower among all parameters, as a high SWE value is generally related to adverse prognosis because of the increase in extracellular matrix components of malignant tumors, the invasion of cancer cells into tissues, or the fibroproliferative reaction (41, 42). A meta-analysis reported that SWE-combined AUC of the NAC response was 0.82 (sensitivity, 79%; specificity, 81%) (43). Although our SWE model cannot independently predict tumor response ($p > 0.05$), great predictive value has been shown in Emax for the combined model, which is consistent with Son that high Emean and Emax values were associated with invasive tumor size, high histological grade, and positive lymphatic vascular invasion ($p < 0.05$), and could predict poor prognosis (44).

Wang summarized in a review that the combined application of various commonly used ultrasound technologies can well predict the response of NAT, with an AUC of 0.71–0.92 (45), and the addition of tumor clinicopathological information will improve the ability of the prediction model to a certain extent (30, 32). Different from previous studies on pathological response, we established the prediction model focused on clinical response, and the combined model shows the best prediction ability with an AUC of 0.808. The factors contributing to the model (HER2+, skin invasion, post-mammary space invasion, myometrial invasion, and Emax) were also highly consistent with the results of univariate analysis, suggesting that particular attention should be paid to these factors. Although in the combined model, compared with pathology and B mode, the addition of SWE does not significantly improve the AUC of the model. This may be attributed to the following reasons. First of all, the research proved that the diagnosis efficiency of SWE alone is lower than that of B-mode (46, 47), which is consistent with the model AUC obtained by our single SWE mode, indicating that the use of SWE needs to be based on conventional US, with additional reference information, rather than being used alone. In addition, SWE is more accurate for small tumors (48) and has limited ability to assess deep lesions (45). However, it still slightly improved the AUC of our prediction model, so the application of SWE in advanced breast cancer is the potential to some extent. It is a supplement to the information in different dimensions of conventional ultrasound while improving the accuracy and sensitivity of the model, although the specificity is slightly reduced, which can give more clinical indications to patients with poor prognoses to pay attention to them. In the future, more samples and groups will be needed for detailed analysis.

Our study has some limitations: (I) this study was performed in a single center, lacking regional representation; (II) the number of patients in the study is modest, so differences in performance according to immunophenotype have not been assessed; and (III)

it is a retrospective study, but the ultrasonic examination method used in this study refers to a multicenter study of our research group (49) with specified unified standards.

5 Conclusions

Our study suggests that in patients with advanced breast cancer treated with NAT and salvage therapy for the M1 stage, the model established by baseline B-mode and SWE ultrasound combined with clinical and pathological indicators can predict the clinical response with better ability. Therefore, a more comprehensive ultrasound examination should be carried out before the intervention to provide critical information for clinicians to formulate personalized treatment strategies in the diagnosis stage.

Data availability statement

The original contributions presented in the study are included in the article/Supplementary Material. Further inquiries can be directed to the corresponding author.

Author contributions

Study conception and design: SW, WW and YP. Administrative support: YP and HZ. Provision of study materials or patient recruitment: XW, JL and HZ. Data collection: SW and ZL. Data analysis and interpretation: SW and WW. All authors contributed to the article and approved the submitted version.

Funding

This work was supported by the Achievement Conversion and Guidance Project of Chengdu Science and Technology Bureau, China (No.2017-CY02-00027-GX).

Acknowledgments

We thank all of the participants recruited for this study.

References

1. Siegel R, Miller K, Jemal A. Cancer statistics, 2020. *CA: Cancer J Clin* (2020) 70 (1):7–30. doi: 10.3322/caac.21590
2. Sung H, Ferlay J, Siegel RL, Laversanne M, Soerjomataram I, Jemal A, et al. Global cancer statistics 2020: globocan estimates of incidence and mortality worldwide for 36 cancers in 185 countries. *CA Cancer J Clin* (2021) 71(3):209–49. doi: 10.3322/caac.21660
3. Singletary SE, Allred C, Ashley P, Bassett LW, Berry D, Bland KI, et al. Revision of the American joint committee on cancer staging system for breast cancer. *J Clin Oncol* (2002) 20(17):3628–36. doi: 10.1200/JCO.2002.02.026
4. Giordano S. Update on locally advanced breast cancer. *Oncol* (2003) 8(6):521–30. doi: 10.1634/theoncologist.8-6-521
5. Gradishar WJ, Anderson BO, Abraham J, Aft R, Agnese D, Allison KH, et al. Breast cancer, version 3.2020, nccn clinical practice guidelines in oncology. *J Natl Compr Canc Netw* (2020) 18(4):452–78. doi: 10.6004/jnccn.2020.0016
6. Eisenhauer EA, Therasse P, Bogaerts J, Schwartz LH, Sargent D, Ford R, et al. New response evaluation criteria in solid tumours: revised recist guideline (Version 1.1). *Eur J Cancer* (2009) 45(2):228–47. doi: 10.1016/j.ejca.2008.10.026

Conflict of interest

The authors declare that the research was conducted in the absence of any commercial or financial relationships that could be construed as a potential conflict of interest.

Publisher's note

All claims expressed in this article are solely those of the authors and do not necessarily represent those of their affiliated organizations, or those of the publisher, the editors and the reviewers. Any product that may be evaluated in this article, or claim that may be made by its manufacturer, is not guaranteed or endorsed by the publisher.

Supplementary material

The Supplementary Material for this article can be found online at: <https://www.frontiersin.org/articles/10.3389/fonc.2023.1096571/full#supplementary-material>

SUPPLEMENTARY TABLE 1

Summary of the clinical and pathological indicators of the patients included in the test set. ER, estrogen receptor; PR, Progesterone receptor; HER2, human epidermal growth factor receptor-2; IHC subtype, immunohistochemistry subtype. *Quantitative data are mean \pm standard deviation; $P < 0.05$, the difference is statistically significant.

SUPPLEMENTARY TABLE 2

Summary of the B-mode US features of the patients included in the test set. BI-RADS, Breast imaging reporting and data system. *Quantitative data are mean \pm standard deviation; Qualitative data are absent/present and percentage; $P < 0.05$, the difference is statistically significant.

SUPPLEMENTARY TABLE 1

The distribution of the clinical and pathological indicators between test and validation sets. ER, estrogen receptor; PR, Progesterone receptor; HER2, human epidermal growth factor receptor-2; IHC subtype, immunohistochemistry subtype. *Quantitative data are mean \pm standard deviation; $P < 0.05$, the difference is statistically significant.

SUPPLEMENTARY TABLE 2

The distribution of the B-mode US features between test and validation sets. BI-RADS, Breast imaging reporting and data system. *Quantitative data are mean \pm standard deviation; Qualitative data are absent/present and percentage; $P < 0.05$, the difference is statistically significant.

SUPPLEMENTARY TABLE 3

The distribution of the SWE parameters between test and validation sets. *Data are mean \pm standard deviation. P values for difference were determined by Mann-Whitney U test; $P < 0.05$, the difference is statistically significant.

7. Ogston KN, Miller ID, Payne S, Hutcheon AW, Sarkar TK, Smith I, et al. A new histological grading system to assess response of breast cancers to primary chemotherapy: prognostic significance and survival. *Breast* (2003) 12(5):320–7. doi: 10.1016/s0960-9776(03)00106-1
8. Wang H, Mao X. Evaluation of the efficacy of neoadjuvant chemotherapy for breast cancer. *Drug Des Devel Ther* (2020) 14:2423–33. doi: 10.2147/DDDT.S253961
9. Yang Y, Liu J, Gu R, Hu Y, Liu F, Yun M, et al. Influence of factors on mammographic density in premenopausal Chinese women. *Eur J Cancer Prev* (2016) 25(4):306–11. doi: 10.1097/cej.0000000000000177
10. Cantisani V, David E, Barr RG, Radzina M, de Soccio V, Elia D, et al. Ultrasound elastography for breast lesion characterization: prospective comparison of us birads, strain elastography and shear wave elastography. *Ultraschall Med* (2021) 42(5):533–40. doi: 10.1055/a-1134-4937
11. Sigrist RMS, Liao J, Kaffas AE, Chammas MC, Willmann JK. Ultrasound elastography: review of techniques and clinical applications. *Theranostics* (2017) 7(5):1303–29. doi: 10.7150/thno.18650
12. Nasief HGR-M, Zagzebski IM, Hall JA, Timothy J. A quantitative ultrasound-based multi-parameter classifier for breast masses. *Ultrasound Med Biol* (2019) 45(7):1603–16. doi: 10.1016/j.ultrasmedbio.2019.02.025
13. Chen J, Ma J, Li C, Shao S, Su Y, Wu R, et al. Multi-parameter ultrasonography-based predictive model for breast cancer diagnosis. *Front Oncol* (2022) 12:1027784. doi: 10.3389/fonc.2022.1027784
14. Mao Y, Lim H, Ni M, Yan W, Wong D, Cheung J. Breast tumour classification using ultrasound elastography with machine learning: a systematic scoping review. *Cancers* (2022) 14(2):367. doi: 10.3390/cancers14020367
15. Guo R, Lu G, Qin B, Fei B. Ultrasound imaging technologies for breast cancer detection and management: a review. *Ultrasound Med Biol* (2017) 44(1):37–70. doi: 10.1016/j.ultrasmedbio.2017.09.012
16. Song EJ, Sohn YM, Seo M. Diagnostic performances of shear-wave elastography and b-mode ultrasound to differentiate benign and malignant breast lesions: the emphasis on the cutoff value of qualitative and quantitative parameters. *Clin Imag* (2018) 50:302–7. doi: 10.1016/j.clinimag.2018.05.007
17. Evans A, Sim YT, Pourreyaon C, Thompson A, Jordan L, Fleming D, et al. Pre-operative stromal stiffness measured by shear wave elastography is independently associated with breast cancer-specific survival. *Breast Cancer Res Treat* (2018) 171(2):383–9. doi: 10.1007/s10549-018-4836-5
18. Amin MB, Greene FL, Edge SB, Compton CC, Gershengwald JE, Brookland RK, et al. The eighth edition ajcc cancer staging manual: continuing to build a bridge from a population-based to a more “Personalized” approach to cancer staging. *CA Cancer J Clin* (2017) 67(2):93–9. doi: 10.3322/caac.21388
19. Allison K, Hammond M, Dowsett M, McKernin S, Carey L, Fitzgibbons P, et al. Estrogen and progesterone receptor testing in breast cancer: ASCO/CAP guideline update. *J Clin Oncol* (2020) 38(12):1346–66. doi: 10.1200/jco.19.02309
20. Goldhirsch A, Wood W, Coates A, Gelber R, Thürlimann B, Senn H. Strategies for subtypes—dealing with the diversity of breast cancer: highlights of the st. gallen international expert consensus on the primary therapy of early breast cancer 2011. *Ann Oncol* (2011) 22(8):1736–47. doi: 10.1093/annonc/mdr304
21. Organized and compiled by the Chinese Society of Ultrasound in Medicine; Liang Ping, Jiang Yuxin. *Chinese Guidelines and recommendations on the clinical use of ultrasound elastography*. Beijing: People's Medical Publishing House (2018). p. 126.
22. Mercado CL. Bi-rads update. *Radiol Clin North Am* (2014) 52(3):481–7. doi: 10.1016/j.rcl.2014.02.008
23. Thill M, Friedrich M, Kolberg-Liedtke C, Albert US, Banys-Paluchowski M, Bauerfeind I, et al. Ago recommendations for the diagnosis and treatment of patients with locally advanced and metastatic breast cancer: update 2021. *Breast Care (Basel)* (2021) 16(3):228–35. doi: 10.1159/000516420
24. Mougalian SS, Hernandez M, Lei X, Lynch S, Kuerer HM, Symmans WF, et al. Ten-year outcomes of patients with breast cancer with cytologically confirmed axillary lymph node metastases and pathologic complete response after primary systemic chemotherapy. *JAMA Oncol* (2016) 2(4):508–16. doi: 10.1001/jamaoncol.2015.4935
25. Zheng S, Li L, Chen M, Yang B, Chen J, Liu G, et al. Benefits of neoadjuvant therapy compared with adjuvant chemotherapy for the survival of patients with Her2-positive breast cancer: a retrospective cohort study at fusc. *Breast* (2022) 63:177–86. doi: 10.1016/j.breast.2022.03.015
26. Gunasekara ADM, Anothaisintawee T, Youngkong S, Ha NT, McKay GJ, Attia J, et al. Neoadjuvant treatment with Her2-targeted therapies in Her2-positive breast cancer: a systematic review and network meta-analysis. *Cancers (Basel)* (2022) 14(3):523. doi: 10.3390/cancers14030523
27. Wuerstlein R, Harbeck N. Neoadjuvant therapy for Her2-positive breast cancer. *Rev Recent Clin Trials* (2017) 12(2):81–92. doi: 10.2174/1574887112666170202165049
28. Ortmann O, Blohmer JU, Sibert NT, Brucker S, Janni W, Wockel A, et al. Current clinical practice and outcome of neoadjuvant chemotherapy for early breast cancer: analysis of individual data from 94,638 patients treated in 55 breast cancer centers. *J Cancer Res Clin Oncol* (2023) 149(3):1195–209. doi: 10.1007/s00432-022-03938-x
29. Srivastava P, Wang T, Clark BZ, Yu J, Fine JL, Villatoro TM, et al. Clinical-pathologic characteristics and response to neoadjuvant chemotherapy in triple-negative low ki-67 proliferation (Tnlp) breast cancers. *NPJ Breast Cancer* (2022) 8(1):51. doi: 10.1038/s41523-022-00415-z
30. Gu J, Polley EC, Denis M, Carter JM, Pruthi S, Gregory AV, et al. Early assessment of shear wave elastography parameters foresees the response to neoadjuvant chemotherapy in patients with invasive breast cancer. *Breast Cancer Res* (2021) 23(1):52. doi: 10.1186/s13058-021-01429-4
31. Woo J, Oh SJ, Song JY, Chae BJ, Choi JE, Lee J, et al. Response to neoadjuvant chemotherapy based on pathologic complete response in very young patients with er-positive breast cancer: a large, multicenter, observational study. *BMC Cancer* (2021) 21(1):647. doi: 10.1186/s12885-021-08355-w
32. Ma Y, Zhang S, Zang L, Li J, Li J, Kang Y, et al. Combination of shear wave elastography and ki-67 index as a novel predictive modality for the pathological response to neoadjuvant chemotherapy in patients with invasive breast cancer. *Eur J Cancer* (2016) 69:86–101. doi: 10.1016/j.ejca.2016.09.031
33. Savaridas SL, Sim YT, Vinnicombe SJ, Purdie CA, Thompson AM, Evans A. Are baseline ultrasound and mammographic features associated with rates of pathological complete response in patients receiving neoadjuvant chemotherapy for breast cancer? *Cancer Imag* (2019) 19(1):67. doi: 10.1186/s40644-019-0251-3
34. Kim R, Chang JM, Lee HB, Lee SH, Kim SY, Kim ES, et al. Predicting axillary response to neoadjuvant chemotherapy: breast mri and us in patients with node-positive breast cancer. *Radiology* (2019) 293(1):49–57. doi: 10.1148/radiol.2019190014
35. Bae M, Shin S, Ryu H, Han W, Im S, Park I, et al. Pretreatment Mr imaging features of triple-negative breast cancer: association with response to neoadjuvant chemotherapy and recurrence-free survival. *Radiology* (2016) 281(2):392–400. doi: 10.1148/radiol.2016152331
36. Lawson BT, Vinnicombe S, Whelehan P, Macaskill EJ, Sim YT, Evans A. Associations between the ultrasound features of invasive breast cancer and breast cancer specific survival. *Clin Radiol* (2020) 75(11):879.e13–e21. doi: 10.1016/j.crad.2020.07.012
37. Evans A, Sim YT, Whelehan P, Savaridas S, Jordan L, Thompson A. Are baseline mammographic and ultrasound features associated with metastasis free survival in women receiving neoadjuvant chemotherapy for invasive breast cancer? *Eur J Radiol* (2021) 141:109790. doi: 10.1016/j.ejrad.2021.109790
38. Choong WL, Evans A, Purdie CA, Wang H, Donnan PT, Lawson B, et al. Mode of presentation and skin thickening on ultrasound may predict nodal burden in breast cancer patients with a positive axillary core biopsy. *Br J Radiol* (2020) 93(1108):20190711. doi: 10.1259/bjr.20190711
39. Stavros A, Thickman D, Rapp C, Dennis M, Parker S, Sisney G. Solid breast nodules: use of sonography to distinguish between benign and malignant lesions. *Radiology* (1995) 196(1):123–34. doi: 10.1148/radiology.196.1.7784555
40. Pfof A, Barr RG, Duda V, Busch C, Bruckner T, Spratte J, et al. A new practical decision rule to better differentiate bi-rads 3 or 4 breast masses on breast ultrasound. *J Ultrasound Med* (2022) 41(2):427–36. doi: 10.1002/jum.15722
41. Lu P, Weaver VM, Werb Z. The extracellular matrix: a dynamic niche in cancer progression. *J Cell Biol* (2012) 196(4):395–406. doi: 10.1083/jcb.201102147
42. Zhou J, Zhan W, Chang C, Zhang X, Jia Y, Dong Y, et al. Breast lesions: evaluation with shear wave elastography, with special emphasis on the “Stiff rim” sign. *Radiology* (2014) 272(1):63–72. doi: 10.1148/radiol.14130818
43. Jin J, Liu Y, Zhang B. Diagnostic performance of strain and shear wave elastography for the response to neoadjuvant chemotherapy in breast cancer patients: systematic review and meta-analysis. *J Ultrasound Med* (2022) 41(10):2459–66. doi: 10.1002/jum.15930
44. Son MJ, Kim S, Jung HK, Ko KH, Koh JE, Park AY. Can ultrasonographic vascular and elastographic features of invasive ductal breast carcinoma predict histologic aggressiveness? *Acad Radiol* (2020) 27(4):487–96. doi: 10.1016/j.jacr.2019.06.009
45. Wang J, Chu Y, Wang B, Jiang T. A narrative review of ultrasound technologies for the prediction of neoadjuvant chemotherapy response in breast cancer. *Cancer Manag Res* (2021) 13:7885–95. doi: 10.2147/CMAR.S331665
46. Sadigh G, Carlos R, Neal C, Dwamena B. Ultrasonographic differentiation of malignant from benign breast lesions: a meta-analytic comparison of elasticity and birads scoring. *Breast Cancer Res Treat* (2012) 133(1):23–35. doi: 10.1007/s10549-011-1857-8
47. Maier AM, Heil J, Harcos A, Sinn HP, Rauch G, Uhlmann L, et al. Prediction of pathological complete response in breast cancer patients during neoadjuvant chemotherapy: is shear wave elastography a useful tool in clinical routine? *Eur J Radiol* (2020) 128:109025. doi: 10.1016/j.ejrad.2020.109025
48. Feng S, Lotz T, Chase JG, Hann CE. Editors. An image based vibration sensor for soft tissue modal analysis in a digital image elastography (Diet) system. *Annu Int Conf IEEE Eng Med Biol Soc* (2010) 2010:25–8. doi: 10.1109/IEMBS.2010.5626070
49. Lin X, Chang C, Wu C, Chen Q, Peng Y, Luo B, et al. Confirmed value of shear wave elastography for ultrasound characterization of breast masses using a conservative approach in Chinese women: a Large-size prospective multicenter trial. *Cancer Manage Res* (2018) 10:4447–58. doi: 10.2147/cmar.S174690



OPEN ACCESS

EDITED BY

Alberto Farolfi,
Scientific Institute of Romagna for the
Study and Treatment of Tumors (IRCCS),
Italy

REVIEWED BY

Laura Kruper,
City of Hope National Medical Center,
United States
Carlos Martinez-Perez,
Medical Research Council Institute of
Genetics and Molecular Medicine (MRC),
United Kingdom

*CORRESPONDENCE

David Dabbs
✉ ddabbs@preludedx.com
Troy Bremer
✉ tbremer@preludedx.com

RECEIVED 13 October 2022

ACCEPTED 11 April 2023

PUBLISHED 19 May 2023

CITATION

Dabbs D, Mittal K, Heineman S,
Whitworth P, Shah C, Savala J, Shivers SC
and Bremer T (2023) Analytical validation
of the 7-gene biosignature for prediction
of recurrence risk and radiation therapy
benefit for breast ductal carcinoma *in situ*.
Front. Oncol. 13:1069059.
doi: 10.3389/fonc.2023.1069059

COPYRIGHT

© 2023 Dabbs, Mittal, Heineman, Whitworth,
Shah, Savala, Shivers and Bremer. This is an
open-access article distributed under the
terms of the [Creative Commons Attribution
License \(CC BY\)](https://creativecommons.org/licenses/by/4.0/). The use, distribution or
reproduction in other forums is permitted,
provided the original author(s) and the
copyright owner(s) are credited and that
the original publication in this journal is
cited, in accordance with accepted
academic practice. No use, distribution or
reproduction is permitted which does not
comply with these terms.

Analytical validation of the 7-gene biosignature for prediction of recurrence risk and radiation therapy benefit for breast ductal carcinoma *in situ*

David Dabbs^{1*}, Karuna Mittal¹, Scott Heineman¹,
Pat Whitworth^{2,3}, Chirag Shah⁴, Jess Savala¹, Steven C. Shivers¹
and Troy Bremer^{1*}

¹PreludeDx, Laguna Hills, CA, United States, ²University of Tennessee, Knoxville, TN, United States,
³Nashville Breast Center, Nashville, TN, United States, ⁴Department of Radiation Oncology, Taussig
Cancer Institute, Cleveland Clinic, Cleveland, OH, United States

Purpose: Ductal carcinoma *in situ* (DCIS), is a noninvasive breast cancer, representing 20–25% of breast cancer diagnoses in the USA. Current treatment options for DCIS include mastectomy or breast-conserving surgery (BCS) with or without radiation therapy (RT), but optimal risk-adjusted treatment selection remains a challenge. Findings from past and recent clinical trials have failed to identify a ‘low risk’ group of patients who do not benefit significantly from RT after BCS. To address this unmet need, a DCIS biosignature, DCISionRT (PreludeDx, Laguna Hills, CA), was developed and validated in multiple cohorts. DCISionRT is a molecular assay with an algorithm reporting a recurrence risk score for patients diagnosed with DCIS intended to guide DCIS treatment. In this study, we present results from analytical validity, performance assessment, and clinical performance validation and clinical utility for the DCISionRT test comprised of multianalyte assays with algorithmic analysis.

Methods: The analytical validation of each molecular assay was performed based on the Clinical and Laboratory Standards Institute (CLSI) guidelines Quality Assurance for Design Control and Implementation of Immunohistochemistry Assays and the College of American Pathologists/American Society of Clinical Oncology (CAP/ASCO) recommendations for analytic validation of immunohistochemical assays.

Results: The analytic validation showed that the molecular assays that are part of DCISionRT test have high sensitivity, specificity, and accuracy/reproducibility ($\geq 95\%$). The analytic precision of the molecular assays under controlled non-standard conditions had a total standard deviation of 6.6 (100-point scale), where the analytic variables (Lot, Machine, Run) each contributed $<1\%$ of the total variance. Additionally, the precision in the DCISionRT test result (DS) had a 95%CI ≤ 0.4 DS units under controlled non-standard conditions (Day, Lot, and Machine) for molecular assays over a wide range of clinicopathologic factor values. Clinical validation showed that the test identified 37% of patients in a low-risk group with a 10-year invasive IBR rate of $\sim 3\%$ and an absolute risk reduction (ARR) from RT of

1% (number needed to treat, NNT=100), while remaining patients with higher DS scores (elevated-risk) had an ARR for RT of 9% (NNT=11) and 96% clinical sensitivity for RT benefit.

Conclusion: The analytical performance of the PreludeDx DCISionRT molecular assays was high in representative formalin-fixed, paraffin-embedded breast tumor specimens. The DCISionRT test has been analytically validated and has been clinically validated in multiple peer-reviewed published studies.

KEYWORDS

DCIS - breast ductal carcinoma *in situ*, DCIS biomarkers and morphogenetic mechanisms, radiation therapy, analytical validation, radiogenomics, immunohistochemistry, DCISionRT

1 Introduction

The diagnosis of ductal carcinoma *in situ* (DCIS) has increased dramatically since the introduction and routine utilization of screening mammography (1). About 50,000 women are diagnosed with DCIS each year in the United States (2). Breast conservation surgery (BCS) followed by radiation therapy (RT) is the mainstay for DCIS treatment. BCS plus RT has been validated as a successful strategy to reduce the in-breast recurrence rate in patients diagnosed with DCIS in multiple RCTs (3), and BCS plus RT has been broadly adopted as a sufficient alternative approach to mastectomy (4–7), but not directly compared with mastectomy in a RCT. However, preventing over and undertreatment with radiotherapy remains the key challenge in the optimal treatment of DCIS given the heterogenous nature of the disease. Although the traditional clinicopathologic factors have been associated with risk of recurrence, they do not accurately determine an individual patient's recurrence risk, or importantly, the clinical benefit from adjuvant radiation therapy (3, 8–15). Additionally, pooled analysis of the multiple randomized clinical trials have shown that traditional clinicopathologic factors have limited capability in risk stratifying the DCIS patients and that there has not been a clinicopathologic patient subpopulation that has not benefited significantly from RT (3).

The goal of primary therapy for DCIS is to prevent invasive in-breast recurrences (IBR), as patient survival overall is excellent, with the choice of local treatment not impacting disease-specific or overall survival (16). At this time, current NCCN guidelines recommend that patients with DCIS should receive either 1) mastectomy, or 2) BCS with adjuvant RT, or 3) BCS alone without adjuvant RT (16). After definitive breast conserving surgery, 70% to 80% of women with DCIS will not have any IBR within 10 years, and 15% or fewer patients will benefit from adjuvant RT (3, 13). Thus, of the population of women treated with BCS, on an average 85% of women will not benefit from RT after BCS for preventing any IBR within 10 years. Consequently, BCS without RT is an option when the individual is considered to be “low-risk”, as for a low-risk patient, the absolute risk reduction of in-breast recurrence may not be large enough to justify the risks

associated with RT (16). The definition of “low-risk” has been described in general, commonly referencing prognostic clinicopathologic factors (nuclear grade, tumor size, patient age, and margin status). Typically, young age, high nuclear grade, tumor size > 2 cm, positive or close margins, or the presence of palpability have been considered high-risk features, while “low-risk” has been defined as the absence of these high-risk clinicopathologic factors, thus allowing for preferential treatment with endocrine therapy in hormone receptor-positive patients (16).

Several factors have been identified to contribute towards local recurrence and different classifiers based on clinicopathological factors have been tested with the goal of guiding patients to an appropriate level of treatment. Herein, Van Nuys Prognostic Index (VNPI) (that combines tumor size, margin size, grade, comedo-necrosis, and patient age) stratifies patients into scores ranging from 4 to 12 that lead to treatment recommendations of BCS, BCS+RT, or mastectomy (17, 18). However, the VNPI criteria does not provide a risk of recurrence after breast conserving surgery with and without radiation therapy and does not predict RT benefit (19).

Another clinicopathological factors-based nomogram combined data from seven variables (age, family history, detection method, grade, necrosis, margin size, and number of excisions), and accounts for the year of surgery and the absence of adjuvant RT and/or hormone therapy to predict the 10-year IBR rates (20). However, the nomogram specifies that all patients have an equally reduced score from radiation therapy, such that all patients are expected to benefit uniformly from RT. Despite the use of clinicopathologic driven risk stratifications, prospective trials have not demonstrated any clinicopathologic criterion which was predictive of a cohort of patients with DCIS that do not benefit with respect to local control from radiation therapy (3). Based on this, there has been no clear-cut low-risk population based on clinicopathologic features (21).

Despite the use of these “low-risk” clinicopathologic-driven risk stratifications, prospective trials have not demonstrated any clinicopathological criterion predictive of a cohort of patients with DCIS that do not benefit with respect to local control from radiation therapy (3). Based on this, there has been no clear-cut low-risk population based on clinicopathologic features (21).

However, improved risk stratification of DCIS may be achieved by employing a robust biological risk assessment, integrating molecular biology with clinical and pathologic factors as suggested by the NCI to provide an integrated assessment of ipsilateral recurrence risk as the basis to guide therapy and help prevent overtreatment and undertreatment (22).

Multiple studies have identified a number of molecular biomarkers that are prognostic for DCIS local recurrence rate including the status of HER-2 amplification (23), negative hormone receptor status (24, 25), and immunohistochemical detection of a range of biomarkers, including COX2 (26, 27), Ki67 (27), p16 (26–28), p53 (29, 30), p21 (31), and BNIP3 (32). But none of these markers have individually addressed the question of the expected differential benefit from radiation therapy. Thus, the utility of these biomarkers was limited and not clinically adopted for risk stratification of DCIS patients. Moreover, a commercialized RNA based 12 gene DCIS test, Oncotype DX DCIS Score[®], was validated retrospectively using a low-risk EORTC clinical trial population and an observational Canadian population (33, 34). The test provides an estimated risk of 10-year total and invasive recurrence risk but does not report any information on the predicted benefit of radiation therapy. Validation studies demonstrated that the test was prognostic but that 10-year IBR risks were higher for the intermediate than the high DCIS Score groups (10-year IBR intermediate DCIS score group 33% vs. 10-year IBR High DCIS score group 27.8%) (34–36) and there was no direct interaction of the DCIS score with RT in the study (35). Of note, the low risk and high risk groups had approximately the same relative benefit from RT (19, 33).

The DCISionRT test is a biosignature that was developed to address this unmet need and is the first genomic test to predict radiation therapy benefit in patients with DCIS. DCISionRT provides a comprehensive assessment of the woman's ipsilateral breast cancer recurrence risk after breast-conserving surgery with and without RT by integrating tumor molecular biology and clinicopathology. The biosignature/test is a multianalyte assay with algorithmic analysis (MAAA). The test integrates protein expression of seven critical genes measured in formalin-fixed paraffin-embedded (FFPE) tumor tissue samples with four clinicopathologic factors (age, tumor extent, tumor palpability, tumor margin status) as inputs to the proprietary algorithm to report a score (37–41).

The DCISionRT test was derived from research performed at UCSF. The investigators identified that the level of P16^{INK4A} in combination with Ki67 provided a significant assessment of subsequent invasive breast event risk. In a subsequent nested case-control study that analyzed a DCIS cohort treated with BCS without RT, invasive-IBR was associated with palpability, young age, and the expression of p16, COX-2, and Ki-67 (27).

Following the discovery research at UCSF, PreludeDx (Laguna Hills, CA) further developed the test to account for the interactions between the different biomarkers and the clinicopathology factors, employing machine learning. A nonlinear algorithm was developed such that the value of a given risk factor depends on the values of other risk factors (37). This enabled the DCIS biosignature to account for the interdependencies and activation of the oncogenic

pathways commonly dysregulated in DCIS such as estrogen response pathway, HER2 pathway, cell cycle, survival and stress response leading to increased proliferation and cell survival. The biosignature was parameterized and tested using multiple cross-validation and produced a continuous score. Parameterization was performed with the training folds and evaluated using the validation folds of the UUH/UMASS study cohort (37). A continuous score ranging from zero to ten, termed the Decision Score (DS), was reported for each patient as the median of the multiple cross-validated results (37).

Furthermore, the results from initial studies using the DCISionRT biosignature showed there was a subset of the patients with high DS scores who had higher risk of recurrence after BCS plus RT treatment. Given the heterogeneous nature of the disease it was hypothesized that the biology underlying these high-risk patients was different than other patients and some specific pathway(s) were driving the aggressiveness and residual risk after BCS plus RT. Interestingly it was observed that a significant percentage of this high risk population was HER2 positive, further validating the findings from previous studies that DCIS shares similar genomic heterogeneity to invasive breast cancer comprising lesions that vary in their clinical presentation and outcomes. Thus, in order to further identify the subset of the patients with a greater risk of recurrence after BCS plus RT, additional pathways regulated by the existing DCISionRT biomarkers that could impact progression of breast cancer and contribute to the resistance of standard therapies were investigated, and the K-RAS pathway was identified as the putative pathway contributing to the aggressiveness in the high risk group. An algorithm was pre-specified to combine biomarkers (used by the DS biosignature) in a novel manner based on the biologic hypothesis that an activated K-RAS pathway would drive a proliferative, aggressive disease profile and thus could identify a subgroup of patients with higher residual risk after adjuvant RT i.e., a Residual Risk Subtype (RRt) (38).

The DCISionRT test has been validated to be prognostic for IBR risk and predictive for RT benefit in multiple clinical validation studies in over 1,600 patients from five different cohorts with long-term outcomes (37, 38, 40–42). In a prospective clinical utility study, RT recommendations were changed for about 40% of DCIS patients when DCISionRT was incorporated into routine treatment decision management, identifying low-risk patients who may avoid unnecessary and costly RT and associated potential toxicities (avoiding overtreatment), as well as identifying higher risk patients to appropriately receive a necessary, beneficial treatment (avoiding undertreatment) (39). In addition, a cost-effective analysis for use of DCISionRT in patients undergoing BCS for DCIS with or without RT has shown that treating the Elevated Risk group patients based on DCISionRT was most cost effective when compared to treating all patients diagnosed with DCIS (43).

To be clinically applicable, a test to guide DCIS treatment strategy must have validated analytical performance for the molecular assays and validated clinical performance for the reported test results. The clinical and analytic validity of a multianalyte molecular assay relies on the analytes, reagents, precise experimental techniques, correct application of controls,

and ultimately, an accurate interpretation of the data based on all the aforementioned factors in the post-analytic phase. Here we report the analytic performance of the DCISionRT test using well-established methods as per the recommended guidelines. The analytic performance of the DCISionRT assay system was performed at the PreludeDx centralized clinical laboratory, including all steps involved in clinical lab implementation. The clinical performance and clinical utility of the DCISionRT test was also summarized with clinical metrics and performance statistics.

2 Materials and methods

2.1 Study design

The analytical validation of each molecular assay was based on the Clinical and Laboratory Standards Institute (CLSI) guidelines for Quality Assurance for Design Control and Implementation of Immunohistochemistry Assays (44) and College of American Pathologists/American Society of Clinical Oncology (CAP/ASCO) recommendations for analytic validation of Immunohistochemical assays (45). Analytical validation demonstrates the assay's ability to measure the analyte of interest in specimens representative of the population of interest in the clinical laboratory. The molecular assay analytic sensitivity, analytic specificity, and analytic accuracy were determined by comparing observed results in representative tissues with known or expected positive and negative expression. Intra-laboratory analytic precision for each molecular assay was determined as the extent of agreement among results obtained by replicate testing of representative tissue specimens under specified variable assay conditions, including different equipment, antibody lots and testing day assessed by two pathologists, while reproducibility was assessed as the percent agreement between different pathologists (45). In-line with the goal of improving DCIS treatment management by ruling out overtreatment with RT, the clinical performance of the test for RT benefit was also reported as summary statistics based on standard definitions (46).

2.2 Analytical validation performance

The protein expression of each gene was assayed using immunohistochemistry in accordance with laboratory Standard Operating Procedures (SOPs). The primary monoclonal antibodies in each of the molecular assays were individually validated with the same SOPs, using cell lines and tissues that were fixed in 10% neutral buffered formalin and paraffin-embedded (FFPE) per CAP/ASCO guidelines (45). The tissue samples were assayed on a Leica BOND III, using monoclonal antibodies with pre-specified titers, a Leica Diluent dilution buffer, and specified pre-treatment and IHC protocols (36, 47). All biomarkers were scored for intensity and percentage (H-score) by board-certified pathologists at the PreludeDx CLIA laboratory. External negative isotype controls for each protein biomarker consisted of tissue samples that were processed with an isotype antibody with the same concentration and assay conditions as the test samples. Cell

lines were selected with a known positive expression for each protein biomarker, and in addition, the HER2 cell lines were selected to have known (negative, 1+, 2+, or 3+) expression (48). For each protein biomarker, tissue control samples with expected negative or positive expression were assayed to confirm that the observed expression was consistent with the expected expression. Normal organ (n=25) tissue samples (n=100) in a tissue microarray (TMA, BIOMAX FDA9ww2) were characterized using the molecular assays and reported in [Supplemental Table 2](#).

2.3 Molecular assay sensitivity, specificity, and accuracy

Analytic sensitivity and analytic specificity for each molecular assay were estimated as positive and negative concordance of the observed results, respectively, with either expected expression for a given tissue type or observed results from a standard referent inter-lab assay for comparison. Accuracy for each molecular assay was estimated as overall concordance of the observed results with results from a referent inter-lab assay (44). The molecular assays were read in a post-analytic phase by board-certified pathologists at the PreludeDx CLIA laboratory or a reference laboratory. A mix of invasive carcinomas, ductal carcinoma *in situ* tumor (DCIS), and normal organ tissue samples were purchased as tissue micro arrays (Biomax). Annual proficiency testing results (CAP) were utilized to augment the analytic validity of molecular assays for specific markers (PR, HER2, P16). The reported assay results for biomarkers PR, KI67, P16, and SIAH2 were summarized as percentages, while HER2 was summarized per CAP/ASCO adapted for DCIS (49), FOXA1 was summarized as a total H-score, and COX2 was summarized as an Allred Score (49). An inter-lab comparison was done for the PgR, Her2 and KI67 for total concordance as these assays were readily performed at other laboratories.

2.4 Molecular assay precision

The intra-lab molecular assay precision was determined by assaying consecutive sections of multiple tissue samples in a constructed tissue micro array over multiple days, using different primary antibody lots and equipment. The DCIS cases selected were each from a unique DCIS patient and were DCIS tumors with no microinvasion. Specifically, fifteen (15) tissue samples were constructed in a tissue micro array and assayed at PreludeDx (CLIA/CAP) in accordance with validated lab SOPs for controlled non-standard conditions (machine n=2, antibody lot n=2, and day of run n=3). At the beginning of a consecutive 5-day validation period, 12 TMA consecutive sections were cut, slide mounted, and stored at room temperature. Two pathologists independently scored the processed tissue samples in the post-analytical phase. Each molecular assay was normalized to a 100-point scale and the dispersion of the mean was calculated by comparing each of the replicate sample average scores from two pathologists to the mean score of the set of replicate samples, which was reported as the %

standard deviation for ease of comparison. CV was also reported as % std/mean score. The variance in the result attributed to each of the analytic factors combined within- and between-run random error was assessed using mixed effects modeling of the following form that was applied to assess the differences between mean vs. replicate biomarker score results using equation 1.

Equation 1:

$$Score_{ij} = SCORE_{ij} + Run_{ij} + Lot_{ij} + Machine_{ij} + \epsilon_{ij}$$

where i is the sample (1-15), and j is the reproducibility state (Run=3, Lot=2, Machine=2); $Score$ is the individual replicate scores from each biomarker assay, $SCORE$ is the mean score for each biomarker assay averaged over j reproducibility states, and $\epsilon_{ij} \sim iid N(0, \sigma_e^2)$ is (independent and identically distributed) random error.

The mixed effect modeling was implemented with the lmer function from the lme4 package in R version 4.1.1. Summary statistics were reported as percent total variance for reproducibility variables (Run, Lot, Machine), standard deviation, and percent of total variance.

2.5 Multianalyte assay with algorithm analysis: reproducibility

In addition to the pre-specified primary aim to analytically validate the multianalyte assay, the reproducibility of the reported MAAA results was determined, with an aim of highly reproducible test results with a total standard deviation (SD) of less than 0.4 DS units. Specifically, the seven biomarker results for each of the replicate DCIS TMA samples assayed with controlled non-standard conditions (machine, antibody lot, and run) were combined with a set of pre-specified clinicopathologic factors using SOPs. The clinicopathologic factors were age (40, 55, or 70 years; representing young pre-menopause, perimenopause, and older post-menopause), extent (5 mm, 15 mm and 45 mm; representing small, medium and larger DCIS), margin status (negative or positive ink on tumor), and palpability (no, yes). The DCISionRT algorithm was used to calculate the Decision Score (DS) for varying clinicopathologic factors ($n=36$) and seven biomarkers for the DCIS tissue samples ($n=15$), which yielded 540 mean DS results for each of the 12 variable assay conditions (machine $n=2$, antibody lot $n=2$, and day of run $n=3$). The variance in the DS result attributed to each of the analytical factors combined within- and between-run random error was assessed using a mixed effects modeling of the following form that was applied to assess the differences between 540 mean vs. 6,480 individual DS results using equation 2.

Equation 2:

$$DS_{ijk} = \overline{DS}_{ijk} + Run_{ijk} + Lot_{ijk} + Machine_{ijk} + \epsilon_{ijk}$$

Mixed effect modeling of precision variance, where i is the sample (1-15), j is the unique clinicopathologic set (1-12), and k is the reproducibility state (Run=3, Lot=2, Machine=2); DS are the average test results from two independent pathologist assessments,

\overline{DS} is the mean DS test result averaged over k reproducibility states, and $\epsilon_{ijk} \sim iid N(0, \sigma_e^2)$ is random error.

The mixed effect modeling was implemented with the lmer function from the lme4 package in R version 4.1.1. Summary statistics were reported as percent total variance for reproducibility variables (Run, Lot, Machine), standard deviation, percent of total variance, and 95% confidence interval of DS results.

2.6 Ethics approvals

Clinical performance of DCISionRT was summarized from previous studies approved by local ethics committees/boards from Uppsala University Regional Ethical Review Board (37), University of Massachusetts Medical School Tissue and Tumor Bank Institutional Review Board (37), the Kaiser Permanente Northwest Institutional Review Board (41), Umeå University Ethics Review Committee (40), and the Royal Melbourne Hospital and Affiliated Hospitals Ethics Review Board (42), as previously published.

2.7 Clinical performance: multianalyte assay with algorithm analysis

The clinical performance of the DCISionRT test for RT benefit was summarized for all validation studies by biosignature risk groups as absolute 10-year IBR rates after BCS treatment with and without RT, absolute risk reductions (ARR), and the number of patients needed to treat (NNT) (37, 38, 40, 41). NNT was defined as $1/ARR$. Summary performance statistics (NPV, PPV, sensitivity, specificity) were calculated based on a confusion matrix and standard definitions for count data (equation 3 presented in Supplementary Table 4) adapted to right-censored event data (equation 4) (46).

Equation 4:

| | RT Benefit | No RT Benefit | Summary Statistics |
|--|---|--|--|
| Test Positive for RT Benefit ($X > z$), N_{POS} | $a = \widehat{TP}$ $= \widehat{ARR}_{KM}(t X > z) * N_{POS}$ | $b = \widehat{FP}$ $= N_{POS} - a$ | $PPV = a/(a+b)$ $= \widehat{ARR}_{KM}(t X > z);$ $N_{POS} = a+b$ |
| Test Negative for RT Benefit ($X \leq z$), N_{NEG} | $c = \widehat{FN}$ $= N_{NEG} - d$ | $d = \widehat{TN}$ $= (1 - \widehat{ARR}_{KM}(t X \leq z)) * N_{NEG}$ | $NPV = d/(c+d)$ $= 1 - \widehat{ARR}_{KM}(t X \leq z);$ $N_{NEG} = c+d$ |
| Summary Statistics | Sensitivity = $a/(a+c) * 100$ | Specificity = $d/(b+d) * 100$ | $\widehat{ARR}_{KM}(t X > z) =$ $\hat{S}_{KM}(t X > z, No RT) -$ $\hat{S}_{KM}(t X > z, RT)$ |

Summary statistics using right censored event data. NPV = negative predictive value; PPV = positive predictive value; \widehat{TP} = estimated true positive; \widehat{TN} = estimated true negative; \widehat{FP} = estimated false positive; \widehat{FN} = estimated false negative; $\widehat{ARR}(t)$ = estimated absolute IBR risk reduction (ARR) from RT by Kaplan-Meier analysis at time t ; $\hat{S}_{KM}(t|X > z, RT)$ = Kaplan Meier IBR rate estimate at time t evaluated for Test Positive group ($X > z$) treated with RT; $\hat{S}_{KM}(t|X > z, No RT)$ = Kaplan Meier IBR rate estimate at time t evaluated for Test Positive group ($X > z$) treated with No RT; $\widehat{ARR}(t|X > z)$ = Estimated ARR by

Kaplan Meier analysis at time t evaluated for Test Positive Group ($X > z$); $\widehat{ARR}(t|X \leq z)$ = Estimated Absolute Risk Reduction at time t evaluated for Test Negative Group ($X \leq z$); X = Test covariate; z = Test covariate threshold; N_{POS} = Number of Patients with Test Positive; N_{NEG} = Number of Patients with Test Negative.

3 Results

3.1 Molecular assay characterization

The molecular assays utilized a selected primary antibody for each biomarker, as characterized in Table 1 (Manufacturer, Clone Type/Host, Isotype, and Immunogen). Isotype responses for all antibodies were negative (0+ 100%) for known positive tissue controls for each antibody. Representative results for organ tissue positive controls are illustrated in Supplemental Figure 1. Detection kit (antibody-negative) controls were negative (0+ 100%) in the consecutive sections of the known positive tissue controls for each antibody in Supplemental Figure 1.

The cell lines were processed and embedded in paraffin similar to the tissue samples. Observed results for each cell line and FFPE tissue control were concordant with previously reported expression profiles (expected results) and are presented in Table 2. Representative molecular assay results in DCIS tissue samples with varying protein expression are shown in Supplemental Figure 2. Summary results for positive or negative expression in normal organ tissues are listed in Supplemental Table 1.

The positive percent concordance (estimating analytic sensitivity) and negative percent concordance (estimating analytic specificity) of the molecular assays with expected results are summarized in Table 3 for specified thresholds for each biomarker. The tissue type used to validate each biomarker is summarized in Table 3 and detailed in Supplemental Table 2.

Tissues with expected negative and positive expression for each biomarker were a major component of validating molecular assays,

including the use of breast cancer tumors, other tumors, and normal organ tissue samples. For the tissue samples that were expected to be positive and negative, the corresponding percent positive concordance (estimating analytic sensitivity) and percent negative concordance (estimating analytic specificity) were $\geq 95\%$ for all of the molecular assays. The total concordance (estimating accuracy/reproducibility) was $\geq 95\%$ for all of the molecular assays with inter-lab comparisons available.

The precision of each molecular assay under controlled non-standard conditions is summarized in Table 4, accounting for differing antibody lots, machines, and runs on non-consecutive days. The overall standard deviation of the dispersion of the mean over replicates under controlled non-standard conditions was 6.6%, and the analytic variables Lot, Machine and Run accounted for ($<1\%$) of the total variance on average.

The reproducibility of the DCISionRT assay system was assessed as the dispersion of the DS mean, under controlled non-standard conditions (antibody lot, machines, and runs on non-consecutive days) in addition to implicit within and between run variances. The analysis of the sources of variance of the dispersion of DS from the DS mean is shown in Table 5. There were 540 mean DS test results that were derived from the molecular assay results for the seven (7) biomarkers and the 15 unique DCIS tumor tissue samples combined with the clinicopathologic factor sets. The reported DS results ranged from 0.8 to 10 with a mean of 5.7 (1st quartile: 2.8, 3rd quartile 9.2). The overall standard deviation of the dispersion of the mean over replicates under controlled non-standard conditions was low (0.20/10 point scale), and the analytic variables Lot, Machine and Run accounted for ($<1\%$) of the total variance on average, where the DS confidence interval was (95%CI: -0.4, 0.4) on a 10-point scale.

3.2 Clinical performance

The absolute risk reduction (ARR) from RT in 10-year IBR rates are reported for DCISionRT Risk groups for the SweDCIS

TABLE 1 Antibody characteristics.

| Protein | Manufacturer | Clone | Type/Host | Isotype | Immunogen |
|-----------|--------------|------------|-------------------|-------------------|---|
| PgR | Leica | I6 | Monoclonal Mouse | IgG1 | N-Terminal Region of PgR form A |
| HER2 | Cell Marque | SP3 | Monoclonal Rabbit | IgG1 | Positions 654 and 655 of isoform a, positions 624 and 625 of isoform b |
| Ki-67 | Dako | MIB-1 | Monoclonal Mouse | IgG1 kappa | cDNA 1002bp fragment |
| COX-2 | Cell Marque | SP21 | Monoclonal Rabbit | IgG | A synthetic peptide from the C-terminus of rat cox2 |
| FOXA1 | Cell Marque | 2F83 | Monoclonal Mouse | IgG1 kappa | Recombinant human GST-FOXA1 protein encompassing amino acids 7-86. |
| p16/INK4A | Ventana | E6H4 | Monoclonal Mouse | IgG _{2a} | Recombinant protein corresponding to full length p16. |
| SLAH2 | Cell Marque | HC/LC C39S | Monoclonal Mouse | IgG _{2a} | Synthetic peptide corresponding to a region near the N-terminus of SLAH |

TABLE 2 Observed and expected molecular assay results in cell lines and tissue controls.

| Gene | Cell Line | Expected Expression | Observed Expression | Tissue Control | Expected Expression | Observed Expression |
|-----------|--|---------------------|---------------------------------------|--|---------------------|---|
| PgR | MCF-7 (50) | Positive | 3+ 50% 2+ 25% 1+ 15% | Tonsil Breast CA | Negative Strong | 0 100% 3+ 95% |
| HER2 | SKB-R3 (51) MDM-MB-453 (52) MDM-MB-175 (53) MDM-MB-231 (51) | 3+ 2+ 1+ 0 | 100% 3+ 99% 2+ 100% 1+ 99% 0 | Tonsil Breast CA | Negative Strong | 0 100% 3+ 100% |
| Ki-67 | RAMOS | Positive | 3+ 80% 2+ 15% 1+ 5% | Cerebrum Tonsil mantle zone (MZ) | Negative Strong | 0 100% 3+ 5%, 2+ 15%, 1+ 30%, 0 50% |
| COX-2 | COLO-205 (54) | Positive | 3+ 75% 2+ 20% 1+ 5% | Uterus Liver cirrhosis | Negative Strong | 0 100% 3+ 10%, 2+ 85%, 1+ 5%, 0 0% |
| FOXA1 | MFC7 (55) | Positive | 3+ 20% 2+ 50% 1+ 25% | Normal uterus endometrium Prostate adenocarcinoma | Negative Strong | 0 100% 3+ 80%, 2+ 10%, 1+ 5%, 0 5% |
| p16/INK4A | Hela (56) | Positive | 3+ 95% 2+ 5% 1+ 0% | HPV-negative ovarian adenocarcinoma HPV-positive squamous CA lymphoid tissue | Negative Strong | 0 100% 3+ 30%, 2+ 50% 1+ 10%, 0 5% |
| SIAH2 | RAMOS | Positive | 3+ 85% 2+ 10% 1+ 5% | Cerebrum Lung carcinoma | Negative Strong | 0 100% 3+ 40%, 2+ 25%, 1+ 5%, 0 30% |

TABLE 3 Positive concordance (sensitivity), negative concordance (specificity), and total inter-lab concordance (accuracy/reproducibility).

| Biomarker | PgR | HER2 | p16/INK4 | Ki-67 | COX2 | SIAH-2 | FOXA1 |
|---------------------------|---------------------------------|---------------------------------|--------------------------|---------------------------------|---|--|--|
| Specificity | 84/88 (95%) | 172/172 (100%) | 108/109 (99%) | 56/56 (100%) | 120/122 (98%) | 53/53 (100%) | 71/71 (100%) |
| Negative threshold | 0-1% | 0+ or 1+ | 0 | <5% | Allred 0 | 0 (H Score) | <25 (H Score) |
| Tissue Types | Normal organ panel | Normal organ panel | Normal organ panel | Normal organ panel | Normal skin and uterus endometrium | Normal cerebrum and adrenal gland | Normal organ panel |
| Sensitivity | 84/88 (95%) | 89/89 (100%) | 49/50 (98%) | 49/49 (100%) | 101/106 (95%) | 113/116 (97%) | 86/90 (96%) |
| Positive threshold | >5% | 3+ | >1% | ≥15% | Allred ≥4 | ≥10 (H Score) | >50 (H Score) |
| Tissue Types | Invasive breast adeno-carcinoma | Invasive breast adeno-carcinoma | Head and neck and cervix | Invasive breast adeno-carcinoma | Liver, DCIS and invasive breast carcinoma | Colon adeno-carcinoma and lung carcinoma | Prostate adenocarcinoma and colon adenocarcinoma |
| Total Percent Concordance | 74/74 (100%) | 215/215 (100%) | 48/50 (96%) | 105/105 (100%) | Not Available | Not Available | Not Available |

randomized clinical trial cohort and an observational cohort combined from Upsala University Hospital, Sweden, and the University of Massachusetts, Kaiser Permanente Northwest, Royal Melbourne, Australia studies (38) in Table 6A. In the SweDCIS RCT validation cohort, 47% of patients (n=240/504) were classified into the DCISionRT Low Risk group and there was a non-significant difference in the 10-year invasive IBR rates for with

versus without RT, with an average difference of 1%, while the remaining patients with elevated DS results (n=264/504) had a 9% ARR in the 10-year invasive IBR rate. In the combined observational cohort (38), there were 37% (338 of 926) of patients categorized into the DCISionRT Low Risk group that had a non-significant 1% difference in the 10-year invasive IBR rate for women treated with versus without RT, while the remaining patients with

TABLE 4 Molecular assay precision: mixed effect modeling.

| Molecular Assay | HER2 | P16 | SIAH2 | KI67 | FOXA1 | COX2 | PR | OVERALL |
|---|---------------|--------------|---------------|--------------|---------------|--------------|---------------|---------------|
| Score Mean | 33 | 10 | 22 | 21 | 92 | 40 | 30 | 38 |
| Score Range (min, max) | 0,100 | 0,100 | 1,80 | 3,80 | 33,100 | 0,100 | 0,100 | 0,100 |
| RUN std (%var) | 0.1 (<1%) | 0.4 (14%) | <0.1 (<1%) | 2.2 (15%) | <0.1 (<1%) | 3.0 (5%) | 0.9 (4%) | <0.1 (<1%) |
| LOT std (%var) | 0.7 (<1%) | 0.2 (3%) | 1.4 (9%) | <0.1 (0%) | <0.1 (<1%) | 0.5 (<1%) | <0.1 (<1%) | <0.1 (<1%) |
| MACHINE std (%var) | <0.1 (<1%) | 0.3 (11%) | <0.1 (<1%) | 0.3 (<1%) | <0.1 (<1%) | 0.5 (<1%) | 0.02 (<1%) | <0.1 (<1%) |
| Standard deviation (100-point scale) | 7.5 | 1.0 | 4.6 | 5.6 | 1.7 | 12.9 | 4.2 | 6.6 |

TABLE 5 Multianalyte assay with algorithm analysis reproducibility: mixed effect modeling.

| Analytic Variable | Reproducibility Variables | | | |
|------------------------------------|---------------------------|---------------|--------------|------------|
| | Reagent Lot (2) | Run (3) | Machine (2) | Within-run |
| DS std, (% var) (% of variance) | 0.005 (0.8%) | 0.018 (0.05%) | 0.013 (0.4%) | 0.20 (99%) |

DS = DS.mean + (1 | MACHINE) + (1 | LOT) + (1 | RUN), n=6480.

TABLE 6 Absolute risk reduction (ARR) by risk group and study.

| A. DCISionRT | Low Risk | | | Elevated Risk | | |
|---|-----------------|----------------------------|-------------------------|---------------|----------------------------|-------------------------|
| Study | N (%) | 10-yr Invasive ARR (95%CI) | 10-yr Total ARR (95%CI) | N (%) | 10-yr Invasive ARR (95%CI) | 10-yr Total ARR (95%CI) |
| Randomized Validation (SweDCIS), Cancers 2021, n=504 (40) | 240 (48%) | 1% (−6% to 8%) | 6% (−1% to 12%) | 264 (52%) | 9% (2% to 17%) | 16% (6% to 25%) |
| Modern observational validation, combined cohort, IJROBP 2022, n=926 (38) | 338 (37%) | 1% (−5% to 6%) | 1% (−4% to 5%) | 588 (63%) | 9% (2% to 16%) | 18% (9% to 26%) |
| Number Needed to Treat (NNT), modern observational validation, IJROBP 2022, n=926 | | 100 | 100 | | 11 | 6 |
| B. Nuclear Grade | Nuclear Grade 1 | | Nuclear Grade 2 | | Nuclear Grade 3 | |
| Study | n (%) | Total ARR | N (%) | Total ARR | N (%) | Total ARR |
| EBCTCG analysis, combined four RCTs, JNCI monographs 2010, n=1614 ³ | 634 (39%) | 16% (9% - 23%) | 343 (21%) | 14% (4%-25%) | 640 (40%) | 16% (8% - 23%) |
| Number Needed to Treat (NNT), EBCTCG 2010, n=1614 ³ | | 6 | | 7 | | 6 |

elevated DS results (n=588/926) had a 9% ARR in the 10-year invasive IBR rate. In both of these validation cohorts, the number of patients needed to treat (NNT) to prevent one invasive IBR within 10 years was about 100 for those in the Low Risk group and about 11 for the remaining patients with elevated DS results.

The ARR in 10-year IBR rate and the corresponding NNT were also summarized by nuclear grade in Table 6B for patients combined from four DCIS randomized clinical trials by EBCTCG (n=1617) (3). In the overall EBCTCG combined cohort, the DCIS to invasive IBR events was about 1:1 over 10 years. For patients with

nuclear grade 1 or 2 DCIS (n=977 of 1617) the ARR in 10-year total IBR rate was 15%, and for patients with nuclear grade 3 disease (n=640 of 1617) the ARR in 10-year total IBR rate was 16%. Based on an equal ratio of DCIS to invasive IBR events, the ARR in 10-year invasive IBR rate is 7.5% for nuclear grade 1 or 2 DCIS, and 8% for nuclear grade 3 DCIS. The corresponding NNT to prevent one invasive breast event in 10 years was 13 for nuclear grade 1 or 2 DCIS and 13 for nuclear grade 3 DCIS.

The clinical performance statistics negative predictive value (NPV) and positive predictive value (PPV) for 10-year RT

benefit, which are corollaries to the ARR in 10-year IBR, are summarized along with sensitivity and specificity for 10-year RT benefit in [Supplemental Table 3A](#) for the combined observational cohort ($n=926$) (38) using Equation 2. The proportion of patients who benefited from RT detected by DCISionRT elevated DS results, termed clinical sensitivity for RT benefit, was 93% for invasive IBR and 96% for total IBR. In contrast, the clinical sensitivity for RT benefit for 10-year IBR based on nuclear grade 3 vs. nuclear grade 1 or 2 DCIS was 38% for invasive IBR and 40% for total IBR for the combined EBCTCG randomized clinical trial cohorts for RT ($n=1617$) (3), [Supplemental Table 3B](#). The proportion of patients not benefiting from RT detected by the DCISionRT Low Risk group (termed clinical specificity for RT benefit, was 38% for invasive IBR and 41% for total IBR in the combined observational cohort ($n=926$) (38), whereas for nuclear grade 1 or 2 DCIS in the combined EBCTCG randomized clinical trial cohorts for RT, the clinical specificity for RT benefit was 60% for invasive IBR and 61% for total IBR (3), [Supplemental Table 3B](#).

4 Discussion

The DCISionRT test is a 7-gene predictive biosignature comprised of multiple molecular assays for protein expression that are algorithmically combined with four clinicopathologic factors to report a continuous DS result and categorical risk groups, with corresponding 10-year total and invasive IBR rates for patients treated with BCS either with or without RT. The DCISionRT test has been previously validated in multiple observational cohort studies and the SweDCIS randomized clinical trial cohort with a prospective-retrospective study design and determined to be prognostic for 10-year IBR risk and predictive for RT benefit (37, 38, 40, 41). The DCISionRT molecular assays provided robust analytic performance for assessing protein expression of the 7 genes in the centralized clinical lab setting. The molecular assays demonstrated high analytic positive concordance rates (analytic sensitivity), negative concordance rates (analytic specificity) and total concordance (analytic accuracy/reproducibility) for the protein expression of 7 target genes.

The molecular assays demonstrated high analytic precision, with very low variation ($<1\%$) due to controlled non-standard conditions (Run, Antibody Lot, and Machine). The reproducibility of the DCISionRT test system was high with a 95% confidence interval of less than 0.4 DS units on a scale of 0–10 (4%), accounting for varying clinicopathologic factor combinations for replicate molecular assays results obtained under controlled non-standard conditions with two independent pathology assessments of each biomarker. In clinical practice, the SOP requires that each of the independent assessments are used to provide preliminary independent DS assessments. If the two preliminary independent DS assessments differ by more than 0.5 units, then the DAP quality control algorithm automatically identifies the biomarker(s) resulting in the difference and requires a consensus score for those biomarker(s). The updated protein expression profile with consensus results is used to finalize and

report the test result to ensure a high level of reproducibility case by case.

Findings from prior RCTs and more recent studies for BCS and RT have demonstrated that patients who had BCS without RT had a 10-year overall IBR rate of $\sim 30\%$ (DCIS plus invasive) and $\sim 15\%$ IBR rate for invasive breast cancer (3). The addition of adjuvant RT to BCS (BCS plus RT) reduced recurrence risk by half, with approximately 8% of patients having invasive breast cancer and the other half having DCIS within 10 years. Thus, 85% or more of patients are not expected to benefit from RT to prevent a subsequent 10-year IBR (either DCIS or invasive) within 10 years. Based on multiple validation studies, the DCISionRT Low Risk group identifies about half (40%) of the 85% of patients not expected to benefit from RT for preventing a subsequent 10-year IBR. The Low Risk group identified by DCISionRT had low 10-year IBR recurrence rates and very low ARR (non-significant 1% absolute difference with or without RT) in 10-year invasive IBR (37, 38, 40, 41). In the Low Risk group, the corresponding NNT to prevent one 10-year invasive IBR was high (about 100, [Table 6](#)), and equivalently, the NPV for RT benefit in 10-year IBR was high for the Low Risk group (99%). As an alternative means to assess a prognostic or predictive test, the clinical sensitivity was high for RT benefit in 10-year IBR (94% for invasive IBR and 96% for total IBR), and the clinical specificity was 38% to 40% for RT benefit. This indicates that the percentage of false negative results from the Low Risk group is quite low and that about 40% of the patients who are expected to not benefit from RT are identified by the Low Risk group. Of note, a test with high sensitivity for a treatment benefit allows patients who will be unlikely to benefit from a treatment to be safely identified. The validated low IBR rate without RT and low ARR in 10-year IBR from RT indicates that the test identifies a low-risk population of patients consistent with NCCN guidelines, who may be considered for de-escalation of RT.

Based on multiple DCISionRT validation studies with patients from four observational and one randomized clinical trial cohorts, patients with higher DS results had elevated 10-year IBR recurrence rates and clinically significant ARR for RT in 10-year IBR (37, 38, 40, 41). The NNT was between 6 and 11 for 10-year total and invasive IBR for those patients with elevated DS indicating that a limited number of these patients would need to be treated to prevent a subsequent breast cancer recurrence.

As with adjuvant RT, not all patients are expected to benefit equally from adjuvant endocrine therapy (ET). The benefit from ET may differ due to patient compliance with ET, and the risk of recurrence after BCS alone and the relative risk reduction obtained from ET may also vary with tumor molecular biology. The DCISionRT test provides 10-year risk estimates for patients treated with BCS alone, which may help in shared decision making for DCIS treatment management. Furthermore, in multivariable analysis of DCISionRT Risk groups, clinicopathologic factors, and treatment with RT and ET, patients treated with ET had a significantly lower IBR rate in multivariable analysis ($HR=0.55$, $p=0.033$) (38). In univariate analyses for ET benefit within DCISionRT Risk groups, only patients in the Elevated Risk group had a significantly lower IBR rate for patients treated with ET versus without ET ($HR=0.34$, $p=0.02$) (57). Thus, patients with

elevated DS results may be expected to have greater absolute risk reductions from ET.

The multivariable analysis also showed that while DCISionRT risk groups contributed significantly to IBR rate, tumor grade and size, and patient age did not have a statistically significant association with IBR rate. Of these factors, nuclear grade is not a clinicopathologic factor in the DCISionRT test, but is a factor commonly used clinically to identify patients expected to benefit from radiation therapy. The analysis of the four randomized DCIS clinical trials for radiation therapy post lumpectomy identified a large number ($n=1617$) of patients with known nuclear grade. For patients with nuclear grade 1 or 2 in the RCTs, the ARR for RT was clinically relevant (15% 10-year IBR) and the corresponding NNT was low. Likewise, for patients with nuclear grade 3, the ARR for RT was clinically relevant (16% 10-year IBR) and the corresponding NNT was low. The results demonstrated that regardless of nuclear grade, radiotherapy was effective in reducing the absolute 10-year risk of any ipsilateral breast event. The performance metrics for nuclear grade from the four RCTs indicated that the NPV was moderate (85%), and the corresponding sensitivity (40%) and specificity (61%) were also moderate for identifying patients who would benefit from radiation therapy. This indicates that patients with nuclear grade 3 as well as those with nuclear grade 1 and 2 are expected to benefit from radiotherapy, consistent with the conclusions of the studies based on standardly reported clinical results. In addition, there are limitations in the accuracy of nuclear grade for DCIS assessed between different sites (58, 59), further limiting the utility of nuclear grade to identify patients with low-risk DCIS.

Prognostic and predictive tests are also evaluated by how they impact clinical practice. The clinical utility of the DCISionRT biosignature was reflected in the change in RT treatment recommendation observed in the prospective clinical utility study (PREDICT) with the incorporation of the DCISionRT test into routine clinical practice. In the PREDICT study, the utilization of the DCISionRT test led to a 40% change in recommendation for radiation therapy post lumpectomy for patients diagnosed with DCIS. Logistic regression analysis of the RT recommendation after DCISionRT testing indicated that the DCISionRT test result had the greatest impact on the RT recommendation, compared to clinicopathologic risk factors, physician specialty, treatment center type, patient preference and patient race (39). The recommendation for treatment with DCISionRT varied with continuous DS. In particular, those with a low DS result ($DS < 2$) were recommended RT less often (26%), about 50% of those with a DS result between 2 and 4 were recommended RT, while RT was recommended for 95% of those with higher DS results ($DS > 4$). In summary, the analytic performance, along with clinical validation and clinical utility studies support the continued clinical adoption of the test to guide shared decision making for DCIS treatment management. The analytic validation indicates the individual biomarkers have high performance and reproducibility and minimal variability due to standard imprecision conditions, resulting in high reproducibility of the DCISionRT test result. The test has been validated to identify patients with low

recurrence risk and minimal to no absolute risk reduction benefit from RT, where 99% of the patients in the low-risk group did not benefit from RT. These patients may be good candidates for treatment with BCS without RT, depending on risk tolerance and other factors specific to the individual patient. In contrast, the test has also been validated to identify patients with significant absolute risk reduction who benefit from RT and might be undertreated by BCS without RT. These patients might be good candidates for treatment with BCS plus RT, depending on the risk tolerance and other factors specific to the individual patient.

Data availability statement

The datasets presented in this article are not readily available because proprietary biomarker and algorithmic data will remain confidential and will not be shared. Requests to access the datasets should be directed to TB, tbremer@preludedx.com.

Ethics statement

The studies involving human participants were reviewed and approved by the Uppsala University Regional Ethical Review Board, University of Massachusetts Medical School Tissue and Tumor Bank Institutional Review Board, the Kaiser Permanente Northwest Institutional Review Board, Umeå University Ethics Review Committee, and the Royal Melbourne Hospital and Affiliated Hospitals Ethics Review Board. Written informed consent for participation was not required for this study in accordance with the national legislation and the institutional requirements.

Author contributions

DD and TB contributed to conceptualization of the study. DD, TB, and KM provided methodology for the study procedures and data analysis. TB was involved in providing resources and project administration, while DD, CS, JS, and PW provided overall supervision of the study. DD, SH, JS, TB, and KM were responsible for data collection. TB provided funding acquisition. DD, SH, JS, KM, SS, and TB were responsible for data curation. KM, SS, and TB contributed to software needed to organize, curate, and analyze the study data, while TB provided formal analysis of the data and KM, SS and TB participated in validation of the data analysis. DD, JS, KM, CS, SS, and TB performed visualization of the data. DD, KM, and TB provided the original draft of the manuscript and CS, PW, SH, and SS participated in review and editing of the final manuscript. All authors contributed to the article and approved the submitted version.

Funding

This study was funded by PreludeDx.

Conflict of interest

DD, SH, and JS are consultant pathologists for PreludeDx. CS is a consultant for ImpediMed, PreludeDX, Videra Surgical and Evicore and has received grant funding from Varian Medical Systems, VisionRT, and PreludeDx. PW has stock and other ownership interests in Reverse Medical, Rebound Medical, Lazarus, Cerebrotech, Targeted Medical Education and Medtronic. PW is on advisory boards for Medtronic, Lumicell, ImpediMed, Cianna Medical, and PreludeDx and has received research funding from InVita, Intact Medical, PreludeDx, Agendia, and ImpediMed. KM and SS are employees of PreludeDx and have stock options for PreludeDx. TB is an employee of PreludeDx, holds intellectual property rights for the DCISionRT test and has ownership interest in PreludeDx.

The authors declare that this study received funding from PreludeDx. Since this is an analytical validation study for a commercially-available Multianalyte Assay with Algorithmic Analyses (MAAA), employees and consultants employed by the

funder were necessarily involved in the study design, collection, analysis, interpretation of data, the writing of this article, and the decision to submit it for publication.

Publisher's note

All claims expressed in this article are solely those of the authors and do not necessarily represent those of their affiliated organizations, or those of the publisher, the editors and the reviewers. Any product that may be evaluated in this article, or claim that may be made by its manufacturer, is not guaranteed or endorsed by the publisher.

Supplementary material

The Supplementary Material for this article can be found online at: <https://www.frontiersin.org/articles/10.3389/fonc.2023.1069059/full#supplementary-material>

References

- Virnig BA, Tuttle TM, Shamlan T, Kane RL. Ductal carcinoma *in situ* of the breast: a systematic review of incidence, treatment, and outcomes. *J Natl Cancer Inst* (2010) 102:170–8. doi: 10.1093/jnci/djp482
- Siegel RL, Miller KD, Fuchs HE, Jemal A. Cancer statistics, 2021. *CA Cancer J Clin* (2021) 71:7–33. doi: 10.3322/caac.21654
- Early Breast Cancer Trialists' Collaborative G, Corrae C, McGale P, Taylor C, Wang Y, Clarke M, et al. Overview of the randomized trials of radiotherapy in ductal carcinoma *in situ* of the breast. *J Natl Cancer Inst Monogr* (2010) 2010:162–77. doi: 10.1093/jncimonographs/lgq039
- Arriagada R, Le MG, Rochard F, Contesso G. Conservative treatment versus mastectomy in early breast cancer: patterns of failure with 15 years of follow-up data. Institut Gustave-Roussy breast cancer group. *J Clin Oncol* (1996) 14:1558–64. doi: 10.1200/JCO.1996.14.5.1558
- Blichert-Toft M, Rose C, Andersen JA, Overgaard M, Axelsson CK, Andersen KW, et al. Danish Randomized trial comparing breast conservation therapy with mastectomy: six years of life-table analysis. Danish breast cancer cooperative group. *J Natl Cancer Inst Monogr* (1992) 11:19–25.
- Fisher B, Anderson S, Bryant J, Margolese RG, Deutsch M, Fisher ER, et al. Twenty-year follow-up of a randomized trial comparing total mastectomy, lumpectomy, and lumpectomy plus irradiation for the treatment of invasive breast cancer. *N Engl J Med* (2002) 347:1233–41. doi: 10.1056/NEJMoa022152
- Poggi MM, Danforth DN, Sciuto LC, Smith SL, Steinberg SM, Liewehr DJ, et al. Eighteen-year results in the treatment of early breast carcinoma with mastectomy versus breast conservation therapy: the national cancer institute randomized trial. *Cancer* (2003) 98:697–702. doi: 10.1002/cncr.11580
- Khan A, Dumitru D, Catanuto G, Rocco N, Nava MB, Benson J. Management of ductal carcinoma *in situ* in the modern era. *Minerva Chir* (2018) 73:303–13. doi: 10.23736/S0026-4733.18.07729-5
- Barrio AV, Van Zee KJ. Controversies in the treatment of ductal carcinoma *in situ*. *Annu Rev Med* (2017) 68:197–211. doi: 10.1146/annurev-med-050715-104920
- Warnberg F, Garmo H, Emdin S, Hedberg V, Adwall L, Sandelin K, et al. Effect of radiotherapy after breast-conserving surgery for ductal carcinoma *in situ*: 20 years follow-up in the randomized SweDCIS trial. *J Clin Oncol* (2014) 32:3613–8. doi: 10.1200/JCO.2014.56.2595
- Emdin SO, Granstrand B, Ringberg A, Sandelin K, Arnesson LG, Nordgren H, et al. SweDCIS: radiotherapy after sector resection for ductal carcinoma *in situ* of the breast. results of a randomised trial in a population offered mammography screening. *Acta Oncol* (2006) 45:536–43. doi: 10.1080/02841860600681569
- McCormick B, Winter K, Hudis C, Kuerer HM, Rakovitch E, Smith BL, et al. RTOG 9804: a prospective randomized trial for good-risk ductal carcinoma *in situ* comparing radiotherapy with observation. *J Clin Oncol* (2015) 33:709–15. doi: 10.1200/JCO.2014.57.9029
- McCormick B, Winter KA, Woodward W, Kuerer HM, Sneath N, Rakovitch E, et al. Randomized phase III trial evaluating radiation following surgical excision for good-risk ductal carcinoma *in situ*: long-term report from NRG Oncology/RTOG 9804. *J Clin Oncol* (2021) 39:3574–82. doi: 10.1200/JCO.21.01083
- Ringberg A, Nordgren H, Thorstensson S, Idvall I, Garmo H, Granstrand B, et al. Histopathological risk factors for ipsilateral breast events after breast conserving treatment for ductal carcinoma *in situ* of the breast—results from the Swedish randomised trial. *Eur J Cancer* (2007) 43:291–8. doi: 10.1016/j.ejca.2006.09.018
- Solin LJ, Gray R, Hughes LL, Wood WC, Lowen MA, Badve SS, et al. Surgical excision without radiation for ductal carcinoma *in situ* of the breast: 12-year results from the ECOG-ACRIN E5194 study. *J Clin Oncol* (2015) 33:3938–44. doi: 10.1200/JCO.2015.60.8588
- NCCN guidelines version 4.2022 breast cancer (2022). Available at: https://www.nccn.org/professionals/physician_gls/pdf/breast.pdf.
- de Mascarel I, Bonichon F, MacGrogan G, de Lara CT, Avril A, Picot V, et al. Application of the van nuys prognostic index in a retrospective series of 367 ductal carcinomas *in situ* of the breast examined by serial macroscopic sectioning: practical considerations. *Breast Cancer Res Treat* (2000) 61:151–9. doi: 10.1023/A:1006437902770
- Gilleard O, Goodman A, Cooper M, Davies M, Dunn J. The significance of the van nuys prognostic index in the management of ductal carcinoma *in situ*. *World J Surg Oncol* (2008) 6:61. doi: 10.1186/1477-7819-6-61
- Solin LJ. Management of ductal carcinoma *In situ* (DCIS) of the breast: present approaches and future directions. *Curr Oncol Rep* (2019) 21:33. doi: 10.1007/s11912-019-0777-3
- Rudloff U, Jacks LM, Goldberg JJ, Wynveen CA, Brogi E, Patil S, et al. Nomogram for predicting the risk of local recurrence after breast-conserving surgery for ductal carcinoma *in situ*. *J Clin Oncol* (2010) 28:3762–9. doi: 10.1200/JCO.2009.26.8847
- Allegra CJ, Aberle DR, Ganschow P, Hahn SM, Lee CN, Millon-Underwood S, et al. National institutes of health state-of-the-science conference statement: diagnosis and management of ductal carcinoma *In situ* September 22–24, 2009. *J Natl Cancer Inst* (2010) 102:161–9. doi: 10.1093/jnci/djp485
- Allegra CJ, Aberle DR, Ganschow P, Hahn SM, Lee CN, Millon-Underwood S, et al. Diagnosis and management of ductal carcinoma *In situ* (DCIS). *NIH Consensus State-of-the-Science Statements* (2009) 26(2):1–27.
- Nofech-Mozes S, Spayne J, Rakovitch E, Kahn HJ, Seth A, Pignol JP, et al. Biological markers predictive of invasive recurrence in DCIS. *Clin Med Oncol* (2008) 2:7–18. doi: 10.1177/117955490800200202
- Lari SA, Kuerer HM. Biological markers in DCIS and risk of breast recurrence: a systematic review. *J Cancer* (2011) 2:232–61. doi: 10.7150/jca.2.232
- Wang SY, Shamlan T, Virnig BA, Kane R. Tumor characteristics as predictors of local recurrence after treatment of ductal carcinoma *in situ*: a meta-analysis. *Breast Cancer Res Treat* (2011) 127:1–14. doi: 10.1007/s10549-011-1387-4
- Gauthier ML, Berman HK, Miller C, Kozakeiwicz K, Chew K, Moore D, et al. Abrogated response to cellular stress identifies DCIS associated with subsequent tumor

events and defines basal-like breast tumors. *Cancer Cell* (2007) 12:479–91. doi: 10.1016/j.ccr.2007.10.017

27. Kerlikowske K, Molinaro AM, Gauthier ML, Berman HK, Waldman F, Bennington J, et al. Biomarker expression and risk of subsequent tumors after initial ductal carcinoma *in situ* diagnosis. *J Natl Cancer Inst* (2010) 102:627–37. doi: 10.1093/jnci/djq101

28. Witkiewicz AK, Rivadeneira DB, Ertel A, Kline J, Hyslop T, Schwartz GF, et al. Association of RB/p16-pathway perturbations with DCIS recurrence: dependence on tumor versus tissue microenvironment. *Am J Pathol* (2011) 179:1171–8. doi: 10.1016/j.ajpath.2011.05.043

29. de Roos MA, de Bock GH, de Vries J, van der Vegt B, Wesseling J. p53 overexpression is a predictor of local recurrence after treatment for both *in situ* and invasive ductal carcinoma of the breast. *J Surg Res* (2007) 140:109–14. doi: 10.1016/j.jss.2006.10.045

30. Hieken TJ, Cheregi J, Farolan M, Kim J, Velasco JM. Predicting relapse in ductal carcinoma *in situ* patients: an analysis of biologic markers with long-term follow-up. *Am J Surg* (2007) 194:504–6. doi: 10.1016/j.amjsurg.2007.07.002

31. Darby S, McGale P, Peto R, Granath F, Hall P, Ekbom A. Mortality from cardiovascular disease more than 10 years after radiotherapy for breast cancer: nationwide cohort study of 90 000 Swedish women. *BMJ* (2003) 326:256–7. doi: 10.1136/bmj.326.7383.256

32. Holmes P, Lloyd J, Chervoneva I, Pequinet E, Cornfield DB, Schwartz GF, et al. Prognostic markers and long-term outcomes in ductal carcinoma *in situ* of the breast treated with excision alone. *Cancer* (2011) 117:3650–7. doi: 10.1002/cncr.25942

33. Rakovitch E, Nofech-Mozes S, Hanna W, Sutradhar R, Baehner FL, Miller DP, et al. Multigene expression assay and benefit of radiotherapy after breast conservation in ductal carcinoma *in situ*. *J Natl Cancer Inst* (2017) 109(4):djw256. doi: 10.1093/jnci/djw256

34. Rakovitch E, Nofech-Mozes S, Hanna W, Baehner FL, Saskin R, Butler SM, et al. A population-based validation study of the DCIS score predicting recurrence risk in individuals treated by breast-conserving surgery alone. *Breast Cancer Res Treat* (2015) 152:389–98. doi: 10.1007/s10549-015-3464-6

35. Torres MA: Genomic assays to assess local recurrence risk and predict radiation therapy benefit in patients with ductal carcinoma *in situ*. *Int J Radiat Oncol Biol Phys* (2019) 103:1021–5. doi: 10.1016/j.ijrobp.2018.10.032

36. Knowlton CA, Jimenez RB, Moran MS. Risk assessment in the molecular era. *Semin Radiat Oncol* (2022) 32:189–97. doi: 10.1016/j.semradi.2022.01.005

37. Bremer T, Whitworth PW, Patel R, Savala J, Barry T, Lyle S, et al. A biological signature for breast ductal carcinoma *In situ* to predict radiotherapy benefit and assess recurrence risk. *Clin Cancer Res* (2018) 24:5895–901. doi: 10.1158/1078-0432.CCR-18-0842

38. Vicini FA, Mann GB, Shah C, Weinmann S, Leo M, Whitworth P, et al. A novel biosignature identifies patients with DCIS with high risks of local recurrence after breast conserving surgery and radiotherapy. *Int J Radiat Oncology Biology Phys* (2022). doi: 10.1200/JCO.2021.39.15_suppl.513

39. Shah C, Bremer T, Cox C, Whitworth P, Patel R, Patel A, et al. Correction to: the clinical utility of DCISionRT((R)) on radiation therapy decision making in patients with ductal carcinoma *in situ* following breast-conserving surgery. *Ann Surg Oncol* (2021). doi: 10.1245/s10434-021-10138-3

40. Wärnberg F, Karlsson P, Holmberg E, Sandelin K, Whitworth PW, Savala J, et al. Prognostic risk assessment and prediction of radiotherapy benefit for women with ductal carcinoma *In situ* (DCIS) of the breast, in a randomized clinical trial (SweDCIS). *Cancers* (2021) 13:6103. doi: 10.3390/cancers13236103

41. Weinmann S, Leo MC, Francisco M, Jenkins CL, Barry T, Leesman G, et al. Validation of a ductal carcinoma *In situ* biomarker profile for risk of recurrence after breast-conserving surgery with and without radiotherapy. *Clin Cancer Res* (2020) 26:4054–63. doi: 10.1158/1078-0432.CCR-19-1152

42. Mann G, Malley OD, Park A, Shackleton K, Collins J, Rose A. DCIS biologic risk signature predicts risk of recurrence and RT benefit after BCS. *SSO Abstracts* (2021). Available at: <https://preludedx.com/wp-content/uploads/2021/06/2021-Society-of-Surgical-Oncology-Abstract.pdf>.

43. Raldow AC, Sher D, Chen AB, Punglia RS. Cost effectiveness of DCISionRT for guiding treatment of ductal carcinoma *in situ*. *JNCI Cancer Spectr* (2020) 4:pkaa004. doi: 10.1093/jncics/pkaa004

44. Hewitt SM, Robinowitz M, Bogen SA, Gown AM, Kalra KL, Otis CN, et al. Quality assurance for design control and implementation of immunohistochemistry assays: approved guideline- second edition. In: *CLSI document I/LA28-A2*, Wayne, PA: Clinical and Laboratory Standards Institute (2011). 2011:31.

45. Fitzgibbons PL, Bradley LA, Fatheree LA, Alsabeh R, Fulton RS, Goldsmith JD, et al. College of American pathologists p, laboratory quality c: principles of analytic validation of immunohistochemical assays: guideline from the college of American pathologists pathology and laboratory quality center. *Arch Pathol Lab Med* (2014) 138:1432–43. doi: 10.5858/arpa.2013-0610-CP

46. Heagerty PJ, Lumley T, Pepe MS. Time-dependent ROC curves for censored survival data and a diagnostic marker. *Biometrics* (2000) 56:337–44. doi: 10.1111/j.0006-341X.2000.00337.x

47. Hardy LB, Fitzgibbons PL, Goldsmith JD, Eisen RN, Beasley MB, Souers RJ, et al. Immunohistochemistry validation procedures and practices: a college of American pathologists survey of 727 laboratories. *Arch Pathol Lab Med* (2013) 137:19–25. doi: 10.5858/arpa.2011-0676-CP

48. Rhodes A, Jasani B, Anderson E, Dodson AR, Balaton AJ. Evaluation of HER-2/neu immunohistochemical assay sensitivity and scoring on formalin-fixed and paraffin-processed cell lines and breast tumors: a comparative study involving results from laboratories in 21 countries. *Am J Clin Pathol* (2002) 118:408–17. doi: 10.1309/97WN-W6UX-XJWT-02H2

49. Wolff AC, Hammond ME, Hicks DG, Dowsett M, McShane LM, Allison KH, et al. American Society of clinical O, college of American p: recommendations for human epidermal growth factor receptor 2 testing in breast cancer: American society of clinical Oncology/College of American pathologists clinical practice guideline update. *J Clin Oncol* (2013) 31:3997–4013. doi: 10.1200/JCO.2013.50.9984

50. Comsa S, Cimpean AM, Raica M. The story of MCF-7 breast cancer cell line: 40 years of experience in research. *Anticancer Res* (2015) 35:3147–54.

51. Subik K, Lee JF, Baxter L, Strzepek T, Costello D, Crowley P, et al. The expression patterns of ER, PR, HER2, CK5/6, EGFR, ki-67 and AR by immunohistochemical analysis in breast cancer cell lines. *Breast Cancer (Auckl)* (2010) 4:35–41. doi: 10.1177/117822341000400004

52. Neve RM, Chin K, Fridlyand J, Yeh J, Baehner FL, Fevr T, et al. A collection of breast cancer cell lines for the study of functionally distinct cancer subtypes. *Cancer Cell* (2006) 10:515–27. doi: 10.1016/j.ccr.2006.10.008

53. Ross S, Crocker LM, Phillips G, Reardor B, Koeppen H, Sliwkowski MX, et al. Evolution of the MDA-MB-175 breast cancer cell line from a low to a high HER2 expressing tumor line. *Cancer Res* (2005) 65(9_Supplement).

54. Li W, Cao Y, Xu J, Wang Y, Li W, Wang Q, et al. YAP transcriptionally regulates COX-2 expression and GCCSys-4 (G-4), a dual YAP/COX-2 inhibitor, overcomes drug resistance in colorectal cancer. *J Exp Clin Cancer Res* (2017) 36:144. doi: 10.1186/s13046-017-0612-3

55. Gong C, Fujino K, Monteiro LJ, Gomes AR, Drost R, Davidson-Smith H, et al. FOXA1 repression is associated with loss of BRCA1 and increased promoter methylation and chromatin silencing in breast cancer. *Oncogene* (2015) 34:5012–24. doi: 10.1038/ncr.2014.421

56. McLaughlin-Drubin ME, Park D, Munger K. Tumor suppressor p16INK4A is necessary for survival of cervical carcinoma cell lines. *Proc Natl Acad Sci USA* (2013) 110:16175–80. doi: 10.1073/pnas.1310432110

57. Whitworth PW, Shah CS, Vicini FA, Rabinovitch R, Margenthaler JA, Wärnberg F, et al. Assessing the benefit of adjuvant endocrine therapy in patients following breast-conserving surgery with or without radiation stratified by a 7-gene predictive DCIS biosignature. *J Clin Oncol* (2022) 40(16_suppl):502–2. doi: 10.1200/JCO.2022.40.16_suppl.502

58. van Dooijeweert C, van Diest PJ, Baas IO, van der Wall E, Deckers IAG. Grading variation in 2,934 patients with ductal carcinoma *in situ* of the breast: the effect of laboratory- and pathologist-specific feedback reports. *Diagn Pathol* (2020) 15:52. doi: 10.1186/s13000-020-00970-8

59. van Seijen M, Jozwiak K, Pinder SE, Hall A, Krishnamurthy S, Thomas JS, et al. Grand challenge pc: variability in grading of ductal carcinoma *in situ* among an international group of pathologists. *J Pathol Clin Res* (2021) 7:233–42. doi: 10.1002/cjp.2201



OPEN ACCESS

EDITED BY

Ira Ida Skvortsova,
Innsbruck Medical University, Austria

REVIEWED BY

Zhong-Hua Wang,
Fudan University, China
Antonella Argentiero,
National Cancer Institute Foundation
(IRCCS), Italy
Sofia Torres,
Centro Hospitalar Lisboa Norte (CHLN),
Portugal

*CORRESPONDENCE

Guohong Song

✉ songguohong918@hotmail.com

Huiping Li

✉ huipingli2012@hotmail.com

[†]These authors share first authorship

RECEIVED 21 October 2022

ACCEPTED 02 June 2023

PUBLISHED 16 June 2023

CITATION

Zhang R, Chen Y, Liu X, Gui X, Zhu A,
Jiang H, Shao B, Liang X, Yan Y, Zhang J,
Song G and Li H (2023) Efficacy of apatinib
250 mg combined with chemotherapy in
patients with pretreated advanced breast
cancer in a real-world setting.
Front. Oncol. 13:1076469.
doi: 10.3389/fonc.2023.1076469

COPYRIGHT

© 2023 Zhang, Chen, Liu, Gui, Zhu, Jiang,
Shao, Liang, Yan, Zhang, Song and Li. This is
an open-access article distributed under the
terms of the [Creative Commons Attribution
License \(CC BY\)](#). The use, distribution or
reproduction in other forums is permitted,
provided the original author(s) and the
copyright owner(s) are credited and that
the original publication in this journal is
cited, in accordance with accepted
academic practice. No use, distribution or
reproduction is permitted which does not
comply with these terms.

Efficacy of apatinib 250 mg combined with chemotherapy in patients with pretreated advanced breast cancer in a real-world setting

Ruyan Zhang[†], Yifei Chen[†], Xiaoran Liu, Xinyu Gui, Anjie Zhu,
Hanfang Jiang, Bin Shao, Xu Liang, Ying Yan, Jiayang Zhang,
Guohong Song* and Huiping Li*

Key Laboratory of Carcinogenesis and Translational Research (Ministry of Education/Beijing),
Department of Breast Oncology, Peking University Cancer Hospital and Institute, Beijing, China

Objectives: This study evaluated the efficacy and safety of apatinib (an oral small-molecule tyrosine kinase inhibitor targeting VEGFR-2) 250 mg combined with chemotherapy in patients with pretreated metastatic breast cancer in a real-world setting.

Patients and methods: A database of patients with advanced breast cancer who received apatinib between December 2016 and December 2019 in our institution was reviewed, and patients who received apatinib combined with chemotherapy were included. Progression-free survival (PFS), overall survival (OS), the objective response rate (ORR), the disease control rate (DCR), and treatment-related toxicity were analyzed.

Results: In total, 52 evaluated patients with metastatic breast cancer previously exposed to anthracyclines or taxanes who received apatinib 250 mg combined with chemotherapy were enrolled in this study. Median PFS and OS were 4.8 (95% confidence interval [CI] = 3.2–6.4) and 15.4 months (95% CI = 9.2–21.6), respectively. The ORR and DCR were 25% and 86.5%, respectively. Median PFS for the previous line of treatment was 2.1 months (95% CI = 0.65–3.6), which was significantly shorter than that for the apatinib–chemotherapy combination ($p < 0.001$). No significant difference was identified in the ORR and PFS among the subgroups (subtypes, target lesion, combined regimens and treatment lines). The common toxicities related to apatinib were hypertension, hand-foot syndrome, proteinuria, and fatigue events.

Conclusion: Apatinib 250 mg combined with chemotherapy provided favorable efficacy in patients with pretreated metastatic breast cancer regardless of molecular types and treatment lines. The toxicities of the regimen were well tolerated and manageable. This regimen could be a potential treatment option in patients with refractory pretreated metastatic breast cancers.

KEYWORDS

breast cancer, apatinib, chemotherapy, efficacy, safety

1 Introduction

Metastatic breast cancer (MBC) remains an incurable disease, with median overall survival (OS) of about 3 years and a 5-year survival rate of around 25%, even in countries without medicine availability problems (1).

Novel therapeutic strategies for MBC have been established in recent years. Cyclin-dependent kinase 4 and 6 (CDK4/6) inhibitors for hormone receptor (HR) positive/human epidermal growth factor 2 (HER2)-negative MBC, trastuzumab emtansine (T-DM1) and T-DXd for HER2 positive MBC, immune check point inhibitor pembrolizumab and sacituzumab govitecan (SG) for metastatic triple negative breast cancer (TNBC), and poly(ADP ribose) polymerase (PARP) inhibitors for HER2 negative MBC with germline BRCA1/2 mutation have become the standard treatment recommended by guidelines. However, the first CDK4/6 inhibitor palbociclib and T-DM1 were approved by China Food and Drug Administration (CFDA) in August 2018 and January 2020 respectively, and they were not included in medical insurance until March 2023; Until today, pembrolizumab and olaparib have not been approved by CFDA for the treatment of metastatic breast cancer, pembrolizumab was approved only for treatment of early TNBC with high risk of recurrence in November 2022, olaparib was approved only for ovarian cancer and prostate cancer in China; T-DXd and SG have not yet launched in Mainland of China until now. So in the real world clinical practice, a considerable number of patients didn't receive these treatments due to drug accessibility and/or expensive cost which was not covered by local medical insurance. Moreover, some patients who received above treatments did not respond to the therapy, and some who experienced initial response still developed resistance inevitably afterwards. In patients with taxane- and anthracycline-resistant human epidermal growth factor 2 (HER2)-negative MBC, traditional chemotherapy agents including capecitabine, vinorelbine, gemcitabine, or platinum agents are usually considered as treatments of choice. There is no evidence suggesting that any chemotherapeutic drugs have superior efficacy in the second and later lines, and new drugs or strategies are required for this population of patients. Some new therapeutic strategies for MBC such as anti-angiogenesis therapy, androgen receptor antagonists, micro-RNA based therapy, proteolysis targeting chimeric molecules (PROTACs) and others are under exploration, some of them have initially shown potential benefits (2, 3).

Previous researches indicated that angiogenesis is vital for tumor growth and metastasis (4, 5). The vascular endothelial growth factor (VEGF) pathway plays an important role in angiogenesis in cancer (6, 7), and VEGF receptor-2 (VEGFR-2) is the key signaling receptor involved in this pathway (8, 9). Therefore, anti-angiogenesis is an important anti-cancer strategy (7). The anti-VEGF monoclonal antibody bevacizumab, when added to chemotherapy, has been demonstrated to significantly increase progression-free survival (PFS) in patients with metastatic triple-negative breast cancer (TNBC) in the first- and second-line settings (10–13).

Apatinib is an oral small-molecule tyrosine kinase inhibitor (TKI) selectively targeting VEGFR-2, and apatinib monotherapy

has been approved by the CFDA for the third-line treatment of gastric cancer based on its remarkable survival benefits (14). Two prospective open-label, multicenter, phase 2 trials preliminarily revealed the satisfying efficacy and acceptable toxicities of apatinib monotherapy in TNBC and non-TNBC (15, 16).

Preclinical studies illustrated that combined treatment with apatinib can improve the efficacy of chemotherapy and reverse chemotherapeutic drug resistance in tumor cells (17) (18–20). Limited studies have explored the efficacy and safety of apatinib combined with chemotherapy in solid tumors including breast cancer, and efficacy and good tolerance were preliminarily observed (21–26).

Based on above results, we performed a retrospective study to further evaluate the efficacy and safety of apatinib combined with chemotherapy in patients with MBC who failed standard treatment in a real-world setting.

2 Materials and methods

2.1 Methods

A database of patients with breast cancer treated with apatinib combined with chemotherapy from December 2016 to December 2019 in the Department of Breast Oncology of Peking University Cancer Hospital and Beijing Institute of Cancer Prevention was reviewed.

The inclusion criteria were as follows: pathologically confirmed locally advanced breast cancer or MBC; failed previous standard treatments; treated with apatinib combined with chemotherapy, and finished at least one cycle of treatment to permit toxicity evaluations.

The estrogen receptor (ER), progesterone receptor (PgR), and HER2 were recorded. For patients who underwent biopsies of the metastatic sites, the status of these receptors was determined on the basis of the latest pathological test before apatinib treatment. ER/PgR negativity was defined as <1% positive tumor cells with nuclear staining on immunohistochemistry (IHC); a HER2-negative status was defined as an IHC score of 0–1; and negativity was defined by fluorescent *in situ* hybridization in accordance with the American Society of Clinical Oncology guidelines.

Tumor assessments were evaluated every two or three cycles of treatment based on the Response Evaluation Criteria In Solid Tumors (RECIST) (version 1.1). PFS was defined as the time interval from initiating apatinib therapy to disease progression or death, whichever occurred first. OS was considered the interval from initiating apatinib therapy to death from any cause or the last follow-up visit. Adverse events (AEs) were assessed according to the National Cancer Institute Common Terminology Criteria for Adverse Events (version 4.03).

2.2 Statistical analysis

Median PFS and OS were calculated using the Kaplan–Meier method, and inter-group comparisons were performed using the

log-rank test. Pearson's χ^2 test or Fisher's exact test was used to analyze treatment efficacy. Cox regression analysis was used to analyze the correlations between factors and prognosis. SPSS version 26.0 was used for all statistical analyses, and $p < 0.05$ was considered statistically significant.

3 Results

3.1 Patient characteristics

In total, 61 patients with MBC who received apatinib combined with chemotherapy were included. All patients were given apatinib 250 mg per day orally, and chemotherapy was based on physician's choice. Patient characteristics at baseline were shown in Table 1.

The median age at the start of apatinib therapy was 49.9 years (range, 31–67 years). Concerning the molecular subtype, 23 patients (37.7%) were diagnosed with TNBC, 32 patients (52.5%) had ER-positive breast cancer, and 6 patients (9.8%) had HER2-positive breast cancer. More than half of the patients had lymph node and chest wall metastasis (54.1% and 55.7%, respectively), 19 patients (31.1%) had liver metastasis, and 16 patients (26.2%) had lung metastasis.

All 61 patients had previously received chemotherapy containing anthracycline or taxane, and 56 patients (91.8%) had received at least one chemotherapeutic regimen for metastatic disease before the use of apatinib. The median number of prior chemotherapy lines was 2 (0–5). Five patients (8.2%) who received apatinib in the first-line setting all had disease-free survival (DFS) shorter than 12 months. Patients with hormone receptor-positive breast cancer had received at least one regimen of endocrine treatment. Patients with HER2-positive disease had progressed on previous anti-HER2 therapy. None of the HR+HER2- patients received CDK4/6 inhibitors and only one of them received everolimus before apatinib, one of the five HER2 positive patients received T-DM1 in a phase III clinical trial before apatinib, and none of the TNBC patients received immunotherapy before apatinib. Among all of the 61 patients, one TNBC patient harbored suspected pathogenic mutation of germline BRCA1, one HR+HER2 patient harbored pathogenic mutation of germline BRCA2, neither of them received PARP inhibitor treatment.

The chemotherapies used in combination regimens were gemcitabine (16, 26.2%), vinorelbine (16, 26.2%), taxanes (15, 24.6%), capecitabine (10, 16.4%), platinum (7, 11.5%), and anthracycline (4, 6.6%). Three patients with HER2-positive disease received anti-HER2 targeted therapy (trastuzumab, pyrotinib, and lapatinib, respectively) along with apatinib and chemotherapy.

3.2 Efficacy

Overall, nine of the 61 patients required treatment discontinuation in the first two chemotherapy cycles because of intolerable toxicities, and the tumor assessment could not be completed. Therefore, 52 patients were included in the analyses of PFS, OS, and clinical responses. With a median follow-up of 7.4

months (range, 2.4–41.7 months), 31 of 52 patients had progressive disease (PD), and 25 deaths occurred. Median PFS was 4.8 months (95% confidence interval [CI] = 3.2–6.4 months, Figure 1: PFS of 52 evaluable patients), and median OS was 15.4 months (95% CI = 9.2–21.6 months, Figure 2: OS of 52 evaluable patients). Median PFS for the previous line of treatment (chemotherapy alone) was 2.1 months (95%CI = 0.65–3.6 months), which was significantly shorter than that of apatinib combined with chemotherapy (4.8 months, 95% CI = 3.2–6.4 months, $p < 0.001$), comparisons were performed using the log-rank test (Figure 3: PFS of apatinib combined with chemotherapy versus PFS of the previous line treatment.).

In total, 13 (25.0%) and 34 (65.4%) patients had a best clinical response of partial response (PR) and stable disease (SD), respectively, and no patients had complete response (CR). The overall response rate (ORR) was 25.0% (13/52), and the disease control rate (DCR) was 86.5% (45/52, Table 2, Figure 4. Best overall response of 52 evaluable patients Figure 5. Duration of treatment and response).

Response and PFS in different subgroups were analyzed as presented in Table 3. Median PFS was longer for patients who achieved PR than for those who did not achieve PR (10.0, 3.7, and 1.3 months for the PR, SD, and PD groups, respectively; $P < 0.001$). The ORR was best in the gemcitabine group (42.9% [6/14]) among all combination regimen groups, and patients for whom the liver or chest wall/lymph nodes were the target lesions displayed satisfying ORRs (33.3% [5/15] and 28.6% [8/28], respectively). Meanwhile, the ORR was 0% (0/5), 18.8% (3/16), and 32.3% (10/31) for the first, second, and third or later lines, respectively, and all the five patients in the first group had a best clinical response of stable disease, and median PFS was similar in different treatment lines. Regarding different molecular types, both the ORR and PFS were worse in the TNBC group than in the ER-positive/HER2-negative and HER2-positive groups. No significant difference was identified in the ORR and PFS among the subgroups by the log-rank test for univariate analysis.

3.3 Safety

A total of 61 patients were analyzed for toxicity. Nine patients discontinued the combination treatment in the first two cycles because of intolerable toxicities which including hypertension (four cases), thrombocytopenia (three cases), fever (one case), anorexia (one case). The most common non-hematologic AEs were hypertension, hand-foot syndrome, proteinuria, fatigue, liver dysfunction and anorexia, whereas hematologic AEs, including neutropenia, anemia and thrombocytopenia, occurred at high rates because of the use of combination therapy (Table 4). Most toxicities were generally grade 1–2 and manageable.

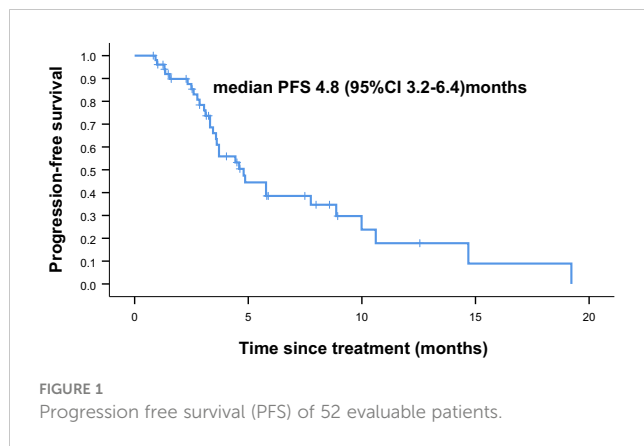
4 Discussion

Our present study reported the efficacy and safety of apatinib combined with chemotherapy in patients with pretreated MBC in a real world setting. In this study, all 52 patients were resistant to standard

TABLE 1 Patient characteristics at baseline.

| Characteristics | Number N=61 | % |
|---|-------------|-------|
| Age | | |
| <60 years | 54 | 88.5 |
| ≥60 years | 7 | 11.5 |
| Histology | | |
| Ductal | 53 | 86.9% |
| Lobular | 2 | 3.3% |
| Metaplastic carcinoma/phyllodes sarcoma | 6 | 9.8 |
| Molecular Subtype | | |
| TNBC | 23 | 37.7 |
| ER positive/Her2 negative breast cancer | 32 | 52.5 |
| HER2 positive breast cancer | 6 | 9.8 |
| Metastatic sites | | |
| Lymph nodes | 33 | 54.1 |
| Chest wall | 34 | 55.7 |
| Bone | 25 | 41 |
| Liver | 19 | 31.1 |
| Lung | 16 | 26.2 |
| Pleural | 16 | 26.2 |
| Brain | 2 | 3.3% |
| Number of prior chemotherapy lines in metastatic setting, median line=2(0-5) | | |
| 0 | 5 | 8.2% |
| 1 | 16 | 26.2 |
| 2 | 20 | 32.8 |
| ≥3 | 20 | 32.8 |
| Combined chemo-regimens | | |
| Gemcitabine | 16 | 26.2 |
| Vinorelbine | 16 | 26.2 |
| Taxanes | 15 | 24.6 |
| Capecitabine | 10 | 16.4 |
| Platinum | 7 | 11.5 |
| Anthracycline | 4 | 6.6 |
| Sequence of chemo and apatinib | | |
| Synchronously | 49 | 80.3 |
| Chemo first | 9 | 14.8 |
| Apatnib first | 3 | 4.9 |

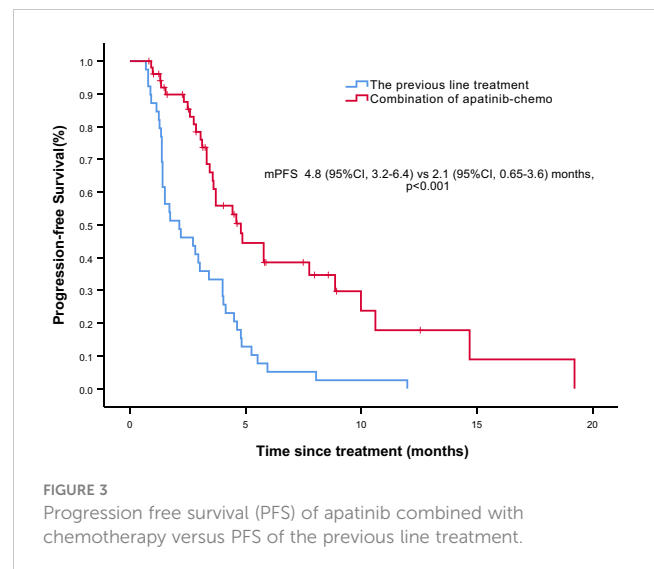
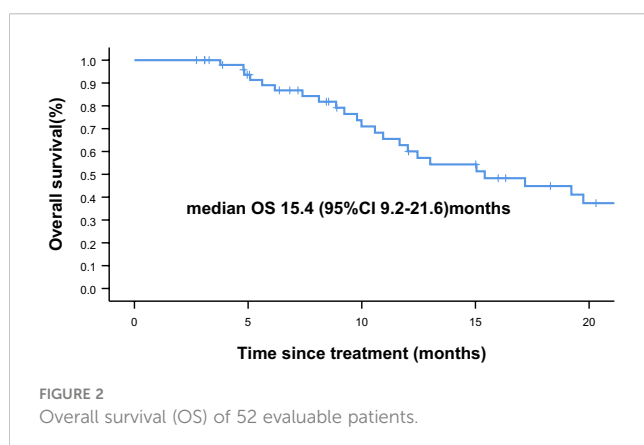
TNBC, triple-negative breast cancer; ER, Estrogen receptor; HER2, human epidermal growth factor receptor 2.



treatment, the median number of prior chemotherapy lines was 2(0-5), and the cohort included patients with TNBC and ER-positive/HER2-negative breast cancer with resistance to chemotherapy and endocrine therapy and patients with HER2-positive breast cancer who progressed on at least one anti-HER2 agent. Because this study started early from the year 2016 to 2019, many new drugs like CDK4/6 inhibitors, T-DM1 and pembrolizumab did not launch in China or were not covered by medical insurance at that time, so nearly all of the patients enrolled in this study did not receive today's standard treatment due to drug accessibility and/or expensive cost but they failed standard treatment at that time.

The ORR was 25%, median PFS and OS was 4.8 and 15.4 months, respectively. These results were nearly consistent with those of previous clinical trials. Meanwhile, our study obtained a very favorable DCR of 86.5% which was higher than that was reported in most of trials.

A number of recent studies have explored the efficacy of apatinib, both alone and in combination, in pretreated MBC. Median PFS for apatinib monotherapy ranged 3.3–4.6 months, and that for the combination of apatinib and chemotherapy ranged 4.4–6.9 months (reviewed in Table Supplement). Median OS in these studies ranged 8.3–20.0 months (15, 16, 24, 27–31). We have reported a prospective multi-center phase II study of apatinib single or combination with endocrine therapy in HER2 negative breast cancer involving chest wall metastasis, the median PFS was 4.9 (95% CI: 2.1–8.3) months (29). Most of these trials were single-armed studies without control group. Only one retrospective study



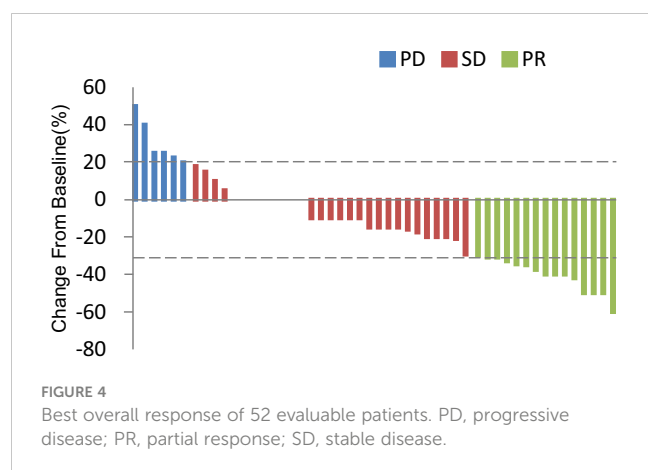
compared apatinib combined with capecitabine to capecitabine alone as the third-line therapy in advanced TNBC. The combination group had longer PFS (5.5 months vs. 3.5 months, $p = 0.001$) and a higher ORR (40.9% vs. 13.4%, $p = 0.042$) than the capecitabine group. As reported in the ASCENT study, median PFS was 5.6 months for sacituzumab govitecan (SG) and 1.7 months for chemotherapy in patients with heavily pretreated metastatic TNBC (32). Our subgroup analysis of patients with TNBC revealed a PFS of 3.7 months for apatinib combined with chemotherapy, however, due to the difference of study design and different enrolled population of studies and other limits, the results of different studies could not be directly compared. Further controlled research is needed to explore superiority of chemotherapy alone or in combination with apatinib.

Notably, although the current study was single-armed without control group, we conducted PFS analysis of the previous line of treatment in the same cohort, and median PFS was only 2.1 months, which was significantly shorter than that of apatinib–chemotherapy combination treatment. The relatively short PFS indicated the aggressiveness of the disease; hence, patients receiving apatinib–chemotherapy combination treatment had a heavier tumor burden and worse condition. Therefore, although it may be somewhat affected by the limitations of the self-controlled case series method, this finding is still valuable. Additionally, some patients

TABLE 2 Best response in evaluated patients (N=52).

| Best response | N (%) | mPFS (months,95%CI) | P value |
|----------------|-----------|---------------------|---------|
| CR | 0 | – | <0.001 |
| PR | 13 (25) | 10.0 (7.7-12.2) | |
| SD | 32 (61.5) | 3.7 (3.5-3.9) | |
| PD | 7 (13.5) | 1.3 (1.3-1.4) | |
| ORR (CR+PR) | 13 (25) | – | |
| DCR (CR+PR+SD) | 45 (86.5) | – | |

CR, complete response; PR, partial response; SD, stable disease; PD, progressive disease; ORR, objective response rate; DCR, disease control rate; mPFS, median progression free survival.



in our study received apatinib plus chemotherapy after a subpar response to initial chemotherapy alone, and a better response was observed in most patients, suggesting that the addition of apatinib can improve the efficacy of chemotherapy.

Another question is whether the addition of chemotherapy to apatinib produces better outcomes than apatinib alone. No clinical trials have directly compared apatinib monotherapy with the combination of apatinib and chemotherapy in breast cancer. Median PFS of apatinib monotherapy reported in clinical trials of breast cancer ranged from 3.3 to 4.6 months, which appeared inferior to the reported PFS of apatinib combination therapy (4.4–6.9 months). Bevacizumab monotherapy provided little clinical benefit in previously treated metastatic colorectal cancer. The median PFS and ORR for bevacizumab alone were 2.7 months and 3.3%, respectively, those for chemotherapy alone were 4.7 months and 8.6%, respectively, and those for the combination of bevacizumab and chemotherapy were 7.3 months and 22.7%, respectively (33). However, as a single agent, apatinib provided remarkable survival benefits in the third-line treatment of gastric cancer versus placebo (14). The exact reason is unclear, but in terms of the mechanism, bevacizumab is a monoclonal antibody directed against VEGFA that acts by binding and neutralizing all VEGFA isoforms (6). It is different that small-molecule TKIs block downstream signaling pathways by inhibiting the activity of VEGF receptors instead of binding to VEGF directly (6). More importantly, apatinib selectively inhibits VEGFR2, which is the key signaling receptor involved in the VEGF pathway. Compared with bevacizumab, apatinib has the advantage of oral bioavailability. Subgroup analysis of one small retrospective study (27 patients) revealed that PFS was even shorter in the apatinib combination group (20 patients, 3.1 months) than in the single-agent apatinib group (7 patients, 3.46 months) (34).

Moreover more studies on apatinib have focused on TNBC because of the limited treatment options for breast cancer of this subtype. Our study also included HER2-positive and ER positive breast cancer. These patients all failed previous available standard treatments. The subgroup analysis of our study suggested that there was no significant difference in PFS and ORR between different subtypes, results seemed to be better in the HER2-positive and hormone receptor-positive groups than in the TNBC group. However, the number of cases in HER2 positive group was too small, and some of them also received anti-HER2 targeted therapy in addition to apatinib

and chemotherapy. In fact, it has been demonstrated that HER2 can increase VEGF protein synthesis by activation of the mTOR/p70S6K cap-dependent translation pathway in human breast cancer cells (35). VEGF might contribute to the aggressiveness of HER2-positive breast cancer (36). Additionally, some studies have suggested that the VEGF pathway could play a role in tamoxifen resistance in ER-positive breast cancer (37). These findings provide some theoretical basis for the effectiveness of apatinib in refractory HER2-positive and ER-positive breast cancers. In addition, subgroup analysis of our study revealed that median PFS for apatinib combined with chemotherapy was similar in different treatment lines, despite no patients obtained partial response in the first line treatment while 18.8% and 32.3% patients got partial response in the second and later lines. This may due to that the sample size for the first line group was too small (only five patients), and the size of their tumor lesions did not meet the measurable criteria, so it could only be evaluated as SD not PR even if the tumor was reduced significantly. Overall, our study suggested that the combination of apatinib and chemotherapy could be a potential treatment option in heavily pretreated MBC regardless of molecular subtypes and treatment lines.

In addition, new combinational regimens containing apatinib in MBC are under exploration (38–40). A phase II study reported the ORR (43.3%) and median PFS (3.7 months) of a combination of the immune checkpoint inhibitor camrelizumab and apatinib (250 mg) in patients with TNBC who received fewer than three lines of systemic therapy regardless of the line of therapy and the PD-L1 status (38). Another phase II study reported a favorable ORR (37.7%) and median PFS (8.1 months) for camrelizumab combined with apatinib (250 mg) and eribulin in heavily pretreated patients with advanced TNBC, and the PD-L1 status was not associated with ORR/PFS (39). And for germline BRCA1/2 mutated HER2 negative MBC, OlympiAD study and other studies have confirmed statistically significant PFS benefit of

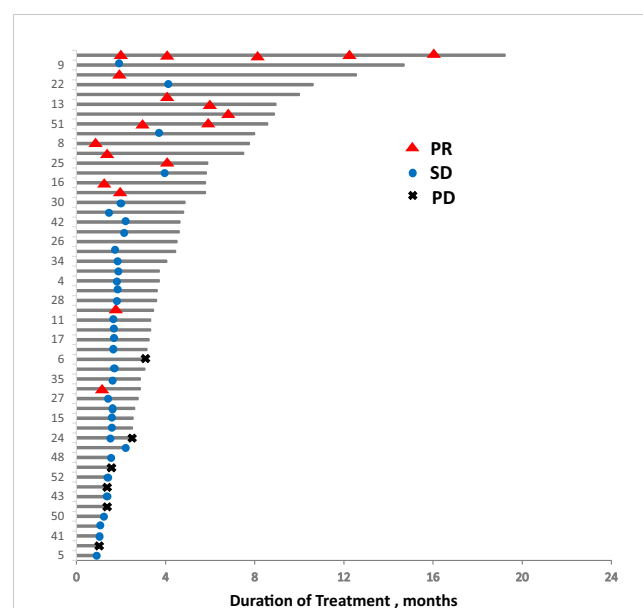


TABLE 3 Response and PFS in different subgroups.

| Subgroup | ORR | | PFS | |
|-------------------------|--------------|---------|---------------------|---------|
| | ORR (N,%) | p value | mPFS (months,95%CI) | p value |
| Subtypes | | | | |
| TNBC | 2/21 (9.5) | 0.081 | 3.6 (2.1-5.0) | 0.184 |
| ER+/HER2- | 8/26 (30.8) | | 5.8 (0.4-11.1) | |
| HER2+ | 3/5 (60.0) | | 7.8 (3.5-12.0) | |
| Target lesion | | | | |
| Liver | 5/15 (33.3) | 0.492 | 3.7 (0.0-9.0) | 0.988 |
| Chest wall/LN | 8/28 (28.6) | | 5.8 (3.0-8.6) | |
| Lung | 0/6 (0) | | 3.3 (-) | |
| Others | 0/3 (0) | | 4.8 (-) | |
| Combined regimen | | | | |
| Gemcitabine | 6/14 (42.9) | 0.422 | 5.8 (2.8-8.8) | 0.805 |
| Vinorelbine | 3/13 (23.1) | | 3.6 (2.6-4.6) | |
| Capecitabine | 1/6 (16.7) | | 19.2 (-) | |
| Taxanes | 2/10 (20.0) | | 4.8 (4.2-5.4) | |
| Others | 1/9 (11.1) | | 4.6 (3.4-5.8) | |
| Treatment line | | | | |
| 1 | 0/5 (0) | 0.407 | 4.8 (4.4-5.2) | 0.655 |
| 2 | 3/16 (18.8) | | 4.4 (3.0-5.9) | |
| ≥3 | 10/31 (32.3) | | 4.9 (2.9-6.8) | |

ORR, objective response rate; mPFS, median progression free survival; LN, lymph node.

poly(ADP ribose) polymerase (PARP) inhibitors compared with chemotherapy treatment (40, 41). A study of fluzoparib (one PARP inhibitor) ± apatinib versus chemotherapy of physician's choice in patients with HER2-negative MBC and germline BRCA mutations is ongoing (NCT number: [NCT04296370](#)).

Concerning safety, owing to the high incidence of hypertension and hand-foot syndrome for high-dose apatinib in previous studies and in real-world clinical practice, in this current study, all patients received apatinib at a dose of 250 mg in combination with

chemotherapy. This lower dose resulted in a lower incidence of AEs with comparable efficacy to high-dose apatinib as reported in previous studies. It is suggested that 250 mg might be the appropriate dose of apatinib when used in combination with chemotherapy, especially in patients who have received multi-line treatments.

In summary, the findings of our present study add to the existing knowledge for apatinib in MBC, it is possible to provide a basis for the treatment of refractory breast cancer patients with apatinib 250 mg combined with chemotherapy.

TABLE 4 Adverse Events graded based on CTCAE 4.0.

| Adverse events | Grade1-2 (n,%) | Grade3-4 (n,%) | All grades (n,%) |
|--------------------|----------------|----------------|------------------|
| Hypertention | 14 (23.0) | 2 (3.3) | 16 (26.0) |
| Hand-foot syndrome | 12 (19.7) | 3 (4.9) | 15 (24.6) |
| Proteinuria | 10 (16.4) | 2 (3.3) | 12 (19.7) |
| Fatigue | 10 (16.4) | 0 | 10 (16.4) |
| Anorexia | 9 (14.8) | 0 | 9 (14.8) |
| Neutropenia | 25 (41.0) | 3 (4.9) | 28 (45.9) |
| Anemia | 25 (41.0) | 3 (4.9) | 28 (45.9) |
| Thrombocytopenia | 10 (16.4) | 2 (3.3) | 12 (19.7) |
| Liver dysfunction | 9 (14.8) | 1 (1.6) | 10 (16.4) |

Nevertheless, there are several limitations in this study. Firstly, retrospective study design: the study relied on a retrospective review of medical records, which means that the data collected may not have been as comprehensive as it would have been in a prospective study. Retrospective studies are limited by the quality and completeness of the medical records, which could have led to missing or incomplete data on the treatment toxicity and the tumor assessment as well. Secondly, the study was lack of control groups, it only included patients who were treated with apatinib combined with chemotherapy, which makes it difficult to determine the extent to which the observed outcomes were due to the apatinib versus chemotherapy. Thirdly, the study only included patients from one institution, which may not be representative of the broader population of breast cancer patients; And the sample size was small, which lead to that it was insufficient to draw conclusions of subgroup analysis, the inferences about the results of subgroup analysis should be cautious.

Further multi-center, prospective and large randomized controlled trials are warranted to directly compare apatinib alone, chemotherapy alone, and combination of apatinib with chemotherapy to clarify the role of apatinib in advanced breast cancer treatment aiming to address these limitations.

Data availability statement

The original contributions presented in the study are included in the article/**Supplementary Material**. Further inquiries can be directed to the corresponding authors.

Ethics statement

The studies involving human participants were reviewed and approved by Ethics Committee of Peking University Cancer Hospital. The patients/participants provided their written informed consent to participate in this study.

References

- Cardoso F, Paluch-Shimon S, Senkus E, Curigliano G, Aapro MS, Andre F, et al. 5th ESO-ESMO international consensus guidelines for advanced breast cancer (ABC 5). *Ann Oncol* (2020) 31(12):1623–49. doi: 10.1016/j.annonc.2020.09.010
- Shadbad MA, Safaei S, Brunetti O, Derakhshani A, Lotfinejad P, Mokhtarzadeh A, et al. A systematic review on the therapeutic potentiality of PD-L1-Inhibiting MicroRNAs for triple-negative breast cancer: toward single-cell sequencing-guided biomimetic delivery. *Genes (Basel)* (2021) 12(8). doi: 10.3390/genes12081206
- Dogheim GM, Amralla MT. Proteolysis targeting chimera (PROTAC) as a promising novel therapeutic modality for the treatment of triple-negative breast cancer (TNBC). *Drug Dev Res* (2023). doi: 10.1002/ddr.22055
- Hanahan D, Weinberg RA. Hallmarks of cancer: the next generation. *Cell* (2011) 144(5):646–74. doi: 10.1016/j.cell.2011.02.013
- Mei B, Chen J, Yang N, Peng Y. The regulatory mechanism and biological significance of the snail-miR590-VEGFR-NRP1 axis in the angiogenesis, growth and metastasis of gastric cancer. *Cell Death Dis* (2020) 11(4):241. doi: 10.1038/s41419-020-2428-x
- Banerjee S, Dowsett M, Ashworth A, Martin L. Mechanisms of disease: angiogenesis and the management of breast cancer. *Nat Clin practice. Oncol* (2007) 4(9):536–50. doi: 10.1038/ncponc0905
- Hicklin DJ, Ellis LM. Role of the vascular endothelial growth factor pathway in tumor growth and angiogenesis. *J Clin Oncol* (2005) 23(5):1011–27. doi: 10.1200/JCO.2005.06.081
- Roviello G, Ravelli A, Polom K, Petrioli R, Marano L, Marrelli D, et al. Apatinib: a novel receptor tyrosine kinase inhibitor for the treatment of gastric cancer. *Cancer Lett* (2016) 372(2):187–91. doi: 10.1016/j.canlet.2016.01.014
- Ferrara N. Vascular endothelial growth factor: basic science and clinical progress. *Endocr Rev* (2004) 25(4):581–611. doi: 10.1210/er.2003-0027
- Gray R, Bhattacharya S, Bowden C, Miller K, Comis RL. Independent review of E2100: a phase III trial of bevacizumab plus paclitaxel versus paclitaxel in women with metastatic breast cancer. *J Clin Oncol* (2009) 27(30):4966–72. doi: 10.1200/JCO.2008.21.6630
- Miles DW, Chan A, Dirix LY, Cortes J, Pivrot X, Tomczak P, et al. Phase III study of bevacizumab plus docetaxel compared with placebo plus docetaxel for the first-line treatment of human epidermal growth factor receptor 2-negative metastatic breast cancer. *J Clin Oncol* (2010) 28(20):3239–47. doi: 10.1200/JCO.2008.21.6457
- Robert NJ, Dieras V, Glaspy J, Brufsky AM, Bondarenko I, Lipatov ON, et al. RIBBON-1: randomized, double-blind, placebo-controlled, phase III trial of chemotherapy with or without bevacizumab for first-line treatment of human

Author contributions

Study conception and design: RZ, GS, HL. Acquisition of data: RZ, YC, XRL, XG, AZ, HJ, BS, XL, YY, JZ. Drafting of the article: RZ, YC. Data analysis and interpretation: RZ, YC, XRL. All authors contributed to the work and approved it for publication.

Acknowledgments

We thank all patients and the staff of Peking University Cancer Hospital who participated in our study. We thank Joe Barber Jr., PhD, from Liwen Bianji (Edanz) for editing the English text of a draft of this manuscript.

Conflict of interest

The authors declare that the research was conducted in the absence of any commercial or financial relationships that could be construed as a potential conflict of interest.

Publisher's note

All claims expressed in this article are solely those of the authors and do not necessarily represent those of their affiliated organizations, or those of the publisher, the editors and the reviewers. Any product that may be evaluated in this article, or claim that may be made by its manufacturer, is not guaranteed or endorsed by the publisher.

Supplementary material

The Supplementary Material for this article can be found online at: <https://www.frontiersin.org/articles/10.3389/fonc.2023.1076469/full#supplementary-material>

epidermal growth factor receptor 2-negative, locally recurrent or metastatic breast cancer. *J Clin Oncol* (2011) 29(10):1252–60. doi: 10.1200/JCO.2010.28.0982

13. Brufsky A, Valero V, Tiangco B, Dakhlil S, Brize A, Rugo HS, et al. Second-line bevacizumab-containing therapy in patients with triple-negative breast cancer: subgroup analysis of the RIBBON-2 trial. *Breast Cancer Res Treat* (2012) 133(3):1067–75. doi: 10.1007/s10549-012-2008-6

14. Li J, Qin S, Xu J, Xiong J, Wu C, Bai Y, et al. Randomized, double-blind, placebo-controlled phase III trial of apatinib in patients with chemotherapy-refractory advanced or metastatic adenocarcinoma of the stomach or gastroesophageal junction. *J Clin Oncol* (2016) 34(13):1448–54. doi: 10.1200/JCO.2015.63.5995

15. Hu X, Cao J, Hu W, Wu C, Pan Y, Cai L, et al. Multicenter phase II study of apatinib in non-triple-negative metastatic breast cancer. *BMC Cancer* (2014) 14:820. doi: 10.1186/1471-2407-14-820

16. Hu X, Zhang J, Xu B, Jiang Z, Ragaz J, Tong Z, et al. Multicenter phase II study of apatinib, a novel VEGFR inhibitor in heavily pretreated patients with metastatic triple-negative breast cancer. *Int J Cancer* (2014) 135(8):1961–9. doi: 10.1002/ijc.28829

17. Mi YJ, Liang YJ, Huang HB, Zhao HY, Wu CP, Wang F, et al. Apatinib (YN968D1) reverses multidrug resistance by inhibiting the efflux function of multiple ATP-binding cassette transporters. *Cancer Res* (2010) 70(20):7981–91. doi: 10.1158/0008-5472.CAN-10-0111

18. Zhang Q, Song Y, Cheng X, Xu Z, Matthew OA, Wang J, et al. Apatinib reverses paclitaxel-resistant lung cancer cells (A549) through blocking the function of ABCB1 transporter. *Anticancer Res* (2019) 39(10):5461–71. doi: 10.21873/anticancer.13739

19. Tong XZ, Wang F, Liang S, Zhang X, He JH, Chen XG, et al. Apatinib (YN968D1) enhances the efficacy of conventional chemotherapeutic drugs in side population cells and ABCB1-overexpressing leukemia cells. *Biochem Pharmacol* (2012) 83(5):586–97. doi: 10.1016/j.bcp.2011.12.007

20. Chen J, Deng S, Zhang Y, Wang C, Hu X, Kong D, et al. Apatinib enhances the anti-tumor effect of paclitaxel via the PI3K/p65/Bcl-xl pathway in triple-negative breast cancer. *Ann Transl Med* (2021) 9(12):1001. doi: 10.21037/atm-21-805

21. Zhang Y, Xu J, Wang Q, Ling G, Mao Y, Cai M, et al. Efficacy and safety of second-line therapy with apatinib combined with chemotherapy as second-line therapy in advanced gastric cancer: a single-arm, open-label, prospective, multicenter study. *Ann Transl Med* (2022) 10(11):641. doi: 10.21037/atm-22-2752

22. Yu Z, Cai X, Xu Z, He Z, Lai J, Wang W, et al. Apatinib plus chemotherapy as a second-line treatment in unresectable non-small cell lung carcinoma: a randomized, controlled, multicenter clinical trial. *Oncologist* (2020) 25(11):e1640–9. doi: 10.1634/theoncologist.2020-0519

23. Yan Y, Li H, Wu S, Wang G, Luo H, Niu J, et al. Efficacy and safety of intermittent versus continuous dose apatinib plus docetaxel as second-line therapy in patients with advanced gastric cancer or gastroesophageal junction adenocarcinoma: a randomized controlled study. *Ann Transl Med* (2022) 10(4):205. doi: 10.21037/atm-22-546

24. Zhu A, Yuan P, Wang J, Fan Y, Luo Y, Cai R, et al. Apatinib combined with chemotherapy in patients with previously treated advanced breast cancer: an observational study. *Oncol Lett* (2019) 17(6):4768–78. doi: 10.3892/ol.2019.10205

25. Jiang Q, Zhang NL, Ma DY, Tan BX, Hu X, Fang XD. Efficacy and safety of apatinib plus docetaxel as the second or above line treatment in advanced nonsquamous NSCLC: a multi center prospective study. *Med (Baltimore)* (2019) 98(26):e16065. doi: 10.1097/MD.00000000000016065

26. Yang M, Liu X, Zhang C, Liao F, Li Z, Luo X, et al. A study of efficacy and safety with apatinib or apatinib combined with chemotherapy in recurrent/advanced ovarian cancer patients. *Cancer Manag Res* (2019) 11:8869–76. doi: 10.2147/CMAR.S223372

27. Li YH, Zhou Y, Wang YW, Tong L, Jiang RX, Xiao L, et al. Comparison of apatinib and capecitabine (Xeloda) with capecitabine (Xeloda) in advanced triple-

negative breast cancer as third-line therapy: a retrospective study. *Med (Baltimore)* (2018) 97(36):e12222. doi: 10.1097/MD.00000000000012222

28. Liu Z, Shan J, Yu Q, Wang X, Song X, Wang F, et al. Real-world data on apatinib efficacy - results of a retrospective study in metastatic breast cancer patients pretreated with multiline treatment. *Front Oncol* (2021) 11:643654. doi: 10.3389/fonc.2021.643654

29. Li H, Geng C, Zhao H, Jiang H, Song G, Zhang J, et al. Multicenter phase II study of apatinib single or combination therapy in HER2-negative breast cancer involving chest wall metastasis. *Chin J Cancer Res* (2021) 33(2):243–55. doi: 10.21147/j.issn.1000-9604.2021.02.11

30. Hu N, Zhu A, Si Y, Yue J, Wang X, Wang J, et al. Single-arm study of apatinib and oral etoposide in heavily pre-treated metastatic breast cancer. *Front Oncol* (2020) 10:565384. doi: 10.3389/fonc.2020.565384

31. Zhu A, Yuan P, Hu N, Li M, Wang W, Wang X, et al. Phase II study of apatinib in combination with oral vinorelbine in heavily pretreated HER2-negative metastatic breast cancer and clinical implications of monitoring ctDNA. *Cancer Biol Med* (2021) 18(3):875–87. doi: 10.20892/j.issn.2095-3941.2020.0418

32. Bardia A, Hurvitz SA, Tolane SM, Loirat D, Punie K, Oliveira M, et al. Sacituzumab govitecan in metastatic triple-negative breast cancer. *N Engl J Med* (2021) 384(16):1529–41. doi: 10.1056/NEJMoa2028485

33. Giantonio BJ, Catalano PJ, Meropol NJ, O'Dwyer PJ, Mitchell EP, Alberts SR, et al. Eastern Cooperative oncology group study: bevacizumab in combination with oxaliplatin, fluorouracil, and leucovorin (FOLFOX4) for previously treated metastatic colorectal cancer: results from the Eastern cooperative oncology group study E3200. *J Clin Oncol* (2007) 25(12):1539–44. doi: 10.1200/JCO.2006.09.6305

34. Lifang Y, L. J, Q. L, S. X, Z. A, S. X, et al. Clinical efficacy of apatinib in patients with heavily pretreated metastatic breast cancer. *Oncol Prog* (2017) 15(4):5. doi: 10.11877/j.issn.1672-1535.2017.15.04.17

35. Klos KS, Wyszomierski SL, Sun M, Tan M, Zhou X, Li P, et al. ErbB2 increases vascular endothelial growth factor protein synthesis via activation of mammalian target of rapamycin/p70S6K leading to increased angiogenesis and spontaneous metastasis of human breast cancer cells. *Cancer Res* (2006) 66(4):2028–37. doi: 10.1158/0008-5472.CAN-04-4559

36. Konecny GE, Meng YG, Untch M, Wang HJ, Bauerfeind I, Epstein M, et al. Association between HER-2/neu and vascular endothelial growth factor expression predicts clinical outcome in primary breast cancer patients. *Clin Cancer Res* (2004) 10(5):1706–16. doi: 10.1158/1078-0432.ccr-0951-3

37. Svensson S, Jirstrom K, Ryden L, Roos G, Emdin S, Ostrowski MC, et al. ERK phosphorylation is linked to VEGFR2 expression and ets-2 phosphorylation in breast cancer and is associated with tamoxifen treatment resistance and small tumours with good prognosis. *Oncogene* (2005) 24(27):4370–9. doi: 10.1038/sj.onc.1208626

38. Liu J, Liu Q, Li Y, Li Q, Su F, Yao H, et al. Efficacy and safety of camrelizumab combined with apatinib in advanced triple-negative breast cancer: an open-label phase II trial. *J Immunother Cancer* (2020) 8(1). doi: 10.1136/jitc-2020-000696

39. Liu J, Wang Y, Tian Z, Lin Y, Li H, Zhu Z, et al. Multicenter phase II trial of camrelizumab combined with apatinib and eribulin in heavily pretreated patients with advanced triple-negative breast cancer. *Nat Commun* (2022) 13(1):3011. doi: 10.1038/s41467-022-30569-0

40. Zhang Q, Shao B, Tong Z, Ouyang Q, Wang Y, Xu G, et al. A phase Ib study of camrelizumab in combination with apatinib and fuzuloparib in patients with recurrent or metastatic triple-negative breast cancer. *BMC Med* (2022) 20(1):321. doi: 10.1186/s12916-022-02527-6

41. Robson ME, Tung N, Conte P, Im S-A, Senkus E, Xu B, et al. OlympiAD final overall survival and tolerability results: Olaparib versus chemotherapy treatment of physician's choice in patients with a germline BRCA mutation and HER2-negative metastatic breast cancer. *Ann Oncol* (2019) 30(4):558–66. doi: 10.1093/annonc/mdz012



OPEN ACCESS

EDITED BY

Paula R. Pohlmann,
University of Texas MD Anderson Cancer
Center, United States

REVIEWED BY

Ning Zhang,
Shandong University, China
Karl Reinhard Aigner,
MEDIAS Burghausen Clinic, Germany

*CORRESPONDENCE

Miguel Sampayo-Cordero
✉ sampayo.mc@gmail.com

RECEIVED 19 September 2022

ACCEPTED 19 June 2023

PUBLISHED 11 July 2023

CITATION

Sampayo-Cordero M, Miguel-Huguet B,
Malfettone A, López-Miranda E, Gion M,
Abad E, Alcalá-López D, Pérez-Escuredo J,
Pérez-García JM, Llombart-Cussac A and
Cortés J (2023) A single-arm study
design with non-inferiority and superiority
time-to-event endpoints: a tool for
proof-of-concept and de-intensification
strategies in breast cancer.
Front. Oncol. 13:1048242.
doi: 10.3389/fonc.2023.1048242

COPYRIGHT

© 2023 Sampayo-Cordero, Miguel-Huguet,
Malfettone, López-Miranda, Gion, Abad,
Alcalá-López, Pérez-Escuredo, Pérez-García,
Llombart-Cussac and Cortés. This is an
open-access article distributed under the
terms of the [Creative Commons Attribution
License \(CC BY\)](https://creativecommons.org/licenses/by/4.0/). The use, distribution or
reproduction in other forums is permitted,
provided the original author(s) and the
copyright owner(s) are credited and that
the original publication in this journal is
cited, in accordance with accepted
academic practice. No use, distribution or
reproduction is permitted which does not
comply with these terms.

A single-arm study design with non-inferiority and superiority time-to-event endpoints: a tool for proof-of-concept and de-intensification strategies in breast cancer

Miguel Sampayo-Cordero^{1*}, Bernat Miguel-Huguet²,
Andrea Malfettone¹, Elena López-Miranda^{1,3}, María Gion³,
Elena Abad¹, Daniel Alcalá-López¹, Jhudit Pérez-Escuredo¹,
José Manuel Pérez-García^{1,4}, Antonio Llombart-Cussac^{1,5}
and Javier Cortés^{1,4,6}

¹Medica Scientia Innovation Research (MEDSIR), Barcelona, Spain, ²Gerència Territorial Metropolitana Sud, Institut Català De La Salut, Hospital Universitari De Bellvitge, Barcelona, Spain, ³Hospital Universitario Ramón y Cajal, Madrid, Spain, ⁴International Breast Cancer Center (IBCC), Quiron Group, Barcelona, Spain, ⁵Hospital Arnau de Vilanova, FISABIO, Universidad Católica de Valencia, Valencia, Spain, ⁶Vall d'Hebron Institute of Oncology (VHIO), Barcelona, Spain

De-escalation trials in oncology evaluate therapies that aim to improve the quality of life of patients with low-risk cancer by avoiding overtreatment. Non-inferiority randomized trials are commonly used to investigate de-intensified regimens with similar efficacy to that of standard regimens but with fewer adverse effects (ESMO evidence tier A). In cases where it is not feasible to recruit the number of patients needed for a randomized trial, single-arm prospective studies with a hypothesis of non-inferiority can be conducted as an alternative. Single-arm studies are also commonly used to evaluate novel treatment strategies (ESMO evidence tier B). A single-arm design that includes both non-inferiority and superiority primary objectives will enable the ranking of clinical activity and other parameters such as safety, pharmacokinetics, and pharmacodynamics data. Here, we describe the statistical principles and procedures to support such a strategy. The non-inferiority margin is calculated using the fixed margin method. Sample size and statistical analyses are based on the maximum likelihood method for exponential distributions. We present example analyses in metastatic and adjuvant settings to illustrate the usefulness of our methodology. We also explain its implementation with nonparametric methods. Single-arm designs with non-inferiority and superiority analyses are optimal for proof-of-concept and de-escalation studies in oncology.

KEYWORDS

time-to-event, non-inferiority, single-arm, phase II, clinical trial, superiority

1 Introduction

Molecular diagnostics and biomarkers have enabled many cancers to be divided into clinical and biological subtypes, some of which have a low risk of relapse or death (1–4). In patients with low-risk breast cancer, de-escalation trials are increasingly being conducted to evaluate therapies that aim to improve quality of life by avoiding overtreatment (1, 5, 6). These trials use non-inferiority designs to investigate de-intensified regimens with efficacy similar to that of standard treatments but with fewer toxic effects (5, 7–9). Although randomized trials provide the strongest evidence (ESMO evidence tier A) for the efficacy of de-escalation strategies (10–13), randomized designs are not always the most efficient option and cannot be used to answer all research questions (14–18). Furthermore, in certain cancer types and phases of clinical development, it is not feasible to recruit the number of patients needed for a randomized clinical trial. In such cases, de-escalation strategies can be investigated using single-arm or non-comparative trials (ESMO evidence tier B) (6, 13, 19–22). Single-arm trials can also be used to evaluate novel therapies, agents with a high expectation of tumor response, rare cancers, salvage therapies, and therapies for late-stage disease, especially when no standard-of-care exists and a robust historical database is available (15, 18, 23). The inclusion of both non-inferiority and superiority primary objectives in single-arm study designs enables informed decisions that rank the magnitude of clinical activity along with other parameters such as safety, pharmacokinetics, and pharmacodynamics data (24–26).

Some treatments have been successful in phase III trials even after producing negative results in phase II single-arm trials. In these situations, a new treatment was deemed non-inferior to standard-of-care therapy when considered in the context of relevant parameters such as safety, duration of clinical benefit, or targeting of a new biological pathway (27, 28). However, the likelihood of a type I error (α) increases when a *post-hoc* non-inferiority analysis is performed after an unsuccessful proof-of-concept trial (25, 29). The probability of such an error can be reduced by including the non-inferiority analysis in the experimental design *a priori* (24–26). It is easy to include non-inferiority and superiority analyses in single-arm one-stage or two-stage studies with response rate as the primary endpoint (24); however, the most reliable and preferred endpoint in cancer studies is overall survival.

It is common to plan proof-of-concept and confirmatory studies in oncology using time-to-event endpoints (19, 30, 31). Most approvals for breast cancer drugs in adjuvant and advanced settings are supported by improvements in overall survival, disease-free survival (DFS), and progression-free survival (PFS) (32). Although there are a few single-arm trials that used a historic control arm to set a non-inferiority threshold for a time-to-event outcome (5, 20, 33), these trials did not include an additional superiority analysis for the primary objective. Here, we propose a single-arm, time-to-event study design that includes both superiority and non-inferiority analyses.

2 Material and methods

2.1 Non-inferiority margin

Single-arm studies with a time-to-event primary endpoint usually include a superiority analysis that aims to show that the probability of survival (e.g., median PFS [mPFS]) with a certain treatment is greater than the probability of survival estimated for an active control arm (mPFS0) in a previous trial (34). Conversely, the risk of progression or death with the treatment, represented by a hazard rate (λ) equal to the Napierian logarithm of 2 ($\text{LN}[2]$) divided by mPFS, is expected to be lower than the risk of progression or death in the active control arm (λ_0) (34). In contrast to such superiority analyses, a non-inferiority analysis aims to show that the effect of a test drug in terms of survival is not inferior to that of the historical comparator by more than a specified amount called the non-inferiority margin (NIM) (29). The NIM calculation is based on the difference in observed effects between the historical comparator and placebo in previous studies, which is represented by a hazard ratio (HR) that is greater than 1 and equal to either the mPFS0 divided by the mPFS in the placebo arm ($\text{mPFS}_{\text{placebo}}$) or the λ in the placebo arm (λ_{placebo}) divided by the λ_0 (7, 24, 29). For example, if the HR is 2.4 with a 95% confidence interval (CI) of 1.44–3.56, the fixed margin method is applied to select the 95% CI lower bound (1.44) and adjust it to retain at least 50% of the historical effect of the active control versus the placebo: $1.44^{(1-0.5)} = 1.2$. Accordingly, the calculated NIM describes a ratio reflecting the largest loss of the effect previously observed in the active control arm that would be clinically acceptable (29).

2.2 Non-inferiority and superiority analyses in a single-arm design

The null hypothesis (H_0) for superiority and non-inferiority analyses in a one-sided test can be defined in terms of survival (mPFS) or hazard (λ) parameters as follows:

$$H_{0,\text{superiority}}: \text{mPFS} \leq \text{mPFS}_0; \lambda \geq \lambda_0 \quad (1)$$

$$H_{0,\text{non-inferiority}}: \text{mPFS} \leq (\text{mPFS}_0/\text{NIM}); \lambda \geq (\lambda_0 \times \text{NIM}) \quad (2)$$

Additionally, the magnitude of the difference between the treatment arm and the historical control (i.e., the effect size) can be defined in terms of mPFS or λ for superiority and non-inferiority analysis as follows:

$$\text{Superiority} : \text{mPFS} - \text{mPFS}_0; \lambda - \lambda_0 \quad (3)$$

$$\text{Non-inferiority} : \text{mPFS} - (\text{mPFS}_0 / \text{NIM}); \lambda - (\lambda_0 \times \text{NIM}) \quad (4)$$

The cutoff for $H_{0,\text{non-inferiority}}$ will be always lower than the cutoff for $H_{0,\text{superiority}}$ (i.e., $\text{mPFS}_{0,\text{non-inferiority}} < \text{mPFS}_{0,\text{superiority}}$), and the converse will be true when H_0 is defined in terms of hazard rates (i.e., $\lambda_{0,\text{non-inferiority}} > \lambda_{0,\text{superiority}}$). At the time of final analysis in a

single-arm trial, the number of patients recruited (n), the events observed, the mPFS, and the λ will be equal for the non-inferiority and superiority analyses. Therefore, the difference in effect size between the superiority and non-inferiority analyses is totally dependent on the magnitude of the preplanned H_0 . In a one-sided test that will accept H_0 if the study mPFS is less than the mPFS of the historical control, H_0 is rejected only if mPFS is greater than mPFS₀ (or λ is less than λ_0). In all these scenarios, the absolute value of the effect size in the non-inferiority analysis will be greater than the absolute value of the effect size in the superiority analysis:

$$|mPFS - mPFS_0| < |mPFS - (mPFS_0 / NIM)| \quad (5)$$

The same is true in terms of hazard rates:

$$\text{If } \lambda < \lambda_0, \text{ then } \lambda_0 < (\lambda_0 \times NIM) \text{ and } |\lambda - \lambda_0| < |\lambda - (\lambda_0 \times NIM)| \quad (6)$$

As the number of events is equal in the superiority and non-inferiority analyses, it follows that the probability of detecting an effect (i.e., the power of the test) will always be greater in the non-inferiority analysis than in the superiority analysis. Therefore, the type II error level (β) planned for the superiority analysis is retained in the inferiority analysis (24, 35).

As stated in the United States Food and Drug Administration's multiple endpoint guidelines, "after demonstrating non-inferiority on the endpoint, it is possible to then test for superiority at an unadjusted alpha" Thus, in a superiority analysis with a time-to-event primary endpoint, analysis of a non-inferiority hypothesis does not inflate the type I error rate when the non-inferiority analysis and NIM are properly pre-specified (29, 36).

The design proposed here can be used to assess both superiority and non-inferiority criteria with the same sample size, type I error rate (α), and β that would be used in a superiority-only strategy. This applies to both parametric (exponential or Weibull distribution estimator) and nonparametric (Kaplan–Meier or life table estimator) approaches (34, 37).

3 Results

3.1 Sample size calculation in a metastatic setting

The following section provides a numerical example of the proposed design for a typical phase II single-arm (proof-of-concept) trial that includes both non-inferiority and superiority analyses in a metastatic setting. Suppose that mPFS for a standard therapy is 12 months. This corresponds to a λ_0 ($\text{LN}[2]/\text{mPFS}[12]$) of 0.058. We would design a study to detect mPFS improvement to at least 18 months ($\lambda_1 = \text{LN}[2]/18 = 0.039$), producing an HR of 0.67 ($\text{HR} = 12/18$). We plan a 12-month accrual period (ap) and a 24-month follow-up period (fp). We design the study to attain 90% power ($1 - \beta$) using the maximum likelihood method for exponential distributions at a nominal one-sided α level of 10%. The maximum accepted α level in our example is higher than what is usually used in confirmatory trials (i.e., one-sided α of 2.5% or two-sided α of 5%). This is appropriate because of the exploratory

nature of our trial. We also assume a 10% dropout rate. The required number of patients and events is calculated as follows, where Z is the standard normal cumulative distribution function for a one-sided test (34):

$$\begin{aligned} \text{Events} &= \frac{(Z_{1-\alpha=0.1} + Z_{1-\beta=0.1})^2}{(\text{LN}(\text{HR} = 0.667))^2} = \frac{(1.282 + 1.282)^2}{(-0.405)^2} = 39.96 \\ &\approx 40 \end{aligned} \quad (7)$$

$$\begin{aligned} \text{Probability of event} &= 1 - \left(\frac{e^{(-\lambda_1 \times \text{fp})}}{\lambda_1 \times \text{ap}} \times (1 - e^{(-\lambda_1 \times \text{ap})}) \right) = \\ &= 1 - \left(\frac{e^{(-0.924)}}{1.39} \times (1 - e^{(-0.462)}) \right) = 0.682 \end{aligned} \quad (8)$$

$$\text{Number of Patients} = \frac{\text{Events}}{\text{Probability of event}} = \frac{40}{0.682} = 58.6 \quad (9)$$

$$\begin{aligned} \text{Drop out correction} &= 58.6 / (1 - \text{dropout rate } [0.1]) = 65.1 \\ &\approx 66 \text{ patients} \end{aligned} \quad (10)$$

The Excel functions to resolve this are "INV.NORM.ESTAND ($1 - (\alpha = 0.1)$)" and "INV.NORM.ESTAND ($1 - (\beta = 0.1)$)"; e^x represents the natural exponential function ("exp(x)" in Excel).

3.2 Final analyses in a metastatic setting

Continuing with this example, it is supposed that by the end of the study 66 patients have been accrued, 54 PFS events have occurred, and the final mPFS is 12 months, with a hazard rate (λ_{obs}) of 0.058. Based on an NIM of 1.2, $H_{0\text{non-inferiority}}$ is an mPFS (mPFS₀/NIM = 12/1.2) of 10 months, which is equivalent to a non-inferiority hazard rate ($\lambda_{\text{NI}} = \text{LN}[2]/10$) of 0.069. Final statistical analyses for the superiority and non-inferiority objectives are performed using the maximum likelihood method for exponential distributions as follows (34):

$$\begin{aligned} \text{Non-inferiority:} \\ \text{p value} &= (1 - \Phi(\sqrt{\text{events}} \times (\text{LN}(\lambda_{\text{obs}}) - (\text{LN}(\lambda_{\text{NI}})))) = \\ &= (1 - \Phi(\sqrt{54} \times (\text{LN}(0.058) - (\text{LN}(0.069)))) = \\ &= 0.09 \text{ (p < 0.1)} \end{aligned} \quad (11)$$

$$\begin{aligned} \text{Superiority:} \\ \text{p value} &= (1 - \Phi(\sqrt{\text{events}} \times (\text{LN}(\lambda_{\text{obs}}) - (\text{LN}(\lambda_0)))) = \\ &= (1 - \Phi(\sqrt{54} \times (\text{LN}(0.058) - (\text{LN}(0.058)))) = \\ &= 0.5 \text{ (p > 0.1)} \end{aligned} \quad (12)$$

The expression " $1 - \Phi()$ " is the standard normal cumulative distribution, which is used to back-transform Z-scores into p values.

3.3 Analysis in an adjuvant setting

Usually, the primary objective of clinical trials in adjuvant settings is DFS. The DFS rate is usually higher than 50%, so the median survival is not estimable. However, the previous analyses can be conducted in an adjuvant setting if the DFS rates are

transformed into hazard rates and HRs. In a study investigating an adjuvant therapy in early-stage breast cancer by Cardoso et al. (2016), the DFS rate without distant metastasis for a standard therapy was 95% at 5 years (60 months). This corresponds to a λ_0 of 0.0009 (5).

$$\lambda_0 = -\text{LN}(0.95)/(60 \text{ months}) = 0.0009 \quad (13)$$

The pre-specified NIM corresponds to a 3% difference in DFS without distant metastases at 5 years (i.e., from 95% to 92%). This corresponds to a $\lambda_{0\text{NI}}$ of 0.0014 (5).

$$\lambda_{0\text{NI}} = -\text{LN}(0.92)/(60 \text{ months}) = 0.0014 \quad (14)$$

The study was designed to attain 80% power at a nominal two-sided α level of 5%. Based on equation (7), the required number of events for this single-arm design is 34. By contrast, 135 events would be needed in a randomized study. The criteria for the primary analysis were met with 748 patients recruited from the primary test population; however, we would need about 3000 patients if we used a comparative design.

4 Discussion

De-intensification strategies are often developed in response to new diagnostics that can select patients who do not need aggressive therapy. Our proof-of-concept example shows how a novel de-intensified treatment can be shown to be non-inferior to the standard of care in selected patients. In such a case, if safety data show that the novel treatment is better tolerated than the standard-of-care, further confirmatory studies should be developed to evaluate the novel treatment. Our method can also be used to explore the efficacy of new drugs. For example, if a new drug achieves the non-inferiority objective, as in our proof-of-concept example, and also shows good tolerability, an appropriate pharmacokinetic profile, and/or a novel molecular target, then it might be expected to show further promising results when combined with standard treatment in a phase II/III randomized trial. Similarly, if a new drug achieves the superiority objective in our study design, this would suggest that it may be effective as a monotherapy (24).

Our approach enables the design of non-inferiority breast cancer studies in settings where it is not feasible to recruit enough patients for a comparative analysis (5, 6, 13). Although the sample size needed for a non-inferiority study is usually expected to be greater than the sample size needed for a superiority study, this is a misunderstanding. Actually, when a non-inferiority study uses the same assumptions as a superiority study, the non-inferiority study will always need fewer patients than the superiority study. The reason that non-inferiority studies are thought to need more patients than superiority studies is because non-inferiority studies assume that two treatments are equally effective, whereas superiority studies never make this assumption (38). In addition to the use of a single-arm primary analysis, there are some other ways to improve the quality of data in de-intensification studies. For example, a randomized non-comparative design can be used, in which the randomized control arm has far fewer patients than

would be needed for a powered comparative analysis (5, 6). Other approaches might be to use an external control based on previous clinical trials, detailed cancer registries, real-world evidence, and synthetic control arms (39).

A single-arm trial designed to analyze both non-inferiority and superiority objectives enables ranking of early efficacy and other parameters such as safety, pharmacokinetics, and pharmacodynamics data (26), making such an approach more informative than a trial designed to analyze only superiority or non-inferiority (24–26). As non-inferiority analysis is allowed, it could be conjectured that this design makes easier that ineffective therapies were assessed as promising. This assumes that evaluation of the treatment is based exclusively on the non-inferiority result, without considering other objectives. Risk-benefit assessments weighing all endpoints are usually performed when establishing development plans for new drugs. Accordingly, our method supports a comprehensive approach to drug development by enabling the totality of the evidence to be considered in favor of a therapy (40, 41).

Non-inferiority analysis can be implemented in time-to-event studies using the log-rank test methodology (42). In addition, our proposed design can be easily implemented with nonparametric methods such as Kaplan–Meier analysis, which usually estimates median survival or survival rates based on CIs. For instance, we would achieve a positive non-inferiority result with a 90% CI of 3.6–5.6, because the lower bound of the CI would be greater than 3.3, the H_0 for the non-inferiority test. Conversely, the superiority objective would not be achieved, because the lower bound of the 90% CI would be lower than 4, the H_0 for the superiority test. The sample size in time-to-event designs based on nonparametric tests can be easily calculated with various methods and online calculators (43–45). The same strategy can be used to prespecify thresholds for null hypotheses under a Bayesian framework (31).

Our method includes the inherent drawbacks of studies that rely on historical controls and non-inferiority analyses. These limitations are common and well-known in non-inferiority comparative study designs because the NIM must be based on historical evidence (46). In randomized controlled designs of non-inferiority, it is necessary to demonstrate assay sensitivity to declare a therapy non-inferior in a single-arm trial (12). Additionally, selection of inappropriate patients, premature discontinuations, and poor compliance all favor conclusions of a lack of difference between experimental and control arms in randomized trials. This can lead to erroneous declarations of non-inferiority of the experimental treatment. This bias is reduced when comparisons are based on a theoretical rate of efficacy deduced from historical controls (12, 46). Accordingly, single-arm designs with non-inferiority analyses that are properly preplanned and conducted are not more challenging than the usual randomized or single-arm designs (5, 24).

Various strategies to evaluate multiple endpoints of efficacy and safety in proof-of-concept trials have been proposed in Bayesian and frequentist paradigms (e.g., EFFT0x, Gumbel model, continual reassessment method, and single-stage and two-stage time-to-event designs). However, these designs do not rank non-inferiority and superiority hypotheses to grade the magnitude of clinical activity in the early clinical stages (19, 47–49).

Altogether, analyses of non-inferiority and superiority in single-arm trials are easily implemented in typical time-to-event designs for adjuvant and metastatic settings. This approach is useful for weighing additional factors such as safety, cost, and biomarkers while also assessing efficacy, making it optimal for proof-of-concept and de-intensification investigations in oncology.

Data availability statement

The raw data supporting the conclusions of this article will be made available by the authors, without undue reservation.

Author contributions

MS-C, AL-C, and JC conceived the study. MS-C, BM-H, DA-L, and EA developed the statistical methods. EL-M, MG, AM, JP-G, JP-E, AL-C, and JC reviewed the methods. MS-C, BM-H, DA-L, and EA conducted the statistical analysis. EL-M, MG, JP-G, AL-C, and JC reviewed the statistical results. MS-C, AM, and JP-G drafted the manuscript. All authors contributed to the article and approved the submitted version.

Funding

The authors declare that this study received funding from Medica Scientia Innovation Research (MEDSIR). The funder was not involved in the study design, collection, analysis, interpretation of data, the writing of this article, or the decision to submit it for publication.

Conflict of interest

Authors MS-C, AM, EL-M, EA, DA-L, JP-E, JP-G, AL-C, JC were employed by company Medica Scientia Innovation Research (MEDSIR).

MS-C declares grants from Medica Scientia Innovation Research MEDSIR, Syntax for Science, Optimapharm, MD

Anderson Cancer Center Madrid, and Ability Pharma that are outside the funding for the submitted work. AM is a medical writer at MEDSIR. JP-G declares a consulting role with Roche, and Daiichi-Sankyo; receiving travel expenses from Roche, to being a part-time employee of MEDSIR during the study period. AL-C declares playing a leadership role with Eisai, Celgene, Lilly, Pfizer, Roche, Novartis, and MSD; intellectual property with MEDSIR and Initia-Research; consulting roles with Lilly, Roche, Pfizer, Novartis, Pierre-Fabre, GenomicHealth, and GSK; membership in the speaker bureaus of Lilly, AstraZeneca, and MSD; research funding from Roche, Foundation Medicine, Pierre-Fabre, and Agendia; and travel expenses from Roche, Lilly, Novartis, Pfizer, and AstraZeneca. JC declares consulting roles with Roche, Celgene, Cellestia, AstraZeneca, Seattle Genetics, Daiichi Sankyo, Erytech, Athenex, Polyphor, Lilly, Merck Sharp&Dohme, GSK, Leuko, Bioasis, Clovis Oncology, Boehringer Ingelheim, Ellipses, HiberCell, BioInvent, Gemoab, Gilead Sciences, Menarini, Zymeworks, and Reveal Genomics; honoraria from Roche, Novartis, Celgene, Eisai, Pfizer, Samsung Bioepis, Lilly, Merck Sharp&Dohme, and Daiichi Sankyo; research funding from Roche, Ariad pharmaceuticals, AstraZeneca, Baxalta GMBH/Servier Affaires, Bayer healthcare, Eisai, F.Hoffman-La Roche, Guardanth health, Merck Sharp&Dohme, Pfizer, Piquar Therapeutics, Puma C, and Queen Mary University of London; intellectual property with MEDSIR, Nektar Pharmaceuticals, and Leuko relative; and receiving travel compensation from Roche, Novartis, Eisai, Pfizer, Daiichi Sankyo, and AstraZeneca.

The remaining authors declare that the research was conducted in the absence of any commercial or financial relationships that could be construed as a potential conflict of interest.

Publisher's note

All claims expressed in this article are solely those of the authors and do not necessarily represent those of their affiliated organizations, or those of the publisher, the editors and the reviewers. Any product that may be evaluated in this article, or claim that may be made by its manufacturer, is not guaranteed or endorsed by the publisher.

References

- Byng D, Retel V, Engelhardt E, Groothuis-Oudshoorn C, van Til J, Schmitz R, et al. Preferences of treatment strategies among women with low-risk DCIS and oncologists. *Cancers* (2021) 13:3962. doi: 10.3390/cancers13163962
- Administration F and D. *Paving the way for personalized medicine: fda's role in a new era of medical product development*. United States: Createspace Independent Pub (2014). p. 64.
- Bartlett JMS, Parelukar W. Breast cancers are rare diseases—and must be treated as such. *npj. Breast Cancer* (2017) 3. doi: 10.1038/s41523-017-0013-y
- Khoury T, Quinn M, Tian W, Yan L, Zhan H. Touching tumor-infiltrating lymphocytes in low risk ductal carcinoma in situ correlates with upgrade to high grade DCIS. *Histopathology* (2021) 80(2):291–303. doi: 10.1111/his.14539
- Cardoso F, van't Veer LJ, Bogaerts J, Slaets L, Viale G, Delaloge S, et al. 70-gene signature as an aid to treatment decisions in early-stage breast cancer. *New Engl J Med* (2016) 375:717–29. doi: 10.1056/NEJMoa1602253
- Pérez-García JM, Gebhart G, Ruiz Borrego M, Stradella A, Bermejo B, Schmid P, et al. Chemotherapy de-escalation using an 18F-FDG-PET-based pathological response-adapted strategy in patients with HER2-positive early breast cancer (PERSEPHONE): a multicentre, randomised, open-label, non-comparative, phase 2 trial. *Lancet Oncol* (2021) 22:858–71. doi: 10.1016/S1470-2045(21)00122-4
- Earl HM, Hiller L, Vallier A-L, Loi S, McAdam K, Hughes-Davies L, et al. 6 versus 12 months of adjuvant trastuzumab for HER2-positive early breast cancer (PERSEPHONE): 4-year disease-free survival results of a randomised phase 3 non-inferiority trial. *Lancet* (2019) 393:2599–612. doi: 10.1016/S0140-6736(19)30650-6
- Pivot X, Romieu G, Debled M, Pierga J-Y, Kerbrat P, Bachelot T, et al. 6 months versus 12 months of adjuvant trastuzumab in early breast cancer (PHARE): final analysis of a multicentre, open-label, phase 3 randomised trial. *Lancet* (2019) 393:2591–8. doi: 10.1016/S0140-6736(19)30653-1
- Giuliano AE, Ballman KV, McCall L, Beitsch PD, Brennan MB, Kelemen PR, et al. Effect of axillary dissection vs no axillary dissection on 10-year overall survival among

women with invasive breast cancer and sentinel node metastasis: the ACOSOG Z0011 (Alliance) randomized clinical trial. *JAMA* (2017) 318:918. doi: 10.1001/jama.2017.11470

10. *Cochrane handbook for systematic reviews of interventions*. Cochrane Training. Available at: <http://training.cochrane.org/handbook> (Accessed January 31, 2020).

11. ICH Harmonised Tripartite Guideline. *ICH topic e 9 statistical principles for clinical trials* (1998). Available at: https://www.ema.europa.eu/en/documents/scientific-guideline/ich-e-9-statistical-principles-clinical-trials-step-5_en.pdf.

12. *Choice of control group and related issues in clinical trials: ICH E10*. Available at: <http://www.ich.org/products/guidelines/efficacy/efficacy-single/article/choice-of-control-group-and-related-issues-in-clinical-trials.html> (Accessed January 31, 2021).

13. Trapani D, Franzoi MA, Burstein HJ, Carey LA, Delaloge S, Harbeck N, et al. Risk-adapted modulation through de-intensification of cancer treatments: an ESMO classification. *Ann Oncol* (2022) 33:702–12. doi: 10.1016/j.annonc.2022.03.273

14. Concato J, Shah N, Horwitz RI. Randomized, controlled trials, observational studies, and the hierarchy of research designs. *New Engl J Med* (2000) 342:1887–92. doi: 10.1056/NEJM200006223422507

15. Gan HK, Grothey A, Pond GR, Moore MJ, Siu LL, Sargent D. Randomized phase II trials: inevitable or inadvisable? *J Clin Oncol* (2010) 28:2641–7. doi: 10.1200/JCO.2009.26.3343

16. Frieden TR. Evidence for health decision making [amp]mdash; beyond randomized, controlled trials. *New Engl J Med* (2017) 377:465–75. doi: 10.1056/NEJMra1614394

17. Sampayo-Cordero M, Miguel-Huguet B, Malfettone A, Pérez-García JM, Llombart-Cussac A, Cortés J, et al. The value of case reports in systematic reviews from rare diseases: the example of enzyme replacement therapy (ERT) in patients with mucopolysaccharidosis type II (MPS-II). *Int J Environ Res Public Health* (2020) 17:6590. doi: 10.3390/ijerph17186590

18. Grayling MJ, Dimairo M, Mander AP, Jaki TF. A review of perspectives on the use of randomization in phase II oncology trials. *J Natl Cancer Inst* (2019) 111:1255–62. doi: 10.1093/jnci/djz126

19. Ortega V, Antón A, Garau I, Afonso N, Calvo L, Fernández Y, et al. Multicenter, single-arm trial of eribulin as first-line therapy for patients with aggressive taxane-pretreated HER2-negative metastatic breast cancer: the MERIBEL study. *Clin Breast Cancer* (2019) 19:105–12. doi: 10.1016/j.clbc.2018.12.012

20. Tolane SM, Guo H, Pernas S, Barry WT, Dillon DA, Ritterhouse L, et al. Seven-year follow-up analysis of adjuvant paclitaxel and trastuzumab trial for node-negative, human epidermal growth factor receptor 2–positive breast cancer. *JCO* (2019) 37:1868–75. doi: 10.1200/JCO.19.00066

21. Llombart-Cussac A, Cortés J, Paré L, Galván P, Bermejo B, Martínez N, et al. HER2-enriched subtype as a predictor of pathological complete response following trastuzumab and lapatinib without chemotherapy in early-stage HER2-positive breast cancer (PAMELA): an open-label, single-group, multicentre, phase 2 trial. *Lancet Oncol* (2017) 18:545–54. doi: 10.1016/S1470-2045(17)30021-9

22. König L, Dreyling M, Dürig J, Engelhard M, Hohloch K, Viardot A, et al. Therapy of nodal follicular lymphoma (WHO grade 1/2) in clinical stage I/II using response adapted involved site radiotherapy in combination with obinutuzumab (Gazyvaro) - GAZAI trial (GAZYvaro and response adapted involved-site radiotherapy): a study protocol for a single-arm, non-randomized, open, national, multi-center phase II trial. *Trials* (2019) 20:544. doi: 10.1186/s13063-019-3614-y

23. Sampayo-Cordero M, Miguel-Huguet B, Malfettone A, Pérez-García JM, Llombart-Cussac A, Cortés J, et al. The impact of excluding nonrandomized studies from systematic reviews in rare diseases: “The example of meta-analyses evaluating the efficacy and safety of enzyme replacement therapy in patients with mucopolysaccharidosis”. *Front Mol Biosci* (2021) 8:690615. doi: 10.3389/fmolb.2021.690615

24. Sampayo-Cordero M, Miguel-Huguet B, Pérez-García J, Páez D, Guerrero-Zotano AL, Garde-Noguera J, et al. Inclusion of non-inferiority analysis in superiority-based clinical trials with single-arm, two-stage simon’s design. *Contemp Clin Trials Commun* (2020). doi: 10.1016/j.conctc.2020.100678

25. Murray GD. Switching between superiority and non-inferiority. *Br J Clin Pharmacol* (2001) 52:219–9. doi: 10.1046/j.0306-5251.2001.01397.x

26. Committee For Proprietary medicinal products (CPMP). *The European agency for the evaluation of medicinal products. points to consider on switching between superiority and non-inferiority* (2000). Available at: http://www.ema.europa.eu/docs/en_GB/document_library/Scientific_guideline/2009/09/WC50003658.pdf.

27. Jardim DL, Groves ES, Breitfeld PP, Kurzrock R. Factors associated with failure of oncology drugs in late-stage clinical development: a systematic review. *Cancer Treat Rev* (2017) 52:12–21. doi: 10.1016/j.ctrv.2016.10.009

28. Monzon JG, Hay AE, McDonald GT, Pater JL, Meyer RM, Chen E, et al. Correlation of single arm versus randomised phase 2 oncology trial characteristics with phase 3 outcome. *Eur J Cancer* (2015) 51:2501–7. doi: 10.1016/j.ejca.2015.08.004

29. U.S. Department of Health and Human Services Food and Drug Administration, Center for Drug Evaluation and Research (CDER) and Center for Biologics Evaluation and Research (CBER). *Non-inferiority clinical trials to establish effectiveness. guidance for industry* (2016). Available at: <https://www.fda.gov/downloads/Drugs/Guidances/UCM202140.pdf>.

30. Carles J, Alonso T, Mellado Gonzalez B, Mendez Vidal MJ, Vazquez Estevez S, González del Alba A, et al. 639P 223Ra in asymptomatic patients (pts) with metastatic castration-resistant prostate cancer (mCRPC) who progressed to first-line abiraterone acetate or enzalutamide. *Ann Oncol* (2020) 31:S525–6. doi: 10.1016/j.annonc.2020.08.898

31. Wu J, Pan H, Hsu C. Bayesian Single-arm phase II trial designs with time-to-event endpoints. *Pharm Stat* (2021) 20(6):1235–48. doi: 10.1002/psl.2143

32. Gion M, Pérez-García JM, Llombart-Cussac A, Sampayo-Cordero M, Cortés J, Malfettone A. Surrogate endpoints for early-stage breast cancer: a review of the state of the art, controversies, and future prospects. *Ther Adv Med Oncol* (2021) 13:175883592110595. doi: 10.1177/17588359211059587

33. Sparano JA, Gray RJ, Makower DF, Pritchard KI, Albain KS, Hayes DF, et al. Adjuvant chemotherapy guided by a 21-gene expression assay in breast cancer. *New Engl J Med* (2018) 379:111–21. doi: 10.1056/NEJMoa1804710

34. Jung S-H. *Randomized phase II cancer clinical trials*. Boca Raton: CRC Press/Taylor & Francis Group (2013). p. 229.

35. U.S. Department of Health and Human Services Food and Drug Administration, Center for Drug Evaluation and Research (CDER) and Center for Biologics Evaluation and Research (CBER). *Multiple endpoints in clinical trials - guidance for industry* (2017). Available at: <https://www.fda.gov/downloads/drugs/guidancecomplianceregulatoryinformation/guidances/ucm536750.pdf>.

36. U.S. Department of Health and Human Services Food and Drug Administration, Center for Drug Evaluation and Research (CDER) and Center for Biologics Evaluation and Research (CBER). *Clinical trial endpoints for the approval of cancer drugs and biologics - guidance for industry* (2018). Available at: <https://www.fda.gov/regulatory-information/search-fda-guidance-documents/clinical-trial-endpoints-approval-cancer-drugs-and-biologics>.

37. *Time to event data analysis. Columbia public health*. Available at: <https://www.publichealth.columbia.edu/research/population-health-methods/time-event-data-analysis> (Accessed January 26, 2021).

38. Chang M. *Introductory adaptive trial designs: a practical guide with r. s.l.* United States: CRC PRESS (2019).

39. Thorlund K, Dron L, Park JJ, Mills EJ. Synthetic and external controls in clinical trials – a primer for researchers. *CLEP* (2020) 12:457–67. doi: 10.2147/CLEP.S242097

40. Lackey L, Thompson G, Eggers S. FDA’s benefit–risk framework for human drugs and biologics: role in benefit–risk assessment and analysis of use for drug approvals. *Ther Innov Regul Sci* (2021) 55:170–9. doi: 10.1007/s43441-020-00203-6

41. Parker RA, Weir CJ. Non-adjustment for multiple testing in multi-arm trials of distinct treatments: rationale and justification. *Clin Trials* (2020) 17:562–6. doi: 10.1177/1740774520941419

42. Kwak M, Jung S-H. Phase II clinical trials with time-to-event endpoints: optimal two-stage designs with one-sample log-rank test. *Statist Med* (2014) 33:2004–16. doi: 10.1002/sim.6073

43. *Sample size calculator | kengo nagashima - the institute of statistical mathematics*. Available at: <https://nshi.jp/en/js/> (Accessed January 26, 2021).

44. *Statistic tools - SWOG cancer research network*. Available at: <https://stattools.crab.org/index.html> (Accessed January 26, 2021).

45. Wu J. Single-arm phase II survival trial design under the proportional hazards model. *Stat Biopharmaceutical Res* (2017) 9:25–34. doi: 10.1080/19466315.2016.1174147

46. Neuenschwander B, Rouyrre N, Hollaender N, Zuber E, Branson M. A proof of concept phase II non-inferiority criterion. *Stat Med* (2011) 30:1618–27. doi: 10.1002/sim.3997

47. Berry SM. *Bayesian Adaptive methods for clinical trials*. Boca Raton: CRC Press (2011). p. 305.

48. Zhong W, Koopmeiners JS, Carlin BP. A trivariate continual reassessment method for phase I/II trials of toxicity, efficacy, and surrogate efficacy. *Stat Med* (2012) 31:3885–95. doi: 10.1002/sim.5477

49. Thall PF, Cheng S-C. Optimal two-stage designs for clinical trials based on safety and efficacy. *Stat Med* (2001) 20:1023–32. doi: 10.1002/sim.717



OPEN ACCESS

EDITED BY

Sharon R. Pine,
University of Colorado Anschutz Medical
Campus, United States

REVIEWED BY

Minghao Wang,
Southwest Hospital, Army Medical
University, China
Otto Visser,
Netherlands Comprehensive Cancer
Organisation (IKNL), Netherlands

*CORRESPONDENCE

Mackenzie Henderson
✉ mhenderson@dsi.com

RECEIVED 10 August 2022

ACCEPTED 21 August 2023

PUBLISHED 06 September 2023

CITATION

Tu N, Henderson M, Sundararajan M and
Salas M (2023) Discrepancies in ICD-9/
ICD-10-based codes used to identify three
common diseases in cancer patients in
real-world settings and their implications
for disease classification in breast cancer
patients and patients without cancer: a
literature review and descriptive study.
Front. Oncol. 13:1016389.
doi: 10.3389/fonc.2023.1016389

COPYRIGHT

© 2023 Tu, Henderson, Sundararajan and
Salas. This is an open-access article
distributed under the terms of the [Creative
Commons Attribution License \(CC BY\)](#). The
use, distribution or reproduction in other
forums is permitted, provided the original
author(s) and the copyright owner(s) are
credited and that the original publication in
this journal is cited, in accordance with
accepted academic practice. No use,
distribution or reproduction is permitted
which does not comply with these terms.

Discrepancies in ICD-9/ ICD-10-based codes used to identify three common diseases in cancer patients in real-world settings and their implications for disease classification in breast cancer patients and patients without cancer: a literature review and descriptive study

Nora Tu¹, Mackenzie Henderson^{1*}, Meera Sundararajan¹
and Maribel Salas^{1,2}

¹Epidemiology, Clinical Safety and Pharmacovigilance, Daiichi Sankyo, Inc., Basking Ridge,
NJ, United States, ²Center for Real-World Effectiveness and Safety of Therapeutics (CREST), University
of Pennsylvania Perelman School of Medicine, Philadelphia, PA, United States

Background: International Classification of Diseases, Ninth/Tenth revisions, clinical modification (ICD-9-CM, ICD-10-CM) are frequently used in the U.S. by health insurers and disease registries, and are often recorded in electronic medical records. Due to their widespread use, ICD-based codes are a valuable source of data for epidemiology studies, but there are challenges related to their accuracy and reliability. This study aims to 1) identify ICD-9/ICD-10-based codes reported in literature/web sources to identify three common diseases in elderly patients with cancer (anemia, hypertension, arthritis), 2) compare codes identified in the literature/web search to SEER-Medicare's 27 CCW Chronic Conditions Algorithm ("gold-standard") to determine their discordance, and 3) determine sensitivity of the literature/web search codes compared to the gold standard.

Methods: A literature search was performed (Embase, Medline) to find sources reporting ICD codes for at least one disease of interest. Articles were screened in two levels (title/abstract; full text). Analysis was performed in SAS Version 9.4.

Results: Of 106 references identified, 29 were included that reported 884 codes (155 anemia, 80 hypertension, 649 arthritis). Overall discordance between the gold standard and literature/web search code list was 32.9% (22.2% for ICD-9; 35.7% for ICD-10). The gold standard contained codes not found in literature/web sources, including codes for hypertensive retinopathy/encephalopathy,

Page Kidney, spondylosis/spondylitis, juvenile arthritis, thalassemia, sickle cell disorder, autoimmune anemias, and erythroblastopenia. Among a cohort of non-cancer patients (N=684,376), the gold standard identified an additional 129 patients with anemia, 33,683 with arthritis, and 510 with hypertension compared to the literature/web search. Among a cohort of breast cancer patients (N=303,103), the gold standard identified an additional 59 patients with anemia, 10,993 with arthritis, and 163 with hypertension. Sensitivity of the literature/web search code list was 91.38–99.96% for non-cancer patients, and 93.01–99.96% for breast cancer patients.

Conclusion: Discrepancies in codes used to identify three common diseases resulted in variable differences in disease classification. In all cases, the gold standard captured patients missed using the literature/web search codes. Researchers should use standardized, validated coding algorithms when available to increase consistency in research and reduce risk of misclassification, which can significantly alter the findings of a study.

KEYWORDS

validation, international classification of diseases (ICD), comorbidities, breast cancer, methodology, Validation study

1 Introduction

International Classification of Diseases (ICD) coding is one of the oldest efforts to systematically classify and track diseases and mortality (1). Its first edition (the International List of Causes of Death) was released in 1893, and there have since been many revisions to ICD coding led by the World Health Organization (2). The ICD Ninth Revision, Clinical Modification (ICD-9-CM) was adopted in the United States in 1979, and the Tenth Revision, Clinical Modification (ICD-10-CM) was adopted in the United States in 2015 (2). ICD-9-CM and ICD-10-CM coding are modified versions of the WHO's ICD-9 and ICD-10 coding systems, and are used in a variety of healthcare settings in the United States. They are frequently used by health insurers for the reimbursement of claims related to health care services. They are also recorded in patients' electronic medical records and are used by many disease registries to record disease state information (3, 4). The presence of ICD-9-CM and ICD-10-CM codes in such a variety of U.S. healthcare data sources has introduced an invaluable source of information for epidemiology studies (5, 6). In research settings, ICD-9-CM and ICD-10-CM codes have been used for many purposes, including classifying patients' disease status, studying the natural history and outcomes of diseases, and documenting comorbidities (6, 7).

However, the use of ICD-9-CM and ICD-10-CM coding for research is also associated with challenges related to the accuracy and consistency of their use, largely due to widespread and variable usage of the codes in administrative claims in the United States. O'Malley et al. (2005) found several sources of error in their coding, including coder training and experience, quality-control processes in place at healthcare facilities, and intentional or unintentional coding errors (8). Similarly, Liebovitz and Fahrenbach (2018)

suggested limitations due to physician time constraints, inability to find codes, and lack of coverage warnings leading physicians to choose different codes, among other limitations (9). Some studies have reported error rates in ICD-9-based coding up to 80% (8). Thus, researchers' decisions regarding which codes to include in research can potentially have a large impact on study results.

There have been many approaches to address this issue. Some researchers have attempted to create and validate standardized coding algorithms that can be used to identify diseases accurately and reliably in a variety of databases. For example, in 2005, Quan and colleagues (10) created and evaluated several ICD-based coding algorithms to identify common comorbidities such as diabetes and chronic pulmonary disease. In the years since these results were published, many researchers have used these coding algorithms in their own research to accurately identify comorbid diseases (10). Alternatively, some organizations that create or maintain databases provide researchers with their own coding algorithms that researchers can use to identify diseases specifically in their database.

One example of this is the Surveillance, Epidemiology, and End Results (SEER)-Medicare database. SEER-Medicare is a linked database that includes claims data for patients enrolled in Medicare who have a cancer diagnosis. SEER-Medicare provides researchers with a code list (the 27 CCW Chronic Conditions Algorithm) that was developed within SEER-Medicare data and can be used to identify common comorbidities within these data (11). This code list includes not only ICD-9-CM and ICD-10-CM codes, but other codes as well, such as Healthcare Common Procedure Coding System (HCPCS) and Current Procedural Terminology (CPT) codes.

In this study, we utilized a SEER-Medicare breast cancer (BC) dataset to understand the implications of using different coding algorithms to identify common comorbidities in patients with BC.

Using the 27 CCW Chronic Conditions algorithm provided by SEER-Medicare as the gold standard to identify comorbidities, we were able to evaluate the implications of using different, often simpler, algorithms that are commonly used for identification of comorbidities in research. For this study, we chose to focus on identification of three common comorbidities in elderly patients with BC: anemia, hypertension, and arthritis.

There were three primary objectives of this literature review and descriptive study. The first objective was to use published literature and online sources to identify and summarize ICD-based codes used to identify anemia, hypertension, and/or arthritis. The second objective was to systematically compare the ICD-based codes identified from the literature/web search to the ICD-9-CM and ICD-10-CM codes included in the SEER-Medicare 27 CCW Chronic Conditions Algorithm (gold standard) to evaluate their discordance. The third objective was to evaluate numerical differences in disease classification in cohorts of breast cancer and non-cancer SEER-Medicare patients using the literature/web search codes compared to the gold standard and determine sensitivity of the literature/web search code list.

2 Materials and methods

2.1 Study design

A literature search was performed in Embase (1980 – 22 February 2021) and Medline (1946 – 22 February 2021) to find literature that reported ICD-9/ICD-10-based codes used to identify at least one of three diseases of interest: anemia, hypertension, and/or arthritis (including both osteoarthritis, OA, and rheumatoid arthritis, RA). The search was limited to articles in English. The full literature search strategy is reported in [Supplementary Table 1](#). Additional sources were evaluated for articles, including PubMed, references of articles retrieved in the literature search, the American Medical Association's (AMA) official 2019 ICD-10-CM codebook (9), healthcare institution guidance publications (12, 13), and online ICD code look-up tools (14–16).

Publications were eligible for inclusion if they reported ICD-9/ICD-10-based codes used to identify at least one disease of interest, regardless of the primary objectives and methods of the publication. We did not limit inclusion of articles to ICD-9-CM and ICD-10-CM only; other modifications of ICD-coding were included as well. If a publication reported both ICD-based codes and other types of codes (e.g., HCPCS, CPT, or National Drug Codes), it was eligible for inclusion. However, only ICD-based codes were evaluated in this study and all other types of codes were excluded (due to feasibility concerns, inconsistencies in use, and limited usefulness in some databases).

Two levels of article screening were performed by one researcher. In level 1 screening, the titles and abstracts of identified publications were reviewed. Articles that were selected to move on after level 1 screening were then reviewed in level 2 screening, in which the full texts of the articles were reviewed. If there was uncertainty about the decision to include a specific publication, a second researcher was consulted.

The following data were extracted from all included articles: ICD-9/ICD-10-based codes for anemia, hypertension, and arthritis, and code descriptions when reported. If descriptions were not reported, they were extracted from ICD code look-up tools. One researcher performed the data extraction in Microsoft Excel and a second researcher performed quality control on the extracted data. Statistical analysis was performed in SAS Version 9.4.

2.2 Statistical methods

To address the first objective, we summarized the ICD-9/ICD-10-based codes identified from the literature/web search for each disease state and provided brief descriptions of these codes.

To address the second objective, we evaluated and summarized the extent to which the ICD-based codes identified in the literature/web search differed from the ICD-9-CM/ICD-10-CM codes in the SEER Medicare 27 CCW Chronic Conditions Algorithm. This was measured using *percent discordance*. *Concordant codes* were defined as ICD-based codes that were in both the 27 CCW Chronic Conditions Algorithm and the literature/web search code list. *Discordant codes* were defined as ICD-based codes found only in either the 27 CCW Chronic Conditions Algorithm or the literature/web search code lists, but not both. *Total codes* were defined as any codes found in either the 27 CCW Chronic Conditions Algorithm or the literature/web search (including both concordant and discordant codes). The *percent discordant* was defined as:

$$\text{percent discordant} = \frac{\text{number of discordant codes}}{\text{total codes}} \times 100\%$$

To address the third objective, we classified cohorts of non-cancer and BC SEER-Medicare patients (2008 – 2016) using the ICD-based codes found in the literature/web search and separately using the 27 CCW Chronic Conditions Algorithm to determine the difference in overall patient counts with each disease when using the different ICD-based code lists. For this analysis, one comprehensive literature/web search code list was created that included all ICD-based codes for any of the three diseases of interest found in any of the 29 references included herein from the literature review. The 27 CCW Chronic Conditions Algorithm was considered the gold standard for this study for multiple reasons, including that it was developed specifically for use in the dataset that we used for this study, and because the literature/web search code list was an aggregated list, and thus did not represent one specific list of codes and has not undergone any validation. Using the 27 CCW Chronic Conditions Algorithm as the gold standard, we calculated sensitivity for the literature/web search code lists for each of the three diseases.

3 Results

3.1 Literature search results

After all duplicates were removed, the literature search retrieved a total of 84 references. Twenty-two additional references were identified through other means, such as searching PubMed and

reviewing references of articles identified in the literature search (12–33). Out of a total of 106 references identified, 29 references met the inclusion criteria and were included in this study (34–40). All ICD-9/ICD-10-based codes extracted from the included literature/web search are reported in Tables 1A and B. All tables report a lowercase *x* in a code to indicate a wildcard, meaning this digit can be replaced with any number. Unless otherwise noted, a code with *n* wildcard places after a base code includes all codes with up to *n* digits after the base code (e.g., M16.xx includes M16.x).

3.2 Discordant code findings

3.2.1 Overall discordance

Overall, 884 total codes were identified from either the literature/web search or SEER Medicare 27 CCW Chronic Conditions Algorithm: 180 were ICD-9-based and 704 were ICD-10-based codes. Of the total codes, 155 (17.5%) were for anemia, 80 (9.1%) were for hypertension, and 649 (73.4%) were for arthritis. There were 291 discordant codes found between the literature/web search code lists and 27 CCW Chronic Conditions Algorithm: 40 discordant ICD-9-based codes and 251 discordant ICD-10-based codes. This resulted in an overall discordance of 32.9% (22.2% for ICD-9-based codes and 35.7% for ICD-10-based codes) between the literature/web codes and the 27 CCW Chronic Conditions Algorithm. Discordant code findings are reported in Tables 2A and B.

3.2.2 Anemia discordance

A total of 59 ICD-9-based anemia codes were identified from either the literature/web search or SEER Medicare 27 CCW Chronic Conditions Algorithm. Of these, there was one discordant code that was found in the literature/web search but not the 27 CCW Chronic Conditions Algorithm (Table 2A). This resulted in an overall discordance of 1.7% for ICD-9-based anemia codes. A total of 96 ICD-10-based anemia codes were identified from either the literature/web search or 27 CCW Chronic Conditions Algorithm. Of these, there were 35 discordant codes (30 of which were found only in the 27 CCW Chronic Conditions Algorithm and 5 of which were found only in the literature/web search; Table 2B). This resulted in an overall discordance of 36.5% for ICD-10-based anemia codes.

3.2.3 Hypertension discordance

A total of 60 ICD-9-based hypertension codes were identified from either the literature/web search or the SEER Medicare 27 CCW Chronic Conditions Algorithm. Of these, there were 26 discordant codes (1 of which was found only in the 27 CCW Chronic Conditions Algorithm and 25 of which were only found in the literature/web search; Table 2A). This resulted in an overall discordance of 43.3% for ICD-9-based hypertension codes. A total of 20 ICD-10-based hypertension codes were identified from either the literature/web search or the 27 CCW Chronic Conditions Algorithm. Of these, there were 6 discordant codes (all of which were only found in the 27 CCW

TABLE 1A All ICD-9-based codes extracted from the literature/web search and SEER Medicare 27 CCW chronic conditions algorithm.

| Disease | Reference | Literature/Web ICD-9-Based Codes | SEER-Medicare 27 CCW Chronic Conditions Algorithm ICD-9-CM Codes |
|----------------------|--|--|--|
| Anemia | Elixhauser (32) | 280.x, 281.x, 285.2x, 285.9, 648.2 | 280.x, 281.x, 282.xx, 283.xx, 284.xx, 285.xx |
| | Golinvax (40) | 280.1, 280.8, 280.9, 281.x, 285.2x | |
| | Nickel (17) | 285.9 | |
| | Other identified codes ¹ (14) | 282.xx, 283.xx, 284.xx, 285.xx | |
| Hypertension | Elixhauser (32) | 401.x, 402.xx, 403.xx, 404.xx, 405.xx, 642.0x, 642.1x, 642.2x, 642.7x, 642.9x | 362.11, 401.x, 402.xx, 403.xx, 404.xx, 405.xx, 437.2 |
| | Quan (33) | 401.x, 402.xx, 403.xx, 404.xx, 405.xx | |
| | Lee (23) | 401.x, 402.xx, 403.xx, 404.xx, 405.xx | |
| | Nickel (17) | 401.x, 402.xx, 403.xx, 404.xx, 405.xx, 437.2, 642.0x, 642.1x, 642.2x, 642.7x, 642.9x | |
| | Vergara (35) | 401.9 | |
| Rheumatoid Arthritis | Kim (19) | 714.xx | 714.0, 714.1, 714.2, 714.3x, 715.xx, 720.0, 721.0, 721.1, 721.2, 721.3, 721.9x |
| | Lacaille (21) | 714.xx | |
| | Widdifield (22) | 714.xx | |
| | Chung (36) | 714.xx | |
| | Huang (38) | 714.xx | |
| | Bernatsky (29) | 714.xx | |

(Continued)

TABLE 1A Continued

| Disease | Reference | Literature/Web ICD-9-Based Codes | SEER-Medicare 27 CCW Chronic Conditions Algorithm ICD-9-CM Codes |
|----------------|--------------|---|--|
| | BCBS (13) | 714.0 | |
| | Yang (30) | 714.0 | |
| | Maclean (18) | 714, 714.0, 714.1, 714.2, 714.4, 714.8x | |
| | Hanly (20) | 714.0, 714.1, 714.2 | |
| Osteoarthritis | Gore (27) | 715.xx | |

¹Other codes were identified through searching the AMA's official codebook; Blue Cross Blue Shield (BCBS).

TABLE 1B All ICD-10-based codes extracted from the literature/web search and SEER Medicare 27 CCW chronic conditions algorithm.

| Disease | Reference | Literature/Web ICD-10-Based Codes | SEER-Medicare 27 CCW Chronic Conditions Algorithm ICD-10-CM Codes |
|----------------------|---|--|---|
| Anemia | Elixhauser (32) | D51.x, D52.x, D53.x, D50.0, D50.8, D50.9 | D50.x, D51.x, D52.x, D53.x, D55.x, D56.x, D57.00, D57.01, D57.02, D57.1, D57.20, D57.211, D57.212, D57.219, D57.3, D57.40, D57.411, D57.412, D57.419, D57.80, D57.811, D57.812, D57.819, D58.x, D59.x ² , D60.x, D61.xxx, D62, D63.x, D64.xx |
| | Ghezala (34) | D51.x | |
| | Zalfani (39) | D50.0 | |
| | Other identified codes ¹ (14–16) | D50.x, D55.x, D58.x, D59.xx, D61.xxx, D62, D63.x, D64.xx | |
| Hypertension | Elixhauser (32) | I10, I11.x, I12.x, I13.xx, I15.x, | I10, I11.x, I12.x, I13.xx, I15.x, I67.4, N26.2, H35.03x |
| | Quan (33) | I10, I11.x, I12.x, I13.xx, I15.x, | |
| | Optum (12) | I10.x, I11.x | |
| | Lee (23) | I10, I11.x, I12.x, I13.xx, I15.x, | |
| Rheumatoid Arthritis | Widdifield (22) | M05.xxx, M06.xxx | M05.0xx, M05.2xx, M05.3xx, M05.4xx, M05.5xx, M05.6xx, M05.7xx ³ , M05.8xx ⁴ , M05.9, M06.xxx ⁵ , M08.xxx ⁶ |
| | Huang (38) | M05.xxx, M06.xxx | |
| | Bernatsky (29) | M05.xxx | |
| | BCBS (13) | M05.4xx, M05.5xx, M05.7xx, M05.8xx, M05.9, M06.0xx, M06.2xx, M06.3xx, M06.8xx, M06.9 | |
| | Hanly (20) | M05.xxx, M06.0xx, M06.8xx, M06.9 | |
| | Luque Ramos (25) | M05.xxx, M06.xxx | |
| | Curtis (37) | M05.xxx, M06.xxx | |
| | Fautrel (28) | M05.xxx, M06.xxx | |
| Osteoarthritis | French (31) | M15.x, M16.xx, M17.xx, M18.xx, M19.xxx | M15.x, M16.xx, M17.xx, M18.xx, M19.xxx ⁷ , M45.x, M47.xxx ⁸ , M48.8Xx ⁹ |
| | Barnabe (26) | M15.x, M16.xx, M17.xx, M18.xx, M19.xxx | |
| | Postler (24) | M16.x, M17.xx | |
| | Other identified codes ¹ (14) | M15.x, M16.xx, M17.xx, M18.xx, M19.xxx | |

¹Other codes were identified through searching the AMA official codebook and/or online code look-up tools; ²This includes D59.1, a nonbillable code; ³excluding M05.7A; ⁴excluding M05.8A; ⁵excluding M06.0A, M06.4, M06.8A; ⁶excluding M08.0A, M08.2A, M08.4A, M08.9A; ⁷excluding M19.19; ⁸excluding M47.14, M47.15, M47.16; ⁹Capital X indicates that the X is part of the code syntax, whereas a lowercase x indicates a wildcard.

TABLE 2A Discordant ICD-9-based codes with code descriptions.

| | ICD-9-Based Code | Brief Code Descriptions |
|---|---|---|
| Only in literature/web search | | |
| Anemia | 648.2 | Anemia complicating pregnancy, childbirth or the puerperium |
| Hypertension | 642.0x, 642.1x, 642.2x, 642.7x, 632.9x | Certain codes for hypertension complicating pregnancy, childbirth or the puerperium |
| Arthritis (RA/OA) | 714, 714.4, 714.8, 714.81, 714.89, 714.9 | Chronic posttraumatic arthropathy; other specified inflammatory polyarthropathies; unspecified inflammatory polyarthropathy |
| Only in SEER-Medicare 27 CCW Chronic Conditions Algorithm | | |
| Anemia | N/A | |
| Hypertension | 362.11 | Hypertensive retinopathy |
| Arthritis (RA/OA) | 720.0, 721.0, 721.1, 721.2, 721.3, 721.9x | Ankylosing spondylitis; certain spondylosis and allied disorders; spondylosis of unspecified site |

TABLE 2B Discordant ICD-10-based codes with code descriptions.

| | ICD-10-Based Codes | Brief Code Descriptions |
|---|---|--|
| Only in literature/web search | | |
| Anemia | D59.10, D59.11, D59.12, D59.13, D59.19 | Other autoimmune hemolytic anemias |
| Hypertension | N/A | |
| Arthritis | M05.1xx ¹ , M05.8A, M06.0A, M06.4 | Rheumatoid lung disease with RA; other RA with RF of other specified site; RA without RF of other specified site; inflammatory polyarthropathy |
| | M19.09, M19.19, M19.29 | Primary OA of other specified site; post-traumatic OA of other specified site; secondary OA of other specified site |
| Only in SEER-Medicare 27 CCW Chronic Conditions Algorithm | | |
| Anemia | D56.x, D57.00, D57.01, D57.02, D57.1, D57.20, D57.211, D57.212, D57.219, D57.3, D57.40, D57.411, D57.412, D57.419, D57.80, D57.811,812,819, D59.1, D60.x | Thalassemia; certain sickle cell disorders; other autoimmune hemolytic anemia ² ; Acquired pure red cell aplasia (erythroblastopenia) |
| Hypertension | H35.03x, I67.4, N26.2 | Hypertensive retinopathy; hypertensive encephalopathy; Page kidney |
| Arthritis | M08.0xx ³ , M08.1, M08.2xx ⁴ , M08.3, M08.4xx ⁵ , M08.8xx, M08.9xx ⁶ , M45.x, M47.0xx, M47.10, M47.11, M47.12, M47.13, M47.2x, M47.8xx, M47.9, M48.8Xx ⁷ | Certain juvenile RAs; juvenile ankylosing spondylitis; juvenile rheumatoid polyarthritis (seronegative); certain pauciarticular juvenile RA; other/unspecified juvenile arthritis; ankylosing spondylitis; other spondylosis with radiculopathy; other/unspecified spondylosis |

¹Excluding M05.19; ²not a billable code; ³excluding M08.0A; ⁴excluding M08.2A; ⁵excluding M08.4A; ⁶excluding M08.9A; ⁷Capital X indicates that the X is part of the code syntax, whereas a lowercase x indicates a wildcard.

Chronic Conditions Algorithm; Table 2B). This resulted in an overall discordance of 30% for ICD-10-based hypertension codes.

3.2.4 Arthritis discordance

For the arthritis code analysis, RA and OA were grouped together to be consistent with the SEER Medicare 27 CCW Chronic Conditions Algorithm, which includes only one overall group for arthritis. A total of 61 ICD-9-based arthritis codes were identified from either the literature/web search or the 27 CCW Chronic Conditions Algorithm. Of these, there were 13 discordant codes (7 were found only in the 27 CCW Chronic Conditions Algorithm and 6 were found only in the literature/web search; Table 2A). This resulted in an overall discordance of 21.3% for ICD-9-based arthritis codes. A total of 588 ICD-10-based arthritis codes were identified from either the literature/web search or the 27 CCW

Chronic Conditions Algorithm. Of these, there were 210 discordant codes (182 were found only in the 27 CCW Chronic Conditions Algorithm and 28 were found only in the literature/web search; Table 2B). This resulted in an overall discordance of 35.7% for ICD-10-based arthritis codes.

3.3 Most frequently identified codes

The most frequent concordant ICD-9/ICD-10-based codes overall (i.e., those identified in both the literature/web search and the SEER-Medicare 27 CCW Chronic Conditions Algorithm), are reported in Supplementary Table 2. The most frequently identified anemia codes were for unspecified anemia, anemia of chronic illness or blood loss, and deficiency anemias (including iron and vitamin B12). The most

frequently identified hypertension codes were for malignant or benign essential/primary hypertension, hypertensive heart disease, hypertensive chronic kidney disease (CKD), hypertensive heart disease and CKD, and secondary hypertension. The most frequently identified arthritis codes were for rheumatoid arthritis and variations thereof (e.g., with visceral involvement, with rheumatoid myopathy; [Supplementary Table 2](#)), osteoarthritis and variations thereof (e.g., of the hip, of the knee; [Supplementary Table 2](#)), rheumatoid bursitis or nodules, Felty's syndrome, and adult-onset Still's Disease.

The most frequently identified discordant codes found only in literature/web sources are listed in [Supplementary Table 3](#). The most commonly found discordant ICD-9-based codes in the literature/web search included certain hypertensive disorders associated with pregnancy and childbirth and certain arthropathies/polyarthropathies ([Supplementary Table 3](#)). The most common discordant ICD-10-based codes in the literature/web search included certain codes for rheumatoid lung disease with RA, RA of unspecified sites, inflammatory polyarthropathy, and certain codes for OA of unspecified sites.

3.4 Classification of non-cancer and breast cancer patient cohorts in the SEER-Medicare database

Finally, to address the third objective of this study we evaluated the numerical differences in disease classification in two cohorts of patients in SEER-Medicare (non-cancer patients and BC patients) using the literature/web search codes compared to the SEER-Medicare 27 CCW Chronic Conditions Algorithm codes. These results are presented in [Tables 3A, B](#). For non-cancer patients, the 27 CCW Chronic Conditions Algorithm identified 129 additional patients with anemia ($p=0.83$), 510 additional patients with hypertension ($p=0.27$), and 33,683 additional patients with arthritis ($p<0.0001$) that were not identified using the literature/web code list. Using the 27 CCW Chronic Conditions Algorithm as the gold standard, the comprehensive literature/web search code list had a 99.96% sensitivity to identify anemia in non-cancer patients, 99.91% sensitivity to identify hypertension in non-cancer patients, and 91.38% sensitivity to identify arthritis (including both OA and RA) in non-cancer patients. For BC patients, the 27 CCW Chronic Conditions Algorithm identified 59 additional patients with anemia ($p=0.88$), 163 additional patients with hypertension ($p=0.66$), and 10,993 additional patients with arthritis ($p<0.0001$) that were not identified using the literature/web code list. Using the 27 CCW Chronic Conditions Algorithm as the gold standard, the comprehensive literature/web search code list had a 99.96% sensitivity to identify anemia in BC patients, 99.92% sensitivity to identify hypertension in BC patients, and 93.01% sensitivity to identify arthritis in BC patients.

4 Discussion

A total of 884 codes were identified for anemia, hypertension, and arthritis. The majority of these codes were ICD-10-based codes

($n=704$), and the remainder were ICD-9-based codes ($n=180$). The discrepancy between number of codes in the ninth and tenth revisions was expected, given that there are almost five times as many ICD-10-CM codes as there are ICD-9-CM codes, largely due to differences in grouping and specificity between the ICD versions (6). The most common codes identified for anemia were for anemias of chronic illness or blood loss, unspecified anemias, and deficiency anemias. The most common codes identified for hypertension were for malignant or benign essential/primary hypertension, secondary hypertension, and hypertensive heart disease and/or hypertensive CKD. Finally, the most common codes for arthritis were for OA and variations thereof, RA and variations thereof, rheumatoid bursitis or nodules, Felty's syndrome, and adult-onset Still's Disease.

When the literature/web search code lists were compared to the SEER-Medicare 27 CCW Chronic Conditions Algorithm, there was variable discordance. Discordance for all codes was less than 50% (overall discordance was 32.9%), and higher discordance was observed for hypertension compared to either anemia or arthritis. Discordance for ICD-9-based codes ranged from 1.7% - 43.3% and discordance for ICD-10-based codes ranged from 30% - 36.5%. There were several codes included in the 27 CCW Chronic Conditions Algorithm that were not found in literature/web sources. These included certain codes for hypertensive retinopathy/encephalopathy, Page kidney, thalassemia, sickle cell disorders, autoimmune hemolytic anemia, erythroblastopenia, spondylitis/spondylosis, and juvenile arthritis conditions. On the other hand, the most common codes found only in the literature/web search included certain codes related to hypertensive disorders of pregnancy/childbirth, certain arthropathies/polyarthropathies, rheumatoid lung disease with RA, and RA of unspecified sites, ([Supplementary Table 3](#)).

There are many possible reasons for the differences between the codes included in the literature/web search code list and the 27 CCW Chronic Conditions Algorithm. Specific codes included in any given study may be driven largely by the population of interest. This is demonstrated clearly by the fact that pregnancy-related hypertensive disorders were not found in the 27 CCW Chronic Conditions Algorithm. Because the SEER-Medicare database primarily contains information about older adults (≥ 65 years old), codes related to pregnancy are less relevant in these patients, which may be why they were excluded. Interestingly, when examining codes found only in the 27 CCW Chronic Conditions Algorithm, there were several codes related to juvenile arthritis. As previously noted, SEER-Medicare includes data on mostly older individuals, so the rationale for including these codes in the code list is unclear. It is possible that since some types of juvenile arthritis are chronic diseases that persist into adulthood, they may remain relevant in older populations (41).

Furthermore, the exact codes used in a study may be based on the specific database being used, or based on previous research that has validated the use of specific codes to identify the disease of interest. As an example, a 2011 article by Kim et al. (19) performed a validation of several code lists to identify RA in Medicare claims data. Since this initial validation, this paper has been cited by over 150 articles, many of which used one of Kim et al.'s code lists to

TABLE 3A Total number of non-cancer SEER-Medicare patients (N=684,376) classified with each disease of interest using codes found in the literature/web search code list compared to the SEER-Medicare 27 CCW chronic conditions algorithm.

| Disease | ICD Code Version | Number of non-cancer patients identified | | Absolute difference | Sensitivity ² | p-value ³ |
|--------------|------------------|--|--|---------------------|--------------------------|----------------------|
| | | Literature/web search | 27 CCW Chronic Conditions Algorithm ¹ | | | |
| Anemia | ICD-9 | 300,876 (44.0%) | 300,876 (44.0%) | 0 (0) | – | 1.00 |
| | ICD-10 | 112,643 (16.5%) | 113,128 (16.5%) | 485 (0.1%) | – | 0.26 |
| | Any | 330,644 (48.3%) | 330,773 (48.3%) | 129 (<0.1%) | 99.96% | 0.83 |
| Hypertension | ICD-9 | 515,380 (75.3%) | 515,845 (75.4%) | 465 (0.1%) | – | 0.36 |
| | ICD-10 | 310,697 (45.4%) | 311,195 (45.5%) | 498 (0.1%) | – | 0.39 |
| | Any | 548,324 (80.1%) | 548,834 (80.2%) | 510 (0.1%) | 99.91% | 0.27 |
| Arthritis | ICD-9 | 324,569 (47.4%) | 356,329 (52.1%) | 31,760 (4.6%) | – | <0.0001 |
| | ICD-10 | 143,426 (21.0%) | 164,825 (24.1%) | 21,399 (3.1%) | – | <0.0001 |
| | Any | 357,280 (52.2%) | 390,963 (57.1%) | 33,683 (4.9%) | 91.38% | <0.0001 |

¹Considered the gold standard for this study; ²Sensitivity refers to the sensitivity of the literature/web search code list when compared to the gold standard, the SEER-Medicare 27 CCW Chronic Conditions Algorithm; ³P-value based on Chi-square test

TABLE 3B Total number of SEER-Medicare breast cancer patients N=303,103 classified with each disease of interest using codes found in the literature/web search code list compared to the SEER-Medicare 27 CCW chronic conditions algorithm.

| Disease | ICD Code Version | Number of breast cancer patients identified | | Absolute difference | Sensitivity ² | p-value ³ |
|--------------|------------------|---|--|---------------------|--------------------------|----------------------|
| | | Literature/web search | 27 CCW Chronic Conditions Algorithm ¹ | | | |
| Anemia | ICD-9 | 120,792 (39.9%) | 120,792 (39.9%) | 0 (0) | – | 1.00 |
| | ICD-10 | 52,584 (17.4%) | 52,789 (17.4%) | 205 (0.1%) | – | 0.49 |
| | Any | 134,900 (44.5%) | 134,959 (44.5%) | 59 (0.0%) | 99.96% | 0.88 |
| Hypertension | ICD-9 | 188,462 (62.2%) | 188,610 (62.2%) | 148 (0.1%) | – | 0.70 |
| | ICD-10 | 125,619 (41.4%) | 125,800 (41.5%) | 181 (0.1%) | – | 0.64 |
| | Any | 203,026 (67.0%) | 203,189 (67.0%) | 163 (0.1%) | 99.92% | 0.66 |
| Arthritis | ICD-9 | 131,529 (43.4%) | 141,881 (46.8%) | 10,352 (3.4%) | – | <0.0001 |
| | ICD-10 | 66,675 (22.0%) | 74,775 (24.7%) | 8,100 (2.7%) | – | <0.0001 |
| | Any | 146,263 (48.3%) | 157,256 (51.9%) | 10,993 (3.6%) | 93.01% | <0.0001 |

¹Considered the gold standard for this study; ²Sensitivity refers to the sensitivity of the literature/web search code list when compared to the gold standard, the SEER-Medicare 27 CCW Chronic Conditions Algorithm; ³P-value based on Chi-square test

identify RA in their own research (19, 42–45). This indicates that a researcher's decision about which codes to use may be based on previous work done to validate those codes in the same or similar databases.

A third potential reason for the differences seen may be due to variable consultation of clinical or coding experts when developing codes lists for specific diseases. When examining the codes found in the literature/web search and the SEER-Medicare 27 CCW Chronic Conditions Algorithm, each contained codes that did not explicitly match the disease name, but may have been included because a clinical expert deemed them appropriate. For example, under the scope of arthritis, the 27 CCW Chronic Conditions Algorithm includes codes for spondylosis and adult-onset Still's disease. Professionals in medical coding and clinicians who specialize in a

particular area of practice may be knowledgeable about common coding practices and diseases that share common features and may be able to use this knowledge to ensure face validity of code lists (46, 47).

Finally, another possible reason for the differences observed may be due to variation in the use of specific codes over time. Common ICD-9-/ICD-10-based coding practices or reimbursement policies for any given disease state may change over time, and this would in turn necessitate a change in the codes used to identify the given disease in a healthcare database. In addition, the code version used in the United States changed in 2015 from ICD-9-CM to ICD-10-CM. Thus, depending on the years included in a specific study, it may be necessary to include one or both of these code versions. These issues may also account for some of the differences in code lists observed in this study.

Regardless of the specific reasons for the variation in coding algorithms, the differences can result in important differences in patient classification. When we classified two cohorts of patients in SEER-Medicare, the literature/web search code list had between 91.38% – 99.96% sensitivity in identifying non-cancer patients and 93.01% - 99.96% sensitivity in identifying BC patients with the three diseases of interest. While the overall sensitivity was high, it should be noted that the sensitivity for the code lists used in individual studies may have been significantly lower than the overall sensitivity, given that we combined all 29 literature/web search code lists into one list for analysis. Interestingly, percent discordance did not necessarily correspond to lower sensitivity. While the highest discordance was identified for hypertension, the lowest overall sensitivity was seen for arthritis: the SEER-Medicare 27 CCW Chronic Conditions Algorithm identified a significant additional number of patients with arthritis in the non-cancer cohort (33,683 additional patients; $p < 0.0001$) and in the BC cohort (10,993 additional patients $p < 0.0001$) that were not identified with the literature/web search codes.

Using the 27 CCW Chronic Conditions Algorithm as the gold standard, the literature/web search code list misclassified a significant number of patients with arthritis. Because these codes are often used to assign patients to exposure or outcome groups, or used for subgroup analyses in epidemiology studies, issues of misclassification can affect the clinical interpretation of a study's results. Whether this misclassification is differential or non-differential may depend on the study design and data source used. If misclassification occurs proportionally between the groups being compared to each other, this will result in non-differential misclassification and will bias the study results towards the null. The extent to which this is an issue for any particular study will depend largely on the disease of interest, its common coding practices, and the database used. However, the differences can be substantial, and this example offers a clear illustration of why researchers must carefully evaluate and determine which codes to include in their research.

This study has a few limitations. The gold standard (the 27 CCW Chronic Conditions Algorithm) and the ICD-10-CM coding system are frequently updated. We used the version of the 27 CCW Chronic Conditions Algorithm that was developed using data through 2016, aligning with the specific dataset used in this study. For this reason, we were able to use it as a gold standard for this study, but this algorithm has since been updated and our results may not reflect the most recent algorithms or ICD-10-CM coding. This study focused on the evaluation of how the literature/web search code list performed against the gold standard, but we were unable to evaluate the performance of the gold standard itself. It should also be noted that this algorithm undergoes continual updating to reflect the most current coding practices and understanding of the relevant disease states. In addition, definitions used to determine disease status in epidemiology studies are not limited to codes (e.g., ICD-9-CM or ICD-10-CM codes), but may incorporate other rules. These can include requirements for patients to have more than one code recorded for the disease, potentially at prespecified time intervals. Though not directly evaluated in the current study, articles that were included in our literature review varied extensively in their definitions of arthritis. Kim et al. (19) required patients to have at least two or three diagnosis codes for RA. Lacaille et al. (21) required at least two

physician visits more than two months apart with a diagnosis code for RA. In contrast, French et al. (31) required only one diagnosis code for OA. Finally, Postler et al. (24) required an outpatient diagnosis of OA in at least two quarters of a single calendar year. These differences in coding algorithms must also be considered when determining the appropriate way to identify and classify patients' disease status.

5 Conclusions

Although it may not be feasible to develop one coding algorithm to identify a specific disease for use across all databases, there is considerable room for improvement in the development of valid coding algorithms and increased consistency of their use in research. Researchers should carefully evaluate what codes to include in their research, and consider the potential implications of these decisions. If significant misclassification occurs because invalid coding algorithms are used to identify patients, this may bias the results of a study and call into question their clinical utility. It is advisable that researchers provide justification for their inclusion and exclusion of certain codes in their publications. Finally, if validated coding algorithms or validated ICD-9/ICD-10-based codes are available for use, researchers should use them in their research. Future work is needed to develop and validate coding algorithms for use in specific databases.

Data availability statement

The data analyzed in this study is subject to the following licenses/restrictions: SEER-Medicare data are not public use data files. Requests to access these datasets should be directed to SEER-Medicare, SEERMedicare@imsweb.com.

Ethics statement

The studies involving humans were approved by SEER-Medicare Review Committee. The studies were conducted in accordance with the local legislation and institutional requirements. Written informed consent for participation was not required from the participants or the participants' legal guardians/next of kin in accordance with the national legislation and institutional requirements.

Author contributions

NT contributed to the development of the research project, contributed to drafting of study materials including statistical analysis plan and study protocol, contributed to statistical analysis of data and quality control, critically reviewed drafts and approved the final manuscript. MH contributed to the development of the research project, contributed to drafting of all study materials, provided input into the statistical analysis plan, contributed to

drafting of manuscript and critical review, approved final manuscript. MeS contributed to drafting of study materials, conducted statistical analysis of the data and quality control, contributed to the drafting of the manuscript, and critically reviewed drafts and approved final manuscript. MaS contributed to the development of the research project, provided input into the statistical analysis plan and interpretation of results, critically reviewed drafts and approved the final manuscript. All authors contributed to the article and approved the submitted version.

Conflict of interest

All authors are employees of Daiichi Sankyo, Inc., the funder of this research. Authors MaS, MeS, and NT own Daiichi Sankyo stock.

References

1. International Statistical Classification of Diseases and Related Health Problems (ICD). Geneva, Switzerland: World Health Organization (2021). Available at: <https://www.who.int/standards/classifications/classification-of-diseases>.
2. ICD-9-CM Code Set. Salt Lake City, Utah, USA: AAPC. Available at: <https://www.aapc.com/resources/medical-coding/icd9.aspx#:~:text=The%20current%20version%20used%20in%20the%20United%20States,%20input%20of%20providers,%20payers,%20and%20other%20key%20stakeholders>.
3. Thought Leadership Team Editorial Staff / AAPC ICD-10 and CMS eHealth: What's the Connection? Centers for Medicare & Medicaid Services (2013). Available at: [https://www.cms.gov/Medicare/Coding/ICD10/Downloads/ICD-10andCMSHealth-WhatstheConnection_071813remediated\[1\].pdf](https://www.cms.gov/Medicare/Coding/ICD10/Downloads/ICD-10andCMSHealth-WhatstheConnection_071813remediated[1].pdf).
4. ICD-O-3 Coding Materials. National Cancer Institute. Available at: <https://seer.cancer.gov/icd-o-3/>.
5. Classifications. World Health Organization. Available at: <https://www.who.int/standards/classifications>.
6. The Role of the ICD-10 in Epidemiology. Louisville, KY, USA: Radius Anesthesia of Kentucky PLLC (2020). Available at: <https://radiusky.com/icd-10-epidemiology/>.
7. International Classification of Diseases, (ICD-10-CM/PCS) Transition - Background. Centers for Disease Control and Prevention (2015). Available at: https://www.cdc.gov/nchs/icd/icd10cm_pcs_background.htm.
8. O'Malley KJ, Cook KF, Price MD, Wildes KR, Hurdle JF, Ashton CM. Measuring diagnoses: ICD code accuracy. *Health Serv Res* (2005) 40(5 Pt 2):1620–39. doi: 10.1111/j.1475-6773.2005.00444.x
9. Liebovitz DM, Fahrenbach J. COUNTERPOINT: is ICD-10 diagnosis coding important in the era of big data? No. *Chest* (2018) 153(5):1095–8. doi: 10.1016/j.chest.2018.01.034
10. Quan H, Sundararajan V, Halfon P, Fong A, Burnand B, Luthi JC, et al. Coding algorithms for defining comorbidities in ICD-9-CM and ICD-10 administrative data. *Med Care* (2005) 43(11):1130–9. doi: 10.1097/01.mlr.0000182534.19832.83
11. Chronic Conditions Data Warehouse. Baltimore, Maryland, USA: Centers for Medicare and Medicaid Services (2022).
12. Hypertension coding tool. Optum (2019). Available at: https://myuha.org/wp-content/uploads/2020/05/Optum_Insider_Hypertension_Coding_Tool-11-20-19.pdf.
13. Rheumatology ICD-10-CM Coding Tip Sheet: Overview of Key Chapter Updates for Rheumatology. Blue Cross Blue Shield of Michigan. Available at: <https://www.bcbsm.com/content/dam/public/Providers/Documents/help/faqs/icd10-tip-sheet-rheumatology.pdf>.
14. ICD-10-CM 2019: The Complete Official Codebook. 1 ed. Chicago, Illinois: American Medical Association (2018). Available at: https://books.google.com/books/about/ICD_10_CM_2019_the_Complete_Official_Cod.html?id=A0V0tgEACAAJ
15. ICD10Data.com. Available at: <https://www.icd10data.com>.
16. ICD9Data.com. Available at: <http://www.icd9data.com/>.
17. Nickel KB, Wallace AE, Warren DK, Ball KE, Mines D, Fraser VJ, et al. Modification of claims-based measures improves identification of comorbidities in non-elderly women undergoing mastectomy for breast cancer: a retrospective cohort study. *BMC Health Serv Res* (2016) 16(a):388. doi: 10.1186/s12913-016-1636-7
18. MacLean CH, Louie R, Leake B, McCaffrey DF, Paulus HE, Brook RH, et al. Quality of care for patients with rheumatoid arthritis. *JAMA* (2000) 284(8):984–92. doi: 10.1001/jama.284.8.984
19. Kim SY, Servi A, Polinski JM, Mogun H, Weinblatt ME, Katz JN, et al. Validation of rheumatoid arthritis diagnoses in health care utilization data. *Arthritis Res Ther* (2011) 13(1):R32. doi: 10.1186/ar3260
20. Hanly JG, Thompson K, Skedgel C. The use of administrative health care databases to identify patients with rheumatoid arthritis. *Open Access Rheumatol Res Rev* (2015) 7:69–75. doi: 10.2147/OARRR.S92630
21. Lacaille D, Anis AH, Guh DP, Esdaile JM. Gaps in care for rheumatoid arthritis: a population study. *Arthritis Rheumatol* (2005) 53(2):241–8. doi: 10.1002/art.21077
22. Widdifield J, Bombardier C, Bernatsky S, Paterson JM, Green D, Young J, et al. An administrative data validation study of the accuracy of algorithms for identifying rheumatoid arthritis: the influence of the reference standard on algorithm performance. *BMC Musculoskelet Disord* (2014) 15:216. doi: 10.1186/1471-2474-15-216
23. Lee DC, Feldman JM, Osorio M, Koziatke CA, Nguyen MV, Nagappan A, et al. Improving the geographical precision of rural chronic disease surveillance by using emergency claims data: a cross-sectional comparison of survey versus claims data in Sullivan County, New York. *BMJ Open* (2019) 9(11):e033373. doi: 10.1136/bmjopen-2019-033373
24. Postler A, Ramos AL, Goronzy J, Günther KP, Lange T, Schmitt J, et al. Prevalence and treatment of hip and knee osteoarthritis in people aged 60 years or older in Germany: an analysis based on health insurance claims data. *Clin Interv Aging* (2018) 13:2339–49. doi: 10.2147/CLIA.S174741
25. Luque Ramos A, Redeker I, Hoffmann F, Callhoff J, Zink A, Albrecht K. Comorbidities in patients with rheumatoid arthritis and their association with patient-reported outcomes: results of claims data linked to questionnaire survey. *J Rheumatol* (2019) 46(6):564–71. doi: 10.3899/jrheum.180668
26. Barnabe C, Hemmelgarn B, Jones CA, Peschken CA, Voaklander D, Joseph L, et al. Imbalance of prevalence and specialty care for osteoarthritis for first nations people in Alberta, Canada. *J Rheumatol* (2015) 42(2):323–8. doi: 10.3899/jrheum.140551
27. Gore M, Tai KS, Sadosky A, Leslie D, Stacey BR. Clinical comorbidities, treatment patterns, and direct medical costs of patients with osteoarthritis in usual care: a retrospective claims database analysis. *J Med Econ* (2011) 14(4):497–507. doi: 10.3111/13696998.2011.594347
28. Fautrel B, Cukierman G, Joubert JM, Laurendeau C, Gourmelen J, Fagnani F. Healthcare service utilisation costs attributable to rheumatoid arthritis in France: Analysis of a representative national claims database. *Joint Bone Spine* (2016) 83(1):53–6. doi: 10.1016/j.jbspin.2015.02.023
29. Bernatsky S, Dekis A, Hudson M, Pineau CA, Boire G, Fortin PR, et al. Rheumatoid arthritis prevalence in Quebec. *BMC Res Notes* (2014) 7:937. doi: 10.1186/1756-0500-7-937
30. Yang DH, Huang JY, Chiou JY, Wei JC. Analysis of socioeconomic status in the patients with rheumatoid arthritis. *Int J Environ Res Public Health* (2018) 15(6):1194. doi: 10.3390/ijerph15061194
31. French ZP, Torres RV, Whitney DG. Elevated prevalence of osteoarthritis among adults with cerebral palsy. *J Rehabil Med* (2019) 51(8):575–81. doi: 10.2340/16501977-2582
32. Elixhauser A, Steiner C, Harris DR, Coffey RM. Comorbidity measures for use with administrative data. *Med Care* (1998) 36(1):8–27. doi: 10.1097/00005650-199801000-00004
33. Quan H, Khan N, Hemmelgarn BR, Tu K, Chen G, Campbell N, et al. Validation of a case definition to define hypertension using administrative data. *Hypertension* (2009) 54(6):1423–8. doi: 10.1161/HYPERTENSIONAHA.109.139279

Publisher's note

All claims expressed in this article are solely those of the authors and do not necessarily represent those of their affiliated organizations, or those of the publisher, the editors and the reviewers. Any product that may be evaluated in this article, or claim that may be made by its manufacturer, is not guaranteed or endorsed by the publisher.

Supplementary material

The Supplementary Material for this article can be found online at: <https://www.frontiersin.org/articles/10.3389/fonc.2023.1016389/full#supplementary-material>

34. Ben Ghezala I, Arendt JF, Erichsen R, Zalfani J, Gammelager H, Frøslev T, et al. Positive predictive value of the diagnosis coding for vitamin B12 deficiency anemia in the Danish National Patient Register. *Clin Epidemiol* (2012) 4:333–8. doi: 10.2147/CLEP.S38229
35. Vergara VA. Identification of ICD-9 codes associated with scleroderma renal crisis. *Clin Exp Rheumatol* (2014) 32(2):S115.
36. Chung CP, Rohan P, Krishnaswami S, McPheeters ML. A systematic review of validated methods for identifying patients with rheumatoid arthritis using administrative or claims data. *Vaccine* (2013) 31(Suppl 10):K41–61. doi: 10.1016/j.vaccine.2013.03.075
37. Curtis JR, Xie F, Zhou H, Salchert D, Yun H. Use of ICD-10 diagnosis codes to identify seropositive and seronegative rheumatoid arthritis when lab results are not available. *Arthritis Res Ther* (2020) 22(1):242. doi: 10.1186/s13075-020-02310-z
38. Huang S, Huang J, Cai T, Dahal KP, Cagan A, Stratton J, et al. Impact of international classification of diseases 10th revision codes and updated medical information on an existing rheumatoid arthritis phenotype algorithm using electronic medical data. *Arthritis Rheumatol* (2018) 70(Supplement 10). Available at: <https://acrabstracts.org/abstract/impact-of-international-classification-of-diseases-10th-revision-codes-and-updated-medical-information-on-an-existing-rheumatoid-arthritis-phenotype-algorithm-using-electronic-medical-data/#:~:text=We%20observed%20that%20an%20existing%20RA%20algorithm%20trained,includin%20ICD10%20had%20a%20minimal%20impact%20on%20classification.>
39. Zalfani J, Frøslev T, Olsen M, Ben Ghezala I, Gammelager H, Arendt JF, et al. Positive predictive value of the International Classification of Diseases, 10th edition diagnosis codes for anemia caused by bleeding in the Danish National Registry of Patients. *Clin Epidemiol* (2012) 4:327–31. doi: 10.2147/CLEP.S37188
40. Golinvaux NS, Bohl DD, Basques BA, Grauer JN. Administrative database concerns: accuracy of International Classification of Diseases, Ninth Revision coding is poor for preoperative anemia in patients undergoing spinal fusion. *Spine (Phila Pa 1976)* (2014) 39(24):2019–23. doi: 10.1097/BRS.0000000000000598
41. Freeman J. *Juvenile Rheumatoid Arthritis (JRA): Does JRA Ever Go Away?* (2018). Available at: <https://www.rheumatoidarthritis.org/ra/juvenile/#:~:text=Juvenile%20chronic%20arthritis%20and%20juvenile%20idiopathic%20arthritis%20are,High%20fevers,%20Rashes%20that%20appear%20with%20fevers,%20Stiffness.>
42. Hunter TM, Boytsov NN, Zhang X, Schroeder K, Michaud K, Araujo AB. Prevalence of rheumatoid arthritis in the United States adult population in healthcare claims databases, 2004–2014. *Rheumatol Int* (2017) 37(9):1551–7. doi: 10.1007/s00296-017-3726-1
43. Curtis JR, Xie F, Yun H, Bernatsky S, Winthrop KL. Real-world comparative risks of herpes virus infections in tofacitinib and biologic-treated patients with rheumatoid arthritis. *Ann rheumatic diseases* (2016) 75(10):1843–7. doi: 10.1136/annrheumdis-2016-209131
44. Pawar A, Desai RJ, Solomon DH, Ortiz AJS, Gale S, Bao M, et al. Risk of serious infections in tocilizumab versus other biologic drugs in patients with rheumatoid arthritis: a multidatabase cohort study. *Ann rheumatic diseases* (2019) 78(4):456–64. doi: 10.1136/annrheumdis-2018-214367
45. Kim SC, Glynn RJ, Giovannucci E, Hernández-Díaz S, Liu J, Feldman S, et al. Risk of high-grade cervical dysplasia and cervical cancer in women with systemic inflammatory diseases: a population-based cohort study. *Ann rheumatic diseases* (2015) 74(7):1360–7. doi: 10.1136/annrheumdis-2013-204993
46. Stein JD, Rahman M, Andrews C, Ehrlich JR, Kamat S, Shah M, et al. Evaluation of an algorithm for identifying ocular conditions in electronic health record data. *JAMA Ophthalmol* (2019) 137(5):491–7. doi: 10.1001/jamaophthalmol.2018.7051
47. Regier DA, Kaelber CT, Roper MT, Rae DS, Sartorius N. The ICD-10 clinical field trial for mental and behavioral disorders: results in Canada and the United States. *Am J Psychiatry* (1994) 151(9):1340–50. doi: 10.1176/ajp.151.9.1340

Frontiers in Oncology

Advances knowledge of carcinogenesis and tumor progression for better treatment and management

The third most-cited oncology journal, which highlights research in carcinogenesis and tumor progression, bridging the gap between basic research and applications to improve diagnosis, therapeutics and management strategies.

Discover the latest Research Topics

[See more →](#)

Frontiers

Avenue du Tribunal-Fédéral 34
1005 Lausanne, Switzerland
frontiersin.org

Contact us

+41 (0)21 510 17 00
frontiersin.org/about/contact

